CHARACTERIZATION OF BABOON REOVIRUS p15 SUGGESTS A NOVEL MODEL OF FAST PROTEIN-MEDIATED MEMBRANE FUSION

by

Sandra Dawe

Submitted in partial fulfillment of the requirements
for the degree of Doctor of Philosophy

at

Dalhousie University
Halifax, Nova Scotia
March 1, 2004

© Copyright by Sandra Dawe, 2004

National Library
of Canada

Acquisitions and
Bibliographic Services

395 Wellington Street
Ottawa ON K1A 0N4
Canada

Bibliothèque nationale
du Canada

Acquisisitons et
services bibliographiques

395, rue Wellington
Ottawa ON K1A 0N4
Canada

Your file Votre référence
ISBN: 0-612-94042-X
Our file Notre référence
ISBN: 0-612-94042-X

The author has granted a non-exclusive licence allowing the National Library of Canada to reproduce, loan, distribute or sell copies of this thesis in microform, paper or electronic formats.

L'auteur a accordé une licence non exclusive permettant à la Bibliothèque nationale du Canada de reproduire, prêter, distribuer ou vendre des copies de cette thèse sous la forme de microfiche/film, de reproduction sur papier ou sur format électronique.

The author retains ownership of the copyright in this thesis. Neither the thesis nor substantial extracts from it may be printed or otherwise reproduced without the author's permission.

L'auteur conserve la propriété du droit d'auteur qui protège cette thèse. Ni la thèse ni des extraits substantiels de celle-ci ne doivent être imprimés ou aturement reproduits sans son autorisation.

In compliance with the Canadian Privacy Act some supporting forms may have been removed from this dissertation.

Conformément à la loi canadienne sur la protection de la vie privée, quelques formulaires secondaires ont été enlevés de ce manuscrit.

While these forms may be included in the document page count, their removal does not represent any loss of content from the dissertation.

Bien que ces formulaires aient inclus dans la pagination, il n'y aura aucun contenu manquant.

Canada

DALHOUSIE UNIVERSITY

To comply with the Canadian Privacy Act the National Library of Canada has requested that the following pages be removed from this copy of the thesis:

Preliminary Pages

Examiners Signature Page (pii)

Dalhousie Library Copyright Agreement (piii)

Appendices

Copyright Releases (if applicable)

This thesis is dedicated to the two women who made it possible:

To Rachel, for giving me the reason to pursue a Ph.D.
And, to Holly, for making me believe that viruses are cool.

TABLE OF CONTENTS

LIST OF FIGURES

LIST OF TABLES

ABSTRACT

The fusogenic reoviruses are the only nonenveloped viruses known to induce cell-cell fusion, which they accomplish through a distinct class of viral nonstructural, membrane fusion-inducing proteins referred to as the Fusion-Associated Small Transmembrane (FAST) proteins. The factor responsible for the unusual fusogenic phenotype of baboon reovirus was identified as the 15-kDa product (p15) of the 5'-open reading frame of the bicistronic S4 genome segment. As p15 shares no significant overall sequence similarity with other FAST proteins and contains a unique repertoire and arrangement of sequence-predicted structural and functional motifs, p15 was designated as a novel member of the FAST protein family. Topological analysis indicated that p15 is a type III (N_{exo}/C_{cyt}) bitopic membrane protein that not only translocates the smallest ectodomain (about 20 amino acids) of any known viral fusion protein, but the p15 ectodomain also lacks a hydrophobic fusion peptide – an essential motif in virtually all other fusogenic proteins. The function of the p15 ectodomain depends on the presence of two atypical features, namely an N-terminal myristate moiety and a short polyproline helix (residues 10-15). A membrane-proximal, cytoplasmic polybasic motif was shown to contribute to p15 fusogenicity independent of its potential contribution to p15 topogenesis. A hydrophobic sequence present within the p15 endodomain is hypothesized to serve as a fusion-promoting motif, flanked by residues (comprising the 'FLX' region) exhibiting similarity to the externalized 'fusion peptides' of other FAST proteins. The FLX motifs could be functionally exchanged among the different FAST proteins and thus, are postulated to represent mechanistically-equivalent fusogenic regions. A model for p15-mediated membrane fusion is proposed in which p15 initiates membrane merger through perturbations of primarily the donor membrane. Unlike the current models of enveloped virus-mediated membrane fusion, p15 is neither predicted to be held in a metastable state, nor to undergo triggered conformational rearrangements that release energy harnessed to drive lipid bilayer mixing. These fundamental differences in the proposed mechanism of p15 action with respect to the fusion proteins of enveloped viruses may reflect the freedom that this nonstructural, 'non-essential' viral protein has had, outside of a receptor-binding constraint, to evolve a minimal fusogenic structure.

LIST OF ABBREVIATIONS AND SYMBOLS

aa	amino acid
A	adenine
Ab	antibody
ADAM	a disintegrin and a metalloprotease
Ala (A)	alanine
Arg (R)	arginine
ARV	avian reovirus
Asn (N)	asparagine
ATR-FTIR	attenuated total reflection Fourier transform infrared
BFA	brefeldin A
BRV	baboon reovirus
C	cytosine
CD	circular dichroism
CRAC	cholesterol recognition-interaction consensus
CsCl	cesium chloride
Cys (C)	cysteine
cyt	cytoplasmic
Da	dalton
DHBV	duck hepatitis B virus
DIC	differential interference contrast
DMEM	Dulbecco's modified Eagle medium
DRV	muscovy duck reovirus
ds	double-stranded
DS	domain swap
EDTA	ethylenediaminetetraacetate
E	envelope glycoprotein (TBEV, SFV)
EEV	extracellular enveloped virus
EM	electron microscopy
Env	envelope glycoprotein (HIV)
ER	endoplasmic reticulum
ERV	endogenous retrovirus
exo	exocytoplasmic
F	fusion glycoprotein (paramyxovirus)
$F(ab')_2$	fragments of IgG resulting from pepsin digestion to remove Fc portion
FAST	fusion-associated small transmembrane
FBS	fetal bovine serum
FITC	fluorescein isothiocyanate
FLX	flexible (domain)
g(1-8)	engineered glycosylation site (1-8)
G	guanine
G	fusion glycoprotein (VSV)
g(B/D/H/L/K)	glycoprotein B, D, H, L or K (herpesvirus)
GFP	green fluorescent protein

Gln (Q)	glutamine
Glu (E)	glutamate
Gly (G)	glycine
gp41, gp160	glycoprotein 41, glycoprotein 160 (HIV-1)
GPI	glycophosphatidylinositol
GTPase	guanine triphosphatase
H1	hydrophobic domain 1
H2	hydrophobic domain 2
HA	hemagglutinin
HBV	hepatitis B virus
HCl	hydrochloric acid
HCV	hepatitis C virus
HD	hemifusion diaphragm
HERV	human endogenous retrovirus
His (H)	histidine
HIV-1	human immunodeficiency virus, type 1
HL	hinged loop
HN	hemagglutinin-neuraminidase, paramyxovirus
HP	hydrophobic patch
HSV-1	herpes simplex virus type 1
IEV	intracellular enveloped virus
IgG	immunoglobulin class G
Ile (I)	isoleucine
KCl	potassium chloride
kDa	kilodalton
KH_2PO_4	potassium phosphate
L	large
Leu (L)	leucine
Lys (K)	lysine
M	medium
MAb	monoclonal antibody
MBP	maltose binding protein
MEM	minimal essential medium
Met (M)	methionine
Mr	molecular mass (in Daltons)
MRV	mammalian reovirus
NaCl	sodium chloride
Na_2CO_3	sodium carbonate
Na_2HPO_4	sodium phosphate
NBD	7-nitrobenz-2-oxa-1,3-diazole, 4-yl
NBV	Nelson Bay virus
NDV	Newcastle disease virus
NMR	nuclear magnetic resonance
nt	nucleotide
ORF	open reading frame

OST	oligosaccharyl transferase
PAGE	polyacrylamide gel electrophoresis
PBS	phosphate buffered saline
Phe (F)	phenylalanine
PFU	plaque forming units
PKA	protein kinase A
pka	consensus sequence for phosphorylation by protein kinase A
PPII	polyproline type II (left-handed)
prM	TBEV precursor membrane protein
Pro (P)	proline
PRS	proline-rich sequence
RIPA	radioimmune precipitation assay
RRV	reptilian reovirus
S	small
sAg	surface antigen
SDS	sodium dodecyl sulfate
Ser (S)	serine
SFBR	Southwest Foundation for Biomedical Research
SFV	semliki forest virus
SNARE	soluble N-ethylmaleimide sensitive factor attachment protein receptor
SRP	signal recognition particle
T	thymine
TBEV	tick-borne encephalitis virus
TETQ	too extensive to quantify
Thr (T)	threonine
TM	transmembrane
TRIC	tetramethyl rhodamine isothiocyanate
Trp (W)	tryptophan
t-SNARE	SNARE associated with target membrane
Tyr (Y)	tyrosine
U	uracil
Val (V)	valine
v-SNARE	SNARE associated with vesicle membrane
VSV	vesicular stomatitis virus
VV	vaccinia virus
WHV	woodchuck hepatitis B virus
X	any amino acid

ACKNOWLEDGEMENTS

For the cDNA cloning of the BRV S-class genome segments, and in particular, that of the subcloned S4 ORF1 (p15), which was used to both identify the BRV fusion protein and for the p15 mutagenesis presented in this thesis, I acknowledge the excellent technical expertise of Jingyun (Jing) Shou. I further acknowledge the efforts of Jing, along with David Mader and Jayme Salsman, in producing the polyclonal antisera against full-length p15. I thank Martin St-Maurice for his assistance with the CD spectroscopy. Finally, I offer heartfelt gratitude to Jennifer Corcoran for her forthright guidance in all things relating to the confocal microscope, without which the subcellular localization of p15 might still be in doubt.

I thank Dr. Roy Duncan for allowing me independence in research so early in my career, for his good humour, and for teaching me, in one manner or another, the Duncan motto: "That which does not kill you, makes you stronger." I also thank Roy for offering me the opportunity to follow his example in lectureship, which provided me with my most gratifying graduate-school experience. "Flame on".

I thank Jennifer Corcoran for all the food and caffeine, and so much more. For laughter when times were good, for strength when times were bad. For thoughtful advice and criticism, in the lab and in life. For sharing protocols, papers, reagents, and frustrations. And for the memory of the day we made "the doll". It was an honour and a pleasure to carry out my graduate research along side you. You inspired and challenged me to do my best work, and confirmed that is worthwhile to set my own high standards and achieve my own goals even if no-one else is looking. I will sorely miss your company across from my future lab benches. Rest easy my friend, for apparently I will not be needing your identity after-all.

I thank Jayme Salsman, Deniz Top, Eileen Clancy, and all other members of the Duncan lab who mixed good science with good laughs and made it a joy in recent years to walk into Tupper Room 7-S. You have been true colleagues, realizing us "fusionologists" are stronger together than we are apart. I regret that we could not have worked together sooner and for longer. I sincerely thank Andrea Makkay for her friendship and support throughout my degree, but especially when I needed it most. I thank Christian Hoy, Claire Barber and Julie Boutilier - the privilege of being part of your education taught me much and solidified my ambitions in this career path. It was a pleasure every day to be challenged by your questions. I also thank all those nearby who unfailingly demonstrated ethical conduct in their pursuit of knowledge, and thereby gave me the will to continue when I doubted.

Martin, I thank you for learning more virology than any enzymolgists should ever have to. Thank you for listening. Mostly, I thank you with all my heart for loving and for sheltering – wherever you are is home. I am deeply grateful for your support of me and for your faith in me, which sustained me through the bleakest times during this degree. I am truly lucky to have a partner in my life who understands and shares my goals. And to our beautiful daughter, Danika, you are my joy, my balance and my oasis from the lab. Your giggles evaporate even the worst failed-experiment days. Thank you for brightening my world. I thank my parents for their patience with my maintaining student status up until my thirtieth birthday, and for their generous financial assistance along the way.

I am eternally grateful to Action Front Data Recovery Labs for dodging the "lost-thesis" bullet for me. Finally, I acknowledge the funding provided by the Natural Sciences and Engineering Research Council of Canada, the Nova Scotia Health Research Foundation, and the Killam Trusts.

CHAPTER 1

AN OVERVIEW OF MEMBRANE FUSION

1.1. Membrane fusion is an essential cellular event

Membrane fusion occurs when two separate lipid bilayers merge into a single continuous membrane, concomitant with the mixing of their encapsulated contents. The process of membrane fusion is essential for a variety of fundamental biological events, including fertilization, virus infection, intracellular vesicle transport, exocytosis, and the formation of key multinucleated cells in muscle (myotubes), bone (osteoclasts), blood (macrophage-derived giant cells), and placenta (syncytiotrophoblasts) (Abe *et al.*, 1999; Dworak and Sink, 2002; Jahn *et al.*, 2003; Pecheur *et al.*, 1999; Potgens *et al.*, 2002). For membrane fusion to ensue, bilayers need to be in close contact. However, the repulsion forces due to hydration as well as electrostatic and steric interactions, impede the close approach of membranes and prevent spontaneous bilayer merger (Stegmann *et al.*, 1989). These thermodynamic barriers necessitate that biological membrane fusion is protein-mediated (Stegmann *et al.*, 1989). Diverse fusion proteins, acting individually or as part of a multicomponent complex, mediate the recognition of membranes to be fused, pull the membranes close together, and destabilize the lipid/water interface to initiate mixing of the lipids in order to accomplish membrane fusion (Jahn *et al.*, 2003). Although different fusion reactions share common features, the molecular mechanism(s) by which protein-mediated membrane fusion proceeds remains poorly understood. Characterization of biological membrane fusion pathways is necessary in order to both better comprehend the key cellular processes that rely on membrane fusion, as well as to develop a

knowledge base from which to manipulate certain membrane fusion events, perhaps through the development of novel contraceptives, inhibitors of virus infection, or proteoliposome-based drug delivery vehicles, for example. This thesis will present analysis of an unusual fusion protein encoded by a nonenveloped virus, culminating in the proposal of a novel model of membrane fusion. This model not only describes an atypical fusion event, but also diverges from those models presently available and thus, expands our current appreciation for how biological membrane fusion can occur.

1.2. Biophysical steps involved in membrane fusion

Although biological membranes are maintained in an overall bilayer configuration, they contain lipids that adopt non-bilayer ('non-lamellar') phases in isolation as a consequence of their morphology (Fig. 1.1). The presence of non-lamellar-forming lipids modulates membrane function by affecting the physical properties of membranes, such as fluidity, thickness, charge, curvature, and interfacial polarity (Epand, 1998). The remodeling of the membranes during fusion is necessarily dependent on their lipid composition. Lipids with a propensity to adopt non-lamellar (bilayer-destabilizing) phases facilitate lipid monolayer bending, and are thus important elements at various stages in the fusion process. Under external forces, pure lipid bilayers can be induced to fuse *in vitro* by varying their curvature and degree of contact. In a biological context, membrane fusion requires proteins to provide the 'external' energy to drive the merger of lipid bilayers. Interplay exists between the proteins and lipids composing a biological bilayer such that the propensity of lipids to form non-lamellar phases can modulate the activity of membrane proteins and, likewise, proteins and peptides can influence the

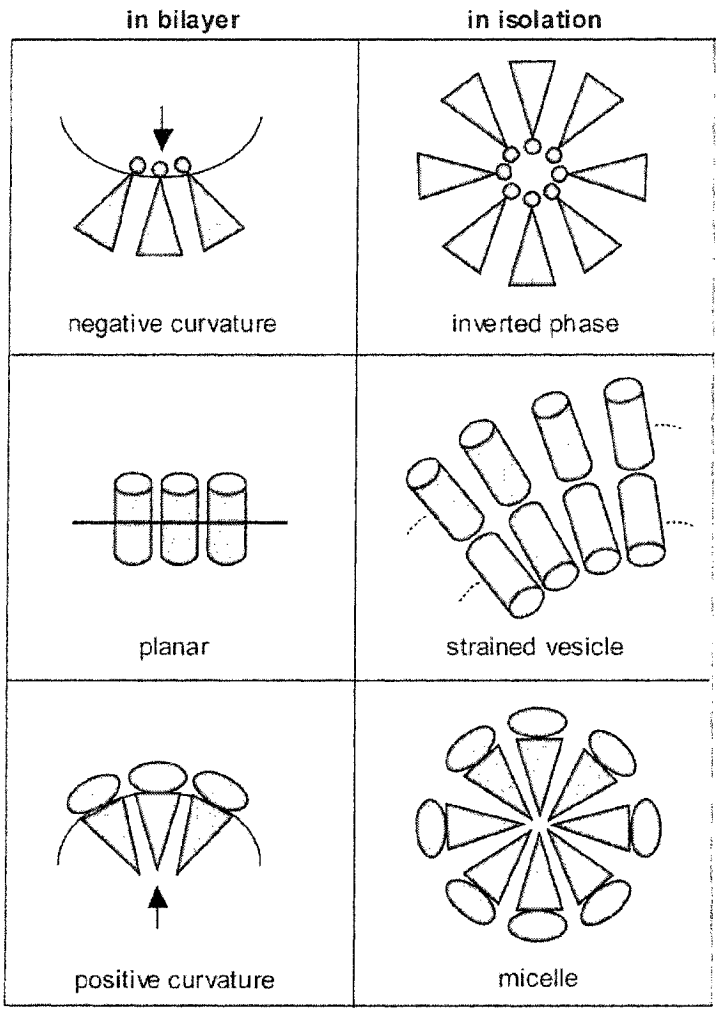

Figure 1.1. **Phospholipid polymorphism.** The left-hand panels represent the bilayer deforming consequences of packing together differently shaped phospholipids; phospholipids with relatively small headgroups promote negative curvature (the surface bends away from the polar headgroups, indicated by arrow), headgroups of size comparable to the cross-section of the acyl chains promote a stable bilayer, phospholpids with a relatively large headgroup promote positive curvature (the surface bends toward the polar headgroups, indicated by arrow). The right-hand panels represent the types of curved lipid phases that the corresponding types of phospholipids can adopt in isolation. Adapted from Epand (1998).

tendency of lipids to form non-lamellar phases (Epand, 1998). Membrane fusion that is mediated by proteins is believed to progress through intermediate lipid arrangements that resemble those occurring during the fusion of protein-free, model membranes, described below and summarized in Figure 1.2 (Chernomordik *et al.*, 1995).

1.2.1. Establishing membrane contact

Contact between membranes is a prerequisite to, but insufficient for, their fusion. Electrostatic repulsion between bilayers together with steric interactions of membrane proteins keeps biological membranes separated by a distance of approximately 10-20 nm (Chernomordik and Kozlov, 2003). Fusion proteins must either pull or push the membranes toward each other and reduce the distance between apposed bilayers to less than a few nanometers (Fig. 1.2A) (Chernomordik and Kozlov, 2003). Alternatively, actin-filled membrane projections (microvilli) that approach cells within 2-3 nm have been implicated as the initiation sites of a variety of cell-cell fusion events (Wilson and Snell, 1998). Further membrane contact requires dehydration of the intervening water layer (Chernomordik and Kozlov, 2003). Strong hydration repulsion prevents large areas of smooth membranes from establishing contact (Chernomordik and Kozlov, 2003). Thus, dehydrated contacts are probably accomplished through small, local points of contact that exhibit a minimal repulsion from the apposing membrane (Fig. 1.2B) (Chernomordik and Kozlov, 2003). The lipid organization of these prefusion, point-like protrusions (semistalks) is predicted to be discontinuous at their tops, with consequent exposure of the hydrophobic interior of the bilayer (Chanturiya *et al.*, 1999). Exposure of the hydrophobic moieties of phospholipids is believed to exert an attractive force between closely apposed membranes, which would facilitate membrane merger (Blumenthal *et al.*,

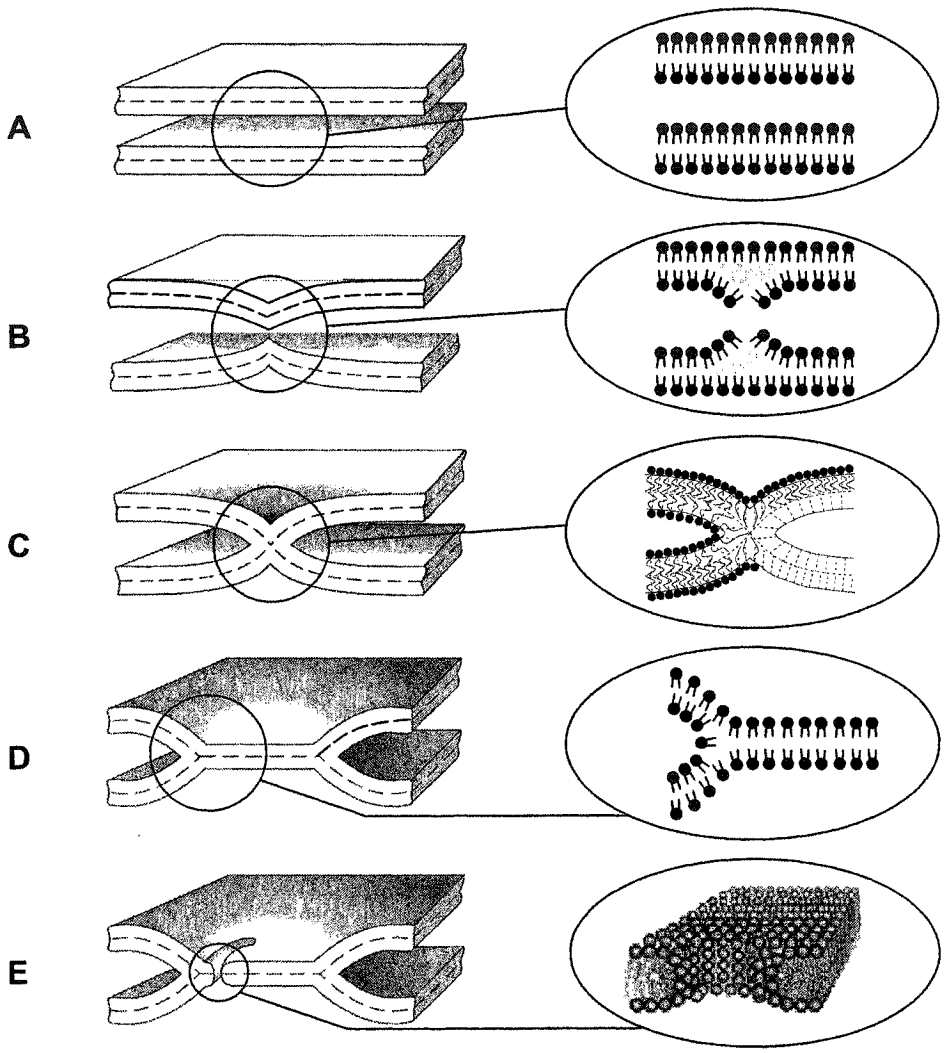

Figure 1.2. **Stages of lipid bilayer fusion.** (A) Establishment of membrane contact within a few nanometres. (B) Pointlike protrusions (semistalks) at the prefusion stage. Note that the hydrophobic interior of both bilayers is exposed to aqueous medium at the tops of both semistalks. (C) Joining of two adjacent semistalks into a fusion stalk; interstices filled by tilted hydrocarbon chains. Note the negative curvature of the contacting monolayers. (D) Radial expansion of the stalk to form the hemifusion diaphragm (HD). (E) Opening of a crack-like fusion pore. Note the positive curvature of the HD leaflets. Ovals at right depict enlarged schematic diagrams of lipid conformations at circled sites. Figure adapted from Chanturiya *et al.* (1999), Chernomordik and Kozlov (2003), and Kozlovsky *et al.* (2002).

2003).

1.2.2. Formation of the fusion stalk

As the ruptured semistalks of approaching monolayers intersect, the first intermediate lipid connection between the two contacting monolayers, the 'fusion stalk', is formed. To avoid energetically unfavorable hydrophobic defects ('interstices') emerging in the middle of the stalk, the hydrocarbon chains of the lipids composing the distal monolayers tilt to fill the void that would otherwise be created once the contacting (*cis*) monolayers bend and connect (Kozlovsky and Kozlov, 2002). As a result, the distal (*trans*) monolayers form sharp corners in front of the stalk center (Fig. 1.2C) (Kozlovsky and Kozlov, 2002). Fusion proteins may facilitate the generation of the fusion stalk by introducing stresses into the bilayer that relax upon, and thereby release the energy needed for, stalk formation (Chernomordik and Kozlov, 2003). Stalk formation is dependent on the lipid composition of the *cis* monolayers. Because the lipid monolayers joined in a stalk are strongly bent (in an inverted direction), formation of the stalk is promoted by lipids of spontaneous negative curvature (i.e. those with head groups more narrow than the cross section of their acyl chains, such as phosphatidylethanolamine) (Kozlovsky *et al.*, 2002, and references therein).

1.2.3. Hemifusion and fusion pore formation

In the favoured stalk-pore hypothesis (Chernomordik *et al.*, 1995; Kozlovsky *et al.*, 2002), the fusion stalk expands radially and brings the distal monolayers together to form a single bilayer referred to as the hemifusion diaphragm (HD; Fig. 1.2D). The edge of the HD is the site where three bilayers (the diaphragm bilayer and the two bilayers of the expanding stalk) join. Expansion of the stalk to form the circular HD requires an

external force (such as the concerted action of multiple fusion proteins) pulling on the diaphragm rim (Kozlovsky *et al.*, 2002). The elastic stresses of lipid tilt and bending in the narrow region along the HD rim are predicted to generate significant lateral tension which may lead to the rupture of the HD and the formation of a crack-like fusion pore expanding along the diaphragm rim (Fig. 1.2E) (Kozlovsky *et al.*, 2002). The probability of fusion pore formation increases as the area of the stressed membrane becomes larger (Kozlovsky *et al.*, 2002). Thus, by pulling on the HD rim, fusion proteins may increase the chance of fusion pore nucleation (Chernomordik and Kozlov, 2003). In contrast to stalk formation and hemifusion, the opening of the fusion pore is dependent on the lipid composition of the *trans* monolayers, and is promoted by lipids of spontaneous positive curvature (i.e. those with head groups wider than their acyl chain(s), such as lysophosphatidylcholine) (Chernomordik and Kozlov, 2003).

1.3. Membrane fusion upon enveloped virus entry

Much of our understanding of protein-mediated membrane fusion has derived from studies of enveloped virus fusion proteins. The enveloped virus fusion proteins are essential structural proteins that enable the virus to enter host cells by inducing fusion of the virus envelope with cell membranes. Typically, a single viral protein accomplishes all the steps required to destabilize and merge two apposed bilayers. Almost all enveloped virus fusion proteins characterized thus far are divided into two classes (Lescar *et al.*, 2001). Class I fusion proteins project out from the viral envelope as spikes, and are encoded by orthomyxoviruses, retroviruses, paramyxoviruses, and filoviruses. Class II fusion proteins lie parallel to the viral envelope, and are encoded by flaviviruses and

alphaviruses. The differences between both of these classes will be discussed in detail below, but, despite their diversity, the fusion proteins of disparate enveloped viruses share common features: they are oligomeric, type I (N_{exo}/C_{cyt}) integral membrane glycoproteins with an externalized hydrophobic fusion peptide (approximately 15-20 amino acids modeled as an asymmetric, amphipathic alpha-helix) that is capable of inserting into membranes in the fusion-activated form of the proteins (Hughson, 1997; White, 1992). Structure-function analysis of several enveloped virus fusion proteins, most notably those of influenza virus and HIV, suggests that the fusion reaction is initiated by a triggered conformational change in a metastable protein that exposes a previously concealed fusion peptide for insertion into, and destabilization of, the target lipid bilayer (Colman and Lawrence, 2003; Hughson, 1997; White, 1992). Further conformational changes involving the reorganization of extended coiled-coil regions (class I) or the reorganization of multimer associations (class II) pull the donor and target bilayers together (Stiasny *et al.*, 2001; Weissenhorn *et al.*, 1999; White, 1992). The ectodomains of these fusion proteins appear sufficient to accomplish hemifusion. The transmembrane (TM) domain and membrane-proximal sequences have been proposed to have a role in destabilization of the donor membrane allowing the fusion reaction to proceed (discussed further in chapter 6) (Melikyan *et al.*, 1995; Peisajovich and Shai, 2003).

This chapter will give an overview of the well characterized class I viral fusion proteins and the leading models (spring-loaded, bending defect, and hydrophobic defect) of protein-mediated membrane fusion that have resulted from their study. The class II and various unclassified viral fusion proteins will be summarized, along with several

examples of intra- and intercellular fusion machines in order to illustrate the diversity evident in biological fusion systems and, thus, to highlight the need for novel models of membrane fusion derived from analysis of fusion proteins other than those encoded by enveloped viruses.

1.3.1. Class I viral fusion proteins and the spring-loaded model of membrane fusion

Influenza HA

The extensively studied influenza hemagglutinin (HA) protein has long been considered the paradigm for protein-mediated membrane fusion. HA is the prototype of the class I viral fusion proteins. The structural organization of HA and the up-to-date, widely accepted "spring-loaded" model of HA-mediated membrane fusion is detailed as follows.

HA is organized as a trimeric spike protein protruding away from the viral surface, anchored in the viral envelope by a single C-terminal TM anchor (Fig. 1.3A). HA is synthesized as an inactive precursor (HA_0) that is proteolytically cleaved into two subunits (HA_1 and HA_2) linked by a single disulfide bond. Cleavage of HA_0 primes HA for subsequent activation of membrane fusion at endosomal pH (Carr *et al.*, 1997). The receptor-binding HA_1 subunit, located distal to the viral envelope, serves as a clamp holding the fusogenic HA_2 subunit in a high-energy, metastable conformation (Carr *et al.*, 1997; Madhusoodanan and Lazaridis, 2003; Skehel and Wiley, 2000). The hypothetical energy released upon the acid-triggered refolding of HA_2 from the high-energy to the lowest-energy form is proposed to be the driving force for membrane fusion (Carr *et al.*, 1997).

Fig. 1.3. **Spring-loaded model for HA-mediated membrane fusion.** (A) Cartoon representation of the entire HA molecule at neutral pH, showing the clamp of HA_1 subunits (grey ovals) holding the primed HA_2 subunits in a metastable, fusion-inactive conformation. (B) Ribbon diagram illustrating the monomeric ectodomain of HA in the neutral-pH- and low pH-induced conformations; details of the transition are given in C. Structural domains are: HA_1 (cyan); central coiled coil (yellow-green-blue); flexible loop/helix (orange); helix-to-loop transition (green) accompanies extension of C-terminal residues (purple). The discontinuous lines indicate parts of the structures that are unknown. (C) To follow the low pH-induced conformational changes in trimeric HA_2, HA_1 is omitted for clarity. (i) In the compact neutral pH form, HA_2 contains a long central triple-stranded coiled coil (orange-purple-yellow), surrounded by an antiparallel layer of three, N-proximal, shorter α-helices (lime) that are connected to the central helices by an extended flexible loop (blue). (ii) At low pH the flexible loop (blue) and short helix (lime) become an extension of the central triple-stranded coiled coil, relocating the fusion peptide (red) from its previously buried position toward the target membrane. (iii) The exposed fusion peptide shallowly inserts into and destabilizes the target membrane. (iv) Multiple HA trimers function in a coordinated manner to effect membrane fusion. Aggregates are either preformed or form rapidly following acidification. (v) The hydrophobic kink region (purple) refolds from a helix to a loop, and the downstream helix (orange) reverses direction to lie antiparallel to the coiled coil. The extended C-termini of HA_2 (green) bind in the grooves between adjacent helices of the coiled coil, causing the trimer to tilt. (vi) The resulting tension pulls the two membranes together and drives their merger. (vii) The fusion peptides and TM domains are brought together, breaking the hemifusion diaphragm. The overall effect of these conformational changes is apparently to deliver the fusion peptide toward the target membrane and to bend the molecule in half so that the fusion peptide and the viral membrane anchor are near the same end of the rod-shaped molecule. Figures (A, B) by Skehel and Wiley are reprinted, with permission, from *Annual Review of Biochemistry*, Volume 69 © 2000 by Annual Reviews www.annualreviews.org. Figure (C) by Gruenke *et al.* (2002) is reprinted, with permission. Copyright © 2002, the American Society for Microbiology. All rights reserved.

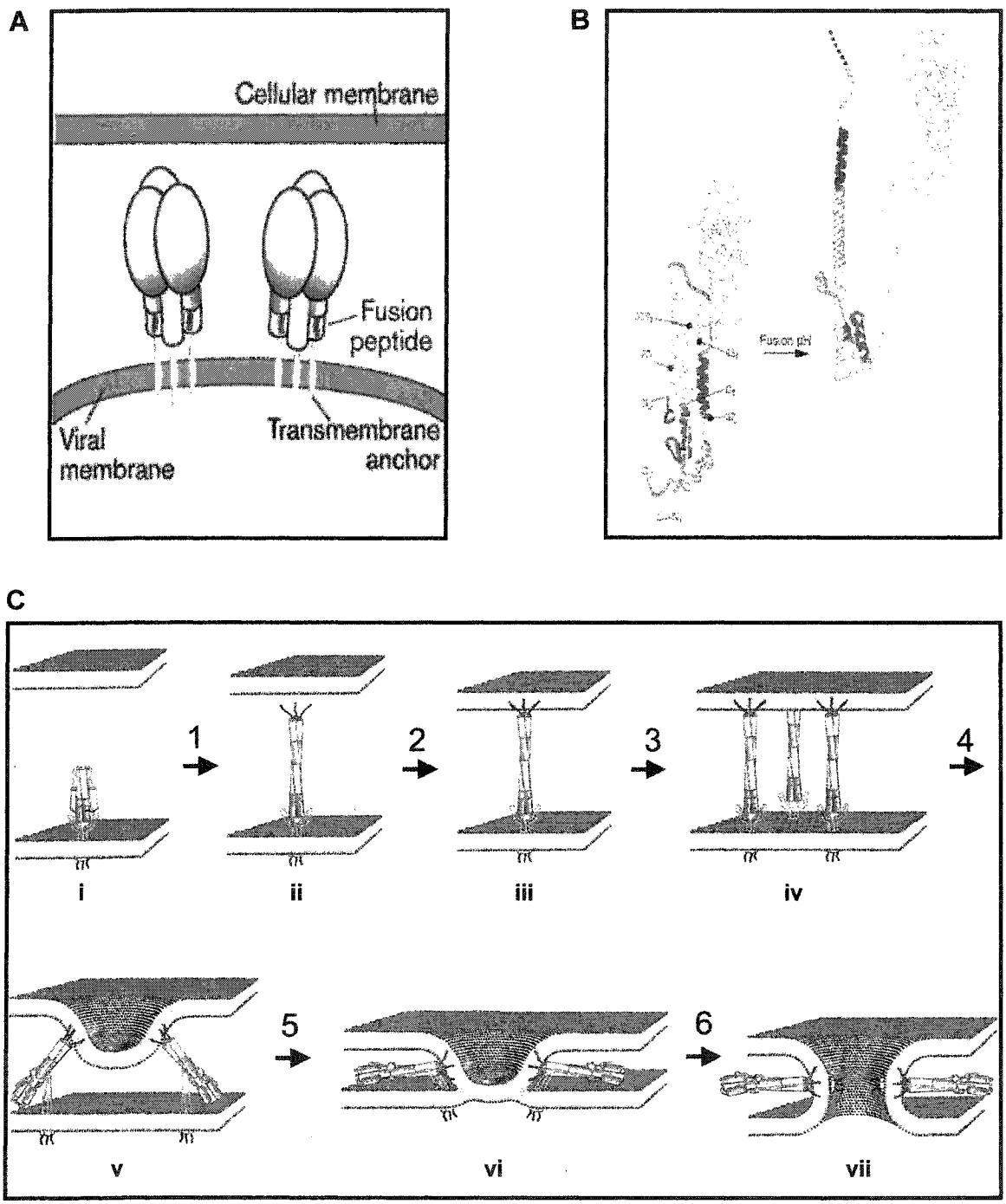
A
Cellular membrane
Fusion peptide
Viral membrane
Transmembrane anchor
B
C
1
2
3
4
5
6
i
ii
iii
iv
v
vi
vii

Figure 1.3.

At neutral pH, the HA ectodomain is stabilized by electrostatic interactions between HA_1 and HA_2. Once bound to a target cell, influenza is internalized by receptor-mediated endocytosis, where the acidic pH triggers the conformational changes in HA which activate the protein for fusion (Carr *et al.*, 1997). Enhanced protonation of the positively-charged HA_1 domain at low pH increases the electrostatic repulsion between the HA_1 subunits (Huang *et al.*, 2003). Partial dissociation of the HA_1 trimeric domain gives rise to a sideward relocation of the HA_1 subunits, apparently enabling the subsequent conformational changes of HA into a fusogenic state by the spring-loaded mechanism (Huang *et al.*, 2003). Using molecular dynamics simulations, it has been calculated that complete dissociation of the HA_1 domain is not necessary for the spring-loaded conformational change (extension of the coiled coil and exposure of the fusion peptide), but that the model with complete dissociation has lower energy (Madhusoodanan and Lazaridis, 2003).

The HA_2 ectodomain contains two regions with a 4-3 hydrophobic (heptad) repeat sequence, which is a feature characteristic of segments that form α-helical coiled coils. As shown schematically in Figure 1.3Ci, at neutral pH the trimeric HA_2 subunit is folded into a long, central, triple-stranded coiled coil, surrounded by a second layer of three, N-proximal, shorter α-helices (Wiley and Skehel, 1987). The short helices are oriented antiparallel to the central helices and are connected to them by a flexible loop (Wiley and Skehel, 1987). The N-terminus of HA_2 contains the hydrophobic fusion peptide, which is buried in a charged pocket between helices at the interface between the two HA subunits, approximately 3.5 nm away from the viral membrane and 10 nm away from the target membrane (Wiley and Skehel, 1987). At low pH, partial dissociation of the HA_1 subunits

opens a central cavity in the HA ectodomain allowing water to enter the HA interior and interact with the loop region of HA_2 that connects the short and long α-helices (Huang *et al.*, 2003). Interaction with water triggers the loop region to adopt a helical conformation, thereby releasing the "spring" and inducing the first major refolding event. As diagrammed in Figure 1.3Cii, the loop-to-helix transformation accompanies the formation of the extended coiled-coil structure of HA_2 (the central, triple-stranded coiled coil found in native HA_2 becomes N-terminally extended by an additional 38 residues) which reorients the previously buried fusion peptide to the distal tip of the HA ectodomain (a relocation of ~ 10 nm) (Skehel and Wiley, 2000). The exposed fusion peptide is then able to insert into, and destabilize, the target membrane (Fig. 1.3Ciii). Alternatively, the fusion peptide may embed into the viral membrane. Models in which this latter conformation mediates membrane fusion are discussed below (section 1.4). As formation of the HA_2 extended coiled-coil structure prevents re-association of the HA_1 head domains, it is considered to be the fusion-committed state, and HA_2 is the only subunit required for further steps in the fusion reaction (Schoch *et al.*, 1991).

The HA fusion peptide is a moderately hydrophobic, 20-amino acid (aa) sequence that is enriched in glycine and alanine residues. These small amino acids endow the fusion peptide with a degree of conformation flexibility that appears to be important for its activity (Tamm, 2003). Typical of fusion peptides, this sequence can be modeled as an amphipathic α-helix, with the hydrophobic residues aligning on one face and the polar residues on the other. Structurally, the HA_2 fusion peptide is oriented in a membrane environment in a kinked 'V'-shaped configuration. The N-terminal arm of the 'V' is characterized by a well-defined α-helix, while the C-terminal arm is disordered at neutral

pH, but forms a short 3_{10}-helix at pH 5 (Tamm, 2003). Acid-induced refolding sequesters all of the bulky apolar residues into the hydrophobic pocket in the cavity of the 'V' and confers an amphipathic character to the fusion peptide (Tamm, 2003). Conserved glutamate residues in the fusion peptide reportedly have unusually high pK_a values (Dubovski *et al.*, 2000) on account of neighbouring hydrophobic amino acids (Bentz and Mittal, 2003). The protonation of these residues at low pH may facilitate deeper insertion of the fusion peptide into the interior of the target bilayer by rendering the outer surface of the 'V' less polar (Tamm, 2003). Nearly a decade ago, Epand *et al.* (1995) determined that the arrangement of positively-charged residues in the polar face of amphipahtic helices controls their effects on membrane stability in a manner analogous to the effect of the molecular shape of phospholipids on bilayers, described above in section 1.2 (Epand *et al.*, 1995). The shape of the amphipathic HA fusion peptide, with a narrow polar face at its apex and a broader nonpolar face at its base, is characteristic of lytic peptides (e.g. melittin) and other fusion peptides that destabilize membranes by inducing negative curvature strain in the outer monolayer (Pecheur *et al.*, 1999). Conformational studies using attenuated total reflection Fourier transform infrared (ATR-FTIR) spectroscopy revealed the fusogenicity of the HA fusion peptide depended on its insertion into the membrane at an oblique angle, and may also correlate with fusion peptide oligomerization (reviewed by Pécheur *et al.*, 1999). While the monomeric form of the HA fusion peptide is α-helical, extended β-conformations appear to mediate its self-association (Nieva and Agirre, 2003, and references therein).

In the extended coiled-coil state, HA_2 bridges the donor and target membranes (anchored in the viral membrane by its TM domain and the target membrane by its fusion

peptide), but further conformational changes are necessary to pull the two bilayers together and accomplish their merger. The extended coiled-coil conformation of HA_2 is an extremely transient intermediate that immediately folds back upon itself (Fig. 1.3Cv). During the refolding of HA_2, the C-terminal end of the original coiled coil undergoes significant rearrangement. A short region unfolds to a loop ('helix-turn' transition), and forms a tight reverse turn, also referred to as the 'hydrophobic kink' (Skehel and Wiley, 2000). The remaining helix that is C-terminal to the hydrophobic kink reverses direction and packs antiparallel against the grooved surfaces of the N-terminal helices, covering the hydrophobic pocket evacuated by the fusion peptide, and forming a stable six-helix bundle (Skehel and Wiley, 2000). The spring-loaded hypothesis proposes that these conformational changes serve to pull the extended HA_2 into a hairpin, bringing the two apposed membranes into contact (Skehel and Wiley, 2000). During refolding, residues downstream of the helix bundle are extruded from their compact association in native HA_2, become extended, and pack within the groove between adjacent helices of the coiled coil (Skehel and Wiley, 2000). Recently, it has been proposed that tension created by binding the C-terminal extended regions into these grooves causes the HA trimer to tilt (Fig. 1.3Cv) and, thus, drives fusion (Gruenke *et al.*, 2002). Tilting of the ~10-15 nm tall HA bundle towards the plane of the bilayer is necessary to achieve close membrane approximation and, as shown in Figure 1.3Cvi, utilizes hinges at the base of both the TM anchor and the fusion peptide (Tamm, 2003).

As the fusing membranes are brought together, the fusion peptide and TM anchor of HA are brought into close proximity (Chen *et al.*, 1999). A direct interaction between the fusion peptide and the TM anchor (Fig. 1.3Cvii), mediated through the conserved

glycine ridge on the upper face of the N-terminal arm of the fusion peptide, is proposed to be involved in the opening of the fusion pore (Tamm, 2003). The final six-helix bundle conformation of HA appears to be stabilized by residues that cap the N-terminal helix ('N-cap' structure) and make extensive contacts with C-terminal residues, thus fixing the N- and C-terminal regions of the bundle together (Chen *et al.*, 1999). The N-cap terminates the triple-stranded coiled coil so that the upstream polypeptide linking the trimeric rod to the membrane-embedded fusion peptide is flexible (Chen *et al.*, 1999). Likewise, the residues C-terminal to the trimeric coiled coil are in an extended (approximately polyproline type II) conformation, and thus serve as a flexible link to the viral membrane and may facilitate the HA conformational changes (Chen *et al.*, 1999).

Although relatively little is known about precisely how close membrane apposition leads to complete fusion, the assembly of higher order HA oligomers is known to be required to form fusion pores. Bentz *et al.* (2003) recently calculated that a minimum of eight HA trimers functioning together at the fusion site are necessary to accomplish membrane merger. However, only two of the eight need undergo the extended coiled-coil conformational change to initiate fusion pore formation (Bentz and Mittal, 2003). Other HA molecules within the aggregate are receptor-bound, and appear not to carry out fusion (Bentz and Mittal, 2003). The neutral pH structure of HA is widely considered to be a high-energy intermediate because it can be induced to unfold to the stable six-helix bundle structure by treatment with low pH, high temperature, or a chemical denaturant (Carr *et al.*, 1997). The energy released upon structural transition from the neutral- to the low pH-form is believed to drive membrane fusion. Analogous spring-loaded models of membrane fusion driven by triggered conformational changes in

a metastable structure have been proposed for several other enveloped virus fusion proteins, of which two are briefly discussed below.

Human immunodeficiency virus Env

The structural organization of the human immunodeficiency virus (HIV) envelope (Env, or gp160) protein is comparable to that described above for influenza HA. The precursor Env is processed into two noncovalently associated subunits - the receptor-binding gp120 and the fusogenic gp41. Unlike influenza however, HIV fuses directly with the plasma membrane of host cells. Thus, the trigger for Env fusogenic activation is not low pH, but rather is a complex set of receptor- and co-receptor-interactions (reviewed by Gallo *et al.*, 2003). The ensuing set of sequential conformational changes in Env include the formation of an extended coiled-coil intermediate and the ultimate adoption of a gp41 stable six-helix bundle. As with HA_2, the transition to this bundle and not just its presence, is believed to provide the energy to drive membrane fusion (Melikyan *et al.*, 2000a). Multiple Env trimers acting cooperatively are believed to be necessary to accomplish the fusion process (Gallo *et al.*, 2003). Similar to that of HA_2, the gp41 N-proximal fusion peptide appears conformationally flexible, exhibiting both α-helix- and β-structure-forming propensities in different environments (Gallo *et al.*, 2003). Recent structure-function analyses indicate that the oligomeric β-sheet conformation, occurring at high concentrations in a membrane environment, is the functional form of the gp41 fusion peptide (Sackett and Shai, 2003; Yang *et al.*, 2003).

Newcastle disease virus F

Membrane fusion induced by paramyxoviruses, such as Newcastle disease virus (NDV), is less well characterized but occurs at the plasma membrane independent of pH.

The fusion protein (F) is synthesized as a precursor, F_0, which is subsequently cleaved into disulfide-linked F_1 and F_2 subunits. Unlike the fusion proteins of either influenza or HIV, however, NDV F requires the co-expression of a separate receptor-binding protein, hemagglutinin-neuraminidase (HN), to accomplish membrane fusion (Morrison, 2003). HN is believed to hold F in a high-energy, metastable state prior to fusion. Conformational changes in HN upon cell attachment are apparently translated into fusion-activating alterations in F. Interestingly, although the influence of HN on the conformation of F is required for membrane fusion, the act of receptor-binding by HN is not (Morrison, 2003). While differences are apparent in the crystal structures of the NDV F ectodomain compared to that of influenza HA, the same theme of a large, trimeric glycoprotein containing significant coiled-coil arrangement and a buried N-terminal fusion peptide prevails. In some paramyxoviruses, a second, internal fusion peptide has been identified that corresponds approximately to the hydrophobic kink region of HA_2 (Morrison, 2003; Peisajovich *et al.*, 2000).

While the fusion proteins of orthomyxoviruses, retroviruses, paramyxoviruses, and filoviruses have been identified as belonging to class I (Blumenthal *et al.*, 2003), less well-characterized fusion proteins of several other virus families display features that predict they too belong to class I. These include the coronavirus spike protein (Bosch *et al.*, 2003) and the baculovirus GP64 (Monsma and Blissard, 1995), as well as the arenavirus glycoprotein, unusual in that it forms tetrameric spikes on the viral envelope (Gallaher *et al.*, 2001). All of the class I fusion proteins are synthesized as precursors requiring proteolytic cleavage for activation, contain N-terminal or N-proximal fusion peptides, and form a coiled-coil postfusion bundle. The fusion proteins of other

enveloped viruses, namely flaviviruses and alphaviruses, are significantly different (as discussed below) and comprise the class II.

1.3.2. Class II viral fusion proteins

Tick-borne encephalitis virus E

As illustrated schematically in Figure 1.4, the structure of the envelope glycoprotein (E) from the flavivirus, tick-borne encephalitis virus (TBEV), is fundamentally different from that of class I fusion proteins such as influenza HA (Rey *et al.*, 1995). Rather than forming a trimeric spike-like projection, at neutral pH the E protein is a head-to-tail dimer oriented parallel to the viral membrane and is thus anchored at its distal ends (Rey *et al.*, 1995). Rather than containing an N-terminal or N-proximal fusion peptide, the fusion peptide of E is comprised of an internal sequence that forms a disulfide- stabilized loop located at the distal tip (furthest away from the TM anchor) of each subunit in the folded dimer (Allison *et al.*, 2001; Rey *et al.*, 1995). The E protein of TBEV is further distinct from class I fusion proteins in that it is composed primarily of β-sheet structure and is not predicted to form coiled coils (Allison *et al.*, 2001). Also, TBEV E is not proteolytically cleaved during maturation, although it is associated with an accessory protein whose cleavage is required for the fusogenic activation of E (Allison *et al.*, 2001). Newly synthesized E proteins associate in heterodimeric complexes with the precursor membrane protein (prM). The interaction with prM is necessary for the proper transport and folding of E, and the ultimate proteolytic cleavage of prM activates the fusogenic potential of E (Allison *et al.*, 1999). Closely packed E homodimers assemble an icosahedral lattice in the mature viral

Figure 1.4. **The E protein of TBEV.** (A) Schematic diagram of a TBEV protein E monomer (not to scale) which, in the native structure, forms a homodimer with a head-to-tail orientation. The three domains (I, II, III) are represented by shaded ovals, and the positions of the fusion peptide at the tip of domain II is indicated. The part below the trypsin cleavage site represents the C-terminal 20% of the E protein, for which the structure is unknown. $H1^{pred}$ and $H2^{pred}$ indicate predicted α-helical regions in the stem, a conserved sequence (CS) element separates these putative helices, and TM1 and TM2 are predicted transmembrane segments. TM2, which normally serves as the signal sequence for nonstructural protein NS1, is depicted as traversing the membrane but it is not known whether it actually remains in the membrane after the cleavage event that separates the E and NS1 proteins during processing of the viral polyprotein. (B) Ribbon diagram of the ectodomain of the TBEV E protein dimer viewed from the top (perpendicular to the virion surface), with the individual subunits colored red and blue. The C-terminal portion of the protein extends downward from domain III at each end of the dimer to anchor the protein in the viral membrane. Domains I, II, and III are labeled, and the fusion peptide at the tip of domain II is colored yellow. (C) Schematic representation of a threefold assembly of E dimers as determined by cryoelectron microscopy. Domains I, II and III are indicated and filled yellow circles represent the fusion peptide. Upon exposure to low pH, the (red and blue) dimers dissociate, transiently exposing the fusion peptide. Then monomers assemble into (red or blue) trimers. Figures (A) and (B, C) by Allison *et al.* (1999, 2001, respectively) are reprinted with permission. Copyright © 1999, 2001, the American Society for Microbiology. All rights reserved.

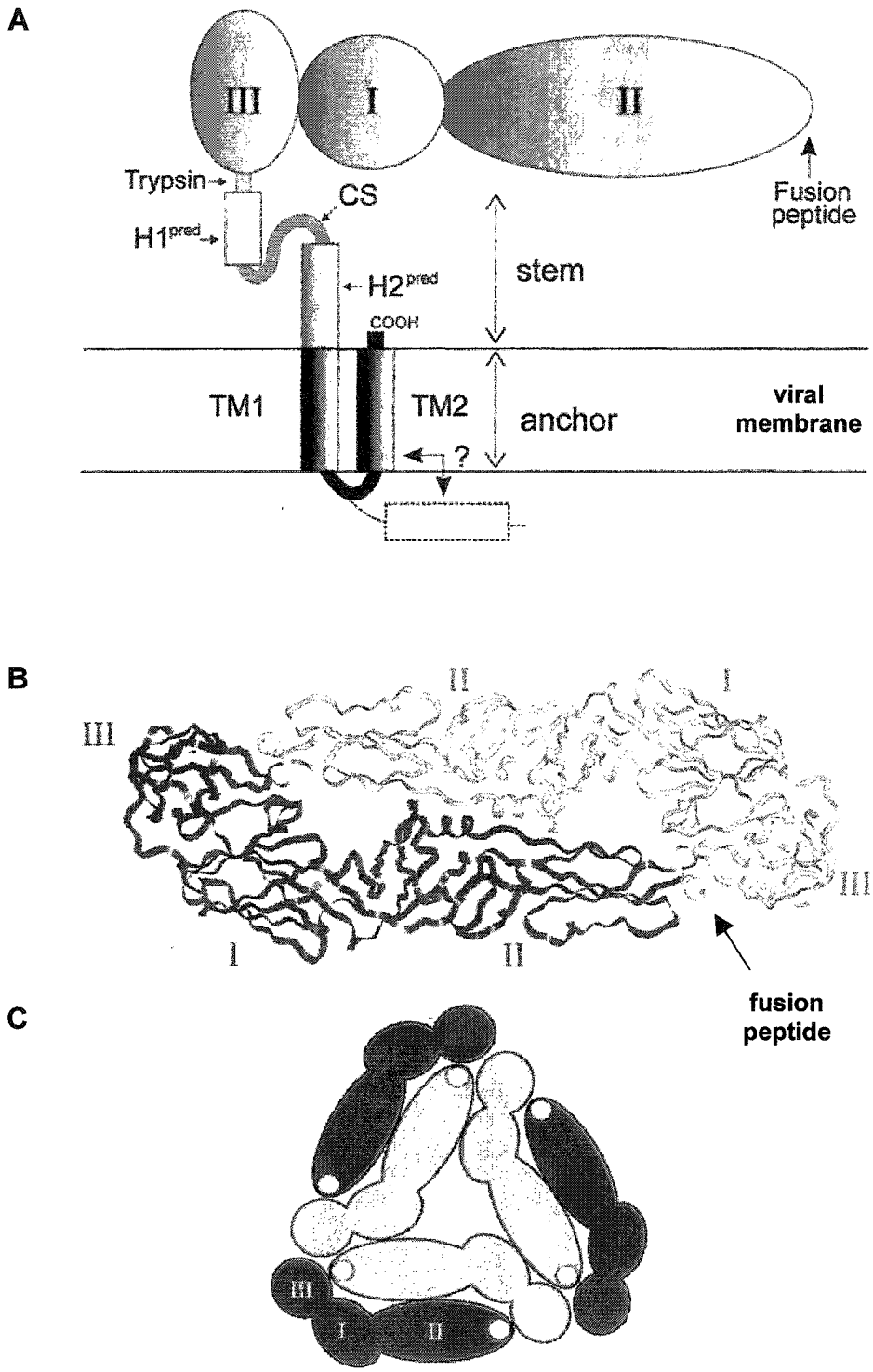
A
III
I
II
Trypsin
CS
Fusion peptide
H1pred
H2pred
stem
COOH
TM1
TM2
anchor
viral membrane
?
B
II
I
III
III
I
II
fusion peptide
C
III
I
II

Figure 1.4.

envelope, in which specific lateral interactions exist between neighboring E dimers (Allison *et al.*, 2001; Allison *et al.*, 1999). Exposure to acidic pH upon receptor-mediated endocytosis triggers the reversible dissociation of the E dimers, followed by the irreversible step of E trimerization (Allison *et al.*, 1999). Low pH induces a conformational change in E that weakens the dimer interactions occurring within the E ectodomain and, consequently, transiently exposes the fusion peptides that were each previously buried in a hydrophobic pocket formed within the partner subunit (Allison *et al.*, 2001). Subsequent formation of the E trimer is mediated by interactions between short α-helices contained within the stem-anchor regions of adjacent E subunits (Allison *et al.*, 1999; Stiasny *et al.*, 1996). The trimeric form of E is more stable than the native dimeric form (Stiasny *et al.*, 2001). Thus, like the class I fusion proteins, the native E protein of TBEV is proposed to represent a kinetically-trapped metastable state that is energetically poised to be converted to the fusogenic form upon exposure to the appropriate trigger (Stiasny *et al.*, 2001).

Semliki Forest virus E1

Although there is no apparent sequence homology between the flavivirus and alphavirus fusion proteins, they exhibit a very similar structural and domain organization and likely evolved from a common progenitor (Lescar *et al.*, 2001). However, significant differences do exist between the fusion proteins of these two virus families. While the TBEV E protein accomplishes both receptor binding and membrane fusion, separate proteins perform these functions in alphavirus Semiliki Forest virus (SFV). The SFV E2 spike protein interacts with cellular receptors, while E1 (the TBEV E homolgoue) promotes membrane fusion. Analogous to the TBEV prM-E association, newly

synthesized E1 interacts with the P62 precursor glycoprotein as a heterodimer (Ferlenghi *et al.*, 1998). Late proteolytic cleavage of P62 into the E2 spike and peripherally-associated E3 protein, primes E1 for membrane fusion (Ferlenghi *et al.*, 1998). On the virion surface, the E1-E2 complex is organized as a trimer of heterodimers, with the E2 trimeric spikes in the center surrounded by obliquely-oriented E1 subunits (Hammar *et al.*, 2003). At low pH the E1-E2 heterodimer separates, unmasking the previously buried fusion peptide (Ferlenghi *et al.*, 1998). E1 swivels around E2 to facilitate E1 trimer interactions (Hammar *et al.*, 2003). There is also a reciprocal relocation of E1 and E2 domains such that the E1 subunits tilt into spike-like projections (Haag *et al.*, 2002). From this vertical orientation, the fusion peptide inserts into the target membrane (Gibbons *et al.*, 2003). Membrane-insertion of the SFV fusion peptide seems to be a cooperative event involving five to six E1 homotrimers (Gibbons *et al.*, 2003).

Both TBEV E and SFV E1 appear to convert from a metastable native conformation to a low energy homotrimer that is essential for the fusion process (Hammar *et al.*, 2003; Kielian, 2002; Stiasny *et al.*, 2001). However, it remains unclear how either the flavivirus or alphavirus fusion proteins accomplish membrane merger beyond the step of fusion peptide exposure and target membrane binding. It has been proposed that a flexible hinge region in the E and E1 ectodomains may mediate a snap-back mechanism bringing the fusion peptide and TM anchor into close proximity, analogous to the hairpin conformation of the post-fusion structures of the class I fusion proteins (Ferlenghi *et al.*, 2001; Lescar *et al.*, 2001). Other flaviviruses have recently been shown to encode class II fusion proteins (Garry and Dash, 2003; Kuhn *et al.*, 2002). Of these, the E1 protein of Hepatitis C virus (HCV) represents a significantly truncated

version of TBEV E lacking the sequence between the TM anchor and the hinge region (Garry and Dash, 2003). Thus, if a fold-back mechanism is involved in action of class II fusion proteins, such rearrangements must not be necessary, at least in the case of HCV E1 (Garry and Dash, 2003).

1.3.3. Non-classified enveloped virus fusion proteins

The fusion proteins of several enveloped viruses, although less well characterized, are clearly distinct from either the class I or class II fusion proteins and, thus, remain unclassified. These examples, discussed below, are important to the field of membrane fusion as they add to the growing realization that there exists a previously unrecognized diversity of pathways to accomplish this essential biological process.

Vesicular Stomatitis Virus G

Vesicular stomatitis virus (VSV), the prototype member of the *Rhabdoviridae*, encodes a single viral glycoprotein (G) that functions as the virus attachment and fusion protein. Although G is a homotrimeric, spike glycoprotein that undergoes low pH-induced conformational changes that promote membrane fusion, significant differences between VSV G and the class I fusion proteins prevent G from joining that classification. Unlike the class I fusion proteins, G does not require proteolytic processing to become fusion competent and, thus, does not appear to be held in a fusion-primed, but inactive, metastable state (Jeetendra *et al.*, 2002). The G protein is not predicted to contain any significant region of α-helical coiled coil, and the conformational changes it undergoes in response to low pH are reversible (Gaudin, 2000b; Yao *et al.*, 2003). This suggests that there is not a large amount of energy released upon conversion from the pre-fusion to the post-fusion forms of G. Furthermore, in contrast to the fusion peptides of class I fusion

proteins, the fusion peptide of G is located internally, is not particularly hydrophobic, and reversibly associates with membranes (Durrer *et al.*, 1995; Fredericksen and Whitt, 1995; Pak *et al.*, 1997). The fusogenicity of G likely depends on the formation of a large complex of G proteins at the fusion site (Yao *et al.*, 2003, and references therein).

Vaccinia virus A27L

An understanding of the entry of vaccinia virus (VV), a member of the *Poxviridae*, into host cells is complicated by the existence of two infectious forms that use different entry pathways (Vanderplasschen *et al.*, 1998). The intracellular mature virus (IMV) form (the most abundant infectious form) contains a single envelope derived from an intermediate compartment between the endoplasmic reticulum and the Golgi apparatus, and enters cells by fusing directly with the plasma membrane. The extracellular enveloped virus (EEV) form contains an additional membrane derived from the *trans*-Golgi cisternae, and enters cells by endocytosis. The 14-kDa protein (A27L) present on the surface of IMV is proposed to function as the fusion protein during both entry pathways, functioning at neutral pH during IMV entry and at acidic pH during EEV entry following disruption of the EEV outer membrane (Vazquez and Esteban, 1999). Evidence implicating A27L as the VV fusion proteins comes from analysis of A27L mutations that eliminate fusion, the observation that insertion of A27L into the genome of nonfusogenic mutant viruses confers fusogenic activity to those viruses, and that monoclonal antibodies specific for A27L block virus-induced syncytium (multinucleated cell) formation (Gong *et al.*, 1990). The 110-aa A27L protein is distinct among viral fusion proteins in that it lacks a TM domain and is instead anchored in the IMV envelope through the interaction of its C-terminal domain with another protein, A17L (Vazquez *et*

al., 1998). The N-terminus of A27L (generated upon signal peptide cleavage) comprises a basic peptide that influences the fusogenic activity of A27L through interaction with heparan sulfate on the surface of target cells (Hsiao *et al.*, 1998). Despite its small size, the trimeric A27L protein is predicted to share similar characteristics with the class I fusion proteins, including a central coiled-coil domain and an N-proximal, α-helical fusion peptide (Vazquez and Esteban, 1999). However, the predicted coiled-coil domain is much shorter than that of the class I fusion proteins, and the proposed fusion peptide does not resemble the hydrophobic, glycine-alanine-rich fusion peptides of class I fusion proteins but rather, contains predominantly charged residues (Vazquez and Esteban, 1999). It is not clear how A27L might function to promote membrane merger but, considering its small size and lack of extended coiled-coil domain, it is unlikely to conform to the class I paradigm.

Hepadnavirus L

The envelopes of various hepadnaviruses consist of multiple versions of the surface antigen (sAg) all expressed from a single open reading frame and sharing a common C-terminal sequence. The common C-terminus comprises the small sAg (S) and contains multiple (probably four) TM domains. Alternate forms of the sAg contain N-terminal extension(s), referred to as the preS domain. The large sAg (L) of both the human and duck hepatitis B viruses (HBV and DHBV, respectively) assumes one of two topologies that differ in the location of the preS domain (Lambert and Prange, 2001; Swameye and Schaller, 1997). When the preS domain is sequestered cytoplasmically, it serves a matrix function mediating interaction with the viral nucelocapsid. In the alternate topology, when the preS domain is translocated across the membrane and exposed on the

viral surface, it mediates cell attachment. Hepadnavirus entry occurs through receptor-mediated endocytosis. Exposure to low pH induces a conformational change in the DHBV L protein resulting in increased hydrophobicity of the virus surface (Cooper *et al.*, 2003). Based on sequence similarity to the fusion peptides of several class I fusion proteins, Rodriguez-Crespo *et al.* (1999) identified a putative fusion peptide at the N-terminus of the S protein of HBV, DHBV, and woodchuck HBV (WHV) which was capable of inducing liposome aggregation, lipid mixing, and leakage from vesicles *in vitro*. Typical of fusion peptides, these hydrophobic stretches at the N-terminus of S are flexible, adopting different conformations in different environments but, as with gp41, β-sheet conformation has been linked to the functionally fusogenic form (Rodriguez-Crespo *et al.*, 1996; Rodriguez-Crespo *et al.*, 2000). Residues downstream of the hepadnavirus putative fusion peptide are predicted to adopt a coiled-coil conformation (Rodriguez-Crespo *et al.*, 1999). Treatment of HBV and WHV virions with V8 protease to remove the preS domain, thereby exposing the putative fusion peptide at the N-terminus of S, significantly enhanced the infectivity of those viruses in certain cell lines (Cooper *et al.*, 2003, and references therein). Therefore, it has been suggested that the proteolytic processing of L subsequent to receptor-binding may activate the protein for membrane fusion (Cooper *et al.*, 2003). Alternatively, conformational changes may regulate exposure of the fusogenic peptide. The identification of an additional membrane-traversing fold between the first and second TM domains of the DHBV L protein led to the proposal that highly folded L molecules may form a spring-loaded, metastable structure that undergoes a low pH-triggered conformational change releasing TM1 onto the surface of the virus particle (Grgacic and Schaller, 2000).

Herpes simplex virus type 1 gB, gH-gL, and gD

Membrane fusion induced by herpesviruses is a complex, pH-independent process that involves the concerted action of at least three conserved viral glycoproteins, designated gB, gH and gL (reviewed by Spear and Longnecker, 2003). The gH and gL proteins form a heterodimeric complex. While gL lacks a TM anchor, it is expressed on the virion surface through its stable association with gH (Dubin and Jiang, 1995). The association with gL is required for the correct processing, folding, and cell surface expression of gH (Hutchinson *et al.*, 1992). The gB, and gH-gL proteins share no homology with the fusion proteins of other virus families and contain no obvious hydrophobic fusion peptides. Most herpesviruses require, in addition to gB and gH-gL, a viral receptor-binding glycoprotein ('fusion ligand') to accomplish membrane fusion. The binding of this additional component of the fusion complex to cellular receptors (so-called 'fusion receptors') may trigger fusion-activating conformational changes in gB, or gH-gL (Cole and Grose, 2003; Spear and Longnecker, 2003). The identity of the fusion ligand varies among viral subfamilies and partially accounts for cell and tissue tropism differences (Spear and Longnecker, 2003). In herpes simplex virus type 1 (HSV-1), as in most alphaherpesviruses, gD functions as the fusion ligand, binding to one of several specific receptors (Milne *et al.*, 2003, and references therein). Milne *et al.* (2003) have shown that, regardless of the affinity of gD for its receptor, membrane fusion will proceed as long as receptor-binding occurs.

The gB component of the fusion complex is the most highly conserved glycoprotein within the *Herpesviridae* and, like typical viral fusion proteins, gB adopts a type I (N_{exo}/C_{cyt}) membrane topology. While the gB proteins of most herpesviruses are

processed into two disulfide-linked subunits, reminiscent of class I fusion proteins, the gB of HSV-1 is not cleaved (Sarimento and Spear, 1979). At 109 amino acids, the C-terminal tail of HSV-1 gB is longer than that of typical enveloped virus fusion proteins and contains α-helical regions that serve to down-regulate cell-cell fusion (Foster *et al.*, 2001). A similar role has been shown for the C-terminal tail of the gB protein of pseudorabies virus (Nixdorf *et al.*, 2000) and Epstein-Barr virus (Haan *et al.*, 2001). A role in the inhibition of syncytium formation for the C-terminal tail has also been shown for select class I fusion proteins of retroviruses and paramyxoviruses (Seth *et al.*, 2003, and references therein). One such example is the F protein of the SER paramyxovirus, which is closely related to the SVF F protein but is 22 aa longer and impaired in its ability to induce syncytium formation (Seth *et al.*, 2003; Tong *et al.*, 2002). Removal of the 22-residue extension completely rescued SER F-mediated cell-cell fusion (Tong *et al.*, 2002). As with herpesvirus gB, syncytial inhibition by the C-terminal tail of SER F is sequence dependent (Seth *et al.*, 2003).

1.4. Alternative models of protein-mediated membrane fusion

Although the spring-loaded mechanism of protein-mediated membrane fusion, described above (section 1.3.1) using the influenza HA protein as an example, is the most popular model, several alternative models have been proposed. During the low pH-induced refolding of influenza HA, the exposed fusion peptide may insert into either the target membrane or the viral membrane (Gaudin *et al.*, 1995; Madhusoodanan and Lazaridis, 2003). Most models, including the spring-loaded theory, consider the population of HA molecules with the fusion peptide inserted into the viral membrane to

be inactive and follow the population with the fusion peptide inserted into the target membrane. However, two models that consider the conformation of HA with the fusion peptide in the donor membrane to be of primary significance are discussed below. The authors of these models reassign the free energy released by the low pH-induced conformational changes of HA so that the energy is more optimally utilized (they argue) than what is described for the spring-loaded mechanism. In the spring-loaded model, extension of the coiled-coil domain, which is expected to release the largest amount of free energy of all the HA conformational rearrangements, functions solely to bring the fusion peptide toward the target membrane, a process that probably occurs nearly spontaneously (Bentz, 2000b). Furthermore, the spring-loaded mechanism hypothesizes that the helix-turn transition associated with the folding-back of the C-terminal α-helices accomplishes the difficult job of bringing the apposed membranes into close contact, although this conformational change should release much less energy than the formation of the extended coiled coil (Bentz, 2000b). The models discussed below assign the relatively large energy released upon formation of the extended coiled coil to the high energy-requiring task of deforming the donor membrane, either through the creation of a bulging dimple (where the fusion peptide remains embedded in the donor membrane) or a hydrophobic defect (where the fusion peptide is extracted from the donor membrane), in order to promote hemifusion. With the largest release of free energy harnessed to create the initial defect at the nascent fusion site, subsequent steps to complete the fusion reaction could proceed down the free energy pathway. The final conformational changes in HA are predicted to facilitate the transition from hemifusion to fusion pore formation. These alternative models, in which HA initiates fusion by inducing deformations of the

donor, not the target, membrane are particularly attractive when considering the class II and several of the unclassified viral fusion proteins (discussed above). Many of these proteins do not appear to have the capability of reaching out to initiate contact with, and destabilization of, the target membrane and, thus, do not obviously conform to the spring-loaded hypothesis.

1.4.1. Bending defect model

Kozlov and Chernomordik (1998) proposed a model of membrane fusion mediated by HA in the acidic pH conformation with the fusion peptide embedded in the donor membrane. Subsequent extension of the rigid coiled-coil domain of HA, while the fusion peptide is inserted in the same membrane as the TM anchor, bends the donor membrane into a saddle-like shape surrounding the HA trimer (Kozlov and Chernomordik, 1998). The resulting mechanical stresses in the bilayer drives the self-assembly of HA trimers into a ring-like cluster that functions as a protein dam, restricting the flow of lipids (Chernomordik *et al.*, 1998; Kozlov and Chernomordik, 1998). The consequence of this restricted lipid flow on the lipidic intermediates of the fusion pathway is discussed below. Formation of the protein dam heavily depends on tight contacts being formed between the TM domains of an estimated minimum of six HA trimers (Kozlov and Chernomordik, 1998). As the HA cluster (already pulling on the membrane) simultaneously tilts away from the center, a lipidic dimple within the ring is formed that protrudes towards the target membrane (Kozlov and Chernomordik, 1998). The dimple is brought into close contact with the target membrane by the receptor-binding interactions of the HA_1 subunit and by the population of HA that inserted the fusion peptide into the target membrane. The bending stresses that accumulate at the tip

of the dimple facilitate its fusion with the target membrane (Kozlov and Chernomordik, 1998). Expansion of the fusion pore would require the subsequent dissociation of the HA cluster.

1.4.2. Hydrophobic defect model

While Kozlov and Chernomordik (1998) proposed that the fusion peptide will remain embedded in the donor membrane until the dimple contacts the target membrane, a modification of the bending defect model was proposed by Bentz (2000a), in which tension resulting from the formation of the extended coiled-coil structure will extract some of the fusion peptides out of the donor membrane and move them toward the target membrane. For those HAs in isolation or in small aggregates not yet in the restricted flow state, lipid diffusion will quickly fill the void in the donor membrane. However, when lipid flow is restricted the space evacuated by the fusion peptides cannot be instantly refilled and, thus, a hydrophobic defect is created with both the acyl chains and portions of the HA TM anchors exposed to water (Bentz, 2000a). The recruitment of lipids from the *cis* monolayer of the apposed target membrane would relieve the hydrophobic defect leading to hemifusion (Bentz, 2000a). The helix-turn transition in the HA coiled coil to form the six-helix bundle, believed to allow close approach of the two fusing membranes, plays an additional role in the hydrophobic defect model. Formation of the helix-turn places a hydrophobic collar (the 'kink' region) just above the hydrophobic defect, and this collar may stabilize the lipids moving from the target membrane into the defect area (Bentz and Mittal, 2003). An analogous 'hydrophobic collar' function has been proposed for similarly-located hydrophobic domains which may become exposed during the

fusogenic refolding of the neuronal SNARE synaptogamin and the TBEV E protein (Bentz and Mittal, 2000).

Support for the hydrophobic defect model of Bentz (2000a) over the bending defect model of Kozlov and Chernomordik (1998) comes from the observation that mutations which increase the hydrophobicity of the HA fusion peptide abolished membrane fusion (reviewed by Bentz, 2000a). Presumably the mutated fusion peptides were too hydrophobic to be extracted from the donor membrane. Furthermore, the well-established role of the fusion peptide in destabilizing the lipid bilayer is better accommodated within the hydrophobic defect model. Also, kinetic analysis indicated that, although formation of the first fusion pore required an aggregation of eight HA trimers, only two are required to adopt the extended coiled-coil conformation (Bentz, 2000b; Bentz and Mittal, 2003). This data fits well with the hydrophobic defect model, as the extraction of just two fusion peptides (one from each of two trimers) from the center of the fusogenic aggregate in a planar bilayer is sufficient to create a large enough hydrophobic defect to cause lipids from the intact monolayer to enter into the defect area (Tieleman and Bentz, 2002). In contrast, the bending defect model is predicted to require the concerted effort of all of the HAs in the aggregate (Kozlov and Chernomordik, 1998).

1.4.3. Restricted hemifusion

The unrestricted flow of lipid molecules present in the *cis* monolayers of two apposed membranes is commonly believed to represent the first step in the fusion process (hemifusion), prior to the opening of a fusion pore and consequent contents mixing. Lipid-mixing assays are commonly employed to measure the ability of a polypeptide to promote hemifusion. However, Chernomordik *et al.* (1998) presented evidence indicating

that the unrestricted hemifusion state (measured by these assays) is an inactivated, side branch in the fusion pathway that occurs when the density of, or the interaction between, activated HA trimers at the fusion site is inadequate. Both the bending defect and hydrophobic defect models (discussed above) incorporate the restricted hemifusion state characterized by Chernomordik *et al.* (1998) as an essential intermediate in the fusion pathway. Restricted hemifusion occurs when the continuity between *cis* monolayers is not accompanied by measurable lipid mixing (Chernomordik *et al.*, 1998). Chernomordik *et al.* (1998) argue that fusion pore formation will only proceed from the tension focused at the site of restricted lipid flow. The alternative unrestricted hemifusion state will not transition directly to the fusion pore formation stage. Thus, the movement of lipid measured by lipid-mixing assays may occur independent of membrane fusion, or occur subsequent to full fusion, but does not represent the initial stage of a competent fusion pathway. Support for the restricted hemifusion state has emerged from analysis of the VSV G fusion protein. A restricted hemifusion intermediate, similar to that characterized for HA by Chernomordik *et al.* (1998), has been described for the VSV G-mediated fusion pathway, and proposed to result from a ring-like clustering of G (Gaudin, 2000a).

1.4.4. Summary of enveloped virus-mediated membrane fusion models

The spring-loaded, bending defect, and hydrophobic defect models are all explicitly two-step processes, each assigning the energy released by the two major refolding events of HA to variant tasks. The high-energy conformational change that accompanies the formation of the extended coiled coil either (1) tethers the donor and target membranes together (spring-loaded hypothesis), (2) induces curvature strain in the donor membrane resulting in HA clustering and formation of a lipidic dimple (bending

defect model), or (3) ultimately extracts the fusion peptide to create a hydrophobic defect in the donor membrane (hydrophobic defect model). The second, low-energy conformational change accompanying the helix-turn transition (1) pulls the apposed membranes together (spring-loaded hypothesis), or translates the defect in the donor membrane to the target membrane, either by (2) inducing maximal growth of the lipidic dimple (bending defect model), or (3) stabilizing the transfer of lipid molecules from the target membrane into the hydrophobic defect (hydrophobic defect model). All of the leading models of enveloped virus class I fusion protein-mediated membrane fusion discussed above require that the fusion protein be held in a high-energy metastable state until triggered to undergo dramatic conformational rearrangements that provide the energy to drive membrane fusion. Elements of these models may apply to other enveloped virus fusion events, mediated by non-class I fusion proteins, as well as apply to the various cellular fusion events discussed below, but in most cases the current models are inadequate.

1.5. Intracellular membrane fusion

1.5.1. Vesicle fusion

Eukaryotic cells are compartmentalized into distinct membrane-bound organelles that are specialized in carrying out diverse cellular processes. Lipid vesicles traffick cellular cargo between organelles, deliver material to the plasma membrane for secretion, and transport endocytosed materials. Precise intracellular vesicle transport and fusion is fundamental to the life of all eukaryotic cells and depends on the participation of a complex of SNAREs (soluble N-ethylmaleimide sensitive factor attachment protein

receptors). All vesicle fusion events require the joining of a SNARE associated with the vesicle membrane (v-SNARE) with two associated with the target membrane (t-SNAREs) into a heterotrimeric complex (Chen and Scheller, 2001). For example, the v-SNARE synaptobrevin, involved in neurotransmitter release, pairs with its cognate t-SNAREs, syntaxin-1A and SNAP-25 (Sutton *et al.*, 1998). These distinct SNAREs represent three families of SNARE proteins conserved in all eukaryotes (Ferro-Novick and Jahn, 1994). Synaptobrevin-2 and syntaxin-1A are each anchored in the vesicle and target membranes, respectively, by a single TM domain while SNAP-25 is associated with the target membrane by acyl groups. As shown in Figure 1.5, the heterotrimeric SNARE complex exhibits a parallel coiled-coil four-helix bundle similar to the antiparallel six-helix bundle of the class I homotrimeric fusion proteins (Skehel and Wiley, 1998; Sutton *et al.*, 1998; Weber *et al.*, 1998). Syntaxin-1A and synaptobrevin each contribute one helix to the core complex while SNAP-25 contributes two (Sutton *et al.*, 1998). Assembly of the SNARE complex is thought to begin distal to the bilayer surfaces and proceed toward the membrane-anchored domains (Sutton *et al.*, 1999). The 'zippering up' of the SNARE complex increases the α-helical content of the SNAREs (monomers are largely unstructured) and pulls the vesicle and target membranes into close proximity (Brunger, 2000). Debate continues over whether formation of the SNARE complex provides sufficient energy to overcome the repulsive forces between apposed membranes and accomplish their merger or whether the complex serves only to juxtapose two membranes and downstream events are required for fusion. Akin to the situation with HA, fusion pore formation in a model membrane system accompanies the

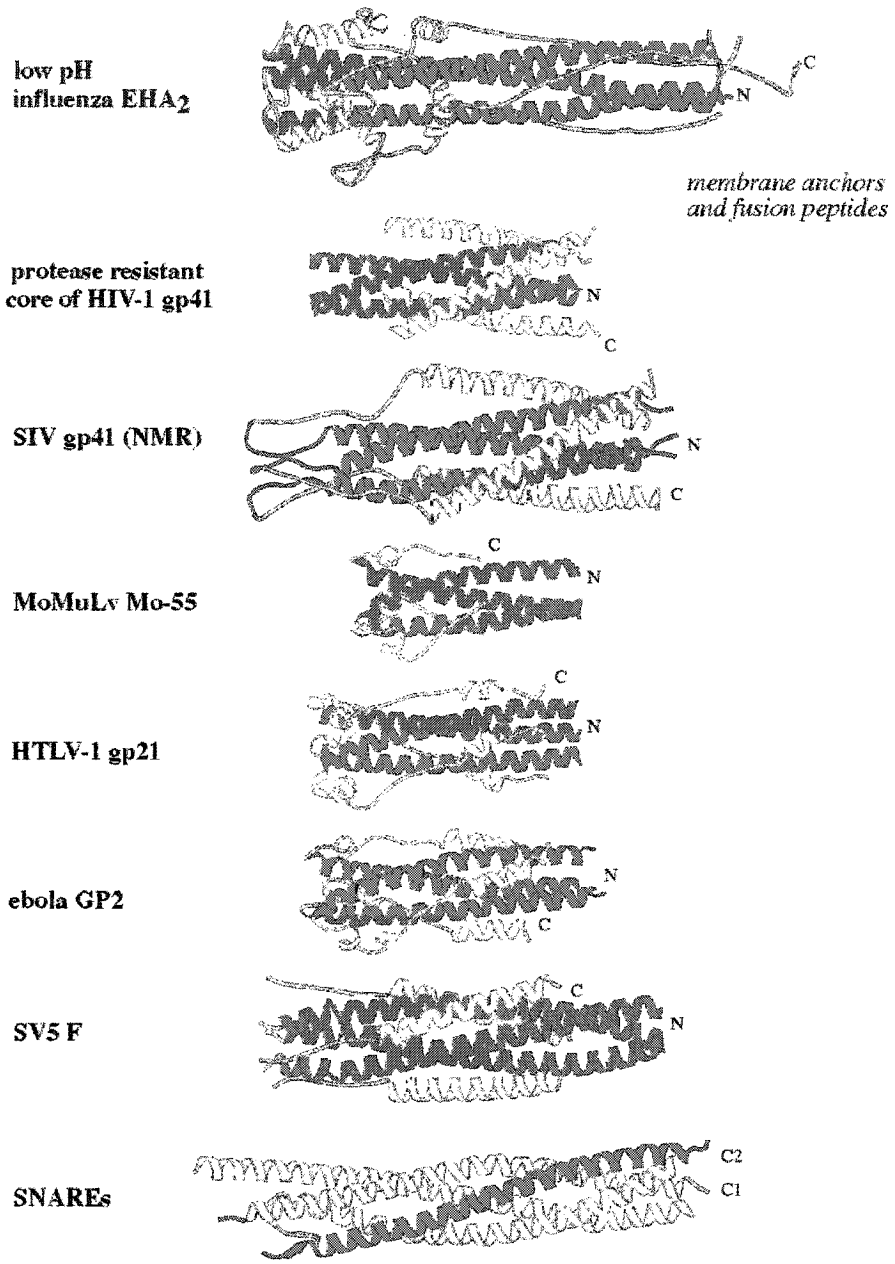

Figure 1.5. **Rod-shaped α-helical bundles of the ectodomains of membrane fusion proteins.** The regions (TM anchors and fusion peptides) that insert in the participating membranes are located at one end (right-hand). Shown are the coiled-coil bundles of influenza virus HA_2, HIV-1 gp41, simian immunodeficiency virus (SIV) gp41, Moloney murine leukemia virus (MoMuLv) TM subunit, human T-cell leukemia virus type 1 (HTLV-1) gp21, Ebola virus GP2, simian virus 5 (SV5) F_1, and the synaptic fusion complex with the v-SNARE synaptobrevin, t-SNARE syntaxin, and the two helical regions of the t-SNARE SNAP-25. N- and C-termini are labeled; C1 and C2 label the C-termini that are inserted, prefusion, in the plasma and vesicle membrane, respectively. Figure by Skehel and Wiley reprinted, with permission, from the *Annual Review of Biochemistry*, Volume 69 © 2000 by Annual Reviews www.annualreviews.org.

assembly of SNARE complexes into a ring-like structure (Cho *et al.*, 2002). Although SNAREs are the core machinery driving intracellular membrane fusion, a number of regulatory proteins, such as the Rab class of small GTPases and their effectors, are required to direct the fusion process *in vivo* by controlling SNARE activity and complex assembly (reviewed by Gerst, 2003). There is also a requirement for calcium (reviewed by Burgoyne and Clague, 2003) and, at least for neurotransmitter release, certain lipids such as cholesterol (Lang *et al.*, 2001) and phosphatidylinositol (reviewed by Blumenthal *et al.*, 2003).

Several proposals have suggested that SNAREs function in a manner analogous to class I fusion proteins, in which formation of the coiled-coil core complex pulls apposing bilayers together and effects their fusion (Skehel and Wiley, 1998; Weber *et al.*, 1998). However, the SNAREs differ from most viral fusion proteins in that they appear to lack a 'fusion peptide'. Nonetheless, Jahn and Südhof (1994) proposed the v-SNARE synaptobrevin contains a fusion peptide-like sequence, located within the center of the coiled-coil domain of the SNARE complex (Sutton *et al.*, 1998). Bentz (2000a) hypothesized that this motif may insert into the donor membrane until the vesicle docks with the target membrane. Formation of the coiled-coil SNARE complex would pull this 'fusion peptide' out of the donor membrane and, if vesicular membrane proteins restricted lipid flow, then the SNARE fusion system could function according to the hydrophobic defect model (Bentz, 2000a).

1.5.2. Outer segment turnover in retinal rod cells

Maintenance of the normal structure of retinal photoreceptor cells, which contain in their outer segment region a stack of flattened membranous disks, requires a

specialized process of membrane fusion. Fusion is involved in both new disk formation and old disk shedding. An integral membrane phospho/glycoprotein with four TM anchors (i.e. a member of the tetraspanin family), called peripherin/rds or peripherin-2, is the candidate fusion protein in photoreceptor rod cells (Boesze-Battaglia *et al.*, 2000). Peripherin/rds is oriented with both termini in the cytoplasm and characterized by a large intradiskal domain between TM3 and TM4 (Loewen *et al.*, 2003). Peripherin/rds forms a disulfide-linked homodimer that associates with itself or with a nonglycosylated homologue (the tetraspanin ROM-1) to assemble a mixture of core homo- and heterotetrameric complexes (Boesze-Battaglia *et al.*, 2000; Loewen *et al.*, 2003). These tetramers further join together through intermolecular disulfide bonds into higher order oligomers believed to be essential for disk rim formation (Loewen *et al.*, 2003). The cytoplasmically-oriented C-terminal region of pheripherin/rds contains a fusion peptide that has been shown to promote membrane aggregation, destabilization, and aqueous contents mixing (Boesze-Battaglia *et al.*, 2000). Interestingly, membrane fusion within retinal rod cells is not the only example involving tetraspanins. Tetraspanins are enriched within secreted vesicles and have been implicated in the regulation of vesicle fusion (Hemler, 2003). They are also involved in several cell-cell fusion events (discussed in section 1.6.2).

1.5.3. Mitochondrial fusion

Mitochondrial fusion serves a number of essential functions (reviewed by Westermann, 2002), such as the defense against accumulated oxidative damage during cellular aging and the development of interconnected mitochondrial networks important for the transmission of energy and calcium signals. Because mitochondria are surrounded

by a double membrane, their fusion requires the coordinated merger of four bilayers. To accomplish this task, mitochondria possess unique membrane fusion machinery unrelated to the SNAREs that mediate other intracellular membrane fusion events (Westermann, 2003). Members of the evolutionarily conserved Fzo family of large GTPase (termed mitofusins) are central components of the mitochondrial fusion machinery (Westermann, 2003). Fzo family members are integral membrane proteins of the mitochondrial outer membrane, with two TM anchors and both termini exposed to the cytosol (Fritza *et al.*, 2001). The two TM anchors are separated by a short polybasic region that is exposed to the intermembrane space and required for Fzo localization to sites of tight contact between the outer and inner membranes (Fritza *et al.*, 2001). The intermembrane-space loop is proposed to connect the outer membrane fusion complex to components in the inner membrane or intermembrane space in order to coordinate fusion of both mitochondrial membranes (Fritza *et al.*, 2001). Each TM segment is flanked by a cytoplasmically-exposed predicted coiled-coil domain that is important for Fzo clustering, and potentially for mediating interactions with partner Fzo members on opposing mitochondria (Westermann, 2003). Thus, mitochondrial Fzo proteins may assemble a *trans*-four-helix bundle required for fusion similar to the SNARE four-helix bundle. Also like the SNARE complex, the mitochondrial fusion machine may utilize energy contributed by GTPase activity, and probably involves accessory proteins since Fzo is known to associate within a larger protein complex (Fritza *et al.*, 2001).

1.6. Intercellular fusion

Cell-cell fusion is a relatively rare, yet essential, process in the life of eukaryotes. Fertilization requires sperm-egg fusion, and other intercellular fusion events generate important specialized multinucleated cells throughout development. For example, multinucleated cells form the placental syncytiotrophoblast lining required for the embryonic development of mammals (Potgens *et al.*, 2002). Striated muscle fibers (myotubes) are formed by the fusion of myoblasts (Abe *et al.*, 1999). In addition, the fusion of certain haematopoietic stem cells is necessary to generate the osteoclasts involved in bone resorption and the giant macrophages associated with chronic inflammation (Namba *et al.*, 2001). These cell-cell fusion events are poorly understood, but are generally accepted to be highly-regulated processes involving complex, multi-component fusion machines. The interactions of a number of complementary molecules localized to specific domains of the sperm and egg plasma membranes govern the recognition and close approximation between the two cell types to be fused (Cuasnicu *et al.*, 2001). It appears that a similar asymmetry in protein-receptor interactions at a specific fusion site regulates the fusion of myoblasts (Ruiz-Gomez *et al.*, 2000), and probably other intercellular fusions.

1.6.1. ADAMs

Several members of the ADAM (a disintegrin and a metalloprotease) protein family are proposed to play key roles in various cell-cell fusion events. The ADAMs are a large group of type I membrane glycoproteins expressed at the cell surface containing four potential functional domains, including a proteolytic domain, an adhesion domain, a fusion domain (containing a hydrophobic 'fusion peptide'), and a signaling domain

(Wolfsberg and White, 1996). Different subsets of these domains are functional in different classes of ADAMs, and only select ADAMs are predicted to be fusogenic. For instance, meltrin-α (ADAM-12) and ADAM-9 are implicated in giant macrophage formation, and meltrin-α is also implicated in osteoclast formation (Abe *et al.*, 1999; Namba *et al.*, 2001). Cyritestin (ADAM-3) and the heterodimer of fertilin-α (ADAM-1) and fertilin-β (ADAM-2), localized on the head of sperm, are involved in gamete fusion. In the general model for ADAM fusogenicity proposed by Wolfsberg and White (1996) the disintegrin domain of fusogenic ADAMs may bind integrins expressed on the target cell. Additional sets of receptor-coreceptor interactions may enhance cell-cell binding. Binding-induced conformational changes in the ADAM complex may expose the fusion peptide, trigger ADAM clustering, and lead to fusion pore formation. The fusion peptides of meltrin-α and fertilin-α appear unordered in aqueous solution but insert into membranes as a β-structure (Wolfe *et al.*, 1999; Muga *et al.*, 1994). Although the model of ADAM fusogenicity is extrapolated from the activity of class I viral fusion proteins, ADAMs significantly differ from these proteins in both their lack of coiled-coil structure and their involvement in multicomponent complexes.

1.6.2. Tetraspanins

In addition to their roles in different intracellular fusion processes (section 1.5.2.), members of the tetraspanin family are also involved in a variety of intercellular fusion events. For example, on the egg surface, the association between the tetraspanin CD9 and the integrin complementary to fertilin-β is necessary for fusion independent of sperm-egg adhesion (Cuasnicu *et al.*, 2001). While tetraspanins facilitate fusion between gametes, myoblasts, and certain virus-infected cells, they paradoxically inhibit the formation of

osteoclasts and giant macrophages (Takeda *et al.*, 2003). The apparent cell-dependent fusogenicity of tetraspanins may reflect a fundamental difference between macrophage and non-macrophage cell lines, especially considering that certain lectins promote macrophage fusion while inhibiting the fusion of gametes, myoblasts and virus-infected cells (Takeda *et al.*, 2003). The role of tetraspanins during fusion is unclear. Tetraspanins appear to organize into a novel type of membrane microdomain distinct from lipid rafts (reviewed by Hemler, 2003). From such microdomains, tetraspanins may modulate the adhesive functions of the integrins with which they complex (Takeda *et al.*, 2003). Alternatively, they might be involved in post-cell adhesion events (Hemler, 2003). Given their four TM domains, it is conceivable that tetraspanins may be well suited to promoting membrane fusion by contributing to the restriction of lipid flow at the fusion site - a necessary prerequisite to hemifusion according to the bending and hydrophobic defect models (section 1.4).

1.6.3. Bindin

A membrane protein of sea urchin sperm cells, known as bindin, is a novel 25-kDa fusion protein that plays a role in fertilization at both the level of adhesion and fusion between sperm and egg (Ulrich *et al.*, 1998). The central part of bindin consists of a hydrophobic region of about 70-80 residues containing a completely conserved 18-residue fusion peptide, called B18, which appears to represent the minimum sequence capable of inducing membrane fusion (Ulrich *et al.*, 1998). The structure and function of the B18 sequence has been extensively characterized *in vitro*. B18 contains a histidine-rich zinc-binding motif, and bindin-induced fusion is more efficient in the presence of zinc (Binder *et al.*, 2000). In solution, B18 is largely unstructured but, upon zinc-binding,

it converts to an α-helical structure that, in a manner characteristic of fusion peptides, binds detergent micelles in a kinked orientation (Glaser *et al.*, 1999). Similar to the HA fusion peptide, B18 shows a tendency to self-associate (through zinc bridges) and, at high concentrations, exhibits a preference for β-sheet conformation (Barre *et al.*, 2003; Tamm *et al.*, 2002). Although previous studies employing membrane-mimicking environments associated B18 fusogenicity to the α-helical form, solid-state NMR spectroscopy analysis (the method of choice for the investigation of peptide binding to intact bilayer membranes) recently implicated the parallel β-sheet conformation as the functional form (Barre *et al.*, 2003).

1.6.4. Syncytin

While other intercellular fusion events involve complex multi-component fusion machines, formation of the syncytiotrophoblast is a unique situation, involving a single captive (probably class I) viral fusion protein. The retrovirus replication cycle involves the integration of a reverse-transcribed form of the RNA genome, as double-stranded DNA, into the host cell genome to form a provirus. As a consequence, retroviruses in germ line cells can be inherited as endogenous elements. About 1% of the human genome harbours replication defective endogenous retroviruses (ERVs) (Lower *et al.*, 1996). The expression of a gene of one such ERV was recently shown to play an important physiological role in humans. The envelope fusion protein of a human endogenous retrovirus (HERV-W), called syncytin, is involved in formation of the placental syncytiotrophoblast layer (Frendo *et al.*, 2003; Mi *et al.*, 2000). Syncytin is a highly fusogenic membrane glycoprotein that induces syncytium formation upon interaction with the type D mammalian retrovirus receptor (amino acid transporter B) (Frendo *et al.*,

2003). While other HERV-W genes have accumulated inactivating mutations, the full-length envelope protein (syncytin) has been selectively preserved, presumably because of its role in placental morphogenesis (Frendo *et al.*, 2003). Thus, it appears that an ancient retroviral infection may have been a pivotal event leading to the evolution of mammals (Frendo *et al.*, 2003).

1.6.5. Fusion of enveloped virus-infected cells

Virus-infected cells that express at their surface viral fusion proteins that do not require low pH-activation or post-virion-budding maturation events can potentially fuse with neighbouring cells to form multinucleated syncytia. Although the process of virus-induced syncytium formation is related to virus entry, often differences with respect to lipid or protein requirements underlie the two events. These distinctions reflect the different evolutionary constraints placed on the processes of virus-cell versus cell-cell fusion. For enveloped viruses, the two processes are not highly divergent since, in most cases, the same machinery is employed and is subject to the constraints of both systems. HSV-1 provides an example of an enveloped virus exhibiting relatively dramatic differences in the requirements for virus entry versus syncytium formation. Despite the fact that the plasma membrane is highly enriched with fusogenic glycoproteins, herpesvirus-mediated syncytium formation is only observed in cells infected with viruses carrying syncytial (*syn*) mutations (Avitabile *et al.*, 2003). In addition to the inhibitory role for the cytoplasmic tail of gB in syncytium formation mentioned above (section 1.3.3.), another membrane protein (gK) is involved in negatively-regulating herpesvirus-induced cell-cell fusion. Most naturally-occuring *syn* mutations target either gB or gK. The activity of gK has not been fully elucidated, but may preclude fusion between the

HSV envelope and virion-encasing vesicles during virus transport, thereby preventing nucleocapsid de-envelopment and promoting virus egress (Avitabile *et al.*, 2003).

1.7 Reovirus FAST proteins

While syncytium formation can be a consequence of the expression of enveloped virus fusion proteins at the cell surface of infected cells, it is highly unusual that a nonenveloped virus, which should not express a fusion protein, would induce cell-cell fusion. Nonetheless, several members of the nonenveloped *Reoviridae* family encode a membrane fusion-inducing protein that accounts for their unexpected syncytial phenotype (Duncan, 1999). The atypical properties exhibited by the reovirus fusion proteins have lead to their designation as a novel class of fusion protein – the Fusion-Associated Small Transmembrane (FAST) protein family (Corcoran and Duncan, 2004; Dawe and Duncan, 2002; Shmulevitz and Duncan, 2000). Being encoded by nonenveloped viruses, the FAST proteins are not required for viral entry or egress, and appear to be nonessential for viral replication (Duncan *et al.*, 1996). As such, the FAST proteins have seemingly evolved free of many of the constraints placed on the fusion proteins of enveloped viruses. The enveloped virus fusion proteins need to be controlled in several ways. Being structural components of the virus particle, they need to be kept stable in harsh external environments. Away from a target membrane they need to be maintained in a way that does not compromise the integrity of the virus envelope. They need a mechanism for ensuring target membrane specificity. Also, their fusogenic activity needs to be tightly regulated such that fusion occurs at the proper time during infection. Given the intrinsic pairing of fusion-promoting and fusion-regulatory machinery in the fusion proteins of

enveloped viruses, it will be cumbersome to isolate which events taking place during the fusion reaction are strictly involved in accomplishing fusion versus its regulation. In comparison, the FAST proteins do not need to be so tightly controlled. Considering the relatively small size and apparent simplicity of the FAST proteins, they make promising candidates for understanding the minimal requirements for biological membrane fusion.

Despite numerous attempts to unify the mechanisms of viral and cellular membrane fusion (for example, see Skehel and Wiley, 1998; Weber *et al.*, 1998; Wolfsberg and White, 1996), no cellular fusion protein identified to date is accurately described by the models of enveloped virus protein-mediated membrane fusion, with the possible exception of the neuronal SNARE complex. Furthermore, increasing numbers of examples of viral fusion proteins are emerging that also do not fit the paradigm. It may be that the leading models of membrane merger are flawed or, possibly, that there exists a formerly unappreciated range of mechanisms to accomplish this vital cellular event. In either case, alternative models of protein-mediated membrane fusion are required.

The identification and characterization of the novel p15 FAST protein of baboon reovirus presented here has revealed a polypeptide whose structural organization is incompatible with the current paradigm of how protein-mediated membrane fusion must proceed. The p15 protein does not appear to be maintained in a metastable state and its fusogenic activity is not predicted to require triggered conformational changes. The absence of a fusion peptide motif from the extremely minimal (20-residue) p15 ectodomain, combined with the cytosolic-localization of a semi-conserved putative FAST protein fusion-inducing sequence, has led to a fresh model of FAST protein-mediated

membrane fusion. In this model, initiation of the fusion process occurs at the donor, rather than the target, membrane, and involves the concerted action of multiple motifs.

CHAPTER 2

MATERIALS AND METHODS

2.1. Virus

Baboon reovirus 10895 (BRV) was isolated from the brain tissue of a baboon with meningoencephalomyelitis (Duncan *et al.*, 1995; Leland *et al.*, 2000) and was obtained from Julia Hilliard (Southwest Foundation for Biomedical Research, San Antonio, TX). The virus was plaque purified, and high titer stocks were grown in African green monkey (Vero) cells as previously described (Duncan and Sullivan, 1998).

2.2. Cells

Vero cells were purchased from the ATCC (CCL-81) and maintained at 37°C in a 5% CO_2 atmosphere in medium 199 with Earle's salts containing 5% heat-inactivated fetal bovine serum (FBS) and 100 U of penicillin and streptomycin per ml. For ease of transfection, quail fibroblast (QM5) cells (which are permissive for BRV infection) were used to express p15 constructs. The QM5 cell line is a clonal derivative of QT6 cells that exhibits a very low spontaneous fusion index (Antin and Ordahl, 1991). QM5 cells were maintained as described for Vero cells, except medium contained 10% heat-inactivated FBS.

2.3. Antibodies

2.3.1. Polyclonal antisera specific for p15 peptides and p16

To generate p16-specific antisera and antisera against p15 subdomains (N-terminus: residues 1-43; C-truncated: residues 1-90; C-terminus: residues 90-140), p16 and the p15 subdomains were cloned in frame with maltose-binding protein (MBP) by

using the *Xmn*I and *Bam*HI sites of the pMAL-c2 vector (New England Biolabs) and transformed into *Escherichia coli* DH5α cells. The MBP-p16 and MBP-p15-(C-terminus) chimeric proteins were separately expressed and purified from *E. coli* on amylose affinity columns, according to the protocol suggested by the suppliers of the pMal-c2 vector, and then used to immunize rabbits. Each rabbit was injected with 0.1 mg of p15-C or 0.5 mg of p16 in Freund's complete adjuvant, administered at three sites (two intramuscular and one subcutaneous), and then boosted three more times with protein in Freund's incomplete adjuvant. Rabbit polyclonal antisera rasied against synthetic peptides corresponding to the p15 N-terminal domain (residues 4-23) or polybasic domain (residues 47-61) was purchased from New England Peptide, Inc.

2.3.2. Polyclonal antisera against full-length p15

To generate antisera against full-length p15, a recombinant baculovirus expressing p15 under the control of the polyhedrin promoter was created using the Bac-To-Bac Baculovirus Cloning and Expression System (Life Technologies). The p15 protein was purified from infected SF21 cells by detergent disruption, affinity chromatography using TALON Metal Affinity Resin (Clonetech), and ion exchange chromatography using HiTrap SP HP ion exchange columns (Amersham Pharmacia Biotech). The purified p15 (500 μg per injection) was used to immunize rabbits using Freund's complete adjuvant for the primary injection and Freund's incomplete adjuvant for five subsequent booster injections at six-week intervals.

2.4. Cloning

The procedures for cDNA cloning and sequencing of the BRV S-class genome segments has been described previously (Duncan, 1999). The full-length cDNAs corresponding to the S1, S2, S3, and S4 genome segments of BRV were cloned into the pBluescript II SK vector (Stratagene) by using the *Not*I site. The S4 genome segment and the p15 ORF were separately subcloned into the pcDNA3 vector (Invitrogen). The forward primer added a *Bam*HI site to the 5' end of the S4- and p15-pcDNA3 constructs. The reverse primers added 3'-terminal *Hpa*I and *Not*I sites to the S4- and p15-pcDNA3 constructs, as well as additional C-terminal Val and Phe residues to p16 or an additional C-terminal Asn residue to p15 (the insertion of the *Hpa*I site before the termination codons was intended to facilitate future in-frame insertions; the additional residues do not affect the function of p15). The p16 ORF was subcloned from the S4 genome segment in pBluescript II, by *Pst*I and *Not*I restriction digestion. The p16 ORF in pBluescript II was subsequently subcloned into pcDNA3 by *Hin*dIII and *Not*I restriction digestion.

Authentic p15 and the G2A, pro1, pro2 and pro5 constructs (described below) were each cloned in frame with GFP, separated by a six-glycine spacer, using the *Hind*III and *Bam*H1 restriction sites of the pEGFP-N1 vector (Clontech).

2.5. Mutatgenesis

2.5.1. Point mutations

The Stratagene Quick-Change mutagenesis method was used to: (1) abrogate the p15 myristylation consensus sequence in the G2A mutant; (2) introduce a TAG stop codon following amino acid 94, 97, 103, 109, 121, or 130 (mutants 94*, 97*, 103*, 109*, 121* or 130*, respectively); (3) replace lysine and arginine residues within the polybasic

domain with alanine: mutant A1 (R51A, K52A, K54A); mutant A2 (R51A, K52A, K54A, K56A, K57A); mutant A3 (R51A, K52A, K54A, K56A, K57A, R58A, K59A); (4) introduce asparagine (N)-linked glycosylation sites (NXS/T) into p15 with mutants g1 (R4N), g4 (R51N), g5 (K52S), g6 (K57S), and g8 (D130S); (5) substitute individual residues within putative the hinged loop (aa 81-90) with mutants P81A, P81I, V85T, P90A and P90I; (6) create a cysteine-less template (C104S) for use to introduce target cysteine residues for biotinylation with mutants V8C, A12C, S53C and S53C/I62C; and (6) to replace residues within the proline-rich region (aa 10-15) as follows. Authentic p15 was used as a template to make the following individual substitutions: Q9A, A12P, P13A, and P15A. Authentic p15 was also used as a template to make the following multiple substitutions: P10A/P14A (construct pro4; aa: $A_{10}PAPAP_{15}$) and P11A/P13A/P15A (construct pro2; aa: $P_{10}AAAPA_{15}$). To make the construct pro1 (aa: $A_{10}AAAAA_{15}$), pro4 was used as a template to replace the remaining three proline residues, P11A/P13A/P15A. Pro1, in turn, was used as a template to generate construct pro5 (aa: $A_{10}PAAAA_{15}$). A12P served as a template to generate both construct P11A (aa: $P_{10}APPPP_{15}$), and construct pro3 (aa: $P_{10}APAPA_{15}$).

2.5.2. Insertion mutations

The Stratagene Excite mutagenesis method was used to: (1) insert the HA antigenic epitope (YPYDVPDYA) into p15 following amino acid 43 (43HA), 54 (54HA) or 140 (140HA); (2) introduce four methionine codons and a TAG stop codon following amino acid 67 in the 67met* mutant; (3) introduce N-linked glycosylation site-containing insertions into p15 with mutants g2 (NFTNHA between aa 9-10), g3 (SAAAACAAAAA between aa 17-18), and g7 (ANASAAACAA between aa 59-60); the glycosylation sites

are underlined; and (4) insert the protein kinase A (PKA) consensus sequence (LRRASLG) following residues 8, 59, or 140 in authentic p15 (8pka, 59pka, 140pka), and constructs G2A (G2A-8pka, G2A-59pka, G2A-140pka), pro1 (pro1-8pka, pro1-59pka, pro1-140pka), pro2 (pro2-8pka, pro2-59pka, pro2-140pka), and pro5 (pro5-8pka, pro5-59pka, pro5-140pka), or following residue 59 in constructs A1 (A1-59pka) and A3 (A3-59pka).

2.5.3. Domain swaps

The Stratagene Excite mutagenesis method was used to simultaneously delete a specified domain (either the putative hinged loop, HL, or flexible, FLX, motifs) from either BRV p15 or reptilian reovirus (RRV) p14, while inserting the corresponding domain from another FAST protein (either avian reovirus [ARV] p10, RRV p14, or BRV p15) as summarized in Table 2.1. The RRV p14 protein in pcDNA3, used as a template for several domain swaps, was obtained from J. Corcoran (Dalhousie University).

The sequence of all constructs was confirmed either commercially (Robarts DNA Sequencing Facility, London, ON), or by cycle sequencing using the Thermo Sequenase Radiolabeled Terminator Cycle Sequencing Kit (USB) according to the manufacturer's instructions.

2.6. Radiolabeled BRV

To prepare radiolabeled BRV, infected monolayers were labeled at 10 h postinfection for 2 h with 100 μCi of [^{3}H]leucine per ml of leucine-free medium and then chased with 1.2 μg of cold leucine/ml for an additional 2 h. Monolayers were rinsed three times with cold phosphate-buffered saline (PBS; 140 mM NaCl, 2.5 mM KCl, 10 mM

Table 2.1. **Summary of FAST protein domain swap construction.**

Construct	Template	Domain Removed	Domain Inserted
DS1	RRV p14	HL (aa 5-13)	p15 HL (aa 81-90)
DS2	BRV p15	HL (aa 81-90)	p14 HL (aa 5-13)
DS3	BRV p15	FLX (aa 90-102)	p14 FLX (aa 13-24)
DS4	BRV p15	FLX (aa 90-102)	p10 FLX (aa 6-17)
DS5	RRV p14	FLX (aa 13-24)	p15 FLX (aa 90-102)
DS6	RRV p14	FLX (aa 13-24)	p10 FLX (aa 6-17)

Na_2HPO_4, and 2 mM KH_2PO_4), scraped from the tissue culture dishes, and passed through a 26.5-gauge needle 10 times. Since BRV is unstable in CsCl, virus was purified by extraction and differential centrifugation. Briefly, cellular debris was removed by centrifugation (20 minutes at 10,000 x *g*), and the virus-containing supernatant was pelleted through a 2-ml sucrose cushion (30% sucrose in medium) for 1 h at 27,000 rpm in an SW40 rotor (Beckman). Concentrated BRV pellets were resuspended in medium.

2.7. *In vitro* transcription and translation

BRV S1 uncapped transcripts were synthesized from *Bam*HI-linearized pBluescript II plasmid by using bacteriophage T3 RNA polymerase. BRV S2 and S3 uncapped transcripts were synthesized from *Sac*II-linearized pBluescript II plasmids by using bacteriophage T7 RNA polymerase. BRV S4 and p16 uncapped transcripts were synthesized from *Xho*I-linearized pcDNA3 plasmids by using bacteriophage T7 RNA polymerase. All p15 uncapped transcripts, except 67met*, were synthesized from *Xba*I-linearized pcDNA3 plasmids using bacteriophage T7 RNA polymerase. All transcripts, except 67met*, were translated in the presence of [^{3}H]leucine (Amersham Biosciences; 0.5 μCi/μL) using nuclease-treated rabbit reticulocyte lysates in the presence or absence of microsomal membranes (Promega). The 67met* transcripts were synthesized from *Afl*II-linearized pcDNA3 plasmid, and translated in the presence of [^{35}S]methionine (Amersham Biosciences; 0.8 μCi/μL). RRV p14 uncapped transcript corresponding to the V9T mutant was obtained from J. Corcoran. Translation reactions were carried out for 1 h at 30°C.

2.8. Membrane fractionation

The membrane-containing fraction of translation reactions was collected after centrifugation for 30 minutes at 10,000 x *g* in a bench-top microfuge at 4°C. The membrane-containing fraction of cell lysate was collected after centrifugation through a sucrose cushion (250 mM sucrose in 20 mM Tris-HCl, pH 7.4) for 30 minutes at 100,000 x *g* in a Beckman TLS-55 rotor at 4°C. In some cases, the membrane pellet was resuspended by vortexing in a solution of either high salt (500 mM NaCl) to remove peripherally associated membrane proteins, or high pH (100mM Na_2CO_3, pH 11.5) to extract lumenal contents, incubated on ice for 30 minutes with periodic vortexing, then re-centrifuged. In the case where infected cell lysate was used, proteins associated with the membrane pellet were extracted with radioimmunoprecipitation assay (RIPA) buffer (50 mM Tris-HCl, pH 8; 150 mM NaCl, 1 mM EDTA, 1% IGEPAL CA-630 [Sigma], 0.5% sodium deoxycholate; 0.1% sodium dodecyl sulfate [SDS]), and the contaminating virus particles were removed by further centrifugation.

2.9. Protease protection assay

Translation reactions performed in the presence of microsomal membranes were subjected to digestion with proteinase K (Qiagen; 0.2 mg/mL) for 30 minutes on ice. Reactions were diluted with stop buffer (PBS containing 1 mM phenyl methyl sulfonyl fluoride) and the membrane fraction was collected as above. The membrane pellet was resuspended in stop buffer, then mixed with boiling protein sample buffer, boiled, and subjected to SDS-polyacrylamide gel electrophoresis (PAGE) or Tricine-SDS-PAGE (Schagger and von Jagow, 1987) and fluorography (Bonner, 1984).

2.10. Transfection

Vero or QM5 cells seeded in 6- or 12-well dishes were transfected when 60-70% confluent using 2-6 μL Lipofectamine (Life Technologies) and 1-2 μg DNA in serum-free medium. With Vero cells, the transfection mix was typically replaced after 10-12 hours (with or without prior addition of FBA 4-6 h post-transfection) with medium containing 5% FBS. With QM5 cells, the transfection mix was typically replaced after four hours with medium containing 10% FBS.

2.11. Radiolabeled cell lysates

To generate infected cell lysate, Vero cells were infected with BRV at a multiplicity of infection of 5 PFU per cell in medium containing 1% fetal bovine serum and radiolabeled 12 h post-infection. Alternatively, QM5 cells expressing p15 constructs were radiolabeled 18-24 h post-transfection (generally, when syncytia contained 5-10 nuclei). Infected or transfected cell monolayers were either (1) leucine-starved 15 minutes, then radiolabeled for 45 minutes with 50 μCi [^{3}H]leucine (Amersham Biosciences) per mL leucine-free MEM (SelectAmine kit; Life Technologies); (2) labeled 4 hours with 20 μCi [^{3}H]myristate (Amersham Biosciences) per mL Eagle's MEM (Life Technologies) containing 1% dialyzed FBS; or (3) incubated 40 minutes with phosphate-free DMEM (Sigma) in the presence or absence of 100 μg/mL cycloheximide, then labeled with 100 μCi [^{32}P]phosphate (Amersham Biosciences) per mL phosphate-free DMEM containing 20 μM forskolin in the presence or absence of 100 μg/mL cycloheximide. Radiolabeled monolayers were rinsed three times with PBS and lysed in cold RIPA buffer containing protease inhibitors (Sigma; 200 nM aprotinin, 1 μM

leupeptin, and 1 μM pepstatin) and phosphatase inhibitors (Sigma; 500 μM nitrophenyl phosphate, 50 μM sodium orthovanadate, 1 mM sodium fluoride, 1 mM EDTA), as required. Cell lysates were harvested and the nuclei pelleted, 1 min at 10,000 x *g* in a bench-top microfuge.

2.12. Immune precipitation

Aliquots of [^{3}H]leucine-labeled, *in vitro*-translated protein (1/10 translation reaction) or radiolabeled cell lysate (equivalent to 1-3 wells of a 6-well plate) were immune precipitated in RIPA buffer containing protease inhibitors for 1 h by using a 1:100 dilution of antisera. Immune complexes were recovered by using fixed *Staphylococcus aureus* cells, washed extensively with RIPA buffer, and released by boiling in Laemmli's SDS protein sample buffer prior to SDS-PAGE and fluorography (Bonner, 1984).

2.13. Antibody inhibition

To test the ability of antisera to inhibit p15-induced syncytium formation, complement-fixed normal rabbit serum or polyclonal rabbit antisera raised against either the p15 C-terminus or N-terminus, diluted 1:10 in culture medium supplemented with 10% FBS, was added to p15-expressing QM5 cells 4 h post-transfection. Antisera were refreshed at 18 h post-transfection. The extent of syncytium formation was measured by syncytial index (see below), 24 h post-transfection, relative to the normal rabbit serum control.

2.14. Metabolic inhibitors

To investigate the intracellular trafficking of p15, cells expressing p15 were treated with an inhibitor of vesicle transport prior to the onset of syncytium formation. Transfected QM5 were incubated with or without brefeldin A (1 μg/mL) for 3 h, beginning 12-15 h post-transfection. Fixed monolayers were examined for evidence of cell-cell fusion.

To assess the N-linked glycosylation status of several p15 mutants, transfected cells were incubated with or without an inhibitor of N-glycan addition, tunicamycin (10 μg/mL), for 2 h prior to radiolabeling (in the presence or absence of tunicamycin) at 16 h post-transfection. Radiolabeled lysates were immune precipitated and analyzed by SDS-PAGE and fluorography (Bonner, 1984).

2.15. Visualization and quantification of syncytium formation

2.15.1. Nuclei staining

Vero or QM5 cells grown in 6- or 12-well plates were transfected as above. Monolayers were fixed and permeabilized with methanol and stained with Wright-Giemsa stain (Diff-Quik) according to the manufacturer's instructions (VWR Scientific) to visualize cell nuclei and polykaryon formation. Images of stained cells were visualized on a Nikon Diaphot inverted microscope at 200x magnification and captured by using computer software Image-Pro Plus (version 4.0).

2.15.2. Syncytial index assay

The relative ability of various p15 mutants to mediate syncytium formation was quantified by a syncytial index assay. The number of syncytial nuclei present in 5 random

fields of view was determined for each transfected cell sample by microscopic examination of Giemsa-stained transfected cell monolayers at 200x magnification. Counting the average number of syncytial nuclei per field typically provides a more accurate measure of a construct's fusogenic potential than measuring either the number of syncytia or the number of nuclei per syncytium (which was used in certain instances). This is particularly evident when comparing the fusogenicity of mutants that induce the formation of many small syncytia versus the formation of few small syncytia. Unless otherwise stated, syncytial index results were reported as the mean +/- the standard error from three separate experiments performed in triplicate.

2.16. Immunostaining

Transfected monolayers were methanol-fixed 20-24 h post-transfection, prior to immunostaining and monolayers were pre-blocked with PBS containing 25 μg/mL whole goat IgG (Jackson ImmunoResearch). Transfected foci were detected (unless otherwise stated) using primary rabbit polyclonal antiserum specific for full-length p15 (diluted 1:600-1:1000). Foci were visualized using secondary goat anti-rabbit $F(ab')_2$ conjugated to either alkaline phosphatase (Jackson ImmunoResearch, diluted 1:1000) or fluorescein isothiocyanate (FITC; Jackson ImmunoResearch, 1:800). For co-immunofluorescence, monolayers were additionally stained using mouse anti-calnexin IgG_1 (BD Transduction Laboratories, 1:1000) and tetramethyl rhodamine isothiocyanate (TRIC)-conjugated goat anti-mouse IgG (Jackson ImmunoResearch, 1:1000). To detect HA-tagged p15 clones, fixed and transfected cells were blocked with whole rat IgG (Jackson ImmunoResearch), and stained using primary mouse monoclonal anti-HA antibody (clone 12CA5; diluted

1:400-1:1000) and secondary rat anti-mouse $F(ab')_2$ conjugated to alkaline phosphatase (Jackson ImmunoResearch; diluted 1:1000). Cells fixed on coverslips and stained for immunofluorescence were mounted on glass slides with fluorescent mounting medium (Dako). Images of immunocytochemically stained cells were captured using a Nikon Diaphot inverted microscope (200× magnification) and computer software Image-Pro Plus (version 4.0). Images of indirectly stained immunofluorescent cells were captured using a Ziess Axiovert microscope (630× magnification) and Axiovision software.

2.17. Visualization of p15 at the cell periphery

To detect cell surface-expressed p15, cells seeded on coverslips of 0.1 mm thickness in cluster plates were transfected as above when subconfluent (to ease visualization of single-cell foci). The intracellular pool of p15 was depleted prior to immunofluorescent staining by 1 h cycloheximide treatment (100 μg/mL) 18-20 hours post-transfection. Monolayers were then methanol-fixed and mounted on glass slides with fluorescent mounting medium (Dako). Indirectly stained immunofluorescent p15-transfected cells, as well as GFP- and GFP-chimera-transfected cells, were visualized and photographed using a Zeiss LSM510 scanning argon laser confocal microscope (1000x magnification). Images shown represent one Z section (approximately 0.1 μM).

2.18. Circular dichroism spectroscopy

The authentic (VQPPAPPPNA) and mutant (VQPAAAPANA) p15 peptides analyzed by CD spectroscopy were synthesized and purified to greater than 95% by Dalton Chemical Laboratories, Inc. Poly-L-proline was purchased from Sigma. All CD spectra were acquired using a Jasco J-810 spectropolarimeter and a quartz cuvette with a

0.1 cm optical path. The p15 peptides were dissolved in phosphate buffer (10mM, pH 7) to a final concentration of 0.2 mg/mL. Measurements were taken between 250 and 200 nm. For measurements using different buffers, the peptides were dissolved to the same concentration in buffer containing either 3 M urea or 4 M NaCl. Owing to the absorbance and light scattering of the buffer components in these solutions at short wavelengths, measurements were taken to 210 nm. Ten scans were acquired and summed for each sample, and the resulting spectrum was smoothed to remove residual noise.

CHAPTER 3

IDENTIFICATION OF p15 AS THE FUSION PROTEIN OF BRV

3.1. Introduction

The handful of nonenveloped viruses reported to have the unusual ability to induce cell-cell fusion are all members of the *Reoviridae* (Duncan *et al.*, 1995). The *Reoviridae* are a large family of nonenveloped viruses that exhibit a double-shelled, icosahedral capsid morphology and whose genomes consist of 10-12 linear segments of double-stranded (ds) RNA (Nibert *et al.*, 1996). Reoviruses are widely distributed in nature, infecting both vertebrate and invertebrate animals, as well as plants (Nibert *et al.*, 1996). The *Reoviridae* currently include ten accepted and two proposed genera (Table 3.1) (Mertens *et al.*, 2000). The different genera display distinct capsid morphologies, host ranges, biological properties, replication strategies, electropherotypes and protein compositions (Murphy *et al.*, 1995; Pereira, 1991). While there are reports of fusogenic rotavirus (Gelberg *et al.*, 1990; Theil and Saif, 1985), orbivirus (Theil and McCloskey, 1991), and aquareovirus (Winton *et al.*, 1987) isolates, the most extensively characterized fusogenic members of the *Reoviridae* belong to the genus *Orthoreovirus* (Blahak *et al.*, 1995; Duncan *et al.*, 1995; Duncan *et al.*, 1996; Duncan and Sullivan, 1998; Duncan *et al.*, 2004; Gard and Compans, 1970; Ni and Ramig, 1993; Petek *et al.*, 1967; Wilcox and Compans, 1982).

Virus isolates classified to the *Orthoreovirus* genus share a well-defined capsid structure by electron microscopy (EM), a conserved 3'-terminal pentanucleotide signature sequence (TCATC-3') in the genomic segment cDNAs, and distinct genome and protein profiles (Duncan, 1999; Murphy *et al.*, 1995; Nibert *et al.*, 1996). While

Table 3.1. **The *Reoviridae*** (adapted from Nibert *et al.*, 1996).

Genus	**Genome Segments**	**Host Range**
Orthoreovirus	10	mammals, birds, reptiles
Rotavirus	11	mammals, birds
Aquareovirus	11	fish, molluscs
Orbivirus	10	arthropods*, mammals, birds
Coltivirus	12	arthropods*, mammals
Seadornavirus	12	arthropods*, mammals
Oryzavirus	10	arthropods*, plants
Phytoreovirus	12	arthropods*, plants
Fijivirus	10	arthropods*, plants
Cypovirus	10	insects
Entomoreovirus (proposed)	11	insects
Mycoreovirus (proposed)	12	fungi

*Serve as vectors for transmission to other hosts.

members of the *Orthoreovirus*, *Orbivirus*, and *Cypovirus* genera all contain 10 genome segments, the *Orthoreovirus* genome exhibits a characteristic migration pattern with three large (L), three medium (M), and four small (S) segments, which encode the corresponding λ, μ, and σ size class proteins. On the basis of host range and comparisons of the S-class genome segments, the *Orthoreovirus* genus can be separated into distinct subgroups categorized as either fusogenic or nonfusogenic based on their ability to induce syncytium formation (Duncan, 1999; Mertens *et al.*, 2000). The nonfusogenic *Orthoreovirus* subgroup is exemplified by the mammalian reovirus (MRV) species, considered the prototypical reovirus. The fusogenic subgroup is currently comprised of four species: (1) avian reovirus (ARV), representing multiple strains of chicken, duck, turkey and goose origins; (2) the mammalian Nelson Bay virus (NBV); (3) reptilian reovirus (RRV), representing several fusogenic isolates from snakes, lizards, and iguanas; and (5) baboon reovirus (BRV), the identification of which is summarized below.

Although the prototypical MRV is not associated with a natural disease state, the fusogenic orthoreoviruses are pathogenic in their natural hosts, a phenotype that may be related to the syncytium-inducing property of these viruses (Duncan *et al.*, 1996; Duncan and Sullivan, 1998). From January, 1993 to January, 1994, an outbreak of meningoencephalomyelitis occurred in a colony of baboons (*Papio cynocephalus*) housed at the Southwest Foundation for Biomedical Research (SFBR, San Antonio, Texas). Virus capable of inducing syncytium formation in Vero cells was isolated from the brain tissues of five of the eight affected juvenile baboons (9578, 10718, 10406, 10607, and 10895) (Leland *et al.*, 2000). From the group of five isolates, the virus isolated from baboon 10895 was selected as the representative strain (Leland *et al.*, 2000). This virus

was classified as an orthoreovirus based on its nonenveloped, double-shelled capsid morphology, as determined by EM, and its genome profile consisting of 10 segments of dsRNA (Duncan *et al.*, 1995; Leland *et al.*, 2000). Thus, baboon reovirus 10895 (herein referred to as BRV), represented the first orthoreovirus to be isolated from baboons, and joined the growing group of orthoreoviruses identified as being capable of inducing syncytium formation – a highly unusual phenotype for nonenveloped viruses.

Comparison of the genome and protein profiles, as well as the antibody epitope conservation, between BRV, MRV, ARV and NBV, supported the classification of BRV as a novel orthoreovirus (Duncan *et al.*, 1995). Although the dsRNA segments of the BRV genome migrate in the pattern characteristic of the orthoreoviruses, with three L, three M, and four S segments, the BRV genome profile is distinct. Most notably, the BRV genome contains an abnormally fast migrating S4 segment, and lacks the distinguishing retarded S1 segment migration that is a hallmark of the fusogenic reoviruses, ARV and NBV (Duncan *et al.*, 1995). The genomes of diverse orthoreoviruses contain a polycistronic S-class segment. Typically, the orthoreovirus S1 segment encodes the σ1/σC cell attachment protein and a small nonstructural protein. The S1 segments of ARV, NBV and RRV contain an additional 5' open reading frame (ORF) encoding the factor responsible for cell-cell fusion – a member of the FAST protein family (Corcoran and Duncan, 2004; Shmulevitz and Duncan, 2000). It was expected therefore that the fusogenic BRV would also encode a FAST protein within its S-class genome segments.

Extensive sequence diversity exists between the gene products of BRV and the homologous gene products of other orthoreoviruses (Duncan, 1999). With the expectation

that this level of evolutionary diversity might offer additional insights into FAST protein structure and function, it was undertaken to identify the BRV fusion-inducing protein. The analysis presented in this chapter indicates that the BRV S4 genome segment is functionally bicistronic, encoding two 140- to 141-amino acid BRV-specific gene products. S4 is the only polycistronic S-class genome segment of BRV. Consistent with the fusogenic orthoreoviruses encoding a fusion-inducing protein on a polycistronic genome segment, the gene product of the 5'-proximal ORF of S4, p15, was identified as the protein responsible for BRV-induced syncytium formation. Sequence analysis revealed that BRV p15 shares no significant similarity, with respect to overall sequence or predicted domain organization, to the p10 proteins of ARV and NBV, or the p14 protein of RRV and, as such, p15 represents a novel member of the FAST protein family.

3.2. Results

3.2.1. BRV sigma-class protein profile

Sequence analysis previously revealed that the BRV S1, S2, and S3 genome segments encoded the major σ-class core, outer capsid, and nonstructural proteins of the virus (Duncan, 1999). Therefore, in order to determine whether BRV encoded a FAST protein homologue within its S-class genome segments, a molecular analysis of the remaining S-class genome segment of BRV, S4, was undertaken. As shown in Figure 3.1A, the gene products of the S1, S2, and S3 genome segments, derived by *in vitro* transcription and translation, corresponded to the dominant σ-class proteins present in [^{3}H]leucine-labeled BRV-infected cell lysates. The products of the S1 ORF (major core

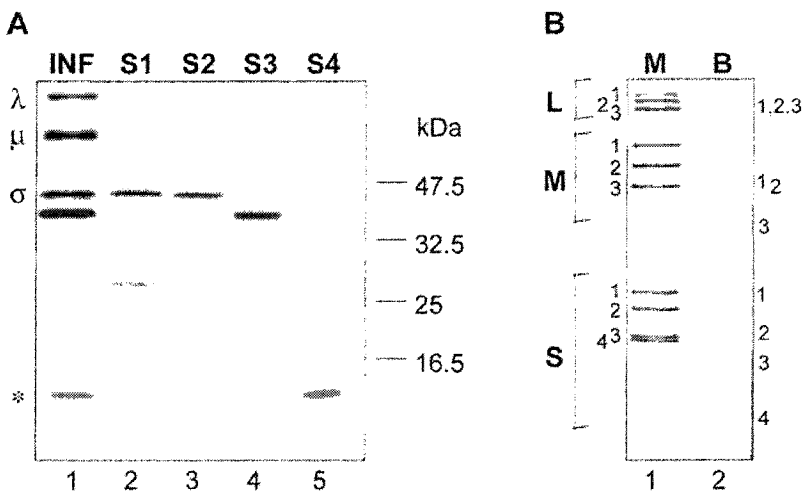

Figure 3.1. **Identification of the σ-class proteins encoded by the BRV S-class genome segments.** (A) The relative gel mobilities of the *in vitro* translation products of the BRV S1, S2, S3, and S4 genome segments, resolved by SDS-15% PAGE, are compared to the dominant viral bands present in [^{3}H]leucine-labeled BRV-infected cell lysate (INF). The positions of the λ-, μ-, and σ-class reovirus proteins are shown at the left. The asterisk denotes the location of an approximately 15-kDa polypeptide present in the infected cell lysate that comigrates with the translation product(s) of the S4 genome segment. The relative mobilities of molecular mass markers are indicated at the right. (B) Double-stranded RNA genome segment profiles of mammalian reovirus type 3, Dearing (M), and baboon reovirus (B) resolved by SDS-10% PAGE and detected by silver staining. The positions of the BRV S1 (1,311 nt), S2 (1,253 nt), S3 (1,150 nt), and S4 genome segments are indicated at the right. Figure 3.1B adapted from Duncan (1999).

protein; 413 codons) and the S2 ORF (major outer capsid protein; 396 codons) co-migrated on SDS-15% polyacrylamide gels (Fig. 3.1A, lanes 2 and 3), slightly behind the product of the S3 ORF (major nonstructural protein; 353 codons; Fig. 3.1A, lane 4). Interestingly, a low-molecular-mass polypeptide of approximately 15 kDa was detected in the BRV-infected cell lysates that co-migrated with a product of the S4 gene (Fig. 3.1A, lane 5). The migration pattern of the S4-specific polypeptide was surprising since the relative gel mobility of the BRV S4 genome segment (Fig. 3.1B) suggested a molecular size of roughly 800 to 900 bp, sufficient to encode a protein at least twice the size of the 15-kDa polypeptide generated by *in vitro* translation of S4.

3.2.2. BRV S4 is functionally bicistronic

Consistent with the *in vitro* translation results, the cDNA sequence of the BRV S4 genome segment indicated the presence of two sequential partially overlapping ORFs rather than a single ORF spanning most of the genome segment (Fig. 3.2). Two independent clones yielded the same sequence, confirming the bicistronic gene arrangement of BRV S4. The first ORF contains 140 codons and encodes a predicted 15-kDa protein (molecular mass of 15,223 Da), termed p15. The second ORF encodes a predicted 16-kDa protein (molecular mass of 16,723 Da), p16, from one of two adjacent in-frame potential initiator methionine codons. Both methionine codons are in a preferred context for an initiator methionine with purines in the -3 and +4 positions (Kozak, 1991; Kozak, 1989), and it is unclear which functions as the initiation site for the 140- to 141-amino acid p16 protein.

Figure 3.2. **The BRV S4 genome segment contains two partially overlapping ORFs.** The cDNA sequence of the BRV S4 genome segment is shown along with the predicted amino acid sequences encoded by two sequential ORFs. ORF1 (nt 25 to 447) encodes p15, a 140-amino acid protein with a predicted molecular mass of 15 kDa. ORF2 (nt 413 to 835) encodes p16, a 140- to 141-amino acid protein with a predicted molecular mass of 16 kDa. The locations of the p15 start codon, the two adjacent potential p16 start codons, and the other two methionine codons that precede the p16 ORF, are underlined. The nucleotides comprising the 5'- and 3'-terminal noncoding regions are in lowercase. Nucleotide and amino acid numbering is indicated at the right.

Figure 3.2

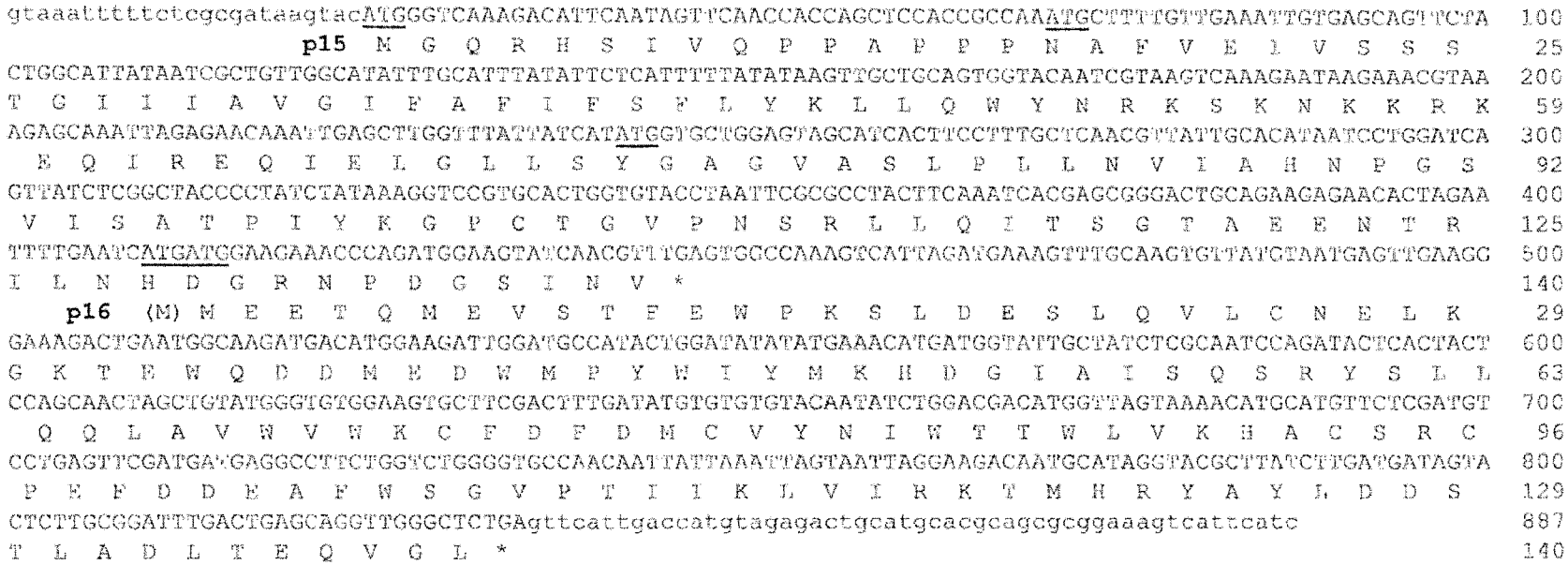
gtaaatttttctcgcgataagtacATGGGTCAAAGACATTCAATAGTTCAACCACCAGCTCCACCGCCAAATGCTTTTGTTGAAATTGTGAGCAGTTCTA 100
p15 M G Q R H S I V Q P P A P P P N A F V E I V S S S 25
CTGGCATTATAATCGCTGTTGGCATATTTGCATTTATATTCTCATTTTTATATAAGTTGCTGCAGTGGTACAATCGTAAGTCAAAGAATAAGAAACGTAA 200
T G I I I A V G I F A F I F S F L Y K L L Q W Y N R K S K N K K R K 59
AGAGCAAATTAGAGAACAAATTGAGCTTGGTTTATTATCATATGGTGCTGGAGTAGCATCACTTCCTTTGCTCAACGTTATTGCACATAATCCTGGATCA 300
E Q I R E Q I E L G L L S Y G A G V A S L P L L N V I A H N P G S 92
GTTATCTCGGCTACCCCTATCTATAAAGGTCCGTGCACTGGTGTACCTAATTCGCGCCTACTTCAAATCACGAGCGGGACTGCAGAAGAGAACACTAGAA 400
V I S A T P I Y K G P C T G V P N S R L L Q I T S G T A E E N T R 125
TTTTGAATCATGATGGAAGAAACCCAGATGGAAGTATCAACGTTTGAGTGCCCAAAGTCATTAGATGAAAGTTTGCAAGTGTTATCTAATGAGTTGAAGG 500
I L N H D G R N P D G S I N V * 140
p16 (M) M E E T Q M E V S T F E W P K S L D E S L Q V L C N E L K 29
GAAAGACTGAATGGCAAGATGACATGGAAGATTGGATGCCATACTGGATATATATGAAACATGATGGTATTGCTATCTCGCAATCCAGATACTCACTACT 600
G K T E W Q D D M E D W M P Y W I Y M K H D G I A I S Q S R Y S L L 63
CCAGCAACTAGCTGTATGGGTGTGGAAGTGCTTCGACTTTGATATGTGTGTGTACAATATCTGGACGACATGGTTAGTAAAACATGCATGTTCTCGATGT 700
Q Q L A V W V W K C F D F D M C V Y N I W T T W L V K H A C S R C 96
CCTGAGTTCGATGATGAGGCCTTCTGGTCTGGGGTGCCAACAATTATTAAATTAGTAATTAGGAAGACAATGCATAGGTACGCTTATCTTGATGATAGTA 800
P E F D D E A F W S G V P T I I K L V I R K T M H R Y A Y L D D S 129
CTCTTGCGGATTTGACTGAGCAGGTTGGGCTCTGAgttcattgaccatgtagagactgcatgcacgcagcgcggaaagtcattcatc 887
T L A D L T E Q V G L * 140

To determine which of the two S4 ORFs produced the estimated 15-kDa band evident in the σ-class protein profile (Fig. 3.1A, lane 5), the individual S4 ORFs were subcloned and separately translated *in vitro*. The presence of specific translation products was detected by immune precipitation with polyclonal rabbit antiserum raised against the products of either ORF1 or ORF2. While both antisera recognized an approximately 15-kDa polypeptide produced in the S4 translation mixture (Fig. 3.3A, lanes 1 to 3), only the anti-p15 serum reacted with the product of ORF1 (Fig. 3.3A, lanes 4 to 6), while only the anti-p16 serum reacted with the product of ORF2 (Fig. 3.4A, lanes 7 to 9). The specific antisera were also used to confirm that both ORFs were functional in virus-infected cells (Fig. 3.3B). Concurrent with the strong inhibition of host cell translation and abundant synthesis of the major λ-, μ-, and σ-class proteins evident in BRV-infected cell lysates, synthesis of both p15 and p16 was detected in cells productively infected with BRV (Fig. 3.3B, lanes 5 to 8). The specificity of the immune precipitations was evident by the absence of the 15-kDa polypeptides in uninfected cells (Fig. 3.3B, lanes 1 to 4) and by the inability of normal rabbit serum to precipitate these proteins (Fig. 3.3B, lanes 4 and 8). These results clearly indicated that the S4 genome segment of BRV is functionally bicistronic, encoding two distinct BRV-specific proteins that co-migrate on SDS-15% polyacrylamide gels.

3.2.3. BRV S4 ORF1 encodes a membrane fusion-inducing protein

Transfection of Vero cells with the S4 genome segment by itself induced syncytium formation (Fig. 3.4), while the other S-class genome segments failed to promote cell-cell fusion (data not shown). Clearly, one or both of the S4 gene products is

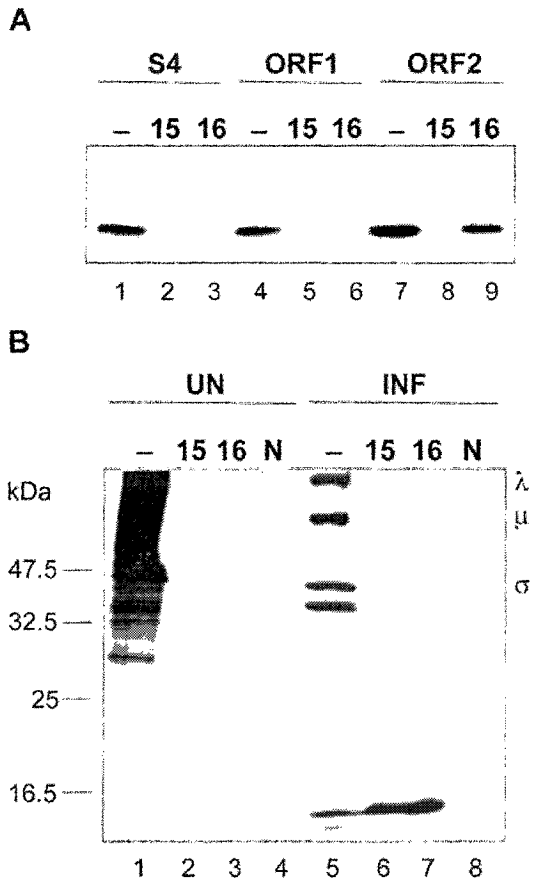

Figure 3.3. **The BRV S4 genome segment is functionally bicistronic.** (A) *In vitro* translation products of the entire S4 genome segment (lanes 1 to 3), S4 ORF1 (lanes 4 to 6), or S4 ORF2 (lanes 7 to 9) were fractionated without prior immune precipitation (-) or after immune precipitation with polyclonal antiserum raised against the product of ORF1, p15 (15), or the product of ORF2, p16 (16). (B) [^{3}H]leucine-labeled uninfected (UN) and BRV-infected (INF) cell lysates were fractionated by SDS-15% PAGE either without prior immune precipitation (-) or after immunoprecipitation with anti-p15-C serum (15), anti-p16 serum (16), or normal rabbit serum (N). The positions of the λ-, μ-, and σ-class reovirus proteins are indicated at the right. The relative mobilities of molecular mass markers are indicated at the left.

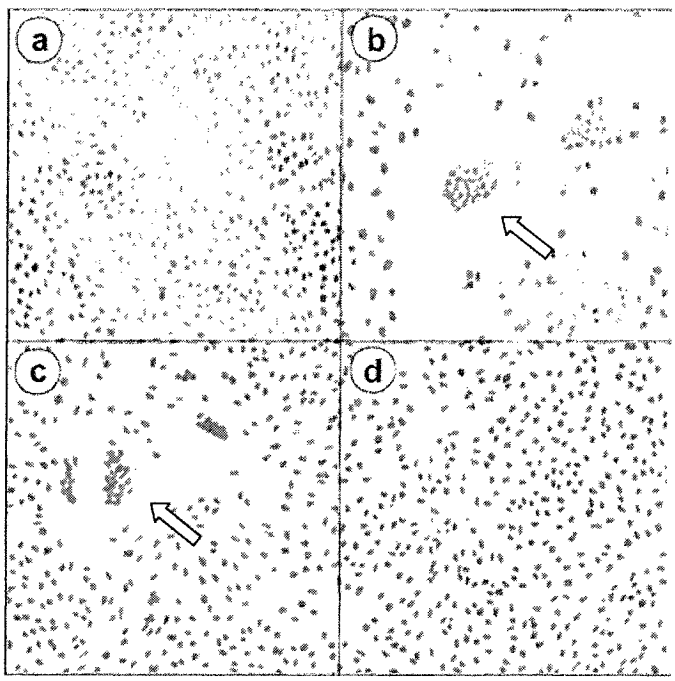

Figure 3.4. **ORF1 of the S4 genome segment encodes the membrane fusion-inducing protein of BRV.** Vero cells were transfected with pcDNA3 (a), pcDNA3-S4 (b), pcDNA3-S4 ORF1 (c), or pcDNA3-S4 ORF2 (d). Transfected monolayers were Wright-Giemsa stained 18 h post-transfection to detect the formation of multinucleated syncytia (examples of which are indicated by the arrows).

responsible for virus-induced syncytium formation. Expression of ORF1 resulted in syncytium formation equivalent to that induced by the entire S4 genome segment, while expression of ORF2 induced no cell fusion (Fig. 3.4). The synthesis of p15 within infected cells correlated with the appearance of syncytia (Fig. 3.5). Furthermore, transfection of increasing concentrations of the ORF1 expression plasmid generated more-extensive syncytium formation (Fig. 3.6). Together, these results indicated that the gene product of the first ORF of the S4 genome segment is the only BRV protein required to induce cell-cell fusion. Sequence comparisons of p15 with the p10 FAST proteins of ARV and NBV, and the p14 FAST protein of RRV revealed no significant overall sequence similarity. Furthermore, BLAST searches failed to identify any obvious sequence similarity to other proteins in the database. It can be concluded, therefore, that the BRV p15 protein represents a novel member of the FAST protein family.

3.2.4 BRV p15 is a nonstructural viral protein

The ability of BRV p15 to become incorporated into virions was examined. Concentrated, radiolabeled virus particles prepared from BRV-infected cell lysates revealed the characteristic reovirus protein profile with the major λ-, μ-, and σ-class proteins in addition to an approximately 15-kDa polypeptide (Fig. 3.7B, lane 1). Since the S4 gene products co-migrate by SDS-15% PAGE, Tricine-SDS-16.5% PAGE was used to better resolve p15 and p16. Under such conditions, the electrophoretic mobility of *in vitro* translated p16 is slightly greater than that of p15, and p16 co-migrated with the smallest σ -class protein observed in BRV particles (Fig. 3.7B, lane 2). Immune precipitation of detergent-solubilized BRV virions with the p15- and p16-specific antisera confirmed the identification of the smallest σ-class particle-associated protein as being p16 and not p15

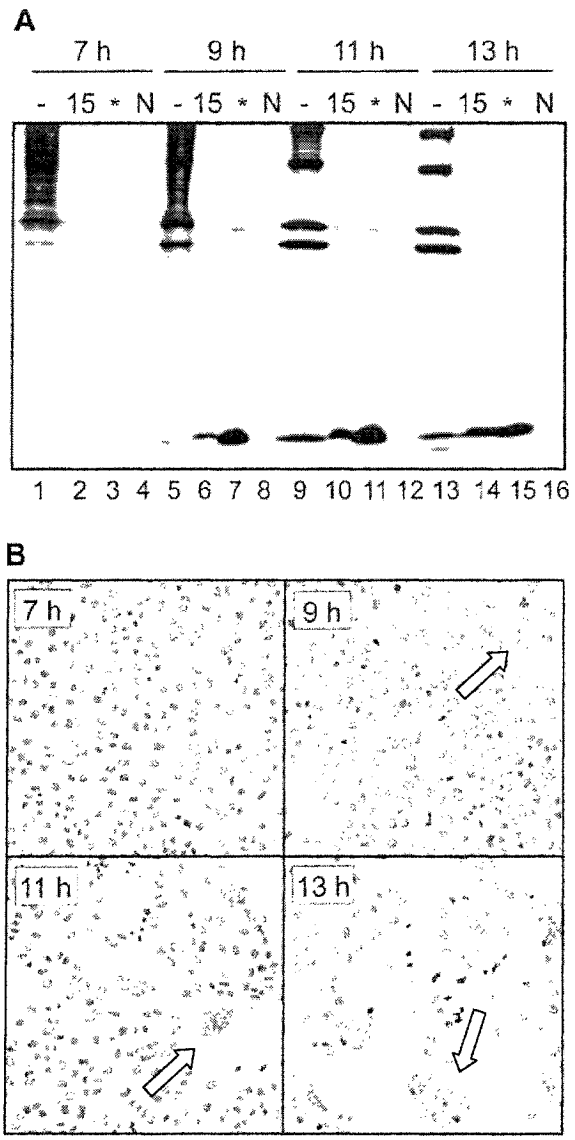

Figure 3.5. **Expression of p15 within BRV-infected cells correlates with syncytium formation.** (A) BRV-infected Vero cell lysates [^{3}H]leucine-labeled and harvested 7 h, 9 h, 11 h, or 13 h post-infection were either not immune precipitated (-), or immune precipitated using antiserum specific for the p15 C-terminus (15), or p16 (*), or normal rabbit serum (N). (B) BRV-infected Vero cells were methanol-fixed and Giemsa-stained at 7 h, 9 h, 11 h, or 13 h post-infection to detect the formation of multinucleated syncytia (examples of which are indicated by the arrows).

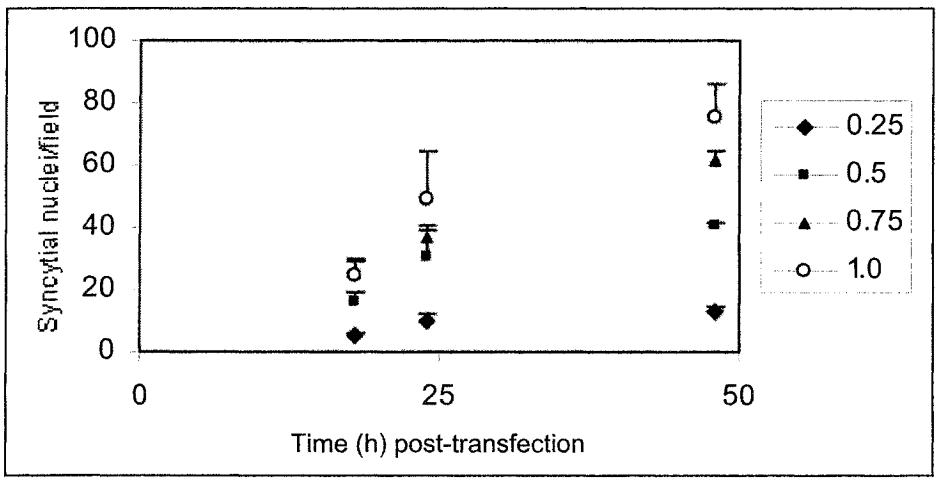

Figure 3.6. **Increasing amounts of BRV p15 lead to enhanced kinetics of syncytium formation.** The extent of syncytium formation present in QM5 cell monolayers at 18 h, 24 h, and 48 h post-transfection with 0.25 μg, 0.5 μg, 0.75 μg, or 1.0 μg of p15 cDNA was measured as the average number of syncytial nuclei per field of view at 20x magnification, for five random fields. The results represent a single experiment performed in triplicate.

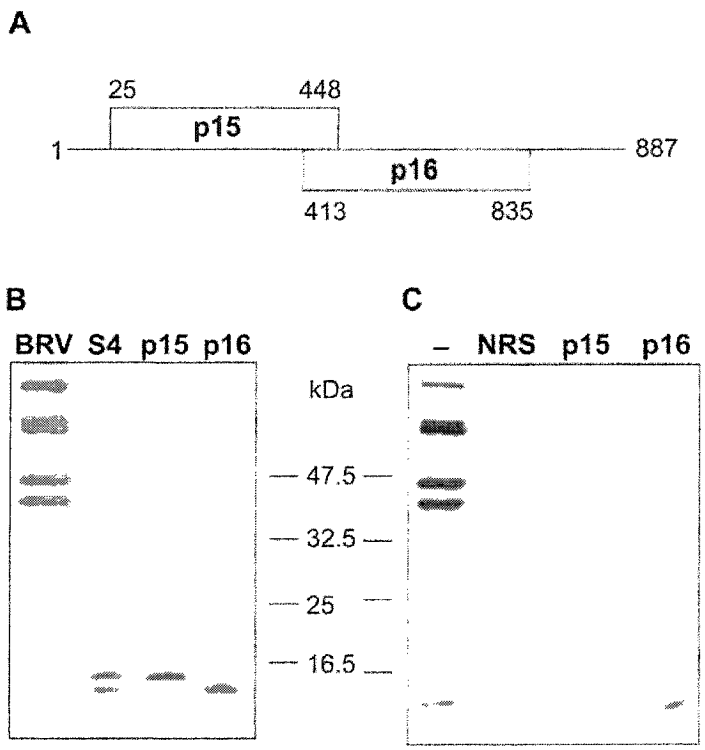

Figure 3.7. **BRV p15 is a nonstructural viral protein.** (A) Schematic diagram of the organization of the p15 and p16 ORFs of BRV S4; nucleotide positions are indicated. (B) The relative gel mobilities of the radiolabeled *in vitro* translation products of BRV S4, S4 ORF1 (p15), and S4 ORF2 (p16) were resolved by Tricine-SDS-16.5% PAGE and compared to the viral bands present in concentrated [^{3}H]leucine-labeled BRV particles. The migration of molecular mass markers is indicated at the right. (C) [^{3}H]leucine-labeled BRV particles either not immune precipitated (-) or immune precipitated using normal rabbit serum (NRS) or antiserum specific for either the p15 C-terminus or p16. The migration of molecular mass markers is indicated at the left.

(Fig. 3.7C). These results indicated that BRV p15 is a nonstructural membrane fusion-inducing protein.

3.2.5. Sequence-predicted structural motifs in p15

Several structural motifs predicted from the p15 amino acid sequence are indicated in Figure 3.8. Two stretches of predominantly apolar amino acids were identified, between residues 21 and 43 (hydrophobic domain 1, H1) and between residues 68 and 87 (hydrophobic domain 2, H2). Both of these apolar regions were identified as presumptive transmembrane (TM) domains using the TMpred (Persson and Argos, 1994), TMAP (Persson and Argos, 1997), SOSUI (Hirokawa *et al.*, 1998), and HMMTOP (Tusnády and Simon, 1998) algorithms. One or both of these domains may function as a signal anchor, as there is no evidence within the amino acid sequence of p15 of an N-terminal signal peptide (a cleavable N-terminal extension comprising 6 to 15 core hydrophobic residues) to direct membrane insertion. The intervening region (residues 44 to 63) between H1 and H2 is highly basic. This region, containing 9 of the 14 positively charged residues present in p15, contributes substantially to the overall basic character of p15 (pI = 9.8). Seven of the positively charged amino acids in this region are clustered in a polybasic domain (residues 51-59) Additional motifs identified in p15 include an N-terminal myristylation consensus sequence (MGXXXS/T) and a proline-rich motif (PPAPPP; residues 10 to 15). The absence of extended heptad repeat sequences implies that p15 does not contain coiled-coil regions, suggesting that p15 cannot promote membrane fusion according to the proposed model for class I viral fusion proteins which involves the critical rearrangment of coiled-coil domins. Furthermore, aside from the predicted TM domains, the hydropathy profile of p15 reveals no additional hydrophobic

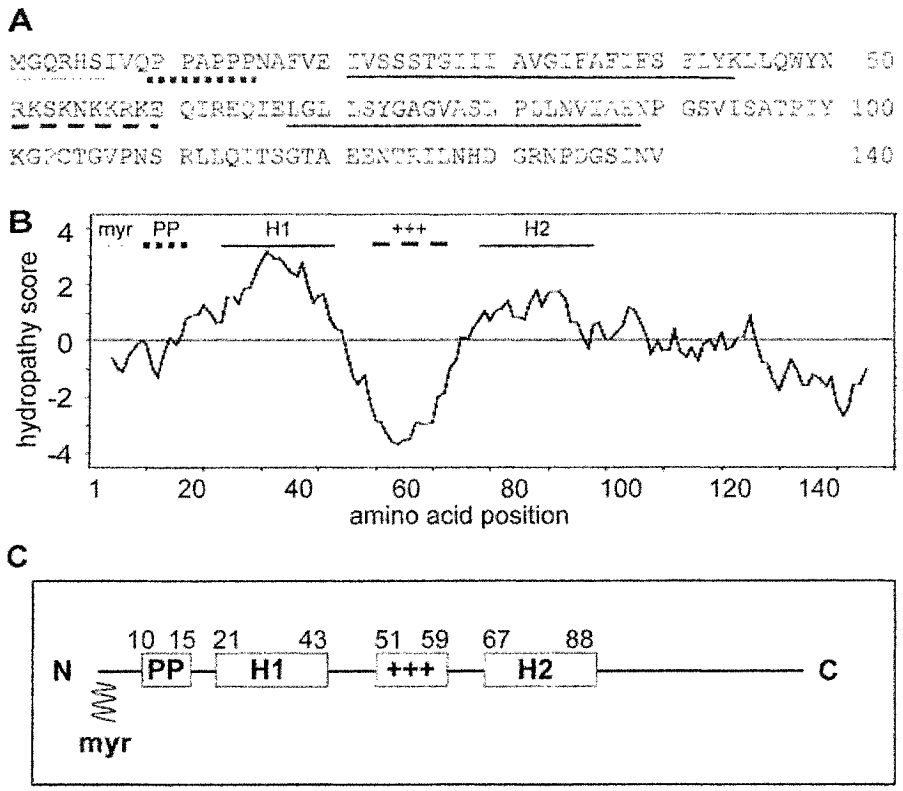

Figure 3.8. **Sequence-predicted structural motifs and hydropathy profile of p15.** (A) The amino acid sequence of p15 with the locations of several predicted structural motifs indicated (as labeled in B), including a myristylation consensus sequence (myr), a polyproline helix (PP), a polybasic region (+++), and two predicted TM domains, H1 and H2; amino acid positions are numbered. (B) The hydropathy profile of p15 as determined by using the hydrophobicity scale of Kyte and Doolittle, averaged over a window of 9 residues. Regions above the solid horizontal line are hydrophobic, while those below the line are hydrophilic. Amino acid positions are indicated. (C) Schematic diagram illustrating the relative positioning of various p15 structural motifs (defined above); amino acid positions are numbered; amino terminus (N); carboxy terminus (C).

clusters of sufficient size or hydrophobicity (i.e., 10-15 residues, hydrophobic index of >0.5) (White, 1990) that might function as a fusion peptide, a motif common to the vast majority of enveloped virus fusion proteins.

3.3. Discussion

3.3.1. Unique nature of the BRV S4 genome segment

Previous sequence analysis determined that the BRV S1, S2, and S3 genome segments encode the major σ-class core, outer capsid, and nonstructural proteins of the virus, homologous to the products of the S2, S3, and S4 genome segments of other reoviruses (Duncan, 1999). It was speculated that the remaining BRV S-class genome segment, S4, might represent a truncated version of the S1 genome segment of other orthoreoviruses. The MRV S1 genome segment is bicistronic, encoding the σ1 cell attachment protein and the small nonstructural protein, σ1NS, implicated in cell cycle arrest (Ernst and Shatkin, 1985; Jacobs and Samuel, 1985; Poggioli *et al.*, 2000; Rodgers *et al.*, 1998). The S1 genome segments of the fusogenic ARV, NBV, and RRV are also polycistronic, containing a 5'-proximal ORF encoding the fusion protein in addition to the downstream genes encoding the σ1 cell attachment protein homologue, σC, and in the case of ARV and NBV, an intervening ORF encoding a small nonstructural protein (p17) of unknown function (Bodelon *et al.*, 2001; Duncan, *et al.*, 2004; Shmulevitz *et al.*, 2002). BRV S4 shares with the S1 segment of the other reoviruses its polycistronic nature and, like the other fusogenic reoviruses, contains a 5'-proximal cistron encoding a small hydrophobic fusion protein. However, there is no significant overall sequence similarity between p15 and either p10 or p14, and these different proteins each possess a unique

repertoire of structural motifs (discussed in section 3.2.5.), suggesting that p15 is a novel member of the FAST protein family. Similarly, analysis of the p16 protein encoded by the downstream ORF in the BRV S4 genome segment revealed that p16 shares no sequence or structural similarity to either the orthoreovirus σ1/σC cell attachment proteins or the small nonstructural proteins σ1NS or p17, the other gene products encoded by the S1 genome segments of the other orthoreoviruses (Dawe *et al.*, 2002). Therefore, the BRV S4 genome segment encodes two novel BRV-specific proteins with no identified homology to any other viral or cellular proteins. Thus, BRV S4 does not represent a truncated version of the typical reoviral S1 segment. Given the lack of a σ1/σC homologue from the S-class genome segments of BRV, together with the appearance of the novel p16 protein, it was hypothesized that p16 served as the functional equivalent of σ1/σC. However, p16 was shown not to function as the cell attachment factor of BRV, as its removal from virions by freon extraction did not inhibit BRV infectivity (Dawe *et al.*, 2002). The role of p16 in the BRV replication cycle remains undefined, and it presently unclear how BRV binds host cells to initiate infection.

Interestingly, the S-class genome segment profile of BRV is comparable to that of an atypical strain of ARV, muscovy duck reovirus (DRV). The S1, S2, and S3 segments of both BRV and DRV encode the major σ-class reovirus core, outer capsid and nonstructural proteins (Duncan, 1999; Kuntz-Simon *et al.*, 2002), and the S4 segment of both viruses is bicistronic (Kuntz-Simon *et al.*, 2002). Unlike BRV however, the DRV S4 segment does represent a shortened version of the typical orthoreovirus S1 segment, encoding a truncated homologue of the σ1/σC cell attachment protein (Kuntz-Simon *et al.*, 2002). The 5' ORF of DRV S4 encodes a novel p10.8 protein, suspected to be a

FAST protein, although it shares no significant sequence similarity the p10 protein of the typical avian reoviruses, nor any other FAST protein identified (Kuntz-Simon *et al.*, 2002). It remains to be determined if p10.8 is responsible for DRV-induced cell-cell fusion.

3.3.2. Bicistronic gene arrangement of BRV S4

The p15 and p16 ORFs are organized on the bicistronic BRV S4 genome segment in an unusual sequential, partially overlapping fashion with start codons that are separated by 388 nucleotides (nt) and whose reading frames overlap by only 38 nt. A similar arrangement of sequential ORFs with minimal overlap exists for the functionally bicistronic S4 genome segment of DRV, the bicistronic S1 genome segment of RRV, and the tricistronic S1 genome segments of ARV and NBV (Bodelon *et al.*, 2001; Corcoran and Duncan, 2004; Kuntz-Simon *et al.*, 2002; Shmulevitz *et al.*, 2002). This situation is unlike the majority of polycistronic viral mRNAs, which contain two or more translation start codons located relatively close together resulting in significant overlap between the ORFs (Samuel, 1989). Leaky scanning (Kozak, 1991; Kozak, 1989) accounts for the ability of ribosomes to initiate translation at two alternate start sites in the majority of these bicistronic viral mRNAs.

Despite the considerable distance separating the two translation start sites on the BRV S4 genome segment, leaky scanning may account for the translation of p16. Although rare, ribosomes are known to scan as much as 900 nt (more than twice the distance separating p15 and p16 on S4) in order to initiate translation (Liu and Hobom, 2000). The initiator methionine codon for p15 (UACAUGG) lies within a suboptimal context, with a pyrimidine at the -3 position, which may enable preinitiation complexes to

scan through the p15 ORF in order to initiate translation of p16 at one of two potential tandem initiator methionine codons, both of which exist in a preferred context for translation initiation (purines at -3 and +4). Scanning preinitiation complexes would also need to bypass two additional suboptimal AUG codons in the +1 reading frame relative to the p15 ORF (Fig. 3.2). These AUG codons precede two minicistrons encoding four or six amino acids, respectively. Extended scanning past multiple upstream AUGs has been previously reported. For example, leaky scanning through 350 nt, including five upstream AUGs, accounts for the translation of the G protein from the borna disease virus unspliced M/G transcript (Schneider *et al.*, 1997).

Although leaky scanning may be solely responsible for translation of the bicistronic BRV S4 genome segment, alternative translation initiation mechanisms are operative with other bicistronic mRNAs whose ORFs are arranged in a sequential manner with minimal overlap. For example, translation of the HBV P protein from the bicistronic C/P mRNA is influenced by enhanced ribosomal reinitiation following the translation of an upstream 7-amino acid minicistron (Fouillot *et al.*, 1993). The efficiency of ribosomal reinitiation is affected by the length of the intercistronic region (Kozak, 1987). The 120-nt distance between the HBV minicistron and the P AUG is within the optimal length of 79-147 nt for reinitiation (Fouillot *et al.*, 1993; Kozak, 1987). Similarly, on BRV S4 the intercistronic distance between the second potential minicistron and the p16 AUG (156 nt) is of a comparable length. After bypassing the p15 AUG, ribosomal complexes may translate one or both of the potential S4 minicistrons in order to facilitate translation reinitiation at the p16 start site. In addition to reinitiation from an upstream minicistron, translation of the HBV P ORF also results from ribosome backscanning over 145 nt to

the P AUG after completing translation of the C protein (Hwang and Su, 1998). A similar backscanning mechanism contributes to expression of the ORF-2 protein of the human respiratory syncytial virus bicistronic M2 gene (Ahmadian *et al.*, 2000). Thus, it is possible that after finishing the translation of p15, ribosomes may scan backwards in order to reinitiate translation at the p16 AUG. Indeed, the 38 nt separating the p15 terminator from the p16 translation start site is within the range (less than 50 nt) required for efficient ribosomal backwards scanning (Peabody and Berg, 1986). Functional translation analysis of the BRV S4 genome segment is required to determine whether leaky scanning alone accounts for p16 expression or whether alternate forms of translational control may be operative.

3.3.3. p15 is a nonstructural, membrane fusion-inducing protein

Transfection analysis identified p15 as a rare example of a membrane fusion-inducing protein encoded by a nonenveloped virus. The absence of detectable p15 in concentrated BRV particles (Fig. 3.6) suggests that p15 is a nonstructural protein of the virus, as are the FAST proteins of ARV and NBV (Shmulevitz and Duncan, 2000). The nonstructural nature of the reovirus FAST proteins dictates that, unlike the fusion proteins of enveloped viruses, the FAST proteins are not involved in virus entry. Neither do the FAST proteins appear to be required for virus release. Prevention of FAST protein-induced cell-cell fusion by the vesicle transport inhibitor brefeldin A demonstrated that syncytium formation is not necessary for the replication or release of fusogenic reoviruses (Duncan *et al.*, 1996). The primary purpose of the FAST proteins appears to be the triggering of syncytium formation as a means of promoting a rapid lytic response and an enhanced rate of virus release, properties that correlate with the relative

pathogenicity of the fusogenic reoviruses (Duncan *et al.*, 1996; Duncan and Sullivan, 1998). Syncytium formation has been detected in the tissues of animals infected with ARV (Kibenge *et al.*, 1985), RRV (Lamirande *et al.*, 1999), and group B rotavirus (Chasey *et al.*, 1989). The potential syncytium-inducing property of p15 *in vivo* may similarly contribute to the pathogenic nature associated with BRV in nonhuman primates (Duncan *et al.*, 1995; Leland *et al.*, 2000).

3.3.4. Topological and functional implications of the p15 structural motifs

The p15 amino acid sequence does not appear to contain an N-terminal signal peptide. Therefore, if p15 integrates into membranes, one of the two predicted TM domains (identified by numerous different search algorithms), H1 or H2, must act as an internal, uncleaved signal anchor. Depending on whether a putative p15 signal anchor initiates the translocation of the N-terminal or C-terminal polypeptide, p15 may adopt either a bitopic type II (N_{cyt}) or type III (N_{exo}) membrane topology Alternatively, the presence of two potential membrane-spanning domains suggests that p15 may adopt a polytopic membrane topology. Since the polybasic region of p15 resides on the C-proximal side of the first predicted TM domain (Fig. 3.8), the basic inside rule (Matlack *et al.*, 1998; von Heijne and Gavel, 1988) supports an external topology for the N terminus of p15. If both of the H1 and H2 regions of p15 function as TM domains, then p15 lacks an essential feature of almost all viral membrane fusion proteins, namely, a fusion peptide motif. Aside from the two predicted TM domains, no other significant stretch of hydrophobic residues in p15 shares properties characteristic of a fusion peptide (White, 1990). If either H1 or H2 actually functions as a fusion peptide, then the relative hydrophobicities, calculated by using the Eisenberg normalized consensus scale

(Eisenberg, 1984), and the glycine-alanine content suggest the C-terminal H2 domain is the more likely of the two to serve as a fusion peptide (hydrophobicity of 0.59 with 30% glycine-alanine content). This would predict an N_{cyt} orientation for p15 (in contradiction to the basic-inside rule), since a putative fusion peptide would be expected to be surface-exposed. It is difficult to accurately predict the topology of a protein from its primary sequence since multiple signals may act cooperatively to determine its orientation and, in some cases (e.g. hepadnavirus L), a protein may adopt more than one topology. Consequently, based on sequence analysis alone, the orientation of p15 in the membrane, including whether p15 is a bitopic or polytopic membrane protein, was unclear.

3.3.5. BRV p15 represents a new class of FAST protein

The only known examples of nonenveloped viruses that induce syncytium formation are all members of the family *Reoviridae* (Duncan, 1999; Duncan *et al.*, 1995). Furthermore, the other S-class genome segment-encoded proteins of BRV share clear sequence similarity to the homologous proteins encoded by other orthoreoviruses (Duncan, 1999). It was, therefore, extremely surprising to find that BRV p15 not only shares no significant sequence similarity with the other reovirus fusion proteins but also that these different reovirus FAST proteins contain a diverse organization of predicted domains. A schematic comparison of the sequence-predicted domains of p15, p10, and p14 is shown in Fig. 3.9.

With a single signal anchor each (and no cleavable signal peptide), p10 and p14 assume a type III (N_{exo}) membrane topology (Corcoran and Duncan, 2004; Shmulevitz and Duncan, 2000). While p15 and p14 contain the consensus sequence for N-terminal myristylation, p10 is internally palmitylated on two conserved, cytoplasmic cysteine

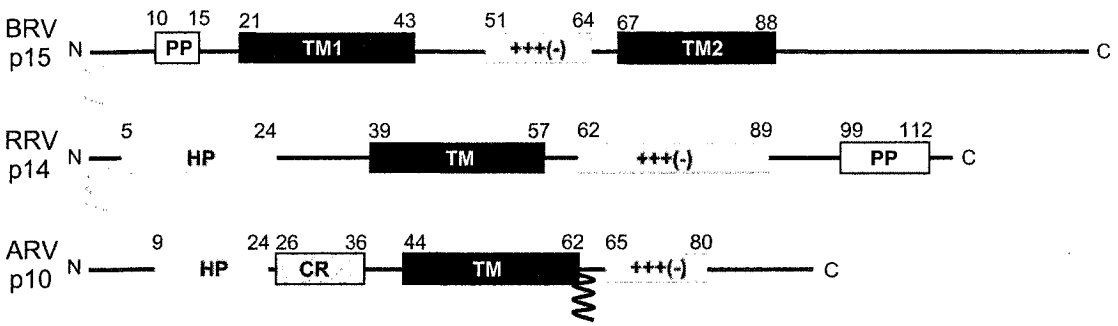

Figure 3.9. **Diversity in the organization of sequence-predicted domains within the FAST protein family.** Structural motifs predicted from the amino acid sequences of BRV p15, RRV p14 and ARV p10 are compared schematically; PP, polyproline sequence; TM, potential transmembrane domain; HP, hydrophobic patch; CR, p10 conserved sequence region; +++(-), charged motif; grey squiggle indicates myristylation consensus sequence; black squiggle indicates predicted palmitylation site; amino acid positions are numbered.

residues adjacent to the transmembrane domain (Shmulevitz *et al.*, 2003). Although the palmitylation status of p15 has not been examined directly, the single cysteine residue (C104) of p15 is unlikely to be palmitylated given its position 17 residues downstream of H2. Palmitylated cysteine residues generally lie within, or immediately adjacent to, a TM domain. Furthermore, the replacement of C104 with serine did not eliminate p15 fusion activity (refer to Fig. 6.9.). Thus, if C104 is palmitylated, the modification is not essential. The C-proximal region of p14 (residues 99 to 112) and the N-proximal region of p15 (residues 10 to 15) each contain a proline-rich motif that is absent from p10. Conversely, while the presence of a fusion peptide within p15 is in question, the N-terminal domains of p10 and p14 each contain a unique hydrophobic patch, which are putative fusion peptides that can be modeled as looped structures (Corcoran, *et al.*, 2004; Shmulevitz *et al.*, 2004b). The hydrophobic patch of p10 is believed to form a cystine-noose, while the absence of cysteine residues within the p14 hydrophobic patch precludes such a structure. The novel structural motifs and domain organization of BRV p15 clearly distinguish this protein from both the p10 fusion protein of ARV and NBV and the p14 fusion protein of RRV.

The BRV p15 protein represents a new member of the reovirus FAST protein family. The features that currently define the reovirus FAST protein family include: (i) their nonstructural nature; (ii) their small size (10-15 kDa); (iii) the presence of at least one TM domain and a second region of significant hydrophobicity; (iv) a membrane-proximal basic cluster; (v) modification by acylation; (vi) the lack of both an obvious fusion peptide and the coiled-coil motif typical of many enveloped virus fusion proteins; and (vii) the ability to trigger membrane fusion in the absence of any other viral proteins.

It remains to be determined whether these shared characteristics contribute to a common mechanism of FAST protein-mediated membrane fusion or whether the unique features of these proteins determine divergent p10-, p14- and p15-induced fusion pathways. It seems clear, however, that the FAST proteins function to promote membrane fusion independent of extensive conformational changes in large, complex, multimeric proteins – the proposed mechanism utilized by the enveloped virus fusion proteins. Further functional analysis of the reovirus FAST proteins is likely to lead to alternative models of protein-mediated membrane fusion.

CHAPTER 4

MEMBRANE ORIENTATION, ACYLATION, AND CELL SURFACE EXPRESSION OF BRV p15

4.1. Introduction

Considering the role of p15 as a syncytium-inducing protein, it is expected that p15 should be membrane-associated and located at the surface of cells. The amino acid sequence of BRV p15 revealed two hydrophobic, potential membrane-spanning regions (H1, aa 21-43; H2, aa 68-87), one, or both, of which could function to anchor p15 in the lipid bilayer. The presence of two prospective TM domains, and the ensuing possibility that p15 adopts a polytopic membrane orientation, distinguishes p15 from other viral fusion proteins. The fusion proteins of the other fusogenic reoviruses, as well as the vast majority of enveloped viruses, are bitopic proteins containing a single membrane anchor. The only exceptions being the multi-spanning envelope protein (L) of hepadnaviruses (Berting *et al.*, 2000; Prange and Streeck, 1995), the VV 14-kDa fusion protein, which does not span the membrane (Vasquez and Esteban, 1999), and the E protein of TBEV, which contains two predicted tandem TM domains (Mandl *et al.*, 1989). However, TM2 of TBE E is not required for E function, and it is not known whether this domain, which serves as the signal sequence for a downstream protein, even remains membrane-embedded after polyprotein processing (Allison *et al.*, 1999).

In general, four classes of membrane proteins can be distinguished on the basis of their orientation in the bilayer and on the topogenic sequences involved in their insertion into the endoplasmic reticulum (ER) (reviewed by Spiess, 1995). Type I membrane proteins (which include the vast majority of enveloped virus fusion proteins) are initially

targeted to the ER by a cleavable, N-terminal signal sequence binding to the signal recognition particle (SRP), which in turn interacts with the SRP receptor at the ER membrane (reviewed by Walter and Johnson, 1994). The ribosome-nascent chain complex is subsequently released from both the SRP and SRP receptor, enabling the signal sequence to interact directly with the Sec61α subunit of the translocon and initiate the translocation of the downstream polypeptide. Translocation is terminated by a hydrophobic stop-transfer sequence which anchors the type I protein in the membrane in an N_{exo}/C_{cyt} orientation. The same Sec61 translocation machinery is also utilized for type II and type III membrane proteins but, in these cases, a single uncleaved topogenic domain, a so-called 'signal anchor', serves as both a signal sequence and as a membrane anchor (High *et al.*, 1991). Type II signal anchors initiate translocation of downstream (C-terminal) polypeptide resulting in an N_{cyt}/C_{exo} orientation, while type III signal anchors initiate translocation of upstream (N-terminal) polypeptide resulting in an N_{exo}/C_{cyt} topology. Determinants for the orientation of the signal anchor include the charge difference between the two flanking segments (positive charges impede translocation while negative charges promote translocation) (Beltzer *et al.*, 1991), the folding behaviour of the N-terminal domain (tightly folded domains hinder or prevent translocation) (Denzer *et al.*, 1995), and the length and hydrophobicity of the signal anchor itself (longer and more hydrophobic sequences favour N-terminal translocation) (Wahlberg and Spiess, 1997). Type IV ('tail-anchored') membrane proteins assume an N_{cyt}/C_{exo} orientation with the TM domain located very close to the C-terminus and are inserted into the ER by a different, as yet poorly understood, post-translational mechanism (Steel, 2002). In multispanning membrane proteins, downstream

transmembrane segments are affected by their own topogenic determinants and may also influence the orientation of the initial signal (Nilsson, 2000; Sato *et al.*, 1998).

BRV p15 does not appear to contain either a cleavable, N-terminal signal sequence of a type I membrane protein, or a C-terminal signal anchor of a type IV membrane protein. Thus, from its sequence, p15 is predicted to be either a single-spanning type II or type III membrane protein, or a polytopic membrane protein with two TM domains. Since the membrane insertion of proteins (particularly multispanning ones) is the result of multiple determinants, it is problematic to accurately predict topology from a primary sequence and, thus, the orientation of p15 must be determined experimentally. In view of the importance of membrane fusion protein ectodomains in promoting lipid bilayer mixing, establishing whether p15 is a bitopic or polytopic membrane protein and determining its orientation in the membrane is essential to elucidating how p15 functions to induce membrane merger.

Another feature by which BRV p15 can be demarcated from other viral fusion proteins is the consensus sequence for N-myristylation (aa 1-6), which, if functional, could potentiate an additional interaction between p15 and the membrane. Although it is not unusual for the fusion proteins of enveloped viruses to be modified by the addition of fatty acid, typically they are palmitylated on TM-proximal cysteine residues. Such is the case with the fusion proteins of retroviruses (Olsen and Andersen, 1999; Yang and Compans, 1996; Yang *et al.*, 1995), orthomyxoviruses (Veit *et al.*, 1991), paramyxoviruses (Caballero *et al.*, 1998), bunyaviruses (Andersson *et al.*, 1997) alphaviruses (Schmidt *et al.*, 1988; Schmidt *et al.*, 1979), rhabdoviruses (Schmidt and Schlesinger, 1979), coronoviruses (Schmidt, 1982) and baculoviruses (Zhang *et al.*,

2003). The p10 FAST proteins of ARV and NBV are also palmitylated in this manner (Shmulevitz *et al.*, 2003).

The role of acylation in the function of viral fusion proteins remains elusive. Studies with many enveloped virus fusion proteins have reported that palmitylation is dispensible for membrane fusion (Smit *et al.*, 2001; Whitt and Rose, 1991; Zhang *et al.*, 2003). The issue is especially contentious with respect to the influenza HA protein. Since Naeve and Williams (1990) initially reported that palmitylation was essential to HA-mediated membrane fusion, several others have countered that the modification is unnecessary (Jin *et al.*, 1996; Naim *et al.*, 1992; Schroth *et al.*, 1996; Steinhauer *et al.*, 1991). However, many of these latter studies were based on lipid-mixing assays, which measure hemifusion only. A recent investigation employing a content-mixing assay concluded that palmitylation of HA is required to specifically mediate the transition from hemifusion to fusion pore formation (Sakai *et al.*, 2002). This study is in contrast, however, with the earlier conclusion of Fischer *et al.* (1998), also based on a content-mixing assay, that palmitylation was not involved in formation of the fusion pore. Nevertheless, Fischer and colleagues (1998) did note that palmitylation was critical for HA-mediated syncytium formation. Despite the confusion over the nature of the contribution of acylation to virus-induced membrane fusion, the conservation of this modification of fusion proteins from diverse virus families hints that it is biologically significant.

In order to begin to elucidate how p15 functions to induce membrane merger, the membrane association and orientation, acylation status, and subcellular localization of this unusual fusion protein must first be determined. This chapter provides evidence that

p15 is a cell surface-expressed, integral membrane protein that is also N-myristylated. The detailed topological analysis undertaken for p15 demonstrates that p15 adopts the N_{exo}/C_{cyt} topology of a type III membrane protein with the H1 domain serving as the sole TM anchor. Thus, with just 20 residues, the p15 ectodomain is the smallest among known viral fusion proteins. Furthermore, in its short ectodomain, BRV p15 lacks a hydrophobic region that could potentially function as a fusion peptide, which is an essential motif of other viral fusion proteins. The unusual features of the p15 ectodomain hint that this protein employs a novel mechanism to induce membrane fusion.

4.2. Results

4.2.1. BRV p15 is an integral membrane protein

Of the predicted motifs in the primary structure of p15, the potential TM domains and the myristylation consensus sequence are of immediate interest since these motifs are known to play a role in protein membrane interactions, including topogenesis and subcellular localization (McCabe and Berthiaume, 1999; Resh, 1999). The presence of two potential TM domains suggested that p15 is an integral membrane protein. This prediction was confirmed through *in vitro* translation of p15 in the presence of microsomes. While p15 translated in the absence of membranes partitioned exclusively to the soluble fraction (Fig. 4.1A, lanes 1 and 2), all of the p15 translated in the presence of microsomal membranes was associated with the pelleted membrane fraction (Fig. 4.1A, lanes 3 and 4). Washing of the membrane pellet with a high-salt buffer failed to extract p15 (Fig. 4.1A, lanes 5 and 6), consistent with p15 assuming an integral membrane topology and suggesting that p15 contains at least one membrane-spanning domain. The

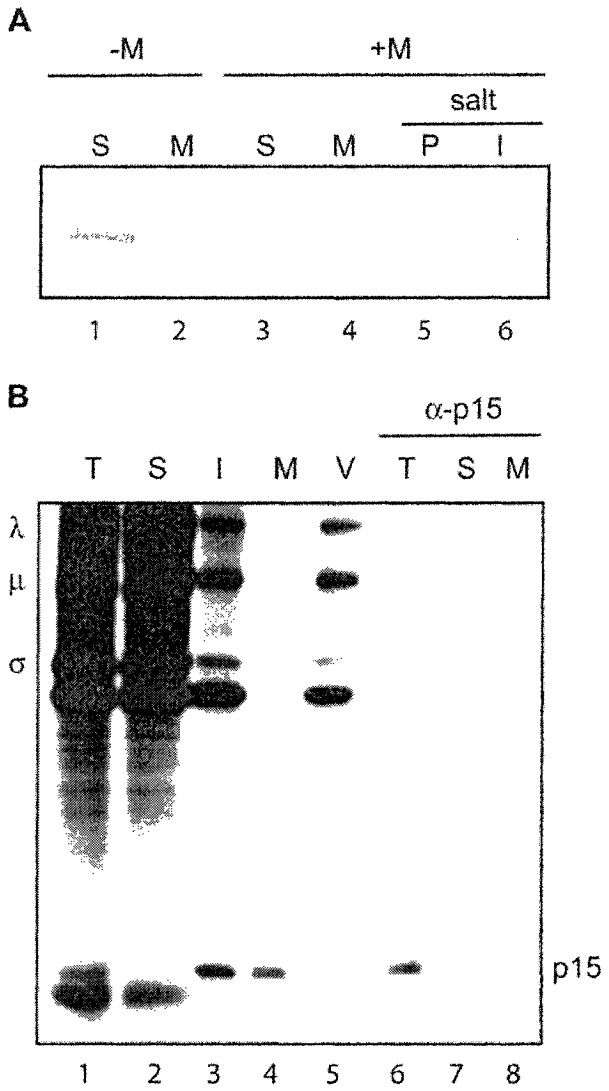

Figure. 4.1. **BRV p15 is an integral membrane protein.** (A) BRV p15 was translated *in vitro* without or with microsomal membranes (-M or +M) then separated into the soluble (S) and insoluble membrane-containing (M) fractions by centrifugation, the latter subsequently extracted with 0.5 M NaCl (salt) and re-centrifuged to separate the peripheral (P) and integral (I) membrane proteins. (B) [^{3}H]Leucine-labeled BRV-infected total cell lysate (T) was fractionated by centrifugation into the soluble (S) and insoluble virus- and membane-containing fraction (I), which was subsequently extracted with RIPA buffer and re-centrifuged to separate the membrane components (M) from the virus particles (V). Various fractions were either not immune precipitated, or immune precipitated using antiserum specific for the C-terminus of p15 (α-p15). The positions of the major λ, μ, and σ class BRV proteins are labeled at the left; the p15 protein at the right.

absence of a mobility shift for p15 translated in the presence of microsomes compared to p15 translated in their absence (Fig. 4.1A) indicated that, as predicted (chapter 3), there is no processing of a signal peptide upon p15 insertion into membranes.

The membrane association property of p15 was confirmed using BRV-infected cells. A p15 band was visible in, and immune precipitated from, the total cell lysate (Fig. 4.1B, compare lanes 1 and 6) as well as the membrane-containing fraction (Fig. 4.1B, compare lanes 4 and 8), but not the soluble fraction of infected cells (Fig. 4.1B, lanes 2 and 7). Concordant with its nature as a nonstructural BRV protein (chapter 3), following detergent extraction of the insoluble virus- and membrane-containing fraction (Fig. 4.1B, lane 3), p15 partitioned with the solubilized membrane component (Fig. 4.1B, lane 4) and was excluded from the re-pelleted virus (Fig. 4.1B, lane 5). These results were consistent with both the *in vitro* translation results and the sequence analysis and confirmed that p15 is an integral membrane protein.

4.2.2. BRV p15 is N-myristylated

To investigate whether BRV p15 was modified by myristylation, infected cells were labeled with [^{3}H]myristate and immune precipitated with p15-specific antiserum. The p15 antiserum specifically precipitated a 15-kDa radiolabeled polypeptide from infected cell lysates that was absent from uninfected cell lysates (Fig. 4.2A). Compared to the [^{3}H]leucine-labeled protein profile of infected cells (Fig. 4.1, lane 1), only a subset of cellular and viral proteins were [^{3}H]myristate-labeled (Fig. 4.2A, lanes 1 and 3), indicating that the radiolabeled myristate moiety was not metabolized into amino acids that would nonspecifically label viral proteins. These results indicated that p15 is a myristylated protein. BRV-infected cell lysates also contained a myristylated polypeptide

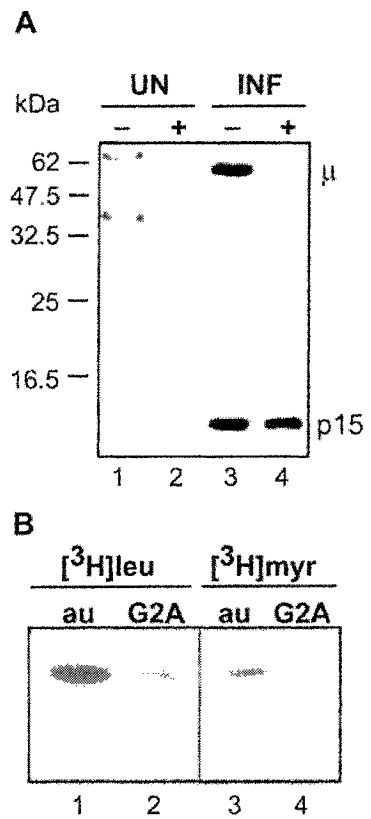

Figure. 4.2. **BRV p15 is myristylated at its N-terminus.** (A) Uninfected (UN) and BRV-infected (INF) [^{3}H]myristate-labeled cell lysates were resolved by SDS-15% PAGE either without prior immune precipitatation (-) or after immune precipitatation with anti-p15 serum (+). The positions of the myristylated μ-class reovirus protein and p15 are shown at the right. The locations of molecular mass markers are indicated at the left. (B) Authentic p15 (au)- or p15 G2A-transfected cell lysates labeled with [^{3}H]leucine (leu) or [^{3}H]myristate (myr) and immune precipitated using anti-p15 serum.

in the μ-class size range, which likely corresponds to the structural protein μ1 of MRV and its homologue in ARV, μ2, which are known to be myristylated (Nibert *et al.*, 1991; Varela *et al.*, 1996).

To confirm that it was the myristylation consensus sequence at the N-terminus (aa 1-6) of p15 that directed acylation of the protein, a mutant of p15 (G2A) was constructed in which the penultimate, myristate-accepting glycine was changed to alanine, thereby preventing the N-terminal myristylation of p15. While both authentic p15 and the G2A mutant were readily labeled with [^{3}H]leucine (Fig. 4.2B, lanes 1 and 2), only authentic p15 was able to incorporate [^{3}H]myristate (Fig. 4.2B, lanes 3 and 4).

The non-myristylated G2A construct interacted with membranes in a manner indistinguishable from that of authentic p15. Like authentic p15, G2A behaved as an integral membrane protein, partitioning into the membrane fraction of an *in vitro* translation mix (Fig. 4.3, lanes 2 and 6) and resisting stripping with 500 mM NaCl (Fig. 4.3, lanes 4 and 8). Thus, myristylation is not required to anchor p15 in the membrane, as expected given the presence of two potential TM domains.

4.2.3. BRV p15 is transported via the secretory pathway

The ability of brefeldin A (BFA), an inhibitor of ER-Golgi transport (reviewed by Pelham, 1991), to inhibit syncytium formation in p15-transfected cells (Fig. 4.4A) suggested that, like the other FAST proteins p10 (Shmulevitz and Duncan, 2000) and p14 (Corcoran and Duncan, 2004), p15 is trafficked through the secretory pathway to the cell surface. Consistent with this supposition, a significant level of co-fluorescence was observed in transfected cells stained for both p15 and the ER marker calnexin (Fig. 4.4B, right panel). While the p15-specific fluorescence predominantly surrounded the nucleus,

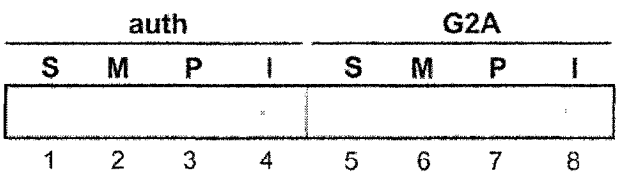

Figure. 4.3. **N-myristylation is not required to anchor p15 in the membrane.** Authentic p15 (auth) or p15 G2A transcripts were translated *in vitro* with microsomes and were separated by centrifugation into the soluble (S) and membrane-containing (M) fractions. The latter was extracted with 0.5 M NaCl and re-centrifuged to isolate the peripheral (P) and integral (I) membrane proteins.

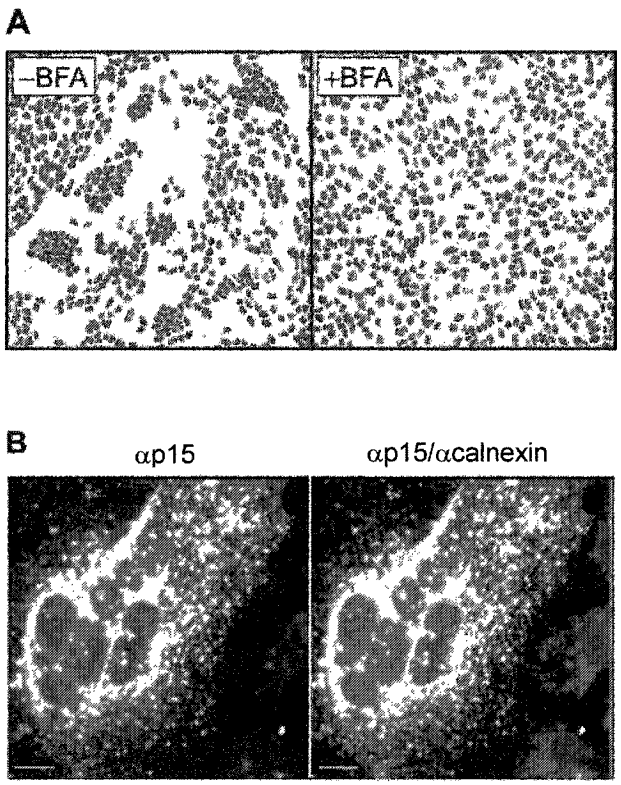

Figure. 4.4. **BRV p15 is transported via the secretory pathway.** Transfected QM5 cells expressing p15 were either: (A) incubated (15 h post-transfection) for 3 h -/+ BFA prior to methanol-fixation and Giemsa staining to visualize multinucleated syncytia, or (B) methanol fixed 24 h post-transfection and co-immunostained using rabbit anti-p15 serum and FITC-conjugated goat anti-rabbit $F(ab`)_2$ (left-hand panel), followed by mouse-anti calnexin and rhodamine-conjugated goat anti-mouse IgG (right-hand panel; yellow in merged image indicates co-localization). Cell images were captured using (A) a Nikon Diaphot inverted microscope (100x magnification), or (B) a Zeiss Axiovert microscope (1000x magnification); scale bar represents 10 μm. The image used to make Figure 4.4B was captured by C. Barber under supervision of S. Dawe.

p15 was also localized to what appeared to be dispersed cytopasmic vesicles extending out to the cell periphery (Fig. 4.4B). Several experimental approaches were used in an attempt to specifically demonstrate p15 at the cell surface.

4.2.4. Approaches to detect cell surface-expressed p15

Attempts were made to generate domain-specific p15 antisera for use as probes to detect cell surface-expressed p15 by indirect immunofluorescence. While the in-house generation of rabbit polyclonal antisera specific for the C-terminus (aa 90-140) of p15 was successful (the specificity of this antisera is illustrated in chapter 3), similar endeavors to raise antisera against the N-terminal 20 or 90 amino acids failed. Consequently, synthetic peptides corresponding to the p15 N-terminus (aa 4-23) and polybasic region (aa 47-61) were designed and used to raise polyclonal rabbit antisera (New England Peptide, Inc.). Unfortunately, these commercially generated antisera failed to react with p15 expressed in transfected cells (Fig. 4.5). Thus, in a final effort to make antiserum capable of recognizing epitopes in either the N-terminal or polybasic domains, polyclonal rabbit antiserum was generated in response to full-length p15 expressed in and purified from baculovirus. The specificity of this antiserum is clear; it readily stained syncytia formed in p15-transfected cells compared to no staining with normal rabbit serum (Fig. 4.5). Although antisera raised against either full-length p15 or the p15 C-terminus recognize p15 expressed within permeabilized infected or transfected cells, these antisera failed to react with p15 at the surface of intact cells (data not shown).

Unable to generate antibodies against the natural N-terminal and polybasic domains of p15, foreign antigenic epitopes were inserted within these domains.

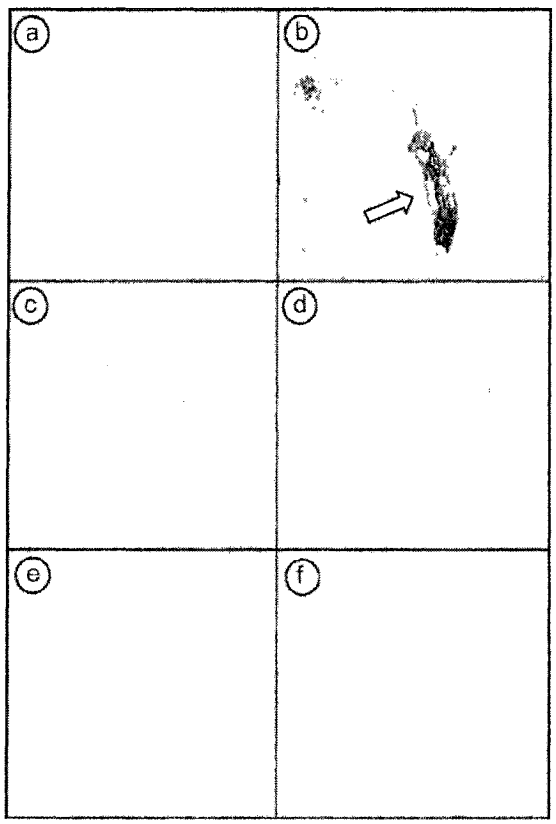

Figure. 4.5. **Antisera raised against synthetic peptides fail to specifically react with p15.** Transfected QM5 cells expressing p15 were methanol-fixed 24 h post-transfection and immunocytochemically stained using normal rabbit serum (a, 1:800; c and e, 1:400), or rabbit antiserum raised against either full-length p15 (b, 1:800), a peptide corresponding to the p15 N-terminus (d, 1:400), or a peptide corresponding to the p15 polybasic region (f, 1:400), and alkaline phosphatase-conjugated goat anti-rabbit $F(ab')_2$. The arrow indicates specific detection of p15-expresing syncytial foci by antiserum against full-length p15. Panels c-f represent prolonged development at the lowest dilution of antiserum tested.

Unfortunately, while the insertion of the HA epitope tag (YPYDVPDYA) at the C-terminus was tolerated, its insertion into various locations within either the N-terminal or polybasic regions (Fig 4.6A) disrupted p15 function, as evidenced by the inability of the tagged constructs to induce syncytium formation (Fig. 4.6B). Furthermore, while the anti-HA antibody readily reacted with its cognate epitope attached to the p15 C-terminus, it failed to adequately stain p15 constructs tagged in other regions of the protein (after residues 7, 43, 54, or 59; Fig. 4.5B). Therefore, in an effort to increase the anti-HA signal, p15 constructs were generated which carried two tandem HA tags inserted after residues 7, 59, or 140. Visualization of transfected p15 foci was not significantly improved using any of the double-HA tagged constructs (Fig. 4.6). For this reason, combined with the fact that they were not functional, these constructs were considered unsuitable for use in immunofluorescence microscopy to detect surface-expressed p15.

Biotinylation was attempted as a possible method to detect functional p15 at the surface of cells. A fusion-competent cysteine-less mutant (C104S) was created from which several p15 constructs were generated carrying cysteine substitutions in the N-terminal domain (V8C and A12C) or the polybasic domain (S53C and S53C/I62C). Of these constructs, only V8C failed to induce the formation of syncytia. In an experiment designed to simultaneously elucidate both p15 topology and surface-expression, cysteine-tagged p15 constructs expressed in transfected cells were treated with a membrane-permeable biotinylation reagent (biotin maleimide) with or without prior treatment with a membrane-impermeant blocker (stilbenedisulfide maleimide). Although a number of biotinylated host cell proteins were isolated by incubation with streptavidin-agarose, p15 was not among them, even in the absence of blocker (Fig. 4.7). The detection of

Figure. 4.6. **Differential Ab-recognition of various HA-tagged p15 constructs.** (A) Schematic diagram illustrating the amino acid positions after which single (HA) or double $(HA)_2$ epitope tags were inserted into p15. (B) Transfected QM5 cells expressing the various single- or double-HA-tagged p15 constructs, methanol-fixed 24 h post-transfection prior to immunocytochemical staining using anti-p15 rabbit polyclonal serum, or mouse anti-HA MAb, and either goat anti-rabbit, or rat anti-mouse, $F(ab`)_2$ conjugated to alkaline phosphatase. The black arrow indicates an example of a single-celled p15-positive foci; the white arrow indicates an example of a p15-positive multinucleated syncytium.

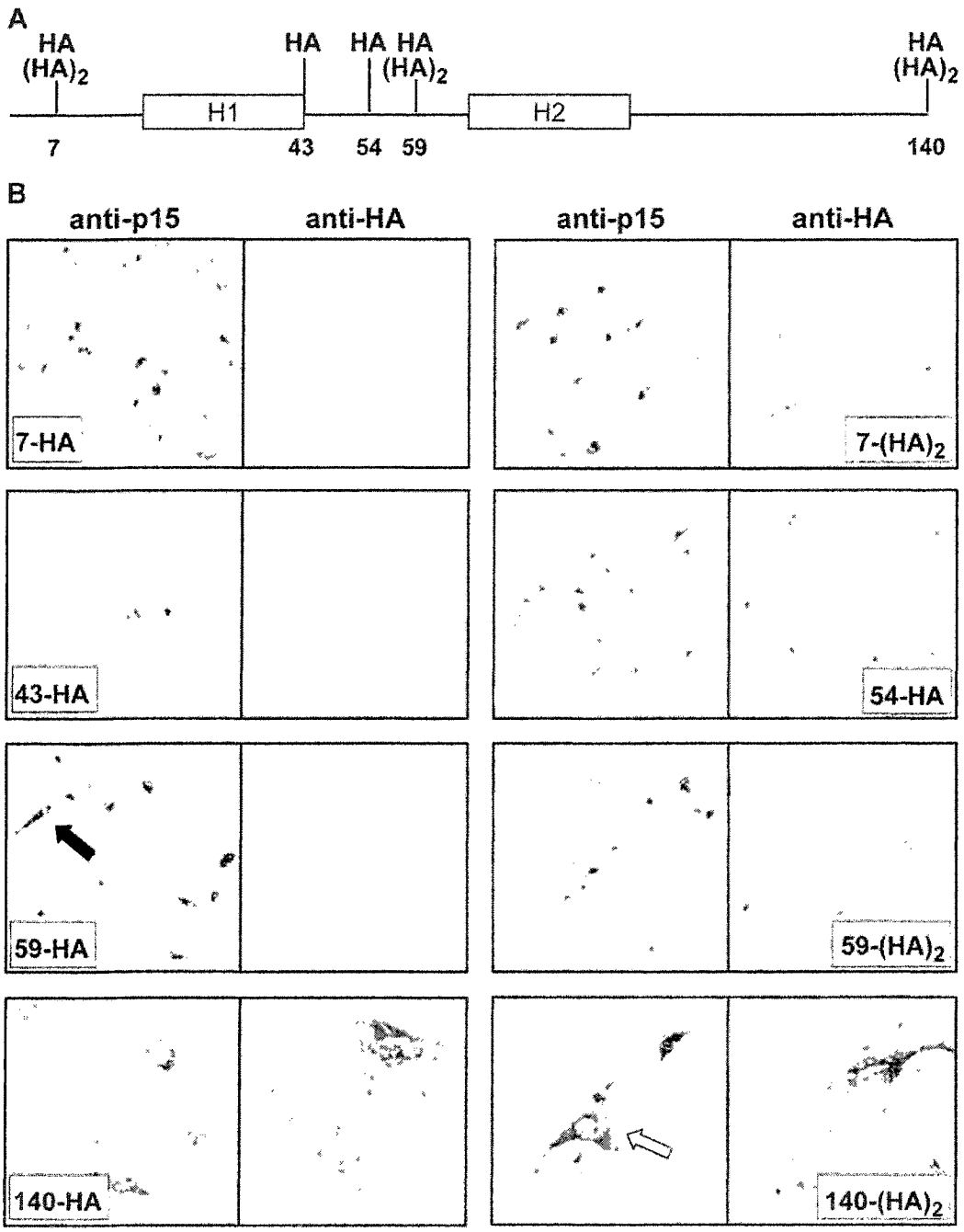
A
HA
(HA)2
HA
HA HA
(HA)2
HA
(HA)2
H1
H2
7
43
54 59
140
B
anti-p15
anti-HA
anti-p15
anti-HA
7-HA
7-(HA)2
43-HA
54-HA
59-HA
59-(HA)2
140-HA
140-(HA)2

Figure 4.6.

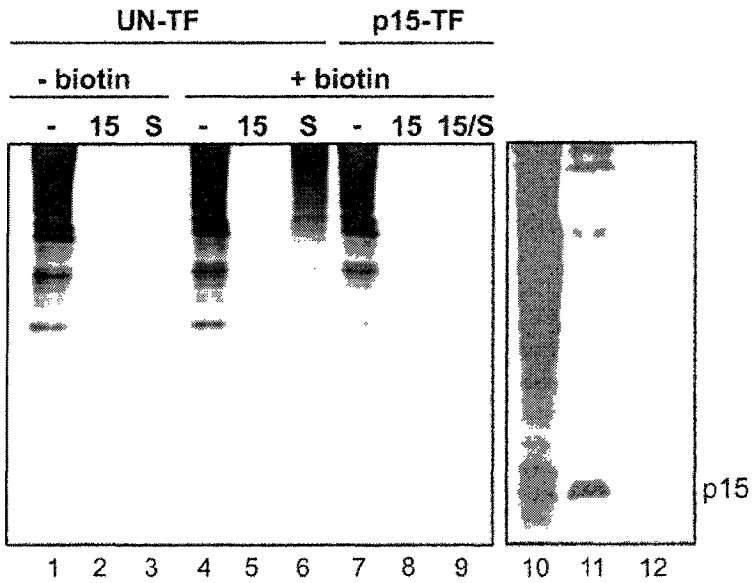

Figure. 4.7. **Failure to detect biotinylated p15.** Untransfected (UN-TF) and p15-transfected (p15-TF) Vero cell lysates treated without (- biotin) or with (+ biotin) biotin maleimide and either not immune precipitated (-), immune precipitated using anti-p15-C serum (15), precipitated using streptavidin-agarose (S), or immune precipitated using anti-p15 serum, boiled and subsequently precipitated using streptavidin-agarose (15/S). Lanes 10-12 are an over-exposure of lanes 7-9. The data shown for authentic p15 is representative of that obtained for constructs C104S, V8C, A12C, S53C and S53C/ I62C.

biotinylated p15 constructs was not facilitated by optimizing the p15 translation start site (Kozak, 1991; Kozak, 1989), or by conducting of the experiment *in vitro*.

Immunofluorescence of permeabilized cells was used as an alternative means to detect plasma membrane-localized p15. The intense intracellular fluorescence of p15 obscured clear visualization of any cell surface-localized p15 (Fig. 4.8A). Therefore, cells were treated with cyclohexamide to stop translation and to both deplete the intracellular p15 pools and allow transport of preexisting p15 to the plasma membrane. Under these conditions, clear ring fluorescence was observed at the cell periphery following antibody staining of permeabilized cells with anti-p15 antiserum (Fig. 4.8B, panel i). As in Figure 4.5, the overall specificity of the anti-p15 antisera (against full-length p15) is demonstrated by the comparative lack of p15 recognition by the normal rabbit serum control (Fig. 4.8B, panel ii). Therefore, p15 is an integral membrane protein that is targeted to the ER, from where a proportion of intracellular p15 is transported to the plasma membrane.

4.2.5. Microsomes protect an N-terminal fragment of p15

The immunofluorescent staining clearly detected a plasma membrane-localized population of p15. However, as it is unknown which of the two potential TM domains (H1, aa 21-43; H2 aa 68-87) function to anchor p15 in the membrane, the topology of p15 remained in question. Difficulties encountered with directly detecting the surface-exposed p15 ectodomain confounded antibody-based determination of p15 topology. Thus, the membrane orientation of p15 was investigated by taking advantage of the ability of microsomal membranes to protect translocated protein domains from proteolysis. When p15 translated *in vitro* in the presence of microsomes was subjected to

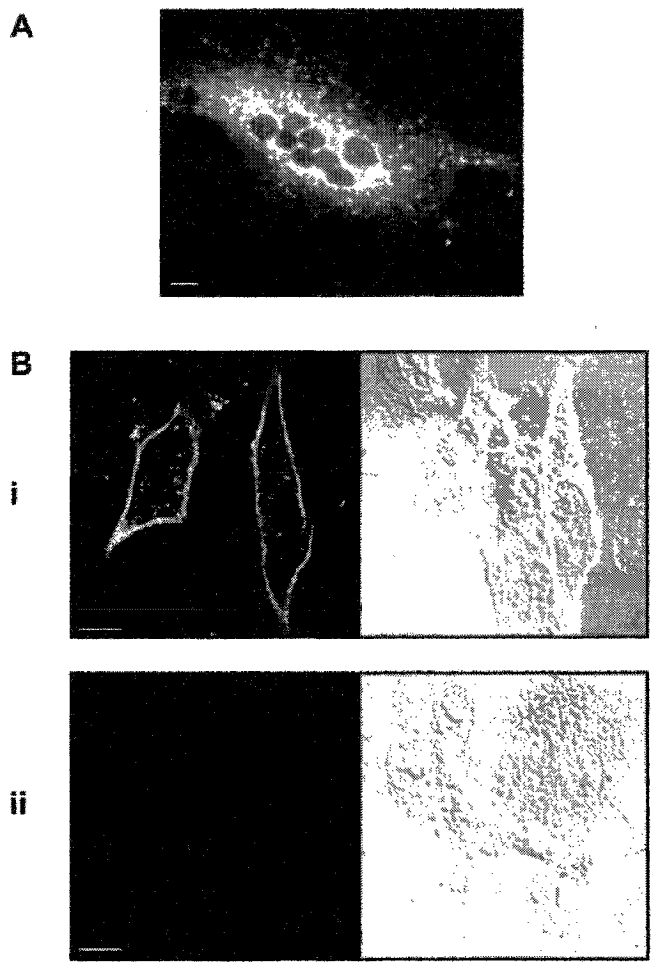

Figure. 4.8. **BRV p15 is trafficked to the plasma membrane.** (A) Transfected QM5 cells expressing authentic p15 methanol-fixed 24 h post-transfection and immunostained using rabbit anti-p15 antiserum and FITC-conjugated goat anti-rabbit $F(ab')_2$. (B) Transfected cells expressing p15 were treated (20 h post-transfection) for 1 h with cycloheximide prior to methanol-fixation and immunostaining using rabbit anti-p15 serum (i) or normal rabbit serum (ii), and FITC-conjugated goat anti-rabbit $F(ab')_2$. Right-hand panel represents merge of fluorescent image (at left) and DIC image. Cell images were captured using a Ziess (A) Axiovert microscope (630× magnification), or (B) LSM510 scanning argon laser confocal microscope (1000x magnification) with technical assistance from J. Corcoran; scale bar represents 10 μm. Images in (B) represent one Z section.

proteinase K digestion, the full-length 15-kDa protein was reduced to an estimated 8-kDa protected fragment (Fig. 4.9B, lanes 1 and 7). Disruption of the microsomes with detergent rendered p15 completely susceptible to degradation (Fig. 4.9B, lane 8). To determine which portion of p15 comprised the protected fragment, several p15 mutants carrying insertions or deletions within various domains (Fig. 4.9A) were subjected to proteinase K digestion. The mobilities of the resulting polypeptides were compared to that of the authentic p15 protected fragment in Tricine-SDS-(16.5%) PAGE (Schagger and von Jagow, 1987). Insertion of a 7 or 11 amino acid tag (8-pka, g3, respectively) in the N-terminal domain of p15 retarded p15 gel mobility (Fig. 4.9B, lanes 2 and 3). The polypeptides resulting from proteinase K digestion of these N-terminally enlarged mutants (Fig. 4.9B, lanes 9 and 10) clearly migrated behind the authentic protected fragment. The mobility shift observed with the digested N-terminally enlarged mutants was proportional to that seen in the absence of protease, and thus, the N-terminal domain of p15 must be contained within the protected polypeptide. Likewise, insertion of a 9-residue epitope tag (54-HA) into the polybasic region of p15, which intervenes between the two potential membrane-spanning segments H1 and H2, similarly retarded the migration of the protein prior to (Fig. 4.9B, lane 4) and following (Fig. 4.9B, lane 11) proteinase K digestion. Therefore, the N-terminal fragment of p15 that is protected by microsomes includes the polybasic domain. In contrast, while deletion of 10 amino acids (130*) or insertion of a 9-residue tag (140-HA) in the C-terminal domain of p15 enhanced (Fig. 4.9B, lane 5) or slowed (Fig. 4.9B, lane 6) the mobility of p15 without proteinase K treatment, these effects were lost after incubation with the enzyme. The polypeptides resulting from proteolysis of the C-terminally truncated and extended p15

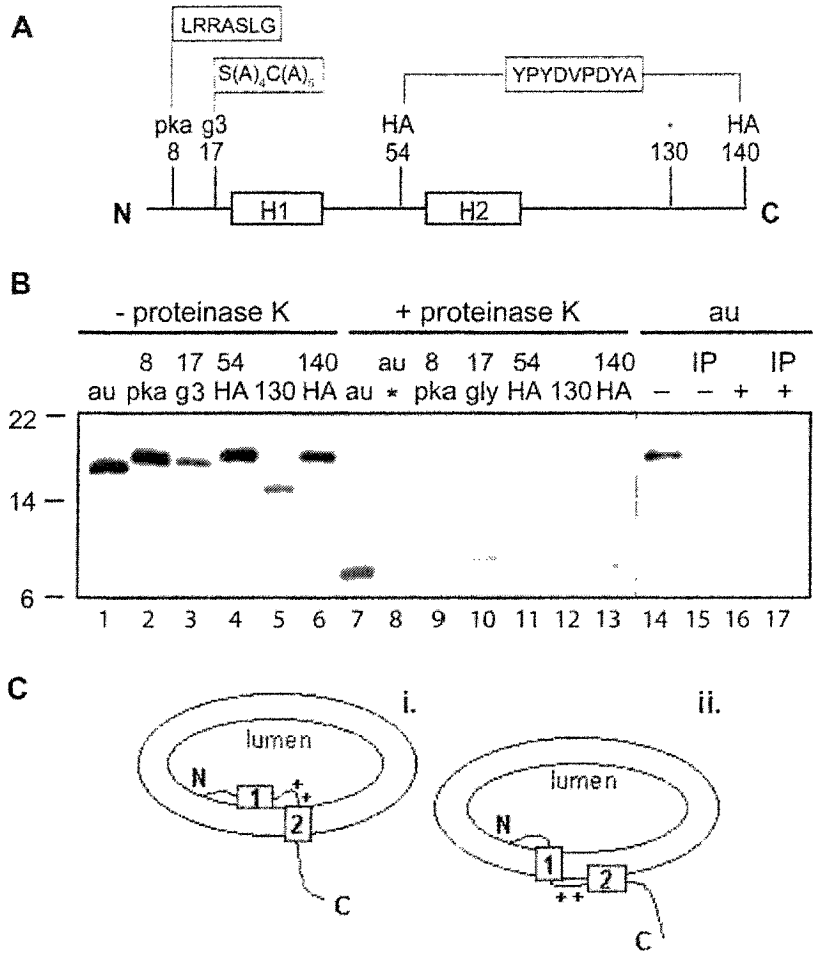

Figure. 4.9. **Microsomes protect an 8-kDa N-terminal fragment of p15.** (A) Schematic diagram indicating the amino acid positions within p15 of various insertions (8-pka, 17-g3, 54-HA, 140-HA), the sequences of which are indicated, and a truncation (130*); boxes indicate the two hydrophobic domains (H1, H2). (B) Authentic p15 (au) and p15 mutants (illustrated in A) translated in vitro with microsomes and incubated -/+ proteinase K; (*) indicates microsome disruption with 1% Triton-X-100; (IP) indicates immune precipitation using antiserum specific for the p15 C-terminus. Translation products were separated by Tricine-SDS-(16.5%) PAGE and subjected to fluorography. (C) Two topological models (i and ii) of p15 in the microsomal membrane. N, amino-terminus; 1, hydrophobic domain 1; 2, hydrophobic domain 2; C, carboxy-terminus.

mutants (Fig. 4.9B, lanes 12 and 13) were indistinguishable from those of the authentic protein. Thus, the C-terminal tail of p15 is clearly susceptible to proteinase K digestion and is, therefore, likely localized to the cytosol. Accordingly, antisera specific for the C-terminal domain of p15 failed to recognize the proteolytic fragment (Fig. 4.9B, lane 17).

Based on the relative gel mobilities of p15 polypeptides before and after proteinase K digestion, two possible models for the orientation of p15 in the microsomal membrane could be envisioned (Fig. 4.9C). Protection of the N-terminal and polybasic domains from protease digestion implied that both of these domains are translocated into the microsomal lumen. Translocation of both the N-terminal and polybasic domains would necessarily implicate H2, the more weakly hydrophobic stretch of p15, as the sole transmembrane anchor (Fig. 4.9C, model i). However, the size of the 8-kDa protected fragment was inconsistent with this membrane orientation, which would be expected to protect a polypeptide of at least 10 kDa. The 8-kDa size of the protected fragment suggested an alternative model whereby the N-terminus of p15 is translocated, H1 spans the membrane and the highly charged polybasic region tightly associates with the cytoplasmic leaflet of the membrane such as to evade proteinase K digestion; the downstream polypeptide would remain protease accessible (Fig. 4.9C, model ii). Additional topological analysis was undertaken to distinguish between these two possible p15 topographies.

4.2.6. BRV p15 constructs fail to be glycosylated

To resolve whether the p15 N-terminus alone, or both the N-terminal and polybasic domains, are translocated across the microsomal membrane into the lumen, the NXS/T consensus sequence for asparagine (N)-linked glycosylation was introduced into

various locations throughout the p15 protein (Fig. 4.10A), which normally lacks signals for N-glycosylation. Potential glycosylation sites g1, g4, g5, g6 and g8 were generated by single amino-acid substitutions in authentic p15, while sites g3 and g7 introduced the NXS/T consensus sequence in the context of an inserted spacer region designed to distance the target asparagine from downstream potentially structured or membrane-interacting domains. Surprisingly, none of the engineered sites directed the N-glycosylation of p15 *in vitro* as evidenced by the lack of any detectable mobility shift of proteins translocated in the presence of microsomal membranes from those translated without membranes (Fig. 4.10B, lanes 3-18). Similarly, each of the engineered sites also failed to become glycosylated when the proteins were expressed in transfected cells (Fig. 4.10C). To illustrate the magnitude of the mobility shift expected (~ 2.5 kDa) for a FAST protein glycosylated at a single site, a version of the RRV p14 FAST protein, p14-gly originally characterized by (Corcoran and Duncan, 2004), was used that carries an engineered N-glycosylation site in its N-terminal ectodomain that is modified with carbohydrate in roughly half of the p14-gly population (Fig. 4.10B, lanes 1 and 2). Insertion of a 6-aa region of p14-gly containing the NXT signal (NFTNHA) into the p15 N-terminal domain (construct g2) also failed to direct the glycosylation of p15 (Fig. 4.10B, lanes 5 and 6). The inaccessibility of the various glycosylation targets hinted that the p15 ectodomain may be a relatively small and/or conformationally restricted region of the protein that prevents glycosylation of introduced target sequences.

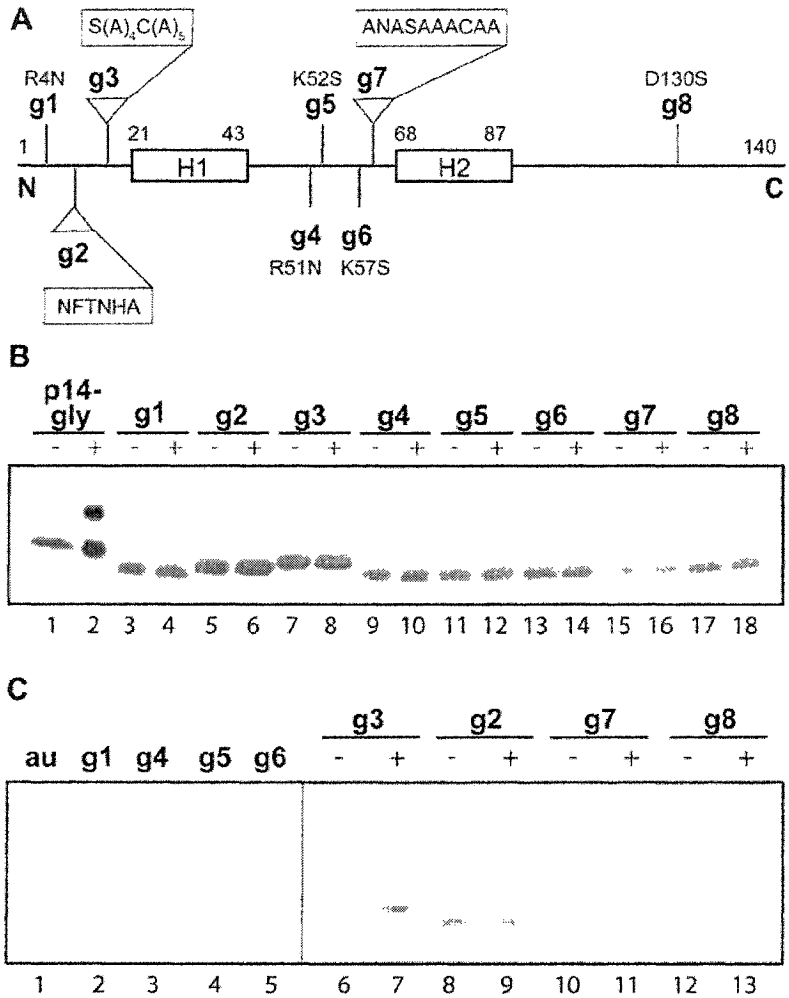

Figure. 4.10. **BRV p15 constructs fail to be glycosylated.** (A) Schematic diagram indicating the relative positions within p15 of various engineered sites for N-glycosylation (g1-g8 in bold); ( ) indicates insertion, the sequences of which are shown; point mutations that generate glycosylation sites are indicated; amino acid positions are numbered above the line; boxes indicate hydrophobic domains, H1 and H2. (B) Various p15 constructs (g1-g8) and p14-gly control translated in vitro -/+ microsomes. (C) Lysates of transfected cells expressing authentic p15 (au) and p15 constructs (g1-g8), in some cases treated with (+) or without (-) tunicamycin, and immune precipitated using anti-p15 serum.

4.2.7. The polybasic and C-terminal domains are cytosolically-exposed

Unable to conclusively determine by glycosylation which p15 domains are translocated into the microsomal lumen, I sought instead to show which p15 domains remain cytosolically-localized. Goder *et al.* (2000) demonstrated the value of using phosphorylation by protein kinase A (PKA) as a sensor of cytosolic localization when elucidating protein topology. The various domains of p15 were individually tagged (after residue 8, 59, or 140) with the consensus sequence (LRRASLG) for serine-phosphorylation by PKA, denoted 'pka' (Fig. 4.11A). Constructs were transfected into cells and analyzed for expression by labeling with [^{3}H]leucine, and for phosphorylation by labeling with [^{32}P]phosphate in the presence of 20 μM forskolin, an indirect activator of PKA. [^{3}H]Leucine-labeling indicated that the various constructs were expressed at comparative levels (Fig. 4.11B, lanes 1-4). [^{32}P]Phosphate was not incorporated into authentic p15 revealing the absence of cryptic phosphorylation signals in the protein (Fig. 4.11B, lane 5). When the phosphorylation tag was inserted in the polybasic domain or at the C-terminus of p15, the tagged proteins were labeled efficiently with [^{32}P]phosphate (Fig. 4.11B, lanes 7 and 8). When the phosphorylation tag was inserted in the N-terminal region however, the construct was less efficiently phosphorylated (Fig. 4.11B, lane 6). Phosphorylation of the N-terminal domain suggested that this region remained cytosolic. However, p15 lacks a signal sequence and uses a TM domain as an internal signal anchor. Thus, the N-terminus of the nascent protein would be accessible to PKA co-translationally until H1 emerged from the ribosome and p15 was targeted to the translocon. Although the N-terminal domain of p15 is small (approximately 27 residues in the tagged construct), it is reasonable to expect a level of phosphorylation of this

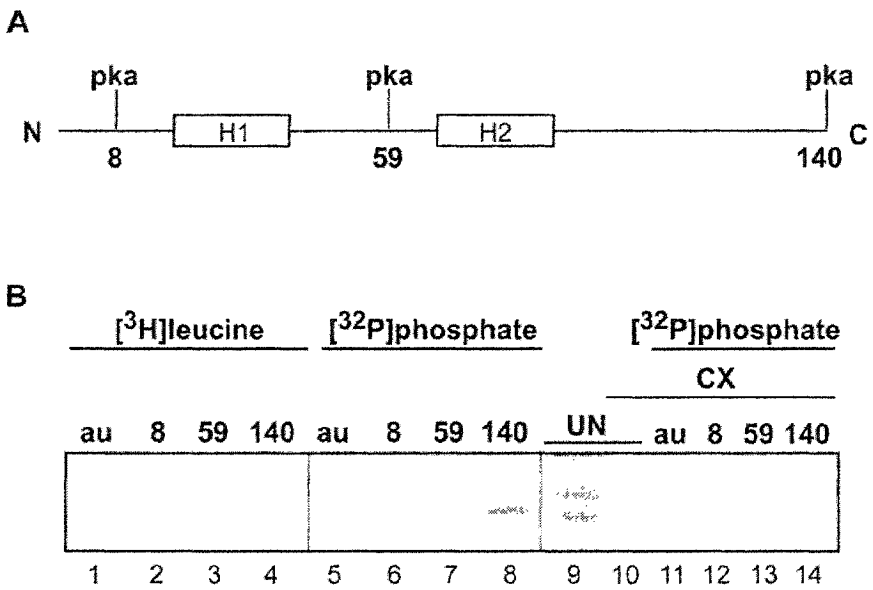

Figure. 4.11. **The N-terminal domain of p15 is translocated across the membrane.** (A) Schematic diagram indicating the amino acid positions within p15 at sites of insertion of the consensus sequence (LRRASLG) for phosphorylation by protein kinase A (pka). (B) Untransfected (UN) or transfected cells expressing authentic p15 (au) and pka-tagged p15 constructs (illustrated in A) radiolabeled with [^{3}H]leucine (lanes 1-4, 9, 10) or [^{32}P]phosphate (lanes 5-8, 11-14); CX indicates the presence of cycloheximide prior to and during radiolabeling. Lysates were immune precipitated using anti-p15 serum.

domain prior to its translocation. Goder *et al.* (2000) were able to detect specific phosphorylation with a 30-residue N-terminal domain under similar conditions. The partial phosphorylation of the p15 N-terminus, therefore, likely reflects the short, transient exposure of this domain to the cytosol prior to its translocation across the ER membrane.

To test whether the observed phosphorylation of the N-terminal tag sequence was indeed restricted to proteins synthesized during the labeling period, phosphate incorporation into the various constructs was analyzed in the presence of the translation inhibitor cycloheximide. Incubation with cycloheximide completely blocked translation, as evidenced by the absence of [^{3}H]leucine incorporation into host cell proteins compared to the abundance of [^{3}H]leucine-labeled bands without cycloheximide (Fig. 4.11B, lanes 9 and 10). Pre-existing p15 constructs tagged in the polybasic and C-terminal domains were still ^{32}phosphorylated efficiently in the presence of cycloheximide (Fig. 4.11B, lanes 13 and 14). In contrast, the N-terminally-tagged construct was not [^{32}P]phosphate-labeled (Fig. 4.11B, lane 12), indicating that the limited phosphorylation observed with this construct in the absence of cycloheximide was the result of transient cytosolic exposure of the N-terminal tag sequence prior to its translocation across the membrane. Therefore, in its final, unique topology, p15 adopts an N_{exo}/C_{cyt} orientation. This topology, along with the lack of a cleavable signal peptide, designates p15 as a type III protein (according to the classification scheme of Spiess, 1995). Taken together, the translocation of the p15 N-terminus and the accessibility of both the polybasic and C-terminal domains to PKA in the cytosol, implicate H1 as the sole TM domain of p15, consistent with topological model ii (Fig. 4.9C).

It should be noted that p15 constructs (authentic and various mutants) pka-tagged in the polybasic region are typically phosphorylated less efficiently. This likely reflects the tight membrane association of the polybasic region (consistent with other topological analyses), and thus the relative inaccessiblility of this domain to PKA. However, it cannot be ruled out that a subpopulation of p15 in an alternate topology co-exists with p15 in the type III/H1-anchored orientation. The only possible alternate topology for p15, based on the post-translational phosphorylation pattern, would be a type III/H2-anchored orientation. It is unclear what functional role, if any, the minor species of p15 displaying this alternate topology might serve.

4.2.8. N-terminus-specific antisera partially inhibits p15-induced cell-cell fusion

To confirm the N_{exo} orientation of p15 at the cell surface, antiserum specific for the p15 N-terminus was used in an attempt to block p15-mediated cell-cell fusion. Although the N-terminus-specific antiserum previously failed to cytochemically stain permeabilized transfected cells expressing p15 (Fig. 4.5), partial inhibition of p15-induced syncytium formation was achieved with a low dilution (1:10) of this antisera (Fig. 4.12). In contrast, similar treatment with antisera specific for the p15 C-terminus did not inhibit p15-induced syncytium formation, and thus the partial inhibition achieved by the N-terminal specific antisera corroborates the N_{exo}/C_{cyt} topological orientation of p15.

4.2.9. The core p15 proteolytic fragment terminates with the polybasic domain

To further investigate the potential membrane interactions of the polybasic and H2 domains of p15, the ability of microsomes to protect truncated forms of the protein from proteinase K digestion was tested. A p15 construct of 94 residues (94*), truncated just downstream of the H2 region, migrated several kDa larger than the authentic

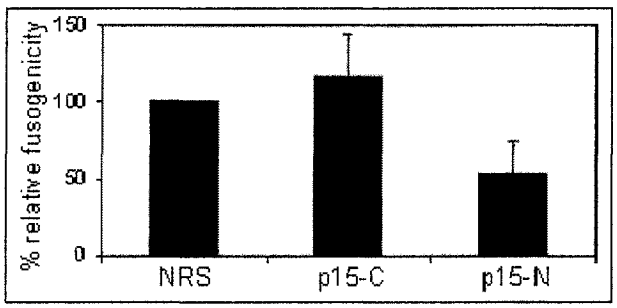

Figure 4.12. **Antiserum specific for the p15 N-terminus partially inhibits syncytium formation.** QM5 cells expressing p15 were incubated, as of 4 h post-transfection, in the presence of normal rabbit serum (NRS), or antiserum specific for either the p15 C-terminal domain (p15-C) or N-terminal domain (p15-N), all diluted 1:10. The percent fusogenicity was measured as syncytial nuclei per field and expressed relative to that formed in the presence of NRS at 24 h post-transfection. The results reported represent the mean plus the standard error of two separate experiments performed in triplicate.

protected fragment (Fig. 4.13A, lanes 3 and 4). Furthermore, the 94* construct was proteinase K digested to the core 8-kDa protected fragment (Fig. 4.13A, lane 6). Clearly, the H2 region does not span the lipid bilayer, consistent with the identification of H1 as the sole TM domain of p15.

To confirm that H1 indeed functions as a signal anchor (both a signal peptide and a TM anchor), the migration of a construct of p15 was analyzed that had been further truncated to remove the entire H2 domain – a 67-residue peptide C-terminally tagged with four methionines to facilitate its detection (67met*). The undigested 67met* peptide co-migrated with the 8-kDa protected fragment (Fig. 4.13A, lanes 2 and 6), proving that the p15 protected fragment consisted of the combined N-terminal, H1 and polybasic domains (Fig. 4.9C, model ii). It is unclear whether the removal of H2 resulted from proteolytic attack in the region downstream of the polybasic core just prior to H2, or whether H2 exists entirely as a protease accessible cytosolic region. The inability of proteinase K to digest membrane-bound 67met* was illustrated by both the absence of a mobility shift in the protease-treated versus untreated peptides, as well as the retention of at least a portion of the C-terminal methionine-tag after proteolysis (Fig. 4.13A, lane 7). The 67met* polypeptide became susceptible to proteinase K digestion once the microsomes were detergent-disrupted (Fig. 4.13A, lane 8). The inaccessibility of 67met* to proteinase K in the presence of intact microsomes suggested that the p15 polybasic domain tightly associates with the cytosolic leaflet of the membrane independent of downstream sequences, including H2. Given that the polybasic domain is expected to interact peripherally with membranes, the ability of 67met* to survive stripping with a high-salt buffer was tested. Membrane-bound 67met* was also subjected to alkaline

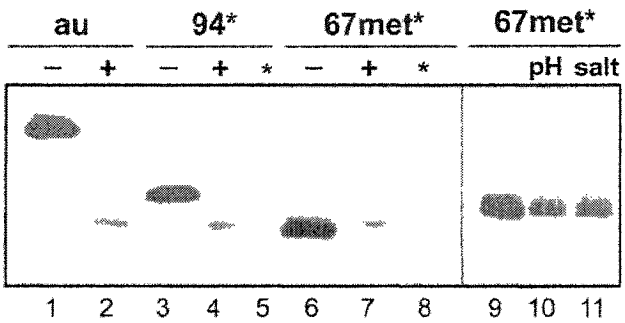

Figure. 4.13. **The H1 domain of p15 functions as a signal anchor.** Authentic p15 (au) and truncated constructs (97*, 67met*) translated *in vitro* with microsomes, either not digested (-) or digested (+) with proteinase K in the absence, or presence (*) of 1% Triton-X-100; alternatively, microsomal-bound 67met* translation products were extracted with either 0.1 M sodium carbonate, pH 11.5 (pH) or 0.5 M NaCl (salt) and centrifuged to isolate integral membrane protein.

treatment to extract any fully translocated polypeptide (Fujiki *et al.*, 1982). The inability of 500 mM NaCl or 100 mM sodium carbonate (pH 11.5) to remove the 67met* polypeptide from microsomal membranes (Fig. 4.13A, lanes 11 and 12) provided further evidence that H1 functions as the signal anchor of p15.

4.2.10. The p15 polybasic domain is not a primary topogenic signal

The possible topogenic role played by the p15 cytosolic polybasic domain, which contains a cluster of seven positively-charged residues preceeding H2, was investigated next. The effect of successive amino acid substitutions within the polybasic region on the fusogenic potential of p15 was quantified by syncytial index, as described in the Materials and Methods section (chapter 2). The individual replacement of three basic residues (R51N, K52S or K57S), as well as the combined replacement of three basic residues in construct A1 (R51A/K52A/K54A) was tolerated (Fig. 4.14A). However, replacement of an additional two basic residues in construct A2 (K56A/K57A), so that only two of the seven positive charges remain, abolished the ability of p15 to induce cell-cell fusion.

Surprisingly, the polybasic region of the protein remained cytosolic and could be tagged with [^{32}P]phosphate in cycloheximide-treated cells when three of the seven basic residues (construct 59(A1)-pka), or the entire seven basic residue cluster (construct 59(A3)-pka), was replaced by alanines (Fig. 4.14B, lanes 2 and 3). Although the pka tag itself reintroduces two arginines into this region of p15, clearly the majority of the cluster of positively charged residues in the polybasic motif is not necessary to generate the N_{exo}/C_{cyt} topology of p15. The relatively reduced radioactivity corresponding to the 59(A3)-pka band (Fig. 4.14B) may indicate that this construct is less stable. Other p15

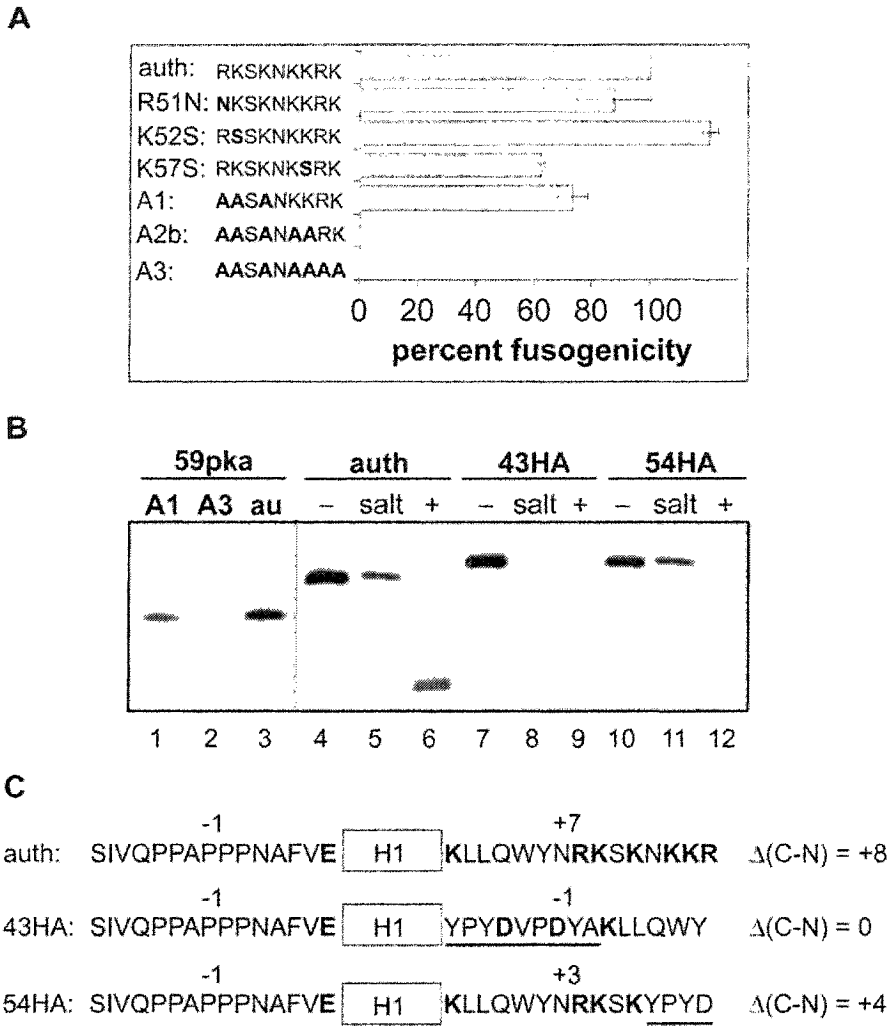

Figure. 4.14. **The p15 polybasic domain is not a primary topogenic signal.** (A) The fusogenicity of various p15 polybasic mutants relative to authentic p15 (the amino acid sequence of each construct, residues 51-59, is shown, with mutated residues in bold) as measured by syncytial index; results are reported as the mean +/- the standard error of three separate experiments performed in triplicate. (B: lanes 1-3) Transfected cells, expressing p15 (au) or p15 polybasic mutants (A1, A3) PKA consensus sequence-tagged after residue 59, treated with cycloheximide prior to, and during, radiolabeling with [^{32}P]phosphate. (B: lanes 4-12) Constructs of p15 translated *in vitro* with microsomes, either extracted with 0.5 M NaCl (salt) or incubated -/+ proteinase K. (C) Calculation using the Hartmann method, of the net charge across H1, considering the relevant 15 flanking residues, for authentic p15 (auth), and constructs 43-HA and 54-HA.

mutants made in the context of the A3 background (polybasic cluster replaced with alanines) are typically detected relatively weakly by [^{3}H]leucine-labeling (data not shown). Alternatively, a portion of the 59(A3)-pka population may exist in which the 'polybasic' region is not ^{32}phosphorylated, possibly because it has been inserted into, or translocated across, the membrane. To address this issue, the phosphorylation pattern of a 59(A3)-pka construct also pka-tagged at its N- and C-termini would need to be analyzed. Thus, it remains plausible that a core of positively-charged residues within the p15 polybasic domain functions as a secondary topological signal.

The polybasic region may be less influential to the translocation of the p15 N-terminus than the charged residues immediately flanking the H1 anchor (E20 and K44). These residues, together with the small size of the N-terminal domain, are likely the primary determinants of the reverse signal anchor orientation of H1. Accordingly, insertion of the anionic HA epitope (YPYDVPDYA) immediately in front of K44 in H1 (mutant 43-HA), which altered the net charge difference across this anchor region from +8 to 0 (calculated according to Hartmann *et al.*, 1989, considering the relevant flanking 15 amino acids; Fig. 4.14C), prevented the integral association of p15 with membranes (Fig. 4.14B, lane 8) and rendered the protein completely accessible to proteinase K (Fig. 4.14b, lane 9). The association of the 43-HA construct with membranes prior to high-salt extraction likely reflects either a peripheral association mediated through H1, H2, and/or the polybasic region, or protein aggregation. In contrast to the situation observed for 43-HA, insertion of the HA epitope immediately following K54 (mutant 54-HA) reduced the charge difference across H1 from +8 to +4 (maintaining the net positive charge) and the

54-HA mutant integrated into membranes in a manner comparable to authentic p15 (Fig. 4.14B, compare lanes 5-6 and 11-12).

4.2.11. N-terminal myristylation is essential to p15-induced membrane fusion

Considering that other integral membrane proteins that are N-myristylated can also translocate their N-termini, including the HBV L protein (Gallina and Milanesi, 1993), the L1R protein of VV (D. Hruby, personal communication), and RRV p14 (Corcoran and Duncan, 2004), it was conjectured that N-myristylation might be a topogenic signal contributing to the efficiency of N-terminal translocation. Thus, the contribution of N-myristylation to the generation and/or maintenance of p15 N_{exo}/C_{cyt} topology was investigated. Proteinase K digestion of G2A yielded an equivalent 8-kDa protected fragment to that generated by proteolysis of authentic p15 (Fig. 4.15A, lanes 1-4). To confirm that the authentic p15 and the non-myristylated mutant did indeed adopt the same unique topology in cells, the pattern of [^{32}P]phosphate incorporation into PKA-consensus sequence-tagged G2A constructs (Fig. 4.15B) was compared to that observed with similar constructs in which the myristylation signal was left intact (Fig. 4.11B). The expression of all three domain-tagged p15(G2A) constructs was confirmed by [^{3}H]leucine-labeling (Fig. 4.15B, lanes 1-3). Like authentic p15, in the presence of cycloheximide, only the polybasic and C-terminal domains of pka-tagged p15(G2A) constructs were phosphorylated (Fig. 4.15B, lanes 4-6). Thus, the nonmyrsitylated G2A mutant is competent in translocating the p15 N-terminal domain. Although the N_{exo}/C_{cyt} topology of p15 appeared unaffected by the myristylation status of the protein, N-terminal myristylation is a modification that is essential to the fusogenic potential of p15. When expressed in transfected cells, the unmyristylated G2A construct failed to induce

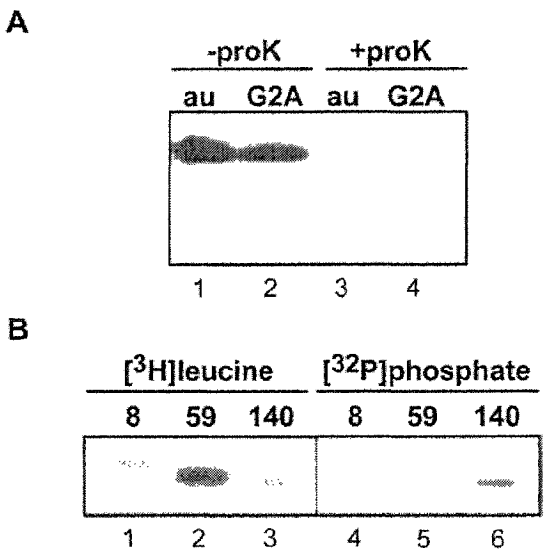

Figure. 4.15. **N-terminal myristylation does not influence p15 topology.** (A) Authentic p15 (au) or p15 G2A transcripts translated *in vitro* with microsomes -/+ digestion with proteinase K (proK). (B) Transfected cells expressing various p15 G2A constructs PKA consensus sequence-tagged after residue 8, 59, or 140, labeled with either [^{3}H]leucine or [^{32}P]phosphate in the presence of cycloheximide. Radiolabeled lysates were immune precipitated using anti-p15 serum.

cell-cell fusion. Immunochemical staining of transfected monolayers revealed that G2A-expressing cells remain as unfused, single-cell foci, while cells expressing authentic p15 form multinucleated syncytia (Fig. 4.16).

It was hypothesized that myristylation may play a role in determining the subcellular localization of p15. To investigate the contribution of myristylation to the intracellular trafficking of p15 to the cell surface, authentic p15 and the G2A mutant were tagged at their C-termini with GFP. Both p15-GFP and p15(G2A)-GFP redistributed GFP from its native diffuse cytoplasmic staining pattern into the extensive punctate staining pattern observed for non-tagged p15 (data not shown). Furthermore, both p15-GFP and p15(G2A)-GFP were competent in localizing a similar population to the cell periphery as evidenced by their pattern of ring fluorescence in cycloheximide-treated cells (Fig. 4.17, panels ii and iii). Thus, N-myristylation is not required to direct p15 to the cell surface. The absence of ring fluorescence displayed by cycloheximide-treated cells transfected with GFP (which is cytosolically-localized) alone (Fig. 4.17, panel i), supported the validity of using this method to detect surface-expressed p15 in permeabilized cells.

4.3. Discussion

4.3.1. BRV p15 is expressed at the cell surface

As expected for a membrane fusion protein, and as demonstrated (Fig. 4.8B), p15 is trafficked to the cell surface from where it presumably initiates cell-cell fusion. For reasons detailed above (section 4.2.4), I was unable to directly demonstrate surface-exposed p15 on intact cells by either immunofluorescence or biotinylation. Thus, in order to detect functional p15 expressed at the cell surface, the translation inhibitor

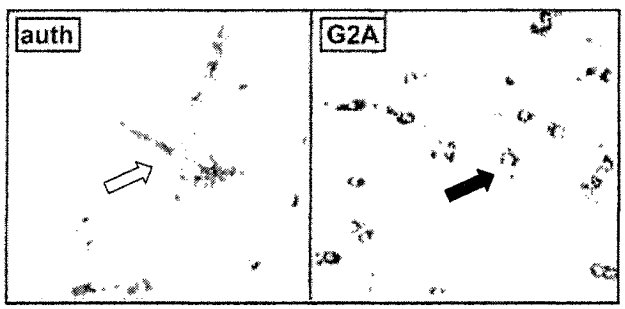

Figure. 4.16. **N-myristylation is essential to p15-induced syncytium formation.** Authentic p15 (auth)- or p15 G2A-expressing transfected QM5 cells methanol-fixed 20 h post-transfection prior to immunocytochemical staining using rabbit anti-p15 serum and alkaline phosphatase-conjugated goat anti-rabbit $F(ab')_2$. The black arrow indicates an example of a single-celled p15-positive foci; the white arrow indicates example of a p15-positive multinucleated syncytium.

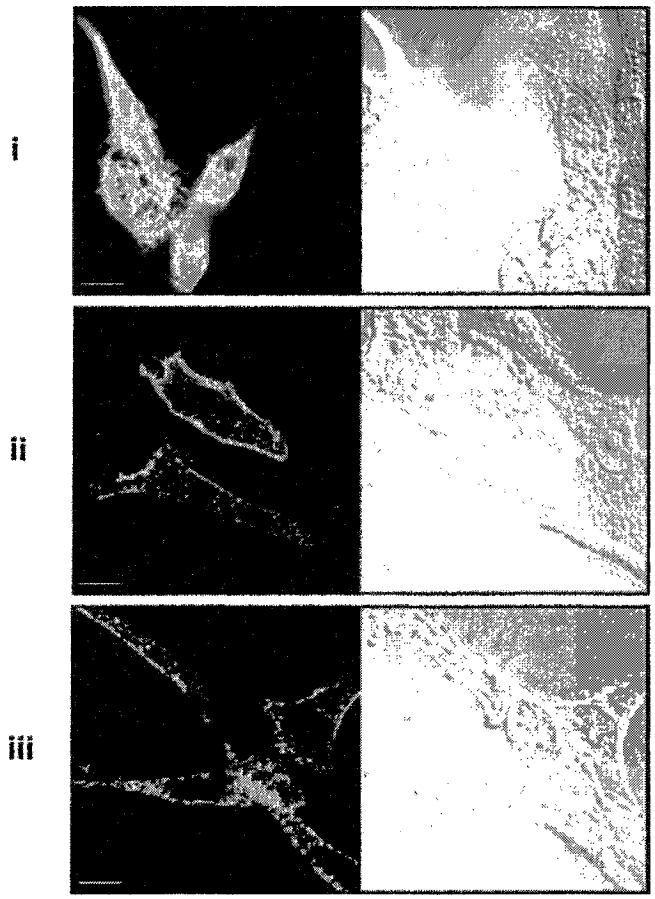

Figure. 4.17. **N-terminal myristylation is not required to traffick p15 to the plasma membrane.** Transfected QM5 cells expressing (i) GFP, (ii) p15-GFP, or (iii) p15(G2A)-GFP, methanol-fixed 20 h post-transfection following 1 h treatment with cycloheximide. Right-hand panel represents merge of fluorescent image (at left) and DIC image. Cell images were captured (with technical assistance from J. Corcoran) using a Zeiss LSM510 scanning argon laser confocal microscope (1000x magnification), single confocal sections are shown; scale bar represents 10 μm.

cycloheximide was used to deplete the intracellular pools of p15 prior to immunofluorescent staining of permeabilized cells using anti-p15 antisera. The resulting ring pattern of fluorescence distinctly revealed a population of p15 localized to the plasma membrane. The inability to modify the p15 N-terminal and polybasic domains by glycosylation or biotinylation, to generate antisera reactive against these regions, or to epitope tag these domains without loss of p15 function together suggest that these areas of p15 may be masked by protein folding, tight membrane associations, or possible protein-protein interactions. It remains possible that the failure to detect biotinylated p15 may reflect the possible inappropriateness of either the biotinylation reagent used or the p15 constructs themselves. Thus, cysteines were introduced into p15 following amino acid 16 or 59 in the context of a spacer region designed to distance the target residue away from a downstream hydrophobic domain (H1 or H2, respectively). Transfected cells expressing these new constructs were subjected to biotinylation with the membrane-impermeable *N*-biotinoylaminoethyl methanethiosulfonate (MTSEA-Biotin) reagent. Technical difficulties with the detection of biotinylated polypeptides using horseradish peroxidase-conjugated NeutrAvidin by Western blot analysis led to the premature rejection of this assay. However, this procedure could be revisited in future analysis in order to confirm the topology and surface expression of p15.

4.3.2. Anchored by H1, p15 is a type III (N_{exo}/C_{cyt}) membrane protein

BRV p15 is clearly an integral membrane protein (Fig. 4.1). The fact that association of p15 with the membrane fraction resisted extraction with high salt indicated that p15 membrane association was unlikely to be peripheral and mediated either by ionic interactions with the polybasic region or by reversible membrane insertion of the

predicted myristate moiety. While these results suggested that p15 spans the membrane, they did not indicate which (or both) of the predicted TM domains (H1, aa 21-43; H2, aa 68-87) in p15 are functional.

In vitro protease protection studies indicated that p15 spans the membrane once, and adopts an N_{exo}/C_{cyt} topology (Fig. 4.9). Analysis in cell culture of the accessibility of various tagged p15 domains to cytosolic PKA confirmed this orientation of p15 and implicated the N-proximal hydrophobic domain (H1) as the p15 TM domain (Fig. 4.10). H1 alone was able to direct the insertion of a truncated form of p15 (67met*) into the membrane, illustrating its function as a signal anchor (Fig. 4.11). The topography of BRV p15 appears similar to that of the NSP4 protein of rotavirus, a member of the *Reoviridae*. Like p15, NSP4 is a nonstructural viral protein, adopting a type III membrane orientation with a hydrophobic domain (H3; residues 63 to 80) which does not span the membrane located downstream of the signal anchor (Bergmann *et al.*, 1989). While protease sites within the NSP4 H3 domain are protected, sites upstream of H3 are accessible to digestion by proteases such as proteinase K (Bergmann *et al.*, 1989). It is not known whether the protection of H3 is due to its burial in the cytosolic face of the lipid bilayer, or possible interactions with the remainder of the protein. Likewise, it remains unclear whether the H2 domain of p15 is laterally embedded in the membrane, hidden within a protein fold or binding interaction, or remains exposed in the cytosol.

Surprisingly, translocation of the p15 N-terminus into the lumen of the ER did not result in the glycosylation of target asparagine residues (Fig. 4.9). Successful N-glycosylation by the oligosaccharyl transferase (OST) enzyme in the lumen of the ER requires adequate spacing (>10 residues) of the acceptor site from the membrane surface

(reviewed by van Geest and Lolkema, 2000).) The engineered N-glycosylation targets within the p15 N-terminal domain were designed to be sufficiently far upstream of the H1 region. However, especially given the small size of the p15 ectodomain (20 residues), perhaps potential N-terminal-membrane interactions mediated by the hydrophobic myristate moiety prevent the accessibility of sites g1 and g2 to OST. It is also possible that the structure or function of the N-proximal polyproline motif (aa 10-15) interferes with the recognition of potential N-glycosylation signals (g1-3) within the region.

Unexpectedly, the polybasic cluster is not a primary topogenic signal for p15, since replacement of the entire cluster with alanines did not alter the cytosolic orientation of (at least) a significant population of p15 (Fig. 4.13B). Rather, it is hypothesized that E20 and K43, which immediately flank H1, are dominant signals determining the N_{exo}/C_{cyt} topology of p15. It is of interest to note that the p14 FAST protein also contains similarly charged residues flanking its TM anchor (E38 and K58). The position of these charged residues, together with the small size (and likely relatively unfolded state) of the p15 N-terminus, would be predicted to favour a reverse signal orientation for H1 (Denzer *et al.*, 1995). Accordingly, displacement of K43 through the upstream insertion of the anionic HA epitope (43-HA) impaired the proper membrane insertion of p15, as evidenced both by the lack of resistance to salt-stripping, and by the lack of protection from proteolysis (Fig. 4.14B). It is noteworthy that the 43-HA construct does not integrate into membranes in either the opposite bitopic (N_{cyt}/C_{exo}) topology, nor as a N_{cyt}/C_{cyt} polytopic protein. Presumably, it is too energetically unfavorable for p15 to translocate the intact highly charged polybasic domain (Krishtalik and Cramer, 1995). While the charged residues flanking H1 appear to be dominant topogenic signals for the

N_{exo} orientation of p15, the polybasic core clearly contributes to maintaining the cytosolic localization of the C-terminal tail. The p15 polybasic cluster also plays an essential role in promoting syncytium formation, even though approximately half of the residues are dispensable for p15 fusogenicity (Fig. 4.13A). Although a critical role for K56, R58, and/or K59 cannot be ruled out (since these amino acids were not individually replaced) it appears that a minimum of three to four positively charged residues within the polybasic cluster are required to accomplish membrane fusion. This analysis corresponds well with the observation that substitution of a single lysine residue within the minimal polybasic cluster (containing just four positively-charged residues) of the p10 FAST protein abolishes the fusogenic ability of p10 (Shmulevitz and Duncan, 2000).

The presence of a polybasic region on the carboxy-proximal side of an internal signal-anchor sequence is a common feature of the FAST proteins (chapter 1; (Corcoran and Duncan, 2004; Shmulevitz and Duncan, 2000). Interestingly, TM domains with an adjacent polybasic region are the hallmark features of a diverse group of small hydrophobic proteins, termed viroporins, encoded by numerous enveloped and nonenveloped viruses (Carrasco, 1995). Although the viroporins are not known to induce membrane fusion, they are involved in interactions that destabilize membranes, leading to cytopathic effects and enhanced virus release. The combination of the TM domains and adjacent polybasic regions in the reovirus FAST proteins may contribute to destabilization of the donor membrane as part of the FAST-mediated membrane fusion reaction. Such a role could account for the essential nature of the polybasic domains, as observed for both p10- and p15-induced syncytium formation.

4.3.3. N-myristylation is essential to p15-induced membrane fusion

The N-terminal myristylation consensus sequence of p15 is utilized, as demonstrated by the ability of p15 to be specifically labeled by [^{3}H]myristate in infected and transfected cell lysates (Fig. 4.2). Analysis of a myristylation-minus mutant (G2A) also indicated that, while myristylation is not required to anchor p15 in the membrane (Fig. 4.3), translocate the p15 N-terminus (Fig. 4.15), or transport p15 to the cell surface (Fig. 4.17), myristylation is necessary for the fusogenic activity of p15 (Fig. 4.16). While fatty acylation of fusion proteins is common, the vast majority of viral fusion proteins that are acylated contain the 16-carbon palmitate post-translationally attached to membrane-proximal cysteine residues rather than the 14-carbon myristate co-translationally attached to an N-terminal glycine residue (for examples see, (Andersson *et al.*, 1997; Caballero *et al.*, 1998; Olsen and Andersen, 1999; Schmidt *et al.*, 1988; Schmidt, 1982; Schmidt and Schlesinger, 1979; Veit *et al.*, 1991; Yang and Compans, 1996; Yang *et al.*, 1995; Zhang *et al.*, 2003). Thus, BRV p15 is a rare example of a myristylated fusion-inducing protein, and the first for which N-myristylation has been demonstrated as being essential to the fusion process (Dawe and Duncan, 2002). Subsequently, myristylation of RRV p14 N-terminus has also been shown to occur and to be critical to p14 function (Corcoran and Duncan, 2004). In addition to the p15 and p14 FAST proteins, the only incidences of viral fusion proteins modified by the addition of myristate are the fusion protein of the Indiana serotype of vesicular stomatitis virus (VSV), which is both palmitylated and myristylated via thioester bonds near its C-terminus (Chen, 1991), and the hepadnavirus L protein, which contains an N-myristylated pre-S domain (Persing *et al.*, 1987). The mechanism of hepadnavirus-mediated membrane fusion remains unclear but may involve

proteolytic cleavage of L to remove the myristylated pre-S domain thereby exposing the potential fusogenic S protein (Berting *et al.*, 2000; Rodriguez-Crespo *et al.*, 1999). Similarly, the amino acid sequence of the precursor fusion (F) protein of NDV contains an apparently conserved N-terminal myristylation consensus sequence (for example, MGSRSS; NCBI accession AAA46675). To my knowledge, the functionality of this sequence has not been tested. Unlike the HBV L and NDV F proteins, there is no evidence to suggest that a precursor protein relationship exists for either BRV p15 or RRV p14 and, thus, the fusogenic forms of these FAST proteins are likely represented by the myristylated species.

The p15 and p14 FAST proteins join a rare group of integral membrane proteins that are known to also be N-myristylated. In addition to the VSV (Indiana serotype) fusion protein and the HBV L protein mentioned above, other examples include cytochrome b5 (Ozols *et al.*, 1984) and the vaccinia virus L1R protein (Wolffe *et al.*, 1995). Although an integral membrane protein does not require myristylation in order to associate with the phospholipid bilayer, the myristate moiety could contribute to important reversible membrane interactions at the N-terminus of the protein, analogous to the well-known "myristyl-switch" mechanisms that allow proteins to cycle between membranes and the cytosol in a regulated fashion (Ames *et al.*, 1997; McLaughlin and Aderem, 1995; Randazzo *et al.*, 1995). Alternatively, the role of myristylation may be unrelated to potential protein-lipid interactions. In many cases, myristic acid has been shown to confer a localized structural effect, with consequences for protein stability (Kennedy *et al.*, 1996; Olsen and Kaarsholm, 2000; Yonemoto *et al.*, 1993) or ligand binding (De Falco *et al.*, 2001; Olsen and Kaarsholm, 2000; Sowadski *et al.*, 1996;

Tholey *et al.*, 2001). The protein-protein interactions promoted by myristylation also include those involved in protein targeting to specific membrane environments, such as raft microdomains at the cell periphery (Ding *et al.*, 2003; Goldberg, 1998; Martin-Belmonte *et al.*, 2000; Resh, 1999; Seykora *et al.*, 1996). The precise role of myristylation in BRV p15 and RRV p14 function remains elusive. While evidence suggests that N-terminal myristylation contributes to the determination of the N_{exo}/C_{cyt} topology for p14 (J. Corcoran, personal communication), there is no clear role for myristylation in the translocation of the p15 N-terminus (Fig. 4.15). Although we observed no obvious requirement for myristylation in the intracellular trafficking of p15 to the cell surface as a whole (Fig. 4.17), it remains possible that myristylation may promote the retention of p15 at specific plasma membrane microdomains which possibly serve as platforms from which to initiate syncytium formation. Alternatively, the myristate moiety may influence either the folding of the p15 N-terminus into a fusion-competent conformation, or mediate potential protein-lipid interactions at the cell-cell interface that are required to trigger membrane fusion.

The topology that has been determined for p15 resembles that of the other FAST proteins (Fig. 4.18). Like p15, neither p10 nor p14 contain cleavable signal sequences and, as such, the N_{exo}/C_{cyt} topology adopted by these unusual fusion proteins is that of the type III class of membrane protein (classification scheme of Spiess, 1995). Typical of type III membrane proteins (which must translocate already formed N-terminal domains), the FAST proteins move relatively short (20-40 aa) and unstructured ectodomains across the membrane. In this regard, the FAST proteins, including p15, contrast markedly from the fusion proteins of enveloped viruses, which are typical type I membrane proteins

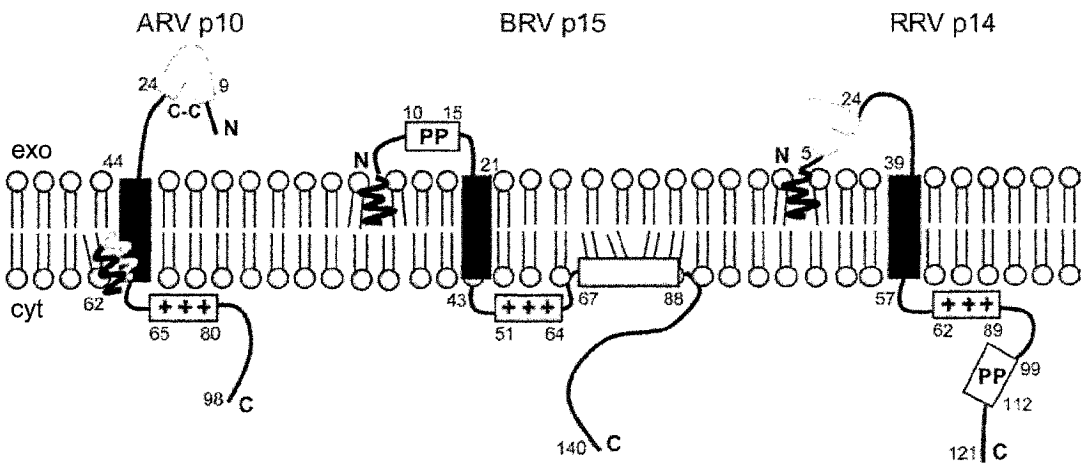

Figure 4.18. **Topological models of the FAST proteins.** Schematic diagrams illustrating the type III membrane orientation of the ARV p10, BRV p15, and RRV p14 proteins; exo, exocytosolic; cyt, cytosolic; N, amino-terminus; C, carboxy-terminus; C-C, putative disulfide bond; PP, polyproline sequence; dark grey box indicates hydrophobic patch; black box indicates TM domain; (+++) denotes charged region; squiggle indicates acylation site; residue positions are numbered.

whose (co-translationally translocated) N-terminal ectodomains comprise the bulk of the polypeptide.

The ectodomains of enveloped viral fusion proteins contain a hydrophobic fusion peptide, which is believed to mediate membrane destabilization during the fusion process (reviewed by (Epand, 2003; Skehel *et al.*, 2001; Tamm *et al.*, 2002). Likewise, the p10 and p14 FAST proteins contain moderately hydrophobic stretches in their ectodomains that are putative fusion peptides (Corcoran *et al.*, 2004; Shmulevitz *et al.*, 2004b). In the case of p15 however, there is no externalized hydrophobic peptide motif. The only hydrophobic segment of p15 that is not membrane-spanning is the cytosolically-localized H2 region. It remains to be determined whether H2 may directly promote membrane fusion from within. It would be unprecedented for a viral fusion protein to contain a hydrophobic peptide with fusion-inducing activity localized to the inner leaflet of the membrane bilayer. Yet, such a possibility must be considered when examining the topology of BRV p15 since this particular FAST protein externalizes no obvious motif with the potential to induce bilayer stress and trigger membrane fusion. Alternatively, considering the well-known protein-protein interaction propensity of proline-rich motifs (for reviews, see: Siligardi and Drake, 1995; Williamson, 1994; Zarripar *et al.*, 2003), it is possible that the polyproline region of the p15 ectodomain (aa 10-15) may recruit a cellular protein partner required to mediate membrane merger. In any case, it is clear that the mode of participation by the p15 ectodomain in membrane fusion must differ significantly from that described for the much larger and more complex ectodomains of enveloped virus fusion proteins.

CHAPTER 5

THE MINIMAL ECTODOMAIN OF THE BABOON REOVIRUS FUSION PROTEIN CONTAINS AN ESSENTIAL POLYPROLINE HELIX

5.1. Introduction

The mechanism of p15-mediated membrane fusion remains to be characterized, but is expected to be novel given both the small size (15 kDa) and unique structural organization of this atypical fusion protein. Although p15 contains two hydrophobic domains, the N-proximal hydrophobic stretch (H1, aa 21-43) was identified as the sole TM segment and is responsible for translocating the p15 N-terminal ectodomain (chapter 4). With just 20 amino acids, the p15 ectodomain is the smallest among known viral fusion proteins and is half the size of the ectodomains of the other FAST proteins. The p15 ectodomain contains the unusual feature of being N-terminally myristylated, a modification that is required for the ability of p15 to induce cell-cell fusion (chapter 4). In addition to its small size and N-myristylation, the p15 ectodomain is distinct in that it lacks a hydrophobic region reminiscent of a fusion peptide, an essential motif in other viral fusion machines. Consequently, it is unclear how p15 may accomplish membrane merger and whether, in the absence of typical fusion-promoting modules, novel motifs within the p15 ectodomain contribute to the fusion process.

Having initially characterized N-myristylation as being essential for p15 fusogenicity, the analysis presented in this chapter details a further unique feature of the p15 ectodomain - the presence of a proline-rich motif, PPAPPP (aa 10-15). Steric interactions between the adjacent prolyl rings within this polyproline cluster are expected to give rise to the formation of a left-handed polyproline (or PPII) helix. Interestingly, the

p15 proline-rich motif is preceded by glutamine, which is favoured at the first position in a PPII helix (Stapley and Creamer, 1999). Furthermore, the N-proximal position of the p15 polyproline motif predicts it to be solvent exposed, which is also the tendency for PPII helices (Adzhubei and Sternberg, 1993; Stapley and Creamer, 1999).

The PPII helix structure is increasingly being recognized as essential to a wide range of biological phenomena. PPII helices are composed of backbone dihedrals of (ϕ, ψ) = (-75°, +145°) resulting in precisely three residues per left-handed turn so that amino acids three positions apart align along one side of the helix. With an axial translation of 3.2 Å, PPII helices are extended structures (stretching twice as long as an α-helix of equal residues), but are also quite flexible as they have few intramolecular hydrogen bonds (Adzhubei and Sternberg, 1993; Bochicchio and Tamburro, 2002). PPII helices tend to occur in short stretches (4-12 amino acids, including a limited number of nonproline residues) on the surface of proteins, frequently found at either the N- or C-termini where they are commonly involved in protein-protein interactions (Adzhubei and Sternberg, 1993; Williamson, 1994; Zarripar *et al.*, 2003). The inherent flexibility of the PPII helix is an important feature facilitating its interactions with other molecules. A PPII helix may also form a flexible link between domains or, if short enough, may promote a bend within a single domain (Holt and Koffer, 2001).

The recognition of proline-rich ligands governs a wide variety of cellular functions, including signal transduction, cytoskeletal rearrangements, transcriptional activation, protein ubiquination, cell motility and the immune response (Holt and Koffer, 2001; Kay *et al.*, 2000; Mayer, 2001; Otte *et al.*, 2003; Rotzchke and Falk, 1994). To date, five different folds that bind proline-rich sequences (PRSs) in the PPII helix

conformation have been identified, namely the SH3, WW, EVH1, profilin, and GYF domains (Bork and Sudol, 1994; Carlsson *et al.*, 1977; Freund *et al.*, 1999; Mayer *et al.*, 1988; Niebuhr *et al.*, 1997; Stahl *et al.*, 1988). The binding mediated by polyproline motifs is generally low affinity, but can be highly specific. Typically, a small (3-6 residue) core within the PRS of a target protein binds a hydrophobic (proline-binding) pocket containing aromatic residues on the surface of its protein partner (Ball *et al.*, 2002; Mayer, 2001). The WW and GYF recognition domains directly contact two adjacent prolines within the PRS core, while the SH3, EVH1 and profilin recognition domains bind two proline residues, three positions apart, which align on one face of the PPII helix module (Ball *et al.*, 2002; Freund *et al.*, 2003; Holt and Koffer, 2001; Ilsey *et al.*, 2002; Yu *et al.*, 1994). Prolines flanking the core binding motif function as a molecular scaffold, promoting the formation of the PPII helix in order to present the core motif in the correct steric and hydrogen bonding conformation for specific interactions at the protein-ligand interface. Additional nonproline residues increase the affinity and specificity of the protein-protein interaction (Feng *et al.*, 1994; Yu *et al.*, 1994).

The PRS present in the p15 N-terminus is not obviously recognizable as a ligand for one of the known PRS-binding folds, and its role in p15 function is not known. It is possible that the p15 PRS may confer a particular structural fold to the p15 ectodomain, or potentiate interactions with a cellular partner, required to accomplish syncytium formation. As part of the effort to understand how p15 promotes membrane fusion, an investigation of the PRS present in the p15 ectodomain was underaken. Although mutagenic analysis suggests the p15 PRS does not conform to a core ligand motif recognized by any known PRS-binding domain, I have determined that the p15 PRS

adopts a PPII helix conformation that is essential for the fusogenicity of this FAST protein.

5.2. Results

5.2.1. BRV p15 contains an essential N-proximal proline-rich domain

To investigate a possible role for the N-proximal polyproline motif (Fig. 5.1A) in p15-induced membrane fusion, a version of p15 (pro1) was constructed in which every proline between residues 10 to 15 was replaced by alanine. In contrast to authentic p15, the pro1 construct lacking the PRS failed to induce the formation of multinucleated syncytia in transfected cells (Fig. 5.1B). Given the presence of a C-proximal PRS within the endodomain of p14 that is of similar sequence to that of the p15 N-proximal PRS (Fig. 5.2A), it was investigated whether the p15 PRS could promote p15 fusogenicity when re-located to the endodomain. While addition of the PRS (QPPAPPP) to the C-terminus of authentic p15 did not inhibit its ability to initiate fusion, addition of this sequence to the C-terminus of pro1 failed to complement the fusion defect of this construct (Fig. 5.2B). Hence, the significance of the proline-rich motif to p15 function is dependent on its localization to the ectodomain.

To determine if any particular residue(s) within the p15 PRS is essential, relative fusogenicity was assessed for of a series of constructs in which individual prolines were replaced by alanine. Alanine was chosen for substitution as it is unlikely to grossly disrupt the predicted PPII helix conformation (Kim *et al.*, 2001). Each construct retained the ability to induce a level of syncytium formation in transfected Vero cells and, thus, no single proline residue within the p15 PRS is critical for fusion (Fig. 5.3).

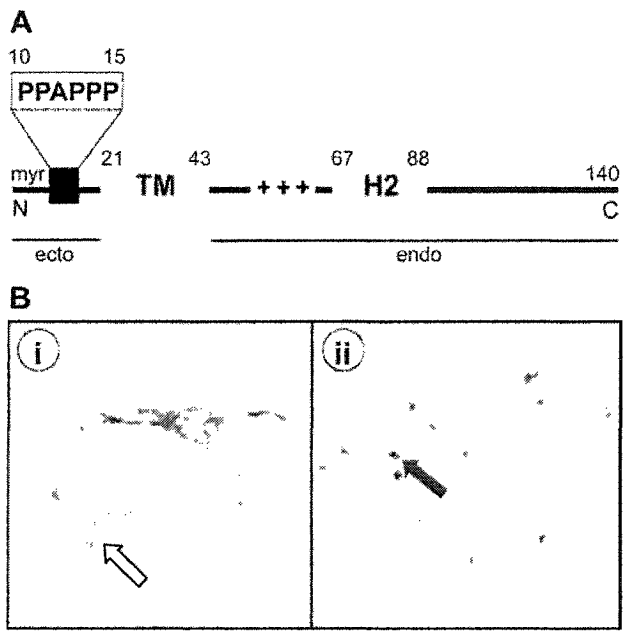

Figure 5.1. **The N-proximal proline-rich sequence is required for BRV p15-induced syncytium formation.** (A) Schematic model of p15 indicating the position (black box) of the proline-rich sequence (PRS), PPAPPP; N, amino terminus; myr, myristate moiety; TM, transmembrane domain; +++, polybasic region; H2, hydrophobic domain 2; C, carboxy terminus; ecto, ectodomain; endo, endodomain; amino acid positions are numbered. (B) Transfected cells expressing (i) authentic p15 (PRS: P_9PAPPP_{15}) or (ii) the pro1 mutant (PRS: A_9AAAAA_{15}) methanol-fixed 20 hours post-transfection prior to immunocytochemical staining using rabbit anti-p15 antiserum (1:1000) and alkaline phosphatase-conjugated goat anti-rabbit $F(ab')_2$ (1:1000). Black arrow indicates example of p15-positive single-cell foci; white arrow indicates example of p15-positive multinucleated syncytium.

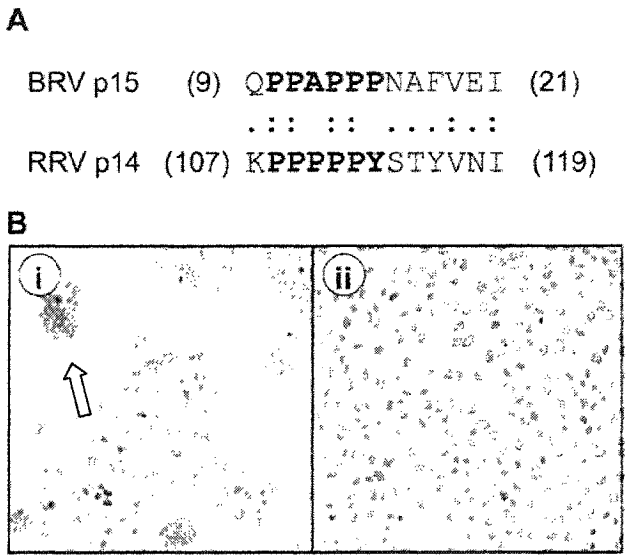

Figure 5.2. **The significance of the p15 PRS is dependent on its localization to the ectodomain.** (A) Comparison of the N-proximal PRS of BRV p15 (residues 9-21) and the C-proximal PRS of RRV p14 (residues 107-119); identical (:) and similar (.) residues are indicated; amino acid positions are bracketed. (B) Transfected cells expressing (i) a p15 construct, or (ii) a pro1 construct (both tagged at their C-termini with the p15 PRS, QPPAPPP) methanol-fixed 20 hours post-transfection prior to Giemsa staining to visualize nuclei and polykaryon formation, an example of which is indicated by the arrow.

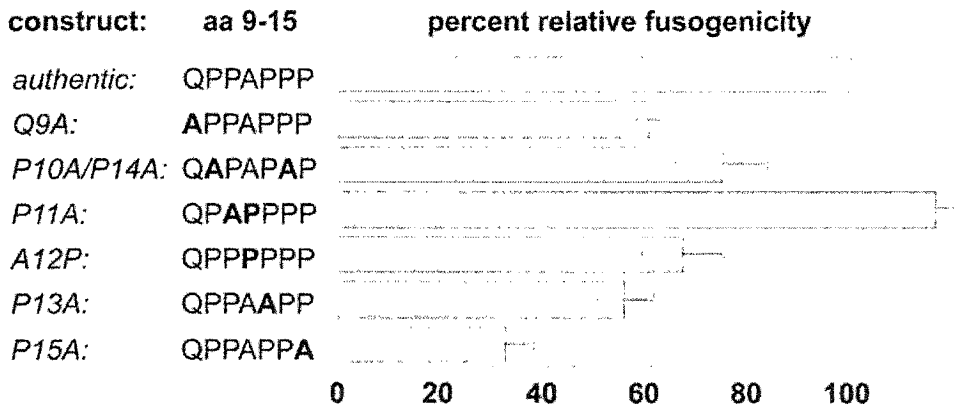

Figure 5.3. **No single residue within the p15 proline-rich sequence is critical.** The fusogenicity of various p15 constructs mutated within the proline-rich sequence relative to authentic p15 was measured by counting the average number of nuclei per syncytia evident in transfected Vero cells. The amino acid sequence of each construct (residues 9 to15) is shown, with mutated residues in bold. Results are reported as the mean +/- the standard error from three separate experiments performed in triplicate.

Similarly, neither the preceeding glutamine residue at position 9 nor the intervening residue at position 12 was found to be essential. The importance of the p15 proline-rich repeat, therefore, must not lie in its primary sequence but rather in its predicted PPII helix conformation.

5.2.2. A p15 proline-rich peptide contains significant PPII conformation

Circular dichroism (CD) spectroscopy is widely considered to be the most reliable method for the identification of PPII helix structure (Bochicchio and Tamburro, 2002). To investigate whether PPII structure is likely to occur in the PRS of p15, a synthetic peptide (VQ**PPAPPP**NA) corresponding to residues 8 to 17 was analyzed by CD spectroscopy. The CD spectra of poly-L-proline is shown (Fig. 5.4A), demonstating the two CD spectral features that are evidence for the presence of PPII helix structure: a weak positive maximum at 230 nm, along with a stronger negative maximum in the vicinity of 200 nm (Ronish and Krimm, 1974). The former is considered to be a hallmark of the structure. The inset shows the CD spectra of poly-L-proline at increasing concentrations, which intensified the signature positive band of the PPII helix at 230 nm. The spectrum of the authentic p15 peptide (VQ**PPAPPP**NA) is typical of peptides possessing at least some PPII helical conformation. Importantly, measurement of the authentic peptide CD spectra in the presence of 3 M urea led to an increase in intensity of the maximum at 230 nm, characteristic of an increase in the proportion of PPII helix structure, whilst 4 M NaCl reduced the maximum markedly (Fig. 5.4B). Such enhancing and inhibitory effects of denaturant and high salt concentration are diagnostic of peptides having PPII helix structure (Park *et al.*, 1997; Woody, 1992).

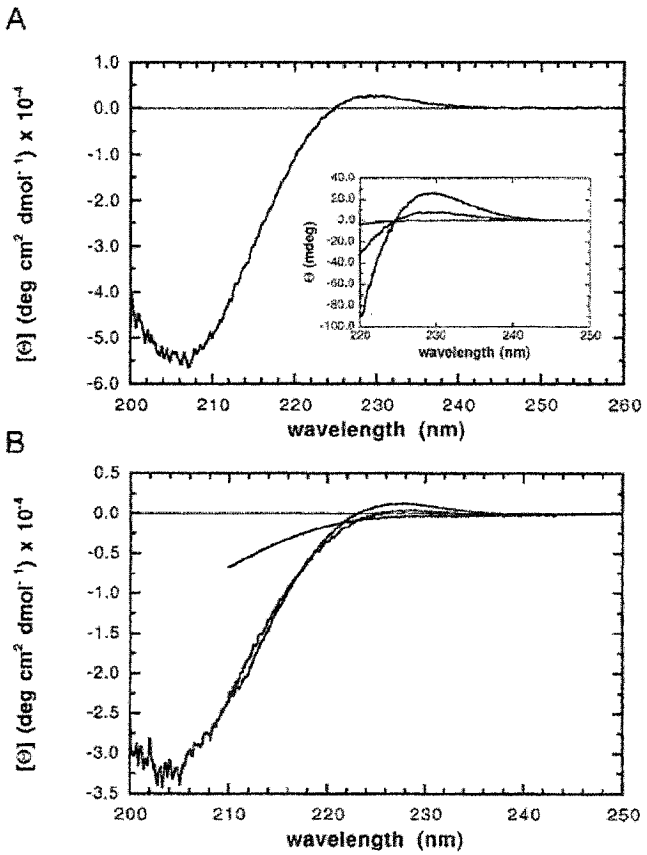

Figure 5.4. **The CD spectra of authentic (VQPPAPPPNA) peptide exhibits significant PPII helix conformation.** (A) CD spectra of polyproline (Mr 5000) at 25°C in 10 mM phosphate buffer, pH 7.5, shows characteristics of a PPII helix. The inset presents unnormalized data measured with three polyproline samples at concentrations of 1.0, 0.35, and 0.03 mg/mL. (B) Effects of denaturant and high ionic strength on the CD spectra of authentic (VQ**PPAPPP**NA) peptide at 25°C in 10 mM phosphate buffer, pH 7.5. Reading downwards at 230 nm, spectra were measured in the presence of 3 M urea, no additional solvent, and 4 M NaCl.

5.2.3. N-proximal PPII structure is essential for p15-induced syncytium formation

It has been reported that PPII helix structure is propagated through two adjacent alanines (Kim *et al.*, 2001). Using short peptides, Kim *et al.* (2001) demonstrated that, although the decrease in PPII helix content going from PAP to PAAP was much greater than that from PPP to PAP, the PAAP peptide still possessed a significant PPII helix character owing to the intrinsic propensity of alanine to adopt this structure. Thus, the PPII helix conformation is likely maintained in all of the mutants analyzed in Figure 5.3, all of which retained the ability to induce syncytium formation. To explore the relevance of PPII helix conformation to p15-induced membrane fusion, the fusogenic potential of several p15 constructs carrying mutations predicted to disrupt the PPII helix structure was analyzed. These constructs (pro2: $P_{10}AAAPA_{15}$ and pro5: $A_{10}PAAAA_{15}$) were compared to constructs (pro3: $P_{10}APAPA_{15}$ and pro4: $A_{10}PAPAP_{15}$) not predicted to lack PPII helix content, but which contained multiple mutations within the proline-rich motif. As shown in Figure 5.5, transfected cells expressing the pro2 and pro5 constructs remained as single cell foci and failed to form syncytia. However, transfected cells expressing the pro3 and pro4 constructs underwent cell-cell fusion (Fig. 5.5). Interestingly, although the proline-rich sequences of constructs pro3 and pro4 differ only in the register of the proline-alanine tri-repeat, the kinetics of fusion induced by pro3 were significantly reduced compared to those of pro4, with the onset of syncytium formation delayed by approximately 24 hours.

To corroborate the supposition that p15-induced membrane fusion is inhibited by a decrease of PPII helical content at the N-terminus (owing to the separation of proline residues within the PRS by three or more alanines), the structure of a peptide

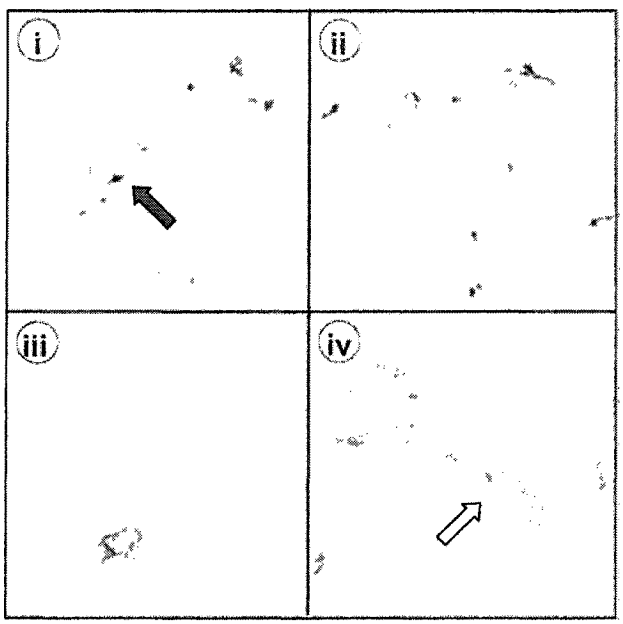

Figure 5.5. **Mutations predicted to disrupt the PPII helix conformation inhibit p15-induced syncytium formation.** Transfected QM5 cells expressing constructs (i) pro5 (PRS: A_9PAAAA_{15}), (ii) pro2 (PRS: P_9AAAPA_{15}), (iii) pro3 (PRS: P_9APAPA_{15}), or (iv) pro4 (PRS: A_9PAPAP_{15}) methanol-fixed 24 (i, ii, iv) or (iii) 48 hours post-transfection prior to immunocytochemical staining using rabbit anti-p15 antiserum (1:1000) and alkaline phosphatase-conjugated goat anti-rabbit $F(ab')_2$ (1:1000). Black arrow indicates an example of a p15-positive single-cell foci; white arrow indicates an example of a p15-positive syncytium.

corresponding to residues 8 to 17 of construct pro2 (VQPAAAPANA) was analyzed. Indeed, the CD spectra of the pro2 peptide lacks evidence for PPII helix conformation. Compared to the CD spectra of the authentic p15 peptide, the pro2 peptide spectra showed a complete loss of the weak positive maximum at 230 nm (Fig. 5.6). Clearly, the loss of PPII helix content within p15 correlates to loss of fusion activity.

5.2.4. A direct role for the PPII helix in p15-induced membrane fusion?

To investigate whether the nonfusogenic proline mutants were compromised in some aspect of p15 function prior to the membrane fusion step, the expression, acylation, membrane association, and topology of constructs pro1, pro2, and pro5 were characterized. Each of these constructs was expressed in transfected cells at a level comparable to authentic p15 (Fig. 5.7A, lanes 1-5). Modification of p15 by the addition of myristate has previously been shown to be essential for p15-induced syncytium formation (chapter 4). As the polyproline region of p15 (aa 10-15) is positioned adjacent to the consensus sequence for N-myristylation (aa 1-6), the effect of fusion-inhibitory proline mutations on the myristylation status of the protein was investigated. The nonfusogenic constructs pro1, pro2, and pro5 incorporated [^{3}H]myristic acid at a level equivalent to authentic p15 (Fig. 5.7A, lanes 6-10). The p15 G2A mutant is shown as a negative control for the specificity of myristylation (Fig. 5.7A, lanes 2 and 7). The membrane affinity of the nonfusogenic proline mutants is indistinguishable from that of authentic p15, as evidenced by their association with the membrane fraction of an *in vitro* translation reaction, as well as their resistance to extraction with a high-salt buffer (Fig. 5.7B). Furthermore, the pro1, pro2, and pro5 constructs integrate into the membrane in the proper N_{exo}/C_{cyt} topology. This is evidenced by the accessibility of the polybasic and

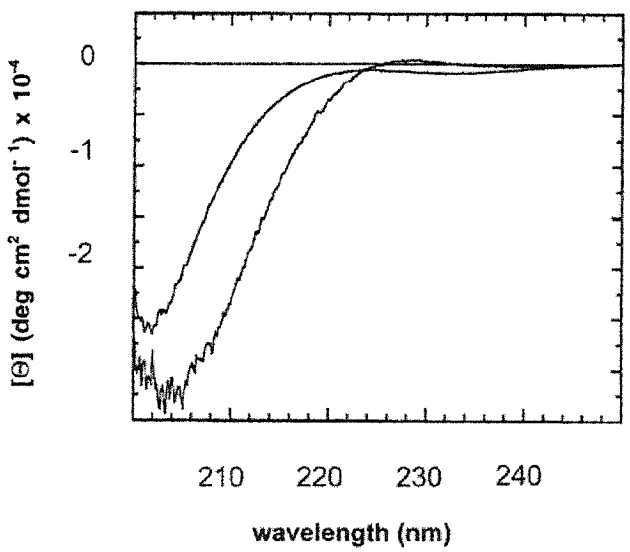

Figure 5.6. **A significant decrease in PPII helix conformation is evident in the CD spectra of the pro2 (VQPAAAPANA) peptide compared to that of the authentic (VQPPAPPPNA) peptide.** Reading downwards at 230 nm, spectra represent the authentic (VQPPAPPPNA) and pro2 (VQPAAAPANA) peptides measured at 25°C in 10 mM phosphate buffer, pH 7.5. Compared to the spectrum of the authentic (VQPPAPPPNA) peptide, the loss of PPII helix conformation in the spectrum of pro2 (VQPAAAPANA) peptide is evident in the loss of the weak positive peak at 230 nm.

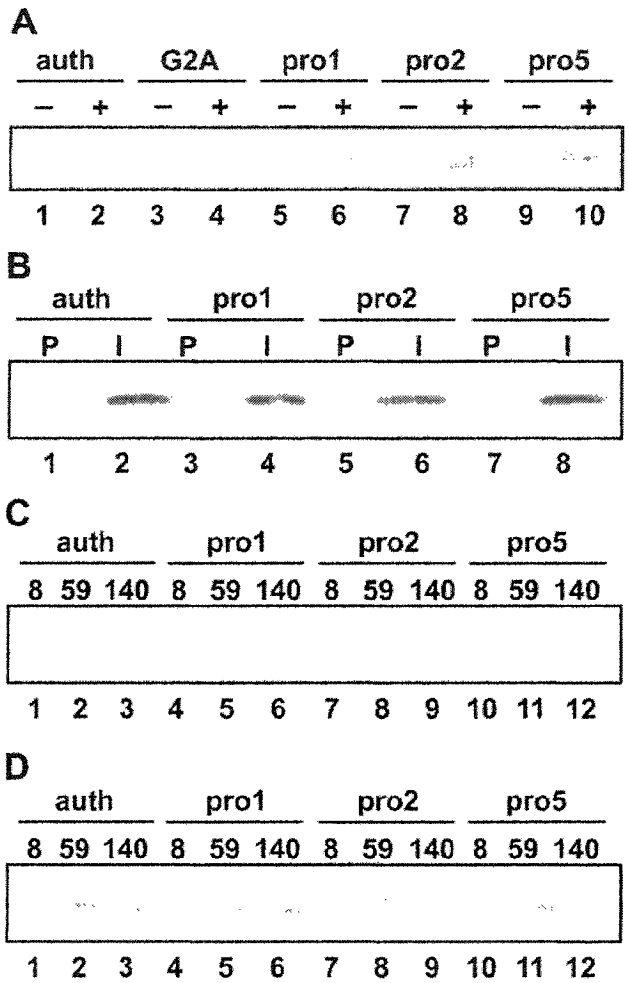

Figure 5.7. **Proline mutations that inhibit syncytium formation do not influence p15 myristylation, membrane association, or topology.** (A) Transfected cell lysates expressing authentic p15 (auth), or p15 constructs (G2A, pro1, pro2, or pro5) labeled with [^{3}H]myristate and either not immune precipitated (-) or immune precipitated using anti-p15 antiserum (+). (B) Authentic p15 (auth), or pro1, pro2, or pro5 transcripts translated *in vitro* with microsomes separated by centrifugation into the soluble and membrane-containing fractions, the latter extracted with 0.5 M NaCl and re-centrifuged to isolate the peripheral (P) and integral (I) membrane proteins. (C and D) Transfected cells, expressing authentic p15 (auth) or constructs pro1, pro2, or pro5, all tagged with the consensus sequence for protein kinase A following residues 8, 59, or 140, (C) treated with cycloheximide (100 mg/mL) prior to, and during, radiolabeling with [^{32}P]phosphate; or (D) radiolabeled with [^{3}H]leucine in the absence of cycloheximide. Lysates immune precipitated using anti-p15 antiserum.

C-terminal domains (but not the translocated N-terminus) to phosphorylation by PKA in the presence of cycloheximide (Fig. 5.7C). As p15 does not contain a signal sequence and the N-terminus of the protein is transiently exposed to the cytosol prior to its translocation, [^{32}P]phosphate-labeling was performed on cycloheximide-treated cells to detect only the phosphorylation of p15 domains in their final membrane orientation (refer to chapter 4). Expression of the non-phosphorylated constructs was confirmed by the incorporation of [^{3}H]leucine in the absence of cycloheximide (Fig. 5.7D).

It was hypothesized that the polyproline motif may contribute to the trafficking of the fraction of p15 that is expressed at the cell surface. As described in chapter 4, the only currently available method to detect p15 present at the cell periphery is to visualize the surface population of permeabilized cells once the intracellular pools of p15 have been depleted by cycloheximide-treatment. Visualization of p15 under these conditions is facilitated by the fusion of GFP to the C-terminus of various p15 constructs. As shown in Figure 5.8, cells transfected with either pro1-GFP, pro2-GFP, or pro5-GFP expressed populations of fluorescent protein at the cell surface, comparable to that of cells transfected with authentic p15-GFP.

5.2.5. Nonfusogenic proline mutants exhibit a dominant-negative phenotype

Consistent with the essential nature of the p15 polyproline helix, the nonfusogenic proline mutants exhibited a dominant-negative effect in Vero cells co-transfected with authentic p15. The ability of p15 to induce membrane fusion was eliminated in cells transfected with a 1:1 ratio of authentic p15 cDNA and cDNA for either pro1, pro2, or pro5 (Fig. 5.9B-D). The dominant negative effect was specific to the polyproline region, as co-transfection of authentic p15 cDNA with cDNA for a nonfusogenic construct

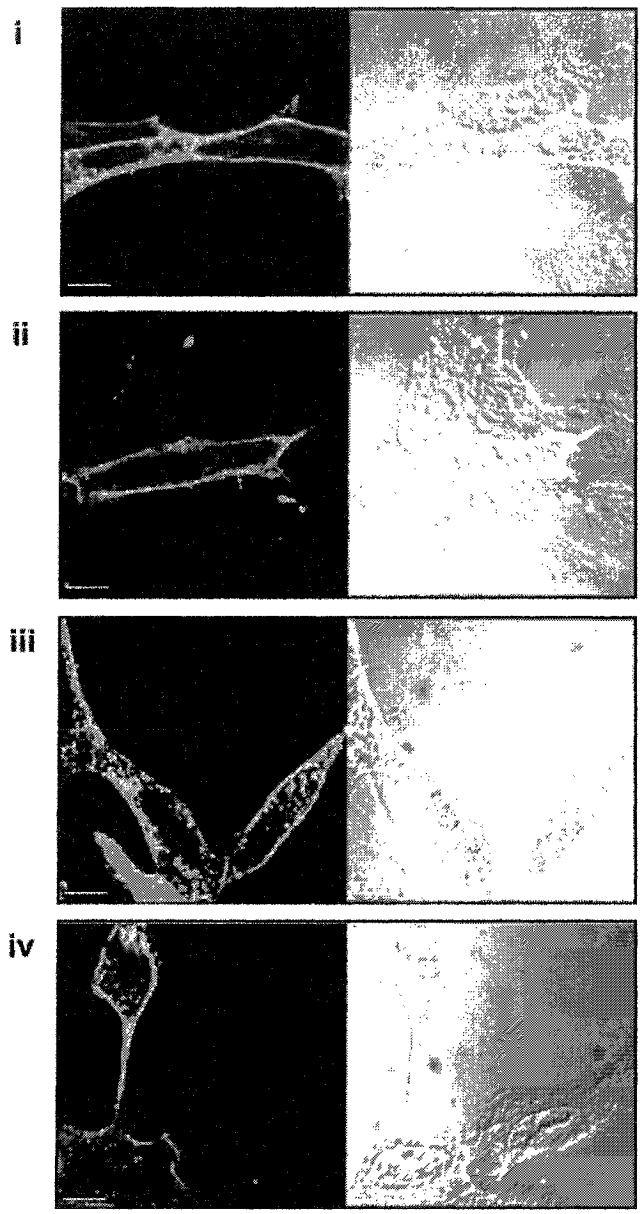

Figure 5.8. **The N-proximal PPII helix is not required to traffick p15 to the cell surface.** Transfected cells expressing (i) pro1-GFP, (ii) pro2-GFP, (iii) pro5-GFP, or (iv) auth-GFP, methanol-fixed 20 h post-transfection following 1 h treatment with cycloheximide. Right-hand panel represents merge of fluorescent image (at left) with DIC image. Cell images were captured (with technical assistance from J. Corcoran) using a Zeiss LSM510 scanning argon laser confocal microscope (1000x magnification); scale bar represents 10 μm.

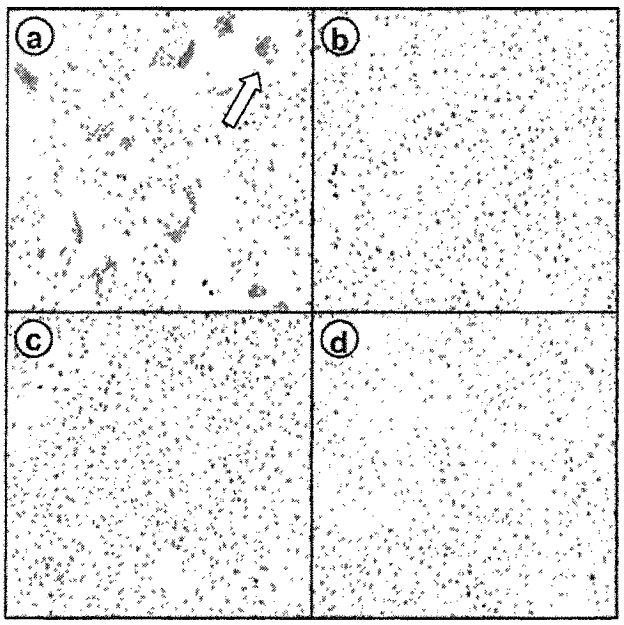

Figure 5.9. **Nonfusogenic p15 constructs containing PRS mutations exhibit a dominant-negative phenotype.** Vero cells were co-transfected using a 1:1 ratio of cDNA for authentic p15 and (a) pcDNA3 vector, (b) QAAAAAA p15 construct, (c) QAPAAAA p15 construct, or (d) QPAAAPA p15 construct. Transfected cells were methanol-fixed 16 h post-transfection and Giemsa stained to visualize the formation of multinucleated syncytia (an example of which is indicated by the arrow).

mutated in the downstream polybasic region (construct 59-HA) did not grossly inhibit p15-induced membrane fusion (Fig. 5.9A). For comparison to the control cells, images shown are of monolayers fixed and Giemsa-stained 18 hours post-transfection. However, it should be noted that the cells co-transfected with authenic p15- and nonfusogenic proline mutant-cDNAs fail to develop syncytia over the full course of the experiment (72 hours). It can be concluded that the proline-rich region of p15 influences neither the protein's expression, N-myristylation, topogenesis, nor trafficking to the cell periphery, and may, therefore, be directly involved in the fusion process.

5.3. Discussion

5.3.1. The PPII helix is an increasingly recognized motif governing virus-host cell interactions

An increasing number of viral proteins have been identified as containing the appropriate PRSs in order to interact with various PRS-recognition domains. Examples of the effects of such recognition processes on viral-cellular interactions include the inhibition of protein kinase R activation by the herpes simplex virus type I Us11 protein (Poppers *et al.*, 2000), the alteration of T-cell receptor signaling by both the HIV-1 Nef protein (Arold *et al.*, 1997) and the herpesvirus Tip protein (Schweimer *et al.*, 2002), the down-regulation of MHC-1 by HIV-1 Nef (Mangasarian *et al.*, 1999), the modulation of B-cell signal transduction by Epstein-Barr virus LMP2A (Ikeda *et al.*, 2000), the processing and stability of the envelope proteins of type C mammalian retroviruses (Weimin Wu *et al.*, 1998), and the budding of retroviruses, rhabdoviruses and filoviruses (Goff *et al.*, 2003; Harty *et al.*, 2000; Yasunda *et al.*, 2003). The matrix function of the

hepadnavirus L protein has been mapped to a PRS (Bruss, 1997) that is designated here as 'PRS-b'. Structural analysis of this region has not been published, nor has speculation that this motif might adopt a PPII helix. However, it is compelling that, while the sequence of this region varies among L proteins of different hepadnaviruses, the positioning of the prolines is conserved (Table 5.1), suggesting a potential role for these prolines in the recognition of hepadnavirus nucleocapsids.

Interestingly, the NS3 protein encoded by various members of the *Orbivirus* genus within the *Reoviridae* family, which is involved in membrane perturbations leading to virus release from host cells, contains an N-proximal PRS which is conserved among serotypes but variable in sequence between serogroups (Table 5.2) (Jensen *et al.*, 1994; Martin *et al.*, 1998; van Niekerk *et al.*, 2003; van Staden and Huismans, 1991).The PRS of NS3 is similar in sequence and location to the PRS of p15. NS3 and p15 are both small, hydrophobic, nonstructural, membrane-active proteins encoded on the smallest genome segment of their respective reoviruses. Presently, there is no evidence that the orbivirus NS3 PRS mediates interaction with any other protein. In the case of bluetongue virus, although NS3 was found to interact with the cellular membrane trafficking protein p11 (calpactin light chain), the binding site is upstream of the NS3 PRS (Beaton *et al.*, 2002). The conservation of a polyproline motif likely to exhibit PPII helix character suggests that such a conformation within the N-terminus of NS3 is important to its function. However, the high degree of sequence variation within this conserved secondary structure motif suggests that it is unlikely to recruit a specific NS3 binding partner. The role of the PRS in orbivirus NS3 function remains unclear. However, it is tempting to speculate that the PRS may be involved in the ability of NS3 to alter

Table 5.1. **The hepadnavirus L protein contains a conserved proline-rich sequence in its pre-S domain that is required for nucleocapsid envelopment.** The L protein 'PRS-b' is compared among hepatitis B virus (HBV), woodchuck HBV (WHV), and duck HBV (DHBV); first and last residues are numbered; prolines are highlighted in bold; positions of conserved prolines are underlined.

Hepadnavirus	Proline-Rich Sequence	NCBI Accession
HBV	**P**$_{105}$T**P**IS**PP**LRNSH**P**$_{117}$	AA065967
WHV	**P**$_{129}$T**P**T**PP**LRDTH**P**$_{141}$	AAA46760
DHBV	**P**$_{78}$ T**P**QEI**P**Q**P**QWT**P**$_{90}$	P03145

Table 5.2. **Proline-rich sequences contained within nonstructural reovirus proteins.** The PRSs of several orbivirus NS3 proteins and orthoreovirus FAST proteins are compared; first and last residues are numbered; prolines are highlighted in bold.

Virus	Proline-Rich Sequence	NCBI Accession
orbivirus NS3 proteins:		
African horse sickness virus	$\mathbf{P}_{22}$YV**PPP**YNFASA$\mathbf{P}_{34}$	BAA02048
Bluetongue virus	$\mathbf{P}_{36}$**P**RYA**P**SA**P**M**P**SS$\mathbf{P}_{50}$	S12593
Broadhaven virus	$\mathbf{P}_{10}$TA**PP**AYAAI$\mathbf{P}_{21}$	P8XRBH
Chuzan virus	$\mathbf{P}_{22}$YQ**PP**AYPTA$\mathbf{P}_{32}$	BAA76554
Epizootic hemorrhagic disease virus	$\mathbf{P}_{25}$YQEQVR**PP**SYV**P**SA**P**IPTAM$\mathbf{P}_{46}$	AAQ62564
Equine encephalitis virus	$\mathbf{P}_{22}$**P**TA**P**M**PP**$_{29}$	AAM83198
Palyam virus	$\mathbf{P}_{22}$YQ**PP**AYPTA$\mathbf{P}_{32}$	PQ0536
orthoreovirus FAST proteins:		
Baboon reovirus p15	$\mathbf{P}_{10}$**P**A**PPP**$_{15}$	AAL01373
Reptilian reovirus p14	$\mathbf{P}_{99}$YE**PP**SRRK**PPPPP**$_{112}$	AAP03134

membrane structure (independent of mediating a specific protein-protein interaction), and that such an activity is shared with the PRS of the BRV p15 protein.

5.3.2. Formation of the N-proximal PPII helix is key to p15 fusogenicity

Through mutational and structural analyses, it has been demonstrated that the N-proximal PRS of p15 folds into an essential PPII helix (Figs. 5.4-5.6). The evidence clearly indicates that the proline-rich motif is not involved in regulating the levels of p15 expression or N-myristylation, and is also not required for either the proper membrane insertion or transport of p15 to the cell surface (Figs. 5.7 and 5.8). Hence, p15 may contain the first example of a polyproline helix that is directly involved in a membrane fusion mechanism. It is noteworthy that a recently identified putative cell-cell fusion protein, HAM-2, required for hyphal fusion in filamentous fungi, contains an N-proximal PRS (QPSAPPPAAPSNFPPPVP) comparable in part to that of p15 (QPPAPPP) (Xiang, 2002).

It has been previously illustrated that p15, like the other FAST proteins, is the only viral protein required to promote syncytium-formation (chapter 3). However, given the well-documented role of various polyproline helices in governing protein-protein interactions, it is possible that p15 may interact (through its polyproline motif) with a cellular ligand required to initiate membrane fusion. A putative protein partner could complex with p15 in the donor membrane, possibly to bridge apposed membranes, or could function as a cellular receptor for p15 in the target membrane. However, several lines of evidence argue against these scenarios. The absence of the p15 polyproline motif from the ectodomains of the other FAST proteins, together with the ability of synthetic peptides corresponding to FAST protein ectodomains to function in lipid-mixing assays

(Corcoran *et al.*, 2004; Shmulevitz *et al.*, 2004b), contradicts a model of FAST protein-induced membrane fusion reliant on a cellular binding partner. An alternative role for a cellular protein partner in FAST protein-mediated fusion could be to aid in the local restriction of lipid flow at the fusion site (refer to the hydrophobic or bending defect models discussed in chapter 1). Such a role for a protein partner cannot be ruled out by the activity of FAST protein peptides in the lipid-mixing assay, since this assay measures unrestricted lipid flow. Nonetheless, the fact that none of the individual residues within the p15 PRS occupy a critical position (Fig. 5.3) is counter-intuitive to one or more of these residues playing a role in specifically binding to a protein partner. Prolines occupy positions *i* and *i+3* on two separate faces of the p15 PPII helix; P10 and P13 align on one plane while P11 and P14 align on another. However, potential p15-ligand interactions are unlikely to be mediated by the coordinated binding of prolines on either face, as prolines of each pair were mutated individually without abolishing p15 function (Fig. 5.3). The robust fusogenicity of construct pro4 (Fig. 5.5), which lacks either a PxxP or a PPx core motif, indicates that the p15 PRS does not fall into any category of known proline-rich ligand, including the binding motifs recognized by SH3, WW, EVH1, profilin and GYF domains. If the p15 polyproline motif does mediate ligand-binding, it may constitute a new class of PPII helix structures governing protein-protein recognition.

The pro3 construct is an intriguing mutant in that the kinetics of pro3-induced syncytium formation are significantly delayed (Fig. 5.5). This effect may reflect the combined P13A and P15A mutations in this construct as, individually, these substitutions were the most deleterious to p15 fusogenicity (Fig. 5.3). It is difficult to explain the pro3 kinetic defect in terms of PPII helix content, as pro3 would be expected to exhibit PPII

helix character equivalent to the pro4 construct, which fuses at close to authentic p15 levels. Although P13 and P15 influence p15 fusogenicity, neither of these residues are strictly required. If P13 and/or P15 form a ligand-binding motif (PxP) recognized by an essential protein partner, clearly the interactions at the protein-protein interface must be promiscuous since alanine is tolerated in those positions. Alternatively, P13 and P15 may provide scaffold-like functions to a distal ligand-binding motif, or to a conformation that facilitates a ligand-independent p15 function. If so, the incomplete inhibition of p15 fusogenicity upon alanine substitution of P13 and P15 would be explained by the ability of alanine to be relatively well accommodated within PPII helix conformation.

5.3.3. The p15 PRS is potentially variable – lessons from HBV L

It is clear that no single residue within the proline-rich region is specifically required for p15 function (Fig. 5.3). This suggests that the positions of the proline residues within the p15 PRS may be variable and thus, the importance of the p15 PRS may lie in the flexibility it might confer to the p15 ectodomain rather than in providing a platform for a specific protein-protein interaction. In the absence of any p15 sequence other than that from the single BRV 10895 isolate, multiple sequence comparisons cannot be made that would illustrate whether the PRS is a conserved BRV p15 motif. The folly of interpreting the specific sequence pattern of a single isolate was realized from analysis comparing the p15 PRS to a sequence present within the hepadnavirus L protein. The L protein of some HBV isolates (e.g. accession # AF052576) contains a PVAPPP motif (comparable to the p15 PPAPPP) in a larger region (residues 63-107) of the pre-S domain that is important for L topogenesis. This region is located upstream of the 'PRS-b' previously discussed (Table 5.2), and thus is designated 'PRS-a'. This portion of L

interacts with the cytosolic heat-shock protein chaperone Hsc70 to repress the co-translational translocation of the pre-S domain (Loffler-Mary *et al.*, 1997). The pre-S domain is post-translationally translocated in about half of the L population. Given the apparent similarity of the pre-S 'PRS-a' and the p15 proline-rich motif, together with the observation that p15 can also integrate into membranes in a post-translation manner *in vitro* (Fig. 5.10), a role for the PRS in facilitating p15 post-translational insertion was proposed. However, this hypothesis was discounted since various proline mutants, including the pro1 construct (all prolines replaced by alanine), were not impaired in their ability to interact post-translationally with membranes *in vitro* (data not shown). Furthermore, attempts to co-immune precipitate p15 using anti-Hsc antiserum were unsuccessful (data not shown). Upon further inspection of the HBV L pre-S domain 'PRS-a', it was found that the pattern of this motif is altered in different isolates, such that only one proline position is completely conserved (Table 5.3). While the proline-rich character of this region of HBV L is clearly maintained, the PRS is variable, with neither the identity nor positioning of the proline residues strictly maintained. Thus, the significance of the initially perceived similarity of this PRS to the p15 PRS is diminished, especially considering that while most of the prolines are variable, much of the flanking nonproline residues are not (refer to Table 5.3). It is not possible to determine whether similar sequence variation exists for the PRS of p15 until p15 sequences from additional BRV isolates become available.

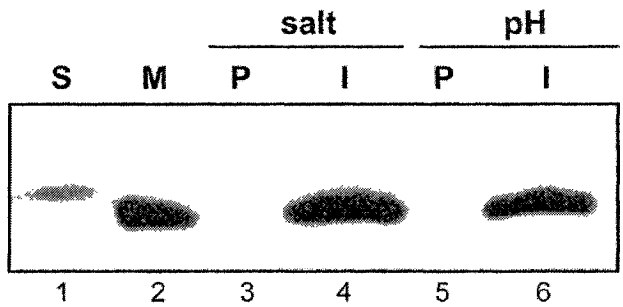

Figure 5.10. **BRV p15 is capable of integrating into membranes post-translationally *in vitro*.** p15 was translated *in vitro* without membranes. Translation reactions were stopped by the addition of cycloheximide (10 μg/mL) and RNase A (1 mg/mL) for 15 min, at which point microsomal membranes were added to the sample. Following a 30 min incubation, reactions were separated by centrifugation through a sucrose cushion into the soluble (S) and membrane-containing (M) fractions, the latter extracted with either 1 M NaCl (salt) or 100 mM Na_2CO_3, pH 11.5 (pH) and recentrifuged to isolate the peripheral (P) and integral (I) membrane proteins.

Table 5.3. **The hepadnavirus L protein contains a variable proline-rich sequence in its pre-S domain within a region controlling L topogenesis.** A proline-rich region ('PRS-a') of the L protein of various HBV L isolates is compared; last residue is numbered; prolines are highlighted in bold; positions of the only absolutely conserved proline is underlined.

Proline-Rich Sequence	NCBI Accession
TTV**P**VA**P**P**P**AST$_{93}$	AF052576
ATV**P**VV**P**P**P**TAST$_{86}$	AAC58021
ATV**P**AV**P**P**P**TAST$_{86}$	AAC58026
ATV**P**AV**P**P**P**AST$_{97}$	AAC35893
TTL**P**AD**P**P**P**AST$_{98}$	AAC35896
TTL**P**AL**P**P**P**AAT$_{86}$	S67506
TTV**P**AA**P**P**P**AST$_{97}$	AAK59317
QTL**P**AN**P**P**P**AST$_{86}$	AAQ90272
TTV**P**TA**P**P**P**AST$_{86}$	SAVLJ3
QTL**P**TN**P**P**P**AST$_{86}$	AAQ90271
ATL**P**TV**P**P**P**AST$_{86}$	AAC58024
TTV**P**TI**P**P**P**AST$_{97}$	CAC87026
TTVSTI**P**P**P**AST$_{97}$	AAO65967
TTV**P**EA**P**H**P**AST$_{97}$	T13469

5.3.4. Are multiple PPII helices required to generate a functional p15 multimer?

The ability of nonfusogenic proline mutants to exhibit a dominant-negative phenotype underscores the importance of the polyproline motif to p15 activity (Fig. 5.8). Although not proof of p15 oligomerization, the dominant-negative effect is consistent with p15 functioning as a homomultimer dependent on the presence of an intact PPII helix in each subunit. If p15 does multimerize, the proline-rich region itself is unlikely to be the multimerization domain. Although polyproline motifs have been implicated in the self-assembly of plant and algae cell wall proteins (Ferris *et al.*, 2001), extracellular matrix proteins (Bochicchio and Tamburro, 2002; Ender *et al.*, 2002; Kieliszewski and Lamport, 1994), and plant storage body proteins (Kogan *et al.*, 2001), in these cases extensive tandem proline-rich repeats confer long regions of PPII helix to the proteins which are then capable of winding into fibrillar supermolecular structures. In the case of the collagen triple-helix (consisting of three extended PPII helices), Feng *et al.* (1996) demonstrated that a minimum of six G-P-X repeats (i.e. at least 18 residues) is required for significant trimer formation. Thus, it is improbable that the short (5-residue) PRS contributes significantly to the possible multimerization of p15.

5.3.5. The N-proximal PPII helix is unique to p15 within the FAST protein family

Within the FAST protein family, the presence of an essential polyproline repeat is a unique feature of the p15 ectodomain. The p10 fusion proteins of ARV and NBV lack a proline-rich domain, and the distinct polyproline sequence contained within the cytosolic C-terminal tail of RRV p14 (Table 5.1) can be removed without eliminating the ability of p14 to mediate syncytium formation (Corcoran *et al.*, 2004). Given that an externalized PPII helix domain is not a feature required for the induction of membrane fusion by all

the FAST proteins, it is likely that the PPII motif contributes to a fusion-competent character of the p15 ectodomain – a character that may be conferred to the ectodomains of the other FAST proteins by distinct features. Such a quality may be related to an extended protein conformation, or to an added degree of flexibility in the protein chain. The flexibility inherent in the N-proximal PPII helix, may assist the reversible 'flipping' of the N-terminal myristate moiety between the donor and target membranes during an initial step in the fusion process (see chapter 7). Further structural analysis is required to determine the precise nature of the participation of the p15 PPII helix in the fusion reaction.

CHAPTER 6

THE FAST PROTEINS ARE MODULAR FUSION MACHINES

6.1. Introduction

Until recently, it was generally accepted that viral fusion proteins contained a single hydrophobic fusion peptide that was solely responsible for the destabilization of the target cell membrane during the fusion process (Peisajovich and Shai, 2003). It was presumed that protein motifs placed well away from the alleged site of fusion initiation at the target membrane did not directly participate in the fusion reaction. However, it is becoming increasingly clear that, in addition to the classical fusion peptide, other regions of viral fusion proteins interact directly with either the donor or target lipid bilayer and contribute to membrane merger (Peisajovich and Shai, 2003). For instance, the heptad repeat (coiled coil) region that has long been implicated in the critical structural reoganization of class I viral fusion proteins (refer to chapter 1), has also been shown, in the cases of influenza HA, sendai F and HIV gp41, to bind membranes and potentiate the activity of the fusion peptide (Epand *et al.*, 1999; Ghosh and Shai, 1999; Kliger *et al.*, 2000; Sackett and Shai, 2002), as well as accomplish hemifusion in the absence of the fusion peptide (Leikina *et al.*, 2001). In addition, the short loop ('hydrophobic kink') following the N-proximal heptad repeat domain of influenza HA and HIV/SIV gp41 has been proposed to have membrane-binding activity (Epand *et al.*, 1999; Peisajovich and Shai, 2001; Santos *et al.*, 1998), and the equivalent region of paramyxovirus (Sendai virus and NDV) F has been identified as a second fusion peptide (Peisajovich *et al.*, 2000). A further membrane-perturbing motif, the pre-TM 'stem' sequence enriched in

aromatic amino acids, has been identified in the fusion proteins of several enveloped viruses, including those of retroviruses, filoviruses, orthomyxoviruses, paramyxoviruses, rhabdoviruses, alphaviruses and flaviviruses (Suarez *et al.*, 2000; Tong *et al.*, 2001). The stem regions of HIV gp41 and Foamy virus Gp47 exhibit a high propensity to partition into, and destabilize membranes, and appear to act together with the fusion peptide to accomplish full membrane fusion (Epand and Epand, 2001; Suarez *et al.*, 2000). Through its membrane-perturbing activity, the stem region of VSV G (together with the G endodomain) not only accomplishes hemifusion, but is able to potentiate the fusogenic activity of heterologous viral fusion proteins when co-expressed with those proteins (Jeetendra *et al.*, 2002). Salzwedel *et al.* (1999) proposed a late-stage role for the stem region of HIV gp41 in disrupting the donor membrane in order to enable fusion pore expansion. The membrane-proximal region of the neuronal SNARE complex is similarly enriched in conserved aromatic (and basic) amino acids, and the insertion of this region into the membrane is proposed to facilitate membrane fusion (Kweon *et al.*, 2003). Whatever the precise nature of the role played by the stem region, it is clear that this motif is membrane-active and likely contributes to the merger of two bilayers in several different systems.

Early models of membrane fusion involving the simple membrane-perturbing action of a fusion peptide paired with a seemingly inert TM anchor are clearly outdated. Our current understanding of membrane fusion reflects a complex process, in which the concerted action of several membrane-interacting domains is required to achieve membrane merger. That multiple regions of the enveloped virus fusion machines have been shown to contribute to the fusion process opens the possibility that there can exist

variation in the combination of fusion-promoting motifs. Thus, it becomes less paradoxical that the reovirus FAST proteins lack both a classical fusion peptide motif and a heptad repeat sequence, presumably in favour of other membrane-active segments.

The FAST proteins appeared highly divergent from one another when their entire amino acid sequences were assessed as a whole (chapter 3). Comparison of the sequence-predicted motifs revealed that the p10, p14 and p15 proteins each contain a unique repertoire of domains. Furthermore, upon determination of the topology assumed by the FAST proteins (all type III, N_{exo}/C_{cyt}), there appeared to be no constraint placed on the conservation of the ecto- or endodomain-localization of select motifs (chapter 4). The polyproline region, acylation site, and the non-TM hydrophobic stretch are located on either side of the membrane depending on which FAST protein is being considered. The diversity evident in the organization of structural features among the FAST proteins is remarkable. The only obvious structural feature that is conserved among p10, p14 and p15, is the presence of a TM anchor flanked by a polybasic cluster in the endodomain. Presumably, this feature alone is insufficient to explain FAST protein fusogenicity. Thus, it was hypothesized that one or more functional domains, common to all FAST proteins and key to the fusion mechanism, remained to be identified.

Analysis presented in this chapter tentatively identifies a putative flexible (FLX) region as such a domain. It is speculated that the FLX sequence of p15 (residues 90-102) and the corresponding semi-conserved sequences within p14 (residues 13-24) and p10 (residues 6-17) are mechanistically equivalent, as these regions can be functionally exchanged among the different FAST proteins. Although a specific role for the FLX motif in FAST protein-mediated membrane fusion has yet to be demonstrated, the FLX

residues of p14 and p10 are contained within externalized hydrophobic patches that have been shown to induce lipid mixing in liposome fusion assays (Corcoran *et al.*, 2004; Shmulevitz *et al.*, 2004b). The intimation that portions of the potential 'fusion peptides' present in the ectodomains of p10 and p14 are functionally equivalent to a motif located within the endodomain of p15 demands a new perspective on the model of how FAST proteins accomplish cell-cell fusion (chapter 7).

6.2. Results

6.2.1. Analysis of the TM-domain and proximal sequence

The presence of a TM anchor flanked by a highly-charged region is a prominent feature shared among the FAST proteins. Comparison of these regions revealed that the greatest degree of similarity (62%) exists between p15 and p14, with the corresponding region of p10 being less well conserved (Fig. 6.1B) However, a similar arrangement of three to five aromatic residues positioned approximately within the C-terminal half of the TM anchor is evident within all the FAST proteins (Fig. 6.1D) – a feature which may confer a conical shape to the membrane-spanning segment. Upstream of the aromatic amino acid-enriched region, the TM sequence of each FAST protein contains a motif that may be involved in TM helix-helix interactions. GxxxG-like motifs, such as that of glycophorin-A (GVxxGV), are known to mediate TM oligomerization (Senes *et al.*, 2000). These motifs consist of small amino acids (G, A, S) at positions *i* and *i*+4 found in association with large aliphatic residues (I, V, L) at neighbouring positions (*i*+/-1 and *i*+/-2). Thus, sequences of the p15 (GIxxAV), p14 (AxLxAL), and possibly p10 (LAxxxG) TM regions potentially promote self-assembly. If the FAST TM domains oligomerize,

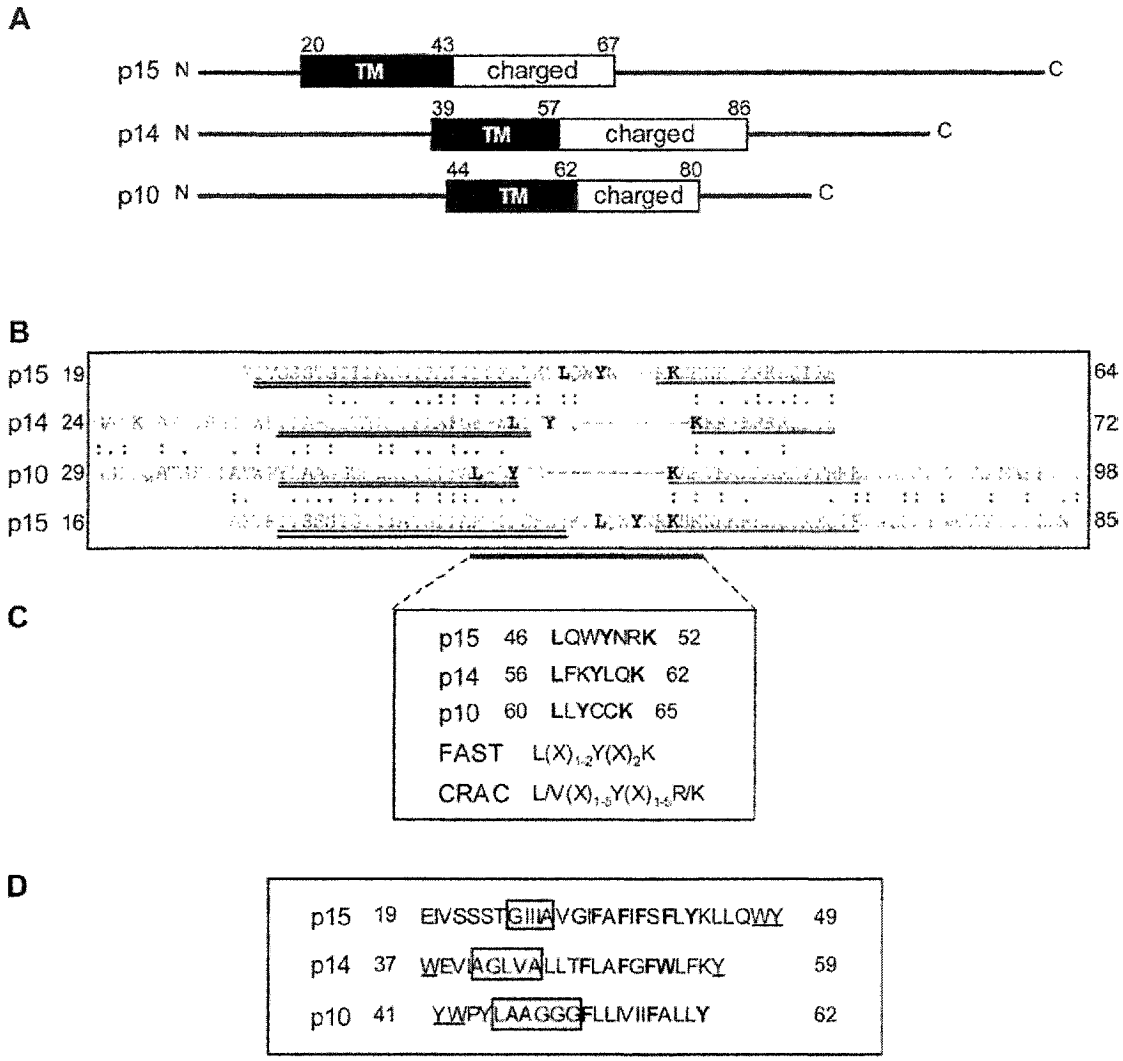

Figure 6.1. **Comparison of the TM domain and flanking charged region among the different FAST proteins.** (A) Schematic diagram indicating the relative positions of the TM domain and flanking charged region within BRV p15, RRV p14 and ARV p10; residue positions are numbered. (B) Pairwise alignments of the TM domain (double-underlined), potential cholesterol recognition motif residues (in bold type), and flanking charged sequence (underlined) of the FAST proteins; identical (:) and similar residues (.) are noted. Alignments are based on the lalign program (Huang and Miller, 1991). (C) Potential cholesterol-binding amino acid pattern of p15, p14, and p10, showing the consensus pattern for the FAST proteins, compared to the published CRAC motif common to all cholesterol-binding proteins (Li and Papadopoulos, 1998). (D) Sided arrangement of TM-domain aromatic residues (in bold type), membrane-proximal aromatic residues (underlined), and potential TM domain-oligomerization, GxxxG-like, motifs (boxed in grey) of p15, p14 and p10. For (B-D) numbers indicate first and last residue positions.

potential pi-pi stacking of proximal TM-domain aromatic residues might stabilize tight helix-helix interactions (Chelli *et al.*, 2002).

In addition, a previously overlooked cholesterol-binding pattern was identified in the membrane-proximal sequences of all the FAST proteins (Fig. 6.1C). This pattern conforms to the cholesterol recognition/interaction amino acid consensus (CRAC) proposed by Li and Papadopoulos (1998). The CRAC is composed of a neutral, hydrophobic residue (L or V) proposed to interact with the hydrophobic side chain of cholesterol, a neutral, polar residue (Y) proposed to interact with the polar 3' hydroxyl of cholesterol, and a basic residue (R or K) that may help create a binding pocket. Each of these key residues may be separated by 1-5 different amino acids (Li and Papadopoulos, 1998). Analysis of p15 indicated, that a polypeptide containing the TM anchor, CRAC, and flanking charged region is not sufficient for FAST protein-mediated membrane fusion since a p15 mutant truncated immediately downstream of the charged region (67met*) failed to promote syncytium formation (see Fig. 6.4). Thus, while the TM domain, CRAC and polybasic cluster likely contribute to the activity of the FAST proteins, other motifs are required to accomplish cell-cell fusion.

6.2.2. Characterization of the 'hydrophobic patch'

Another feature common to all the FAST proteins is the presence of a non-membrane-spanning, weakly to moderately hydrophobic segment; the so-called hydrophobic patch (HP). The HP regions of p10 (residues 9-24) and p14 (residues 8-25) are located in the ectodomains of these proteins, and have been demonstrated to possess fusion peptide-like activity in lipid-mixing assays (Corcoran *et al.*, 2004; Shmulevitz *et al.*, 2004b). In contrast, the p15 HP is not present in the ectodomain but, rather, in the

endodomain. The HP region of p15 (designated the H2 domain, chapter 4) was examined for similarity to either of the HP motifs of the other FAST proteins and was found to bear little resemblance to either the p10 or p14 HP. The p15 H2 domain does exhibit similarity (47%) to a moderately hydrophobic region of C-terminal sequence within p10 (residues 78-98). In fact, the primary sequences of these two regions are 36% identical. The significance of this similarity, if any, is not known.

Although the p15 H2 domain as a whole appeared unrelated to other FAST protein HP motifs, analysis of the sequences flanking H2 did reveal similarity to sequences contained within the p14 or p10 HPs. The similarity of cytoplasmically-localized sequences of BRV p15 to the externalized HPs (putative fusion peptides) of the other FAST proteins was surprising. Given the absence of an externalized HP motif within p15, the possibility that p15 endodomain sequence(s) may be functionally equivalent to the putative fusion peptides of the other FAST proteins was intriguing. For ease of comparison, these sequences of the p15 endodomain were separated into two regions, designated hinged loop (HL) and flexible (FLX) (Fig. 6.2). The HL region overlaps with the H2 domain and extends downstream, encompassing proline 81 to proline 90. Given the ability of proline to introduce a kink into a polypeptide backbone and to act as a molecular hinge (Cordes *et al.*, 2002), it was hypothesized that the region of p15 between proline 81 and proline 90 might fold into a short loop flanked by proline-based hinges. The FLX motif consists of the sequence stretching from proline 90 to glycine 102, predicted to adopt a combination of random coil and extended strand conformations using Guermeur's hierarchial neural network (Combet *et al.*, 2000). The relative positioning of the HL and FLX domains within p15 and the corresponding

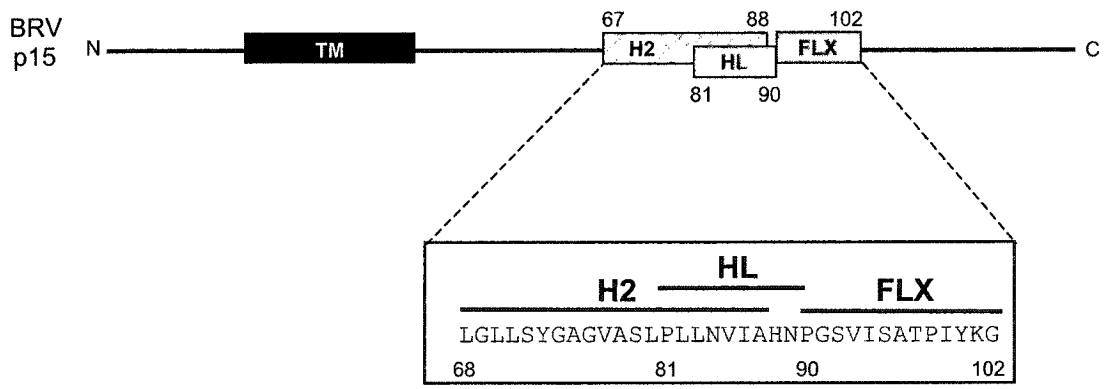

Figure 6.2. **Assignment of subdomains within the amino acid sequence of the p15 C-terminal tail.** The amino acid sequence of the p15 endodomain between residues 67 and 102 is assigned nomenclature for potentially functional domains: Hydrophobic domain 2 (H2), residues 67-88; putative hinged loop (HL), residues 81-90; and flexible (FLX) region, residues 90-102.

regions identified within the other FAST proteins is indicated, along with pairwise alignment of these sequences relative to p15 (Figs. 6.3A and B).

6.2.3. The C-terminal tail is dispensable for p15 fusogenic activity

To begin to address the importance of the sequences downstream of the previously discussed H2 domain, a series of C-terminal truncations were engineered. The positions of the p15 truncations are shown (Fig. 6.4A). Truncations are named as the last amino acid before the introduced (*) stop codon (e.g. 130* consists of the first 130 amino acids of p15). The expression and proper size of the truncated polypeptides were confirmed through immune precipitation of transfected cell lysates (Fig. 6.4B). The presence of a contaminating host band migrating closely with authentic p15, made it difficult to assure that there was no read-through translation of the various introduced stop codons to produce full-length p15. Thus, the unique size of the truncated polypeptides was verified *in vitro*. Transcripts corresponding to the nonsense mutant series were translated *in vitro* and immune precipitated using antisera against full-length p15 (Fig. 6.4C). These same transcripts were also translated in the presence of microsomal membranes and, after fractionation, the resulting membrane-bound polypeptides were analyzed (Fig. 6.4D). As expected, given the maintenance of the H1 signal anchor, all of the truncated polypeptides were found to associate with the membrane fraction of the translation reaction. Slight differences in the migration of the 103*, 97* and 94* constructs, not evident on the 15% polyacrylamide gels shown, were detected following Tricine-SDS-(16.5%) PAGE (data not shown). However, detection of these differences came at the expense of resolution of the mobility differences between authentic p15 and the 130* and 121* constructs. The decrease in radioactivity in samples

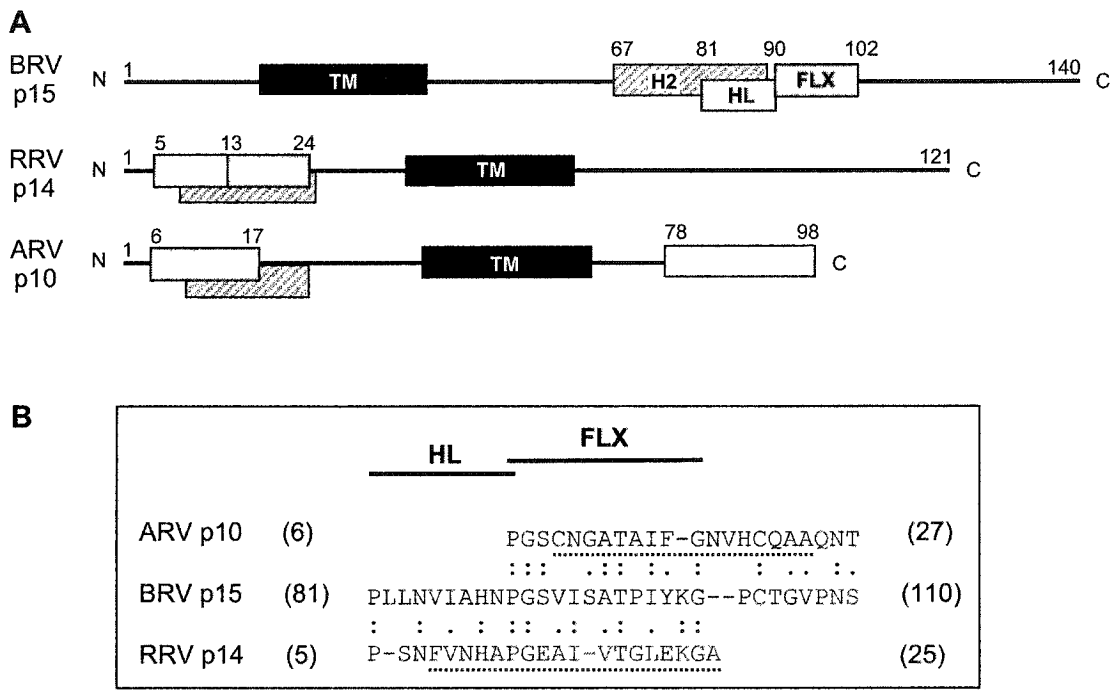

Figure 6.3. **Identification of regions within other FAST proteins displaying similarity to the p15 C-terminal subdomains, H2, HL and FLX.** (A) Schematic representation of the relative positioning of similar domains among the different FAST proteins; TM domain (black box); HP, including p15 H2 (hatched box); HL (light grey box); FLX (dark grey box); p10 sequence similar to p15 H2 (white box); amino acid positions are numbered. (B) Pairwise sequence alignment, using the lalign program (Huang and Miller, 1991), of the HL and FLX subdomains within the different FAST proteins relative to p15; positions of identical (:) and similar (.) residues are indicated; dotted lines denote locations of the p10 and p14 HPs; first and last residue positions are bracketed.

Figure 6.4. **The fusogenic potential of p15 decreases with progressive C-terminal truncation.** (A) Amino acid sequence of the p15 endodomain (residues 90-140) including the FLX domain; arrows and numbers indicate the position of the last amino acid in each truncated mutant. (B) [^{3}H]Leucine-labeled untransfected (UN) QM5 cell lysates, or lysates of cells expressing authentic p15 (auth) or p15 constructs truncated after residue 130, 121, 109, 103, 97 or 94, were immune precipitated using antiserum generated against the full-length p15 protein; (*) indicates position of a host cell background band. (C) Authentic p15 and truncated p15 mutants (as above) translated *in vitro* and immune precipitated using antiserum against full-length p15. (D) The membrane fraction of *in vitro* translation reactions of authentic p15 and truncated p15 mutants (as above). (E) The fusogenicity of various truncated mutants (as above) in QM5 cells relative to authentic p15 at 24 h post-transfection was measured by counting syncytial nuclei per 200x field of view. Results reported represent the average plus the standard error of three separate experiments performed in triplicate.

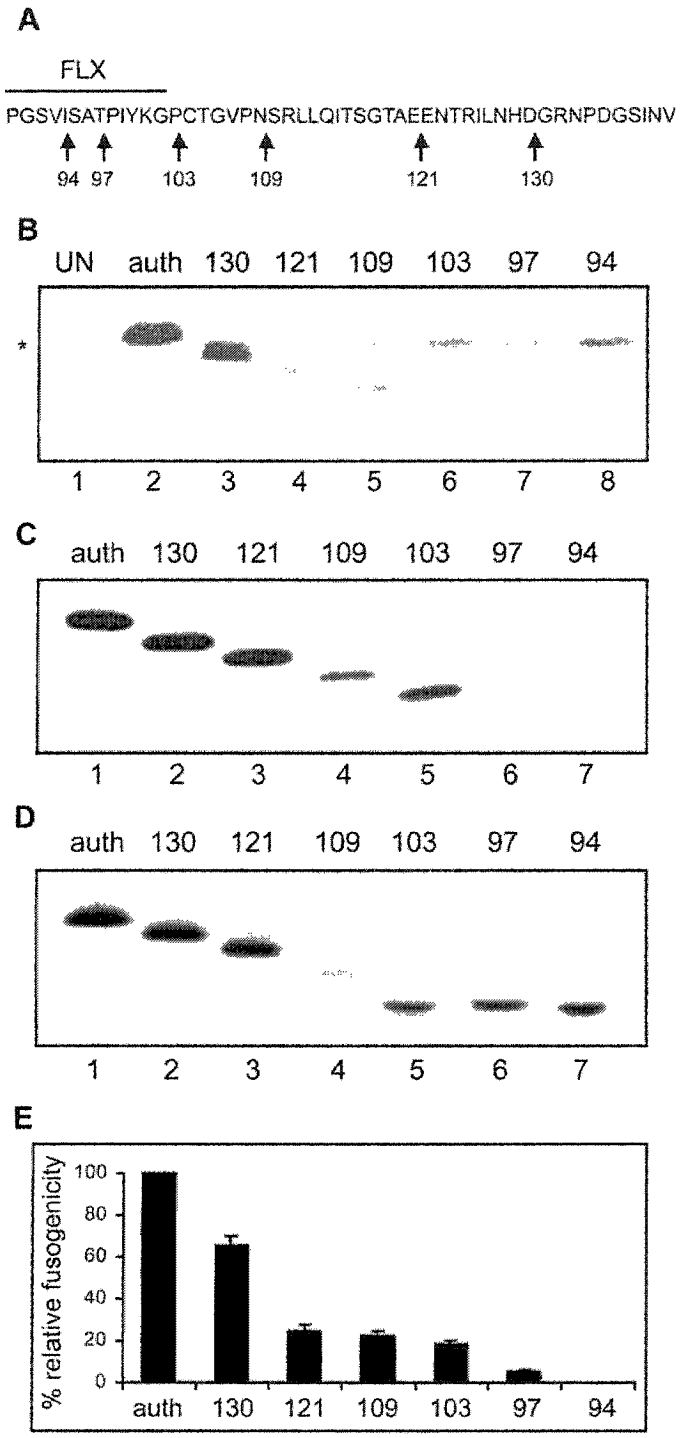
A
FLX
PGSVISATPIYKGPCTGVPNSRLLQITSGTAEENTRILNHDGRNPDGSINV
94 97 103 109 121 130
B
UN auth 130 121 109 103 97 94
*
1 2 3 4 5 6 7 8
C
auth 130 121 109 103 97 94
1 2 3 4 5 6 7
D
auth 130 121 109 103 97 94
1 2 3 4 5 6 7
E
% relative fusogenicity
100
80
60
40
20
0
auth 130 121 109 103 97 94

Figure 6.4.

corresponding to the 97* and 94* mutants following immune precipitation (Fig. 6.4C, lanes 6 and 7) was not evident in the membrane-bound samples (Fig. 6.4D, lanes 6 and 7) and, thus, likely reflects a loss of epitopes upon truncation rather than inefficient expression of the shortened constructs. However, given that the decrease in radioactivity upon immune precipitation of transfected cell lysates is evident with all truncated polypeptides smaller than 130 residues (Fig. 6.4B), it is plausible that the length of the C-terminal tail influences p15 stability.

The relative fusogenicity of the truncated p15 polypeptides was assessed (Fig. 6.4E). The ability of p15 to accomplish cell-cell fusion decreased steadily with each successive truncation. Protein stability did not account entirely for the observed decreases in p15 fusogenicity with the truncated mutants since the 94*, 97* and 103* constructs differed markedly in their fusogenic potential (Fig. 6.4E) but exhibited no discernible differences with respect to expression, stability, or membrane association (Fig. 6.4B, lanes 6-8 and D, lanes 6-8). Surprisingly, nearly half of the p15 endodomain (almost a third of the entire protein) could be removed (97*) while maintaining a minimal level (<10%) of fusogenic activity (Fig. 6.4D). Further truncation within the FLX domain (94*) abrogated the fusogenic potential of p15. Thus, the newly identified HL and FLX sequences (residues 81-102) are located within the minimal p15 polypeptide required to accomplish syncytium formation.

6.2.4. Analysis of the p15 putative hinged loop domain

The putative HL domain of p15 exhibits similarity to the N-proximal portion of the p14 fusogenic HP. A preliminary mutagenic analysis was undertaken to explore a possible role for this region in p15-induced cell-cell fusion (Fig. 6.5). The prolines at

Figure 6.5. **Functional analysis of the p15 HL region in comparison to the corresponding motif within the p14 ectodomain.** (A) Schematic representation of the putative p15 HL region compared to the N-terminal portion of the p14 HP, known to exist as a loop; numbers indicate residue positions; identical residues are shaded; arrows show orientation of the N-H-A tripeptide. (B) Relative fusogenicity of p15 HL point mutants, measured at 24 h (white bars) or 72 h post-transfection (grey bars) but compared to the level of authentic p15-induced syncytium formation at 24 h post-transfection since the level of cell-cell fusion induced by authentic p15 beyond this time point is too extensive to quantify (TETQ). The results reported represent the mean plus or minus the standard error of three experiments performed in triplicate. (C) The locations of the exchanged HL domains for each mutant, DS1 and DS2, are indicated, with the inserted sequence enlarged; numbers denote amino acid positions relative to the authentic protein corresponding to each domain.

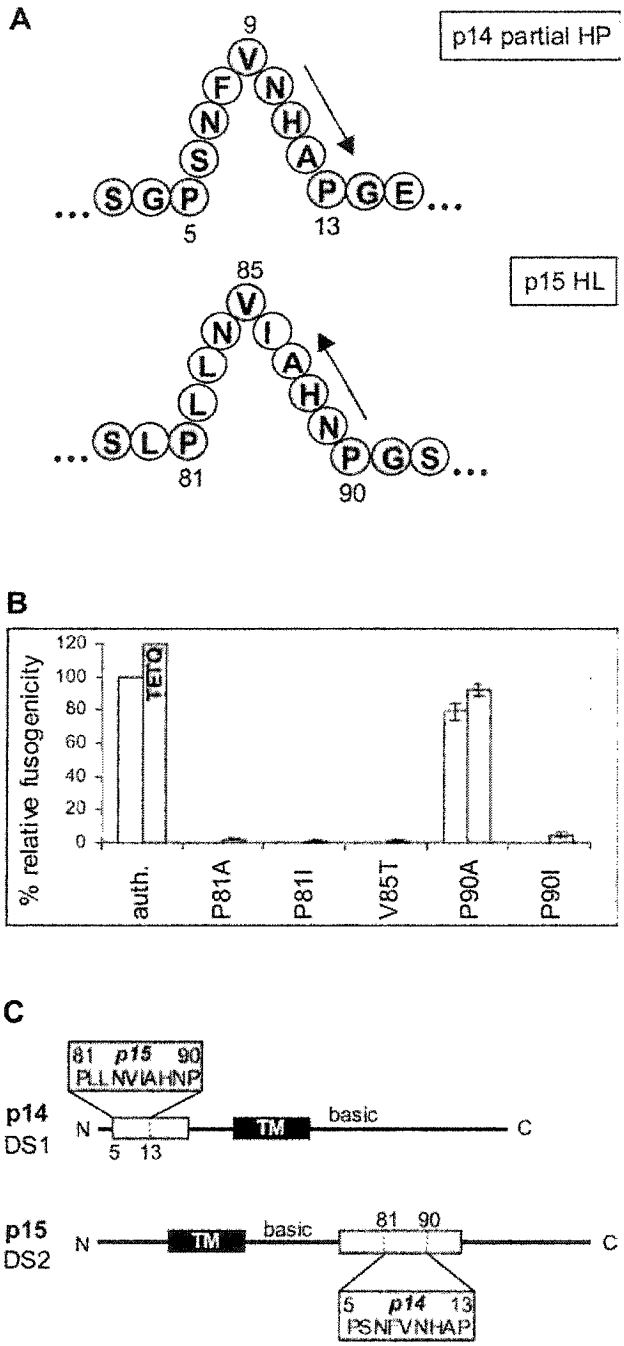
A
p14 partial HP
9
V
F
N
N
H
S
A
...S G P
P G E...
5
13
p15 HL
85
V
N
I
L
A
L
H
N
...S L P
P G S...
81
90
B
% relative fusogenicity
120
100
80
60
40
20
0
TETQ
auth.
P81A
P81I
V85T
P90A
P90I
C
81 p15 90
PLLNVIAHNP
p14
DS1
N
5 13
TM
basic
C
p15
DS2
N
TM
basic
81 90
C
5 p14 13
PSNFVNHAP

Figure 6.5.

positions 81 and 90 were targeted for mutagenesis since these residues potentially form the "hinges" of the putative HL. Replacement of P90 with alanine was well tolerated, akin to the effect of the P13A substitution within the p14 HP (Corcoran *et al.*, 2004). The P81A mutation was much more deleterious, reducing the ability of p15 to induce cell-cell fusion by greater than 95%. Replacement of P81 or P90 by the bulkier isoleucine, which would be expected to more strongly interfere with the putative hinges than alanine, virtually abolished p15 fusogenicity. The replacement of valine 9, positioned near the apex of the loop within the p14 HP, by threonine (V9T) has been shown to eliminate p14 fusogenic activity (Corcoran *et al.*, 2004). Thus, the effect of a similar substitution of the central valine (V85) within the p15 HLA was analyzed. The ability of the p15 V85T mutant to induce syncytium formation was severely impaired (Fig. 6.5B). By 72 h post-transfection, the relative fusogenicity of V85T remained less than 2% that of authentic p15 measured at 24 h post-transfection (authentic p15-induced cell-cell fusion was too extensive after 24 h post-transfection to be accurately quantified). The fusion-inhibitory effects of point mutations within HL indicate that this region contributes to the fusogenic potential of p15. Given the degree of sequence similarity of p15 HL to a portion of the p14 HP, and the comparable effect of equivalent mutations on these regions, it was of interest to determine whether p15 HL could functionally substitute for its apparent counterpart in p14 and vice versa. The exchange of these regions to create domain swap (DS) mutants 1 and 2 (Fig. 6.5C), however, led to the loss of fusion activity in both p15 and p14 (see Fig. 6.7A). This result suggests that either the HL regions are not functionally equivalent, or that their function is dependent upon their context within the native sequences.

6.2.5. Analysis of the p15 potentially flexible motif

As illustrated in Figure 6.6A, the FLX region of p15 (residues 90-102) shares partial identity with sequences within both the p14 HP (residues 13-24) and the p10 HP (residues 6-18). As shown, all three regions were predicted to consist of random coil and extended β-sheet secondary structure, which hints at the possible conformational flexibility of these motifs. In order to investigate whether the FLX motif is an isolated domain that can be functionally exchanged among the various FAST proteins, several domain swaps (mutants DS3-6) were engineered (Fig. 6.6B). In contrast to the results of the HL domain swap, each of the FAST protein chimeras resulting from the exchange of the FLX region retained their fusogenic potential (Fig. 6.7A).

6.2.6. The p15 ectodomain is relatively intolerant to mutation

In order to garner an overall perspective of key regions contributing to the fusogenic potential of p15, the relative fusogenicity of numerous p15 mutants, including those previously discussed (chapters 4-6), was analyzed. The results indicate that the p15 N-terminal ectodomain is highly sensitive to mutation. The introduction of 6 to 11 amino acid insertions into the short, 20-residue ectodomain (refer to Fig. 6.8A) eliminated the ability of p15 to accomplish cell-cell fusion (Fig. 6.8B). Several point mutations in the region, aside from individual proline substitutions, were similarly devastating to p15 fusogenicity (Fig. 6.8B). Although not all of the p15 ectodomain mutants were screened for their myristylation status (an essential modification for p15- induced cell-cell fusion), it was demonstrated that the I7A, 7-HA and V8A constructs were properly modified by the addition of myristate (data not shown). Thus, together with the observation that the nonfusogenic proline mutants retain authentic-like levels of N-myristylation (chapter 5),

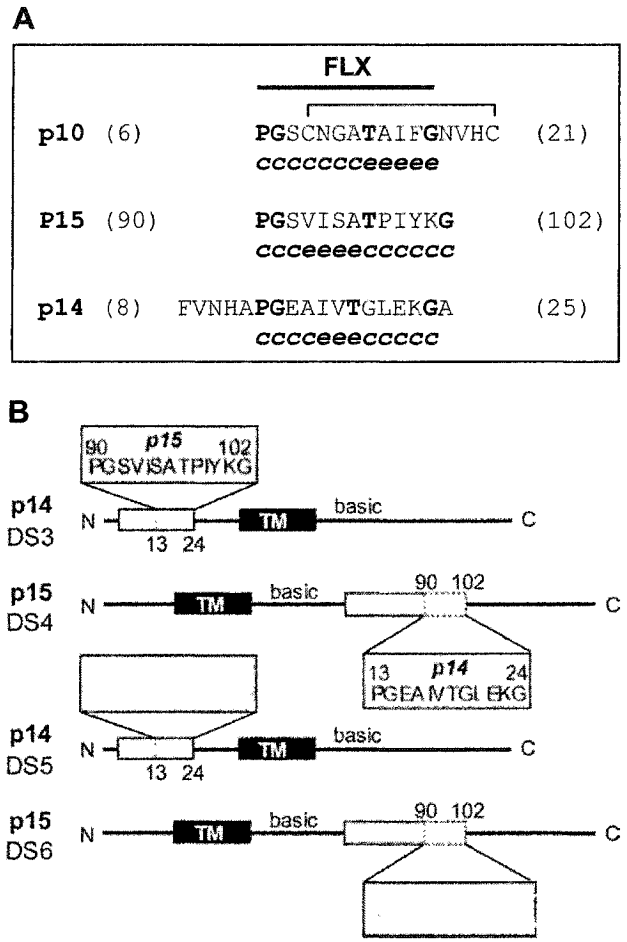

Figure 6.6. **Construction of various FAST protein FLX domain swap (DS) mutants.** (A) The FLX regions of p10, p15 and p14 used to engineer the DS mutants is shown in relation to the p10 and p14 HP sequences (position of the predicted p10 disulfide bond is indicated; identical residues are in bold type), and with the Guermeur's hierarchial neural network-predicted (when part of the larger ecto- or endodomain) secondary structure (random coil, *c*, or extended strand, *e*) specified below; amino acid positions are bracketed. (B) The locations of the exchanged FLX domains for each DS mutant (3-6) is indicated, with the inserted sequence enlarged; numbers denote amino acid positions relative to the authentic protein corresponding to each domain.

A

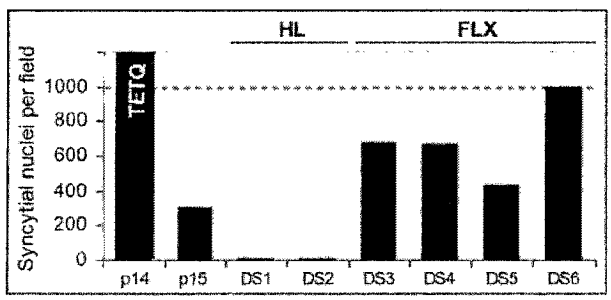

B

construct	description
DS1	p14 with substituted p15 HL sequence
DS2	p15 with substituted p14 HL sequence
DS3	p15 with substituted p14 FLX sequence
DS4	p15 with substituted p10 FLX sequence
DS5	p14 with substituted p15 FLX sequence
DS6	p14 with substituted p10 FLX sequence

Figure 6.7. **Relative fusogenicity of the various domain swap (DS) mutants.** (A) The average number of syncytial nuclei per 200x field of view (5 fields counted) in QM5 cells transfected with each HL domain swap mutant (DS1 and DS2) and each FLX domain swap mutant (DS3, DS4, and DS6) compared to cells transfected with either authentic p14 or authentic p15 at 14 h post-transfection. The approximate number of total nuclei per 200x field of view (1000) is indicated by the horizontal dashed line and represents complete fusion of the monolayer. The level of fusion evident in the p14-transfected cells was too extensive to quantify (TETQ) and is indicated as being greater than complete fusion as the fused monolayer has partially lifted off the substratum. (B) A brief description of each DS mutant is provided for reference.

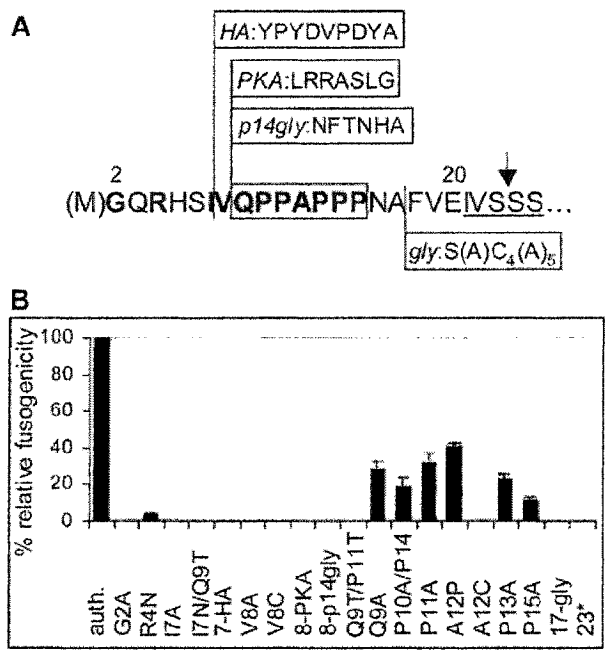

Figure 6.8. **Summary of p15 ectodomain mutants.** (A) Authentic amino acid sequence of p15 ectodomain with positions of point mutations highlighted in bold and locations of insertions indicated by vertical line (insertion sequence boxed); numbers correspond to amino acid positions; shaded box indicates region corresponding to point mutations analyzed in chapter 5; beginning of TM sequence is underlined; arrow indicates position of stop codon (mutant 23*). (B) The fusogenicity of various p15 ectodomain mutants relative to authentic p15 at 24 h post-transfection as determined by syncytial index in QM5 cells. Results presented represent the mean plus the standard error of three separate experiments performed in triplicate.

it can be assumed that all p15 constructs mutated at or downstream of residue 7 are appropriately acylated. It remains possible that the inhibitory effect of the R4N substitution may reflect an influence of the R4 residue on the efficiency of p15 N-myristylation. While the replacement of alanine 12 with proline was tolerated, the substitution of cysteine at this position completely inhibited p15-induced fusion of QM5 cells. Although not quantified, previous analysis demonstrated the ability of the A12C mutant to induce a moderate level of syncytium formation in Vero cells (data not shown). The A12C construct is one of several p15 mutants for which dramatic differences were noted in the relative fusogenicity amongst cell types (discussed further in chapter 7).

Compared to the p15 ectodomain, the endodomain is relatively tolerant of mutation, accommodating numerous point mutations, deletions and insertions (Fig. 6.9). In addition to the remarkable tolerance of the p15 endodomain to truncation reported above, the p15 C-terminus could be moderately extended without complete loss of fusion activity (and with enhancement of fusion activity in the case of the pka- and HA-tags). The addition of GFP (a protein nearly twice the size of p15) to the p15 C-terminus prevented syncytium formation. Relative to other locations hosting point mutations, the HL and FLX regions appear as hot spots within the p15 endodomain in which several alterations are particularly inhibitory to p15-induced fusion.

6.2.7. Numerous p15 mutants exhibit a dominant-negative phenotype

It was hypothesized that distinct p15 domains may act in a concerted manner to promote membrane fusion. In an initial attempt to identify such key motifs, numerous non-fusogenic p15 mutants were screened for their ability to exhibit a dominant-negative

Figure 6.9. **Summary of p15 endodomain mutants.** (A) Authentic amino acid sequence of p15 endodomain with locations of insertions indicated by vertical line (insertion sequence boxed); numbers correspond to amino acid positions; shaded box indicates region corresponding to point mutations (including A1 and A2) analyzed in chapter 2; arrows indicates positions of stop codons (mutants*). (B) The fusogenicity of various p15 endodomain mutants relative to authentic p15 at 24 h post-transfection as determined by syncytial index in QM5 cells; TETQ (too extensive to quantify). Results presented represent the mean plus the standard error of three separate experiments performed in triplicate.

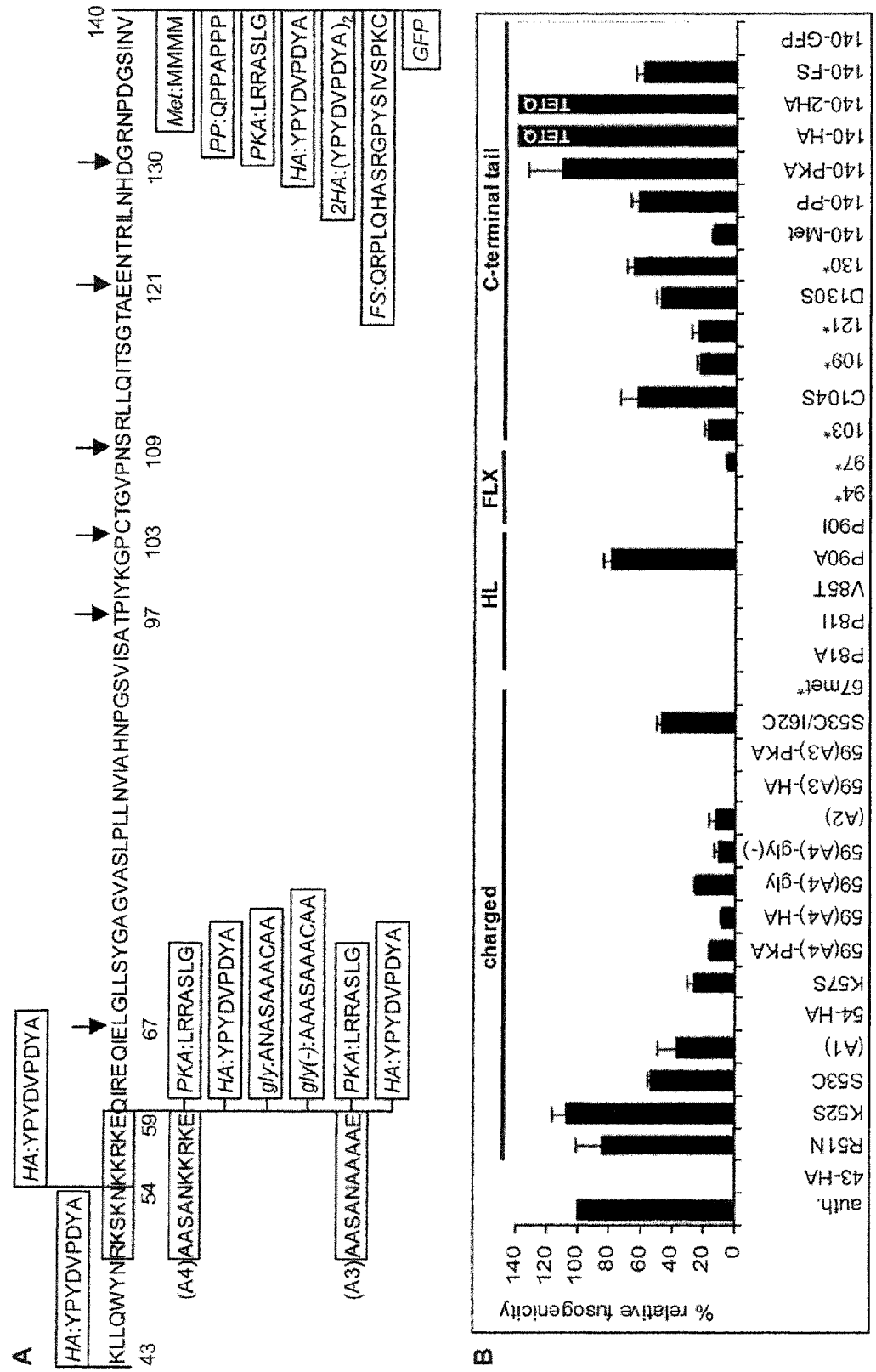
A
HA:YPYDVPDYA
KLLQWYNRKSKNKKRKE
43
54
59
QIREQIELGLLSYGAGVASLPLLNVIAHNPGSVISATPIYKGPCTGVPNSRLLQITSGTAEENTRILNHDGRNPDGSINV
67
97
103
109
121
130
140
(A4)AASANKKRKE
PKA:LRRASLG
HA:YPYDVPDYA
gly:ANASAAACAA
gly(-):AAASAAACAA
(A3)AASANAAAAE
PKA:LRRASLG
HA:YPYDVPDYA
Met:MMMM
PP:QPPAPPP
PKA:LRRASLG
HA:YPYDVPDYA
2HA:(YPYDVPDYA)2
FS:QRPLQHASRGPYSVSPKC
GFP
B
charged
HL
FLX
C-terminal tail
TETC
TETC
% relative fusogenicity
0
20
40
60
80
100
120
140
auth.
43-HA
R51N
K52S
S53C
(A1)
54-HA
K57S
59(A4)-PKA
59(A4)-HA
59(A4)-gly
59(A4)-gly(-)
(A2)
59(A3)-HA
59(A3)-PKA
S53C/I62C
67met*
P81A
P81I
V85T
P90A
P90I
94*
97*
103*
C104S
109*
121*
D130S
130*
140-Met
140-PP
140-PKA
140-HA
140-2HA
140-FS
140-GFP

Fig. 6.9.

phenotype. The extent of syncytium formation in monolayers of QM5 cells co-transfected with authentic p15 cDNA and mutant p15 cDNA in a 1:1 ratio was measured by syncytial index (Fig. 6.10). While the extent of syncytium formation detected in the co-transfected QM5 cells was measured relative to the control of equal amounts of authentic p15 cDNA and empty vector (pcDNA), it should be noted that transfection with double the amount of authentic p15 cDNA reduced the level of p15 fusogenicity to approximately 65% (dashed line, Fig. 6.10). Thus, as a conservative estimate, only those mutants which, when co-expressed with authentic p15, reduced p15 fusion activity to a level significantly less than 65% relative fusogenicity were considered to be truly dominant negative. With this consideration, most of the mutants tested exerted at least a partial inhibitory effect on the level of authentic p15-induced cell-cell fusion. A few mutants (7-HA, V8A, A12C, and 59(A3)-gly) completely inhibited p15-induced syncytium formation when measured at 24 h post-transfection. Several mutants (V8C, 17-gly, 23*, 43-HA, 59(A3)-HA, and 67met*) were classified as not dominant negative. Two of these constructs (23* and 43-HA) would not be expected to interfere with authentic p15 activity in any specific manner considering the 23-amino acid polypeptide (23*) lacks any hydrophobic segment, and the 43-HA construct fails to properly insert into membranes (chapter 4). The stability of neither the severely truncated 67met* construct nor the V8C mutant is known, but the small size and unpaired cysteine residue of these constructs, respectively, potentially targets them for degradation (Fra, 1993), and possibly accounts for their lack of interference with authentic p15 fusogenicity. The remaining two non-fusogenic, non-dominant negative, constructs (17-gly, mutated in the ectodomain, and 59(A3)-HA, mutated in the endodomain) were chosen as possible candidates for a complementation

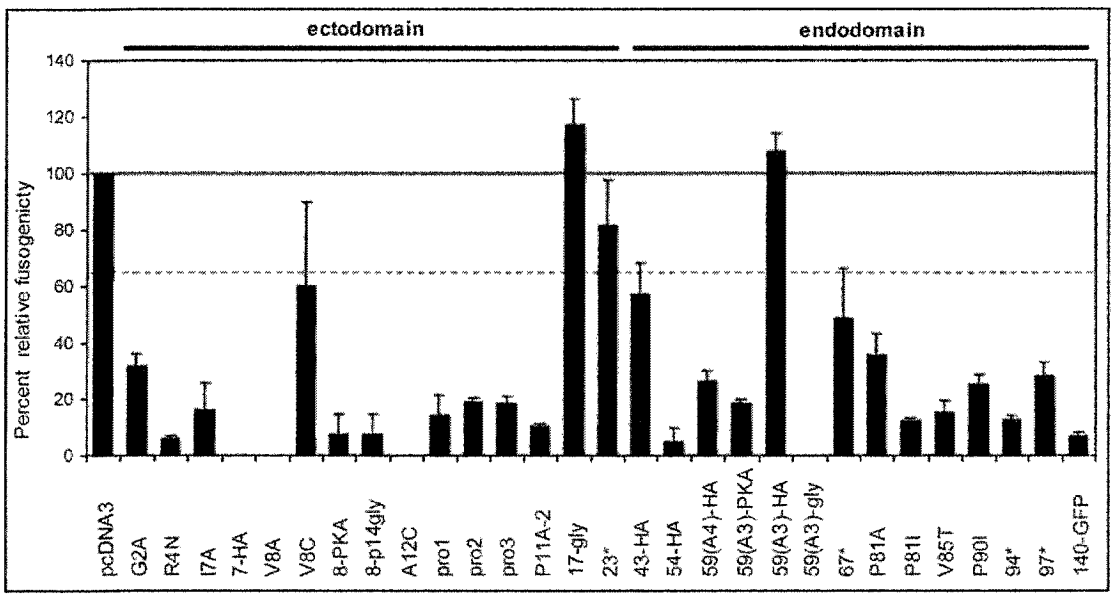

Figure 6.10 **Numerous nonfusogenic p15 mutants exhibit a dominant negative phenotype.** QM5 cells were co-transfected using a 1:1 ratio of authentic p15 cDNA and either vector (pcDNA3) DNA or cDNA for a nonfusogenic p15 mutant. The extent of syncytium formation in cells co-expressing authentic and mutant p15 was measured by enumeration of the syncytial nuclei per 200x field of view at 24 h post-transfection relative to cells co-transfected with p15 and vector DNA (solid horizontal line indicates 100% relative fusogenicity). The dashed horizontal line indicates the level of fusion observed with cells transfected with twice the amount of authentic p15 cDNA

study.

6.2.8. Isolated fusion defects in p15 can be complemented in *trans*

If distinct p15 domains function cooperatively to induce membrane fusion, it should theoretically be possible for a pair of non-fusogenic p15 constructs, each mutated in a separate domain, to complement each other when co-expressed and together achieve a level of fusogenic activity so long as neither mutant is grossly misfolded. The extent of syncytium formation in cells transfected with both 17-gly and 59(A3)-HA was measured by syncytial index and compared to that of cells expressing either 17-gly, 59(A3)-HA, or authentic p15 alone (Fig. 6.11A). A minimal level of cell-cell fusion was achieved (estimated to be less than 10% authentic levels at 48 h post-transfection) when the 17-gly and 59(A3)-HA constructs were expressed together. In order to monitor the extent of syncytium formation over a longer time course, each transfected monolayer was lifted from the culture dish with PBS and split 1:3. After two additional days, cells were fixed and Giemsa-stained to visualize multinucleated syncytia (Fig. 6.11B). The extent of syncytium formation in the co-transfected sample did not appear to increase upon the longer incubation over that measured at 72 h. These results indicated that *trans*-complementation of p15 fusogenic activity is possible but, at least with this set of mutants, is very inefficient.

6.3. Discussion

The FAST proteins appear to be organized as modular membrane fusion machines, representing a collection of fusion-promoting motifs that are arranged in a unique pattern for each protein. While distinct motifs may perform analogous functions

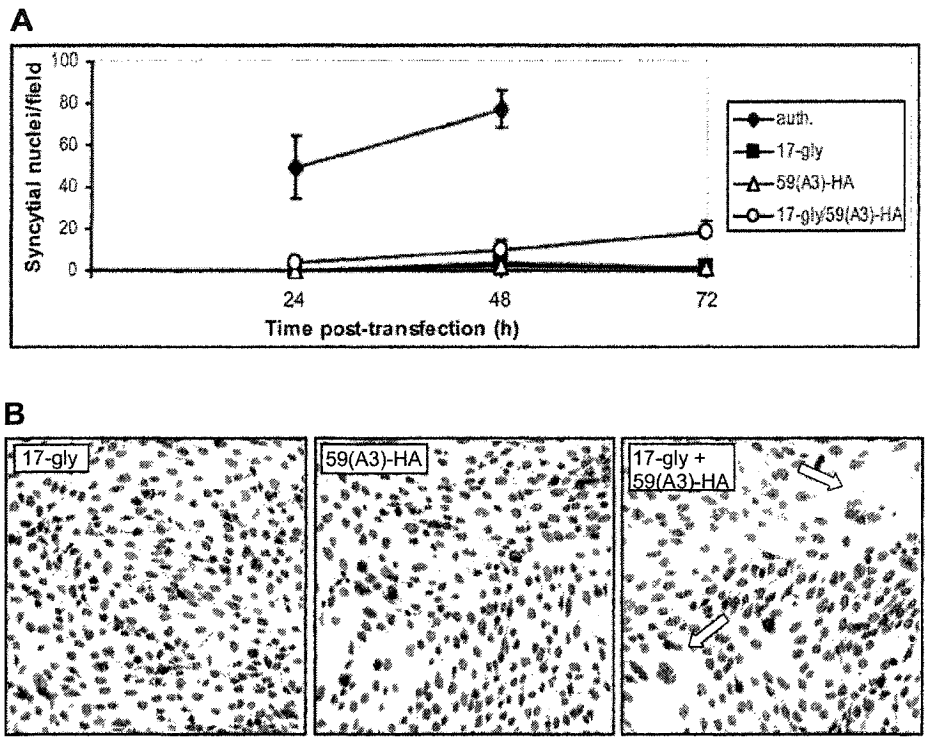

Figure 6.11. **Restoration of p15 fusion activity upon co-expression of complementing, nonfusogenic, non-dominant negative p15 mutants.** (A) Syncytial nuclei per 200x field of view measured for monolayers of QM5 cells expressing authentic p15, or nonfusogenic mutants 17-gly or 59(A3)-HA, or co-expressing 17-gly and 59(A3)-HA, at 24 h, 48 h, and 72 h post-transfection. Results represent a single experiment performed in triplicate. (B) Cells expressing 17-gly or 59(A3)-HA, or co-expressing 17-gly and 59(A3)-HA, were split 1:3 72 h post-transfection and allowed to regrow to confluency prior to methanol-fixation and Giemsa staining 5 d post-transfection. Arrows indicate small syncytia.

in the different FAST proteins, in this chapter it was sought to identify those domains that are common to all the FAST proteins. Such domains are of interest because their conservation hints that they potentially accomplish critical steps in FAST protein-mediated cell-cell fusion. The sequence alignments presented in this chapter are inherently p15-biased, and were made over relatively short regions. The sequence analysis, therefore, was intended as a guide to direct future functional investigations and not as unequivocal evidence of motif conservation.

6.3.1. Role of the TM anchor and flanking residues in FAST protein function

TM anchor

TM domains have been shown to influence the fusion activity of several enveloped virus fusion proteins, particularly at the stage of formation and/or growth of the fusion pore. Point mutations in the TM domain of VSV G (Cleverley and Lenard, 1998) or Moloney murine leukemia virus Env protein (Taylor and Sanders, 1999), truncations to the TM domain of the paramyxovirus simian virus 5 F (Bagai and Lamb, 1996) or influenza HA (Armstrong *et al.*, 2000), as well as replacement of the TM domain of HA by glycophosphatidylinositol (GPI) (Kemble *et al.*, 1994; Melikyan *et al.*, 1995) have been reported to arrest the fusion process at the stage of hemifusion. Others have described the formation of non-expanding fusion pores with GPI-anchored HA (Markosyan *et al.*, 2000) and with simian immunodeficiency virus Env protein truncated within the TM anchor (Lin *et al.*, 2003). Melikyan, *et al.* (2000b) proposed that the TM domain may affect the creation and expansion of fusion pores by interacting with and destabilizing the hemifusion diaphragm. It has also been suggested that interactions between TM domains may assemble fusion protein clusters required to achieve the

restricted hemifusion intermediate (Bentz, 2000a; Kozlov and Chernomordik, 1998) or fusion pore formation (Lin *et al.*, 2003).

The presence of a TM anchor flanked by a charged region (basic in character but also containing several negatively-charged residues) is a prominent feature common to all the FAST protein family members. Given that the TM domain of the FAST proteins functions as a signal anchor, this domain, together with the flanking sequences, is presumed to possess features that direct the membrane insertion of the FAST proteins in the correct topology. However, by analogy with other fusion proteins, it is suspected that the TM segment is involved in the process of membrane merger beyond simply anchoring the FAST proteins in the donor bilayer in the proper orientation. The TM domain may influence FAST protein fusogenicity through its potential for conformational flexibility, oligomerization, and/or clustering. Each of these possibilities is discussed below. Compared to other TM domains, residues with β-branched hydrophobic side-chains occur with high frequency in the TM segments of fusogenic proteins, including the cellular SNAREs and enveloped virus fusion proteins, and are believed to endow these domains with a structural plasticity required for their fusion activity (Cleverley and Lenard, 1998; Langosch *et al.*, 2001). The importance of structural plasticity of TM segments in a late stage of membrane fusion has been demonstrated with VSV G (Dennison *et al.*, 2002), and the SNARE proteins (Langosch *et al.*, 2001). Conformational flexibility and some propensity to adopt β-sheet conformations may enable local deformation or even transient unfolding of TM segments that facilitates the restructuring of the lipid bilayer during membrane fusion (Langosch *et al.*, 2001). Also, flexible, rather than rigid, TM domains would better facilitate the formation of a lipid-

restricting protein dam (Bentz and Mittal, 2000), which is a prerequisite to fusion in several models (refer to chapter 1). Functionally-relevant plasticity may also exist in the TM domains of the FAST proteins, which are similarly high in β-branched amino acids. Compared to a large database of unrelated TM segments (TMbase; Hofmann and Stoffel, 1993), isoleucine is over-represented more than two-fold in the p15 TM domain, and leucine is over-represented approximately 1.5-fold in the p10 and p14 TM domains.

The FAST proteins also contain GxxxG-like motifs (Fig. 6.1D) that may mediate TM domain-oligomerization and/or p15 clustering and thereby potentially facilitate the establishment of restricted lipid flow at the fusion site. The size and shape of the TM domain may also contribute to p15 clustering. When the length of a TM anchor does not match the width of the bilayer, a thickness perturbation is introduced that creates an energetic dilation corona around the TM segment and yields an attraction between like TM domains (Fournier, 1999). The p15 TM region is of sufficient length (20 aa) that it may locally expand the membrane, thereby influencing TM-TM interactions. Furthermore, the sided arrangement of aromatic residues may give the p15 TM anchor a conical shape, which would be expected to tilt the proximal lipids and curve the membrane (Fournier, 1999). Although tilt perturbations typically repel one another, if the tilt difference is small and the dilation corona (from a thickness perturbation) extends further than the tilt difference corona, then the formation of a TM anchor array is favoured, with the axis of each anchor rotated with respect to one another in order to minimize the curvature strain of the membrane (Fournier, 1999). Thus, both the size and shape of the p15 TM anchor is predicted to introduce curvature energy into the donor membrane that may influence the level of p15 self-assembly and/or the formation of

high-energy lipid intermediates during fusion. Preliminary evidence suggests that while the more closely related TM segments of p15 and p14 can be swapped, the TM anchor of p10 cannot be functionally exchanged for that of p15 (E. Clancy, personal communication). This hints that the role played by the TM domain is more complex than to simply serve as a reverse (type III) signal-anchor, and that the TM segment may function in a cooperative manner with other motifs to accomplish FAST protein-mediated membrane fusion.

Cholesterol-binding motif

A conserved membrane-proximal cholesterol-binding pattern of amino acids was identified in the FAST proteins (Fig. 6.1C). This pattern ($L(X)_{1-2}Y(X)_2K$) within the FAST proteins is in accordance with that postulated by Li and Papadopoulos (1998) to represent a common cholesterol recognition/interaction amino acid consensus (CRAC) ($L/V\text{-}(X)_{1-5}\text{-}Y\text{-}(X)_{1-5}\text{-}R/K$), present in all proteins shown to interact with cholesterol. A similar sequence (LWYIK) capable of binding cholesterol was recently identified within HIV gp41, immediately adjacent to the TM domain (Vincent *et al.*, 2002). This sequence is contained within the interfacial region of gp41 known to be essential for fusion activity (Vincent *et al.*, 2002). The presence of sphingomyelin and cholesterol promotes aggregation of the gp41 interfacial region leading to membrane destabilization at the site of fusion (Vincent *et al.*, 2002). Cholesterol influences the fusogenicity of several other enveloped virus fusion proteins, including those of influenza, flaviviruses, and alphaviruses (Razinkov and Cohen, 2000; Stiasny *et al.*, 2003; Waarts *et al.*, 2002). Cholesterol-dependent clustering of SNAREs is required for efficient intracellular fusion events (Lang *et al.*, 2001). Similarly, cholesterol has been shown to be necessary for

FAST protein-induced syncytium formation (J. Salsman, unpublished data). Within p15, residues R51, K52 and K54 each occupy a position that fits the CRAC motif and, thus, potentially contribute to cholesterol interactions. While the individual substitution of each of these residues was well tolerated (chapter 4), simultaneous replacement of all three residues (mutant A1) reduced the relative fusogenicity of p15 by approximately 65% (Fig. 6.10). This effect was originally interpreted to reflect the fusogenic contribution of the polybasic cluster as a whole. However, it is also conceivable that it may reflect the cholesterol-dependence of p15. An impaired ability of mutant A1 to interact with cholesterol may account for the reduced efficiency with which this construct induces cell-cell fusion. If so, the influence of cholesterol on p15 function may mirror that of this lipid on the activity of influenza HA. Although non-raft-associated HA is fusogenic, the clustering of HA molecules within cholesterol-enriched raft microdomains appears to increase the efficiency of HA-mediated membrane fusion both by effectively concentrating HA (Takeda *et al.*, 2003), and through the enhancing effect of cholesterol on the expansion of fusion pores (Razinkov and Cohen, 2000). Further studies are required to specifically determine what role, if any, cholesterol plays in the mode of action of p15.

Membrane-proximal tryptophan

Conserved aromatic amino acid-rich motifs in the membrane-proximal region of the ectodomains of several enveloped virus fusion proteins have been identified as playing an important role during membrane fusion (Suarez *et al.*, 2000). Surprisingly, the presence of only a single tryptophan residue within this motif of HIV-1 gp41 was sufficient to mediate fusion at a level approximately 70% that of wild-type (Salzwedel *et*

al., 1999). Considering this finding, it is interesting that the FAST proteins all contain at least one membrane-proximal tryptophan, positioned on the same side of the membrane as the putative fusion-peptide motif (Fig. 6.1D). These residues are located in the ectodomains of p14 (W37) and ARV p10 (W42, Y41), respectively, while p15 contains W48 (and Y49) located in the endodomain. It is noteworthy that the two FAST proteins considered the most highly fusogenic, RRV p14 and NBV p10, each contain a tryptophan residue flanking both sides of the TM anchor. The contribution of any of these residues to the activity of the FAST proteins has not been investigated.

Charged domain

The sequences flanking the TM domains of the FAST proteins on the cytoplasmic side are characterized by the presence of a number of charged residues. The polybasic cluster of the charged region of p15 appears to bind tightly to the cytosolic leaflet of the membrane and influences the fusogenic activity of the protein without affecting its topology (chapter 4). Mutations in the charged regions of p10 similarly disrupt its fusogenic potential (Shmulevitz and Duncan, 2000). Thus, it is hypothesized that the charged region plays an essential role at some stage of FAST protein-mediated cell-cell fusion. Perhaps by binding to phospholipid headgroups and introducing nonlamellar lipid structures, the charged region of the FAST proteins potentiates the proposed fusogenic activity of the TM domains and facilitates fusion pore formation in a manner similar to the pore-forming activities of certain cationic-hydrophobic peptides. In particular, the continuous bending of the membrane in the formation of torroidal pores induced by peptides such as melittin, magainin, and protegrin (Yang *et al.*, 2001) is reminiscent of the membrane bending required to form a fusion pore (Chizmadzhev *et al.*, 1999). It is

noteworthy that the expression of the N-terminal 90 amino acids of p15 was highly toxic to *E. coli*, precluding attempts to bacterially express and purify this construct for antibody production (chapter 4). Such toxicity was not observed upon expression of the p15 N-terminal 20 amino acids and was thus attributed to the membrane-perturbing activity of the TM anchor and flanking charged region (residues 21-67), but may also involve the downstream H2, HL, and/or FLX regions (discussed below). This latter possibility is supported by the observation that the region of the rotavirus nsp4 protein (which displays a similar topology to p15, refer to chapter 4) downstream of the TM anchor, but encompassing the flanking charged region and adjacent hydrophobic patch, exhibited membrane-destabilizing activity that was toxic to *E. coli* (Browne *et al.*, 2000).

6.3.2. The p15 C-terminal tail is dispensable

Successive C-terminal truncation of p15 reduced the fusogenic potential of the protein in a step-wise manner (Fig. 6.4D). It is unclear whether the decreased abilities of the truncated p15 proteins to promote syncytium formation reflects the loss of specific fusion-enhancing motifs or, rather, a non-specific length requirement. Assessing the fusogenicity of p15 constructs in which portions of the C-terminal tail have been replaced by heterologous sequence would address this issue. Interestingly, while the larger FAST proteins, p14 and p15, can be truncated while retaining fusion-inducing activity, neither are functional when truncated to a size approximating that of the smaller (minimal?) p10 FAST protein, which cannot be functionally truncated (Corcoran and Duncan, 2004; Shmulevitz, 2001). The C-terminal tail of p15 may enhance the stability of the protein (Fig. 6.4B) or potentially contribute to the efficiency of p15 sorting to sites of fusion initiation on cell surface protrusions (refer to chapter 7). The newly identified semi-

conserved FAST protein HL and FLX motifs lie immediately upstream of the dispensable C-terminal tail and, thus, are contained within the minimal p15 structure required to promote fusion.

6.3.3. Role of hydrophobic patch regions in FAST protein function

HL domain

The HL sequence of p15 was conjectured to form a hinged loop based on the positioning of boundary prolines (P81 and P90) as attractive candidates for possible hinges. Flexible, short (~10 residues) hinged domains (often called 'loops' or 'lids') are common features gating access to membrane channels and enzyme active sites. The hinged lid of triose-phosphate isomerase (EC 5.3.1.1) is a well-documented example. Residues 167-176 (underlined, E**P**V<u>WAIGTGLAA</u>T**P**E; NCBI accession #ISBYT) form a rigid loop (the 'lid') that is mobile on flanking proline-based hinges (Yuksel *et al.*, 1994, and references therein). Whether or not the putative hinged region of p15 actually adopts such a structure remains to be determined. However, subsequent to the suggestion that a hinged loop may form within the p15 endodomain, the corresponding region of p14 (P5 to P13) was determined by NMR (using a synthetic ectodomain peptide) to form a loop (Corcoran *et al.*, 2004). This finding lends credibility to the prediction of HL in p15. Nonetheless, the apparently equivalent HL regions of p15 and p14 could not be functionally exchanged (Figs. 6.5 and 6.7). This suggests that HL is not a self-contained functional motif but may require presentation within the context of its native flanking sequences or of distal residues that are positioned proximal to HL in the folded native protein. Hinged loops form noncovalent interactions with other protein domains that often control the mobility of the hinged loop (Hayward, 1999). Creating the p14 and p15

HL chimeras likely disrupted possible hydrogen bonds and/or salt-bridges between each HL sequence and other domains, especially considering the drastic relative relocation of HL in each construct (from ectodomain to endodomain and vice versa). Alternatively, HL activity may depend upon its sequence orientation. Within native p14, the C-proximal HL sequence is closest to the TM anchor, while in p15 it is the N-proximal sequence that lies closest to the TM anchor. If the orientation of the p15 HL were reversed upon its insertion into p14, the N-H-A tripeptide of the p14 sequence would be preserved (refer to Fig. 6.5). It would be worthwhile to investigate the ability of the HL motif to be functionally exchanged between p15 and p14 in the reverse orientation, or in the context of additional flanking sequence.

FLX domain

While the putative HL domain is only present in the sequences of p15 and p14, the adjacent FLX domain is apparent in the sequences of all three FAST proteins and is thus more attractive as a possible candidate for a semi-conserved fusion-promoting motif. A comparison of the FAST protein FLX sequences and predicted secondary structures is given (Fig. 6.6A). These regions are enriched in glycine and alanine residues and, as such, may be conformationally flexible. Domain-swap analysis indicated that the p10 FLX region could functionally replace the analogous regions in both p14 and p15. Likewise, the FLX regions of p15 and p14 could be functionally exchanged. It could be interpreted that the cross-acceptance of this domain across the FAST protein family simply reflects its non-essential role in the fusion process. This could be tested by replacement of the FLX domain with heterologous sequences or scrambled versions of the FLX sequences. However, mutational analysis of this region within the p10 and p14

FAST proteins argues for its importance. The FLX region of p10 (residues 6-19) closely overlaps with the p10 HP motif (residues 9-24). Mutational analysis of the p10 HP identified several amino acid positions (contained within the FLX sequence) that were critical to the fusogenic activity of p10 (Shmulevitz *et al.*, 2004b), suggesting the FLX region does have a key role to play. Similarly, several point mutations within the FLX sequence of the p14 HP were also disruptive to fusogenic activity (Corcoran *et al.*, 2004). Furthermore, in a liposome fusion assay a synthetic peptide (p10ehp) corresponding to residues 6-24 of p10 (which includes the entire FLX motif) induced lipid mixing at a level twice that of a peptide (p10hp) corresponding to the core p10 HP (residues 9-21) (Shmulevitz *et al.*, 2004b). The p10 HP is believed to form a loop stabilized by disulfide bonds (a 'cystine noose') between cysteines at positions 9 and 21 (Shmulevitz *et al.*, 2004b). The enhanced lipid mixing induced by the p10ehp was thought to result from an increased propensity of the peptide to form a cystine noose (Shmulevitz *et al.*, 2004b). Alternatively, the enhanced lipid mixing of p10ehp might reflect FLX-activity. The p10 FLX sequence exchanged here did not include residues N18 to C21 and, consequently, could not form the putative cystine noose. Although the analysis presented in this chapter does not address whether a cystine-stabilized loop is formed within the native p10 HP, it is clear that such a structure cannot explain the functional significance of the p10 FLX motif in the context of the other FAST proteins. If the p10 FLX sequence is, in fact, a fusion peptide, it is exceptional that it is functional when positioned within the p15 endodomain. It would be informative to assess the ability of p10 to trigger membrane fusion upon replacement of the p10 HP region with either the p14 or p15 FLX motifs.

Predicted membrane interactions

The potential of the H2, HL and FLX subregions of the p15 endodomain to interact with membranes was analyzed using the whole-residue Wimley-White hydrophobicity scales (Jaysinghe *et al.*, 2000; White and Wimley, 1999). Like other hydrophobicity scales based on bulk-phase partitioning, the Wimley-White octanol scale predicts the preference of a protein segment to insert into the hydrocarbon core of the bilayer interior, except the Wimley-White scale takes into account the cost of transferring the peptide bonds into the membrane and is thus more realistic. The Wimley-White interface scale, which predicts the preference of a region of a peptide chain to partition into the hydrated interfacial portion of a lipid bilayer, has been of particular value in identifying previously unrecognized domains within the fusion proteins of enveloped viruses that interact with membranes at the hydrophobic interface (Nieva and Suarez, 2000; Suarez *et al.*, 2000). Such regions, typically enriched in aromatic amino acids, have been shown to play a crucial role in the fusion process (Suarez *et al.*, 2000).

On the basis of their weak to moderate hydrophobicity scores, the following model for the insertion of the H2 and HL regions of p15 into the bilayer is proposed. (1) Soon after it is translated, much of the hydrophobic H2 domain (residues 68-81) may initially partition into the interface region of the cytoplasmic face of the bilayer. At this early stage, the flanking HL region (residues 81-90; encompassing the remainder of the H2 sequence) is hypothetically held away from the bilayer. The presence of the H2 domain within the interface, parallel to the membrane surface, would not be expected to significantly perturb the membrane structure (White and Wimley, 1999) and, thus, nascent p15 in this orientation would not be expected to compromise the intracellular

membranes it depends on for transport to the surface. (2) If the HL region subsequently swings into contact with the surface of the membrane, its insertion into the interface as an extension of the H2 domain would be somewhat favoured ($\Delta G \sim -2$ kcal/mol). The presence of H2 and HL simultaneously in the interfacial region is predicted to facilitate deeper insertion of the H2 sequence into the hydrocarbon interior of the membrane, as H2 is expected to prefer the nonpolar environment (water-bilayer $\Delta G = -3.4$ kcal/mol). The HL proline(s) likely facilitate the necessary turn of the membrane-embedded polypeptide so that it emerges from the same side of the bilayer from which it entered. The deep insertion of H2 would be driven primarily by the contribution of HL, as the transition from the interface to the hydrocarbon core of the bilayer is predicted to release just 0.6 kcal/mol in the case of H2, but 2.2 kcal/mol in the case of HL. This process would be facilitated by either an increase in the α-helical content of H2/HL or the adoption of an oligomeric β-sheet structure, as the formation of internal hydrogen bonds lowers the energy cost of transferring them into the hydrocarbon interior (White and Wimley, 1999). Precedence for the insertion of a fusogenic peptide into membranes as an oligomeric β-sheet structure has been demonstrated by analysis of the sea urchin bindin B18 (Barre *et al.*, 2003), meltrin-α (Wolfe *et al.*, 1999), fertilin-α (Muga *et al.*, 1994), HIV-1 gp41 (Sackett and Shai, 2003), and HBV S fusion peptide (Rodriguez-Crespo *et al.*, 1996). Also, Yang *et al.* (2003) have shown that artificial oligomerization (by cross-linking) of the gp41 fusion peptide leads to parallel β-sheet structures that show the full fusion activity (measured by lipid mixing) even at very low peptide to lipid ratio. Interestingly, modeling the HP regions of all three FAST proteins as a β-sheet (and CD analysis of the p10 and p14 HPs indicates significant β-sheet structure) reveals a glycine face that is

potentially equivalent to the glycine ridge of other fusion peptides that are modeled as an α-helix (Pecheur *et al.*, 1999). The glycine ridge is believed to function in the self-association and/or late-stage TM-association of these fusion peptides. The glycine face of p15 H2 in β-sheet conformation might promote self-assembly, thus satisfying the requirement for a hydrogen-bonded structure for H2 membrane-insertion. Insertion of H2/HL may introduce significant packing defects and tension into the lipid bilayer that might relax upon membrane fusion. (3) Late-stage interaction between H2 and the TM anchor (analogous to the final association between the HA fusion peptide and TM anchor) could possibly lead to the formation of a fusion pore and/or contribute to the dissociation of clustered p15 molecules necessary to achieve complete fusion (refer to chapter 7). This predicted sequence of membrane interactions may happen spontaneously, or occur as part of a triggered p15-induced mechanism of membrane fusion. Insertion of approximately 20 amino acids of the p15 endodomain encompassing the H2/HL region (shown in chapter 4 to not span the bilayer) could potentially be disruptive to the integrity of the membrane. Thus, it seems likely that insertion of this entire region would be delayed until the onset of the fusion reaction, perhaps governed by the level of p15 self-assembly. Monomeric H2 in the predicted β-sheet conformation could provide the energy barrier to H2 membrane insertion prior to oligomerization at the fusion site.

The energy gain upon the insertion of the sequences comprising the H2 and HL domains into the membrane would be small. For comparison, the energy of insertion of the TM anchor of the FAST proteins (-10 to -13 kcal/mol), and of insertion of the stem region of HIV gp41 into the interface (-8 kcal/mol), is more significant. However, the fusion peptide of gp41 is predicted to insert into the interface with roughly the same

efficiency (-3 kcal/mol) as the p15 H2 domain. Furthermore, the fusion peptide of bindin (a well-characterized membrane binding and fusion-inducing peptide) is predicted to insert into the interface with a free energy of transfer (-1 kcal/mol) that is less than that for p15 H2.

Similar to the so-called hydrophobic patches of p10 and p14, the p15 FLX domain exhibits no strong preference for either the aqueous, interface, or membrane environments on the basis of its Wimley-White hydrophobicity score (water-bilayer ΔG = ~0 kcal/mol). Nonetheless, the p10 and p14 HPs are presumed to interact with membranes as they promote lipid mixing (Corcoran *et al.*, 2004; Shmulevitz *et al.*, 2004b). The p15 FLX sequence may also interact with lipid, perhaps being dragged into contact with the membrane upon entrenchment of the H2 and HL domains into the bilayer interior.

The structure of a synthetic peptide corresponding to the p14 ectodomain has been determined by NMR (Corcoran *et al.*, 2004). Although a discrete loop corresponding to the p14 HL region was clearly evident, the remainder of the p14 ectodomain (including the FLX sequence) appeared relatively disordered (Corcoran *et al.*, 2004). By analogy, it is plausible that the p10 and p15 FLX regions exist in a similarly disordered state, at least in solution. It is not known what conformation the FLX regions adopt in a membrane environment. It is possible that the observed lack of regular secondary structure in the p14 FLX motif reflects the region's intrinsic conformational plasticity – an essential property of classical fusion peptides and other fusion-promoting motifs. Flexible sequences are also known to flank fusion peptides. As it is not considered hydrophobic and is not predicted to prefer a membrane environment, it is unlikely that the p15 FLX

motif functions like a typical fusion peptide. However, given the proximity of the FAST protein semi-conserved FLX motif to proposed fusogenic sequences, it may be fusion-promoting by virtue of supporting some function (perhaps conformational flexibility) of a neighboring (or overlapping, in the case of p14 and p10) 'fusion peptide'.

It is intriguing that the FLX motif of p15 and p14 is immediately preceded by sequences that resemble regions immediately preceding internal fusion peptides identified in other viruses. The HL domains of p15 and p14 can be described as containing the sequence $P(X)_3V(X)_{3-4}P$, with the proline and valine residues located at the base or apex of the loop, respectively. Similar sequence, $P(X)_5V(X)_5P$, is found directly flanking the fusion peptide of SFV E1 (a class II fusion protein), as well as the "fusion peptide" of rotavirus VP4 (which can be induced to mediate syncytium formation from without). Further structural and functional analysis is required to precisely determine the nature of the H2, HL and FLX regions and their role(s), if any, during FAST protein-triggered membrane merger.

6.3.4. Does fusogenicity require accumulation of a critical mass of p15 molecules?

The ability of various nonfusogenic p15 mutants to *trans*-inhibit authentic p15 function (Fig. 6.9), together with the ability of two nonfusogenic p15 mutants (17-gly and 59(A3)-HA) to *trans*-complement each other and restore a minimum level of p15 activity (Fig. 6.10), hints that multiple p15 molecules must work together in close association to trigger cell-cell fusion. It is unlikely that the partial dominant-negative effect exerted by numerous nonfusogenic p15 mutants is the result of global disruption of intracellular transport pathway(s), or sequestration of a limiting host factor required for p15 transport, given that it has been shown for (at least some of) these mutants there exists no defect in

subcellular localization (chapters 4 and 5). Preliminary evidence of purified FAST protein-mediated liposome-cell fusion (D. Top, personal communication) argues against the need for a cellular partner in the donor membrane. However, it remains possible that the dominant-negative effect results from competition for a limiting host factor in the target membrane. Both the dominant-inhibition and complementation behaviours of nonfusogenic p15 mutants can also be explained by the need to concentrate functional p15 molecules at the initiation site to accomplish membrane merger. The need to accumulate a critical mass of fusogenic complexes is a common theme in models of membrane fusion (chapter 1), and reflects the balance between the activity of various fusion-promoting motifs and the energy barrier preventing spontaneous membrane fusion. By diluting the concentration of functional p15 molecules at the site of fusion initiation, the dominant-negative mutants may interfere with the fusion process by effectively lowering the local energy available to overcome the barriers to cell-cell fusion. The observed complementation of two nonfusogenic p15 mutants can also be explained by an accumulation of p15 polypeptides at the site of fusion, if we assume that individual domains function separately, but in a cooperative manner, to accomplish membrane merger. Assuming the intact ectodomain of the 59(A3)-HA construct carries out its function(s) at its specific step(s) in the fusion process, as does the intact endodomain of the 17-gly construct then, by acting on the membrane together in close proximity, these two individually fusion-incompetent mutants appear to accomplish (albeit inefficiently) the fusion of neighbouring cells. The proposed accumulation of p15 molecules may involve (but not necessarily so) multimeric p15 complexes. In light of the finding that the RRV p14 FAST protein self-associates in multimeric complexes

(Corcoran *et al.*, 2004), and considering the proposed function of several TM domain features in p15 self-assembly, it would be worthwhile to investigate the oligomerization potential of p15.

CHAPTER 7

WORKING MODEL OF p15-MEDIATED MEMBRANE FUSION

7.1. Summary of salient findings

Analysis presented in the preceding chapters has demonstrated that the p15 protein, encoded by the 5'-proximal ORF of the BRV S4 genome segment, is a novel member of the FAST protein family. BRV p15 is a small (140 aa), nonstructural viral protein, the expression of which is both necessary and sufficient to induce syncytium formation in cell culture. A fraction of p15 is transported to the cell surface from where it presumably initiates the merger of adjacent cells. Adopting a type III (N_{exo}/C_{cyt}) topology, p15 externalizes a myristylated, minimal (20-aa) ectodomain, which is not only the smallest among known viral fusion proteins but also lacks a classical fusion peptide motif – an essential feature of virtually all other fusogenic proteins. Within p15, the only non-TM segment of significant hydrophobicity (the H2 domain) is located in the endodomain. Overlapping H2 are sequences (the HL and FLX regions) bearing similarity to the externalized hydrophobic patches (putative fusion peptides) of both the ARV p10 and RRV p14 FAST proteins. Most notably, the FLX sequence could be functionally exchanged among various FAST proteins, suggesting that the semi-conserved FLX motifs of p10, p14 and p15 are mechanistically equivalent and may represent novel, fusion-promoting domains that function on either side of the lipid bilayer.

7.2. Proposed model of p15-mediated membrane fusion

7.2.1. Requirement for pre-existing close cell-cell contact

Given its small size, it is unlikely that the p15 ectodomain is responsible for either initiating contact with a neighbouring cell or undergoing dramatic structural rearrangements to bring apposed lipid bilayers into close proximity. Therefore, it can be assumed that, in order to initiate cell-cell fusion, p15 must be present in the plasma membrane at sites of pre-existing close cell-cell contact. If dispersed randomly across the cell surface, p15 may only be fusogenic when located at points of membrane juxtaposition. Alternatively, p15 may be specifically targeted to such regions. Interestingly, syncytial Vero cells infected with the fusogenic NBV were shown under EM to exhibit numerous elongated processes that formed close contacts with adjacent uninfected cells (Wilcox and Compans, 1982). Recently, immunogold-labeled RRV p14 was observed under EM at similar cellular extensions in transfected cells (J. Salsman, unpublished data). Cell-surface protrusions (microvilli) have been proposed as the preferential site of numerous cell-cell fusion events, including fertilization, the formation of myotubes, giant macrophages, and syncytiotrophoblasts, as well as Sendai virus-, VV-, and HIV-induced syncytia (Gallo *et al.*, 2003; Wilson and Snell, 1998, and references therein). Microvilli likely promote cell-cell fusion both because of their role in cell-cell adhesion, as well as their high degree of membrane curvature strain (Wilson and Snell, 1998). Apparently lacking receptor-binding capacity, the FAST proteins may utilize fusion-promoting cellular protrusions as sites from which to contact a target membrane and initiate syncytium formation. The first molecular determinant responsible for targeting transmembrane proteins to cell surface protrusions was recently identified. Two

dileucine-like motifs positioned approximately 20 amino acids apart in the membrane-proximal region of the cytoplasmic tail of the insulin receptor were shown to play a crucial role in maintaining the receptor preferentially on microvilli (Shackleton *et al.*, 2002). Interestingly, the cytoplasmic tail of p15 contains two dileucine motifs, LL (82-83) and LL (112-113) positioned 30 residues apart. The contribution of these motifs to the sorting of p15 is not known.

7.2.2. Initiation of fusion at the donor membrane

The previous model of FAST protein-mediated membrane fusion, based on analysis of the p10 protein, was in accordance with the most popular theory of how biological membrane fusion must proceed – a membrane-anchored protein exposes a hydrophobic fusion peptide that inserts into and destabilizes the target membrane to initiate the fusion process (Shmulevitz, 2001). However, characterization of the BRV-encoded FAST protein calls into question the validity of such a model to describe the activity of p15. The lack of an externalized fusion peptide in p15, together with the apparent conservation of a FAST protein 'fusion peptide' motif within the p15 endodomain, suggests that initiation of FAST protein-triggered membrane fusion may focus preferentially, or entirely, on the donor membrane. Assuming the two membranes to be fused are held together in close proximity, destabilization of the donor membrane alone might lead to the formation of a hemifusion diaphragm and ensuing full fusion in a manner reminiscent of the bending defect and hydrophobic defect models described in chapter 1. In these models, the target membrane merges with the deformed donor membrane in order to alleviate either extreme bending stresses at the tip of a bulging dimple (Kozlov and Chernomordik, 1998) or to repair a hydrophobic defect created by

the extraction of the fusion peptide (Bentz, 2000a). Various means by which BRV p15 may perturb the donor membrane are summarized in Figure 7.1. The action of any of these motifs, discussed below, is expected to be augmented by the concentrated accumulation of p15 at sites of fusion initiation, possibly as a homomultimer.

N-terminal myristate fluctuations

The N-terminal myristate moiety of p15 (chapter 4) is likely in equilibrium between a membrane-embedded and exposed state. While myristic acid promotes membrane interaction, it is insufficiently hydrophobic to achieve stable membrane binding (Peitzsch and McLaughlin, 1993). Furthermore, transient exposure of the myristate moiety in the intermembrane space may contribute to the dehydration of the fusion site, thereby facilitating close membrane apposition. The reversible interaction between myristate and the donor membrane potentially creates a hydrophobic defect in the outer (*cis*) leaflet of the lipid monolayer, which could lead to the formation of a semistalk (refer to Fig. 1.1b). Assuming close cell-cell contact, the bulging semistalk in the donor membrane may reach, and consequently disrupt the continuity of, the *cis* monolayer of the target membrane. Alternatively, as there are no hydrophobic regions of the p15 ectodomain in which myristate might hide, it remains possible that while the myristylated N-terminus of p15 is in flux it may transiently interact with the adjacent target lipid monolayer, thereby inducing semistalk formation within both *cis* leaflets in the contact zone. Exposure of the hydrophobic interior of each bilayer at the tops of these bulging semistalks would presumably drive their merger to form the fusion stalk intermediate. The presence of myristate in the intermembrane space may also serve to stabilize the transfer of lipids from the target bilayer to the hydrophobic defect in the

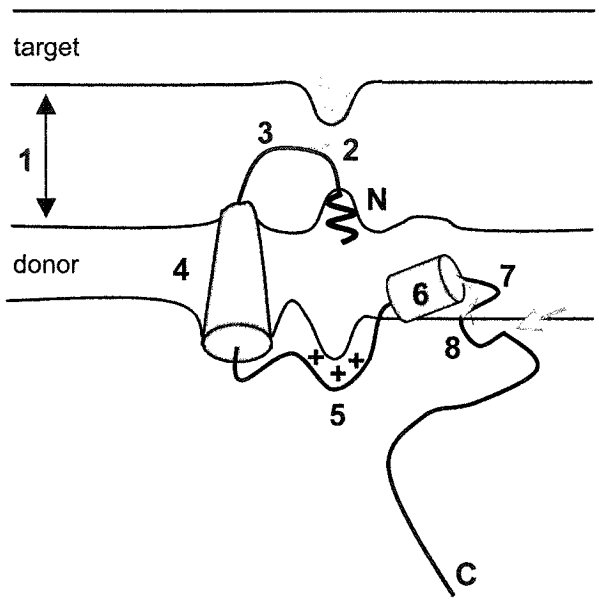

Figure 7.1. **Potential means of p15-induced perturbations of the donor membrane.** (1) Given expression of p15 at sites of close cell-cell contact, perturbations of the donor membrane may trigger the process of fusion with the apposed target membrane. Such p15-induced donor membrane perturbations may be introduced and/or aided through any of the following means: (2) Reversible membrane interactions of the myristylated N-terminus; (3) Flexibility of the ectodomain, possibly facilitated by the PPII helix; (4) TM-introduced expansion of the lipid bilayer; (5) Strong anionic phospholipid binding by the polybasic domain; (6) Insertion of the H2 and HL domains; (7) Formation and possible rotational motion of the putative HL; and (8) Conformational plasticity of the putative FLX region. The minimum length of p15 required to induce syncytium formation is indicated by the arrow. Grey lines shadow segments of p15 potentially in motion. The donor and target membranes are labeled, as are the p15 N- and C-termini. One p15 monomer is shown, but the proposed action of points (2-8) would be enhanced by the concentration of p15 at the site of fusion initiation, possibly as a homomultimer mediated through TM anchor or H2 self-associations.

donor bilayer, analogous to the proposed function of the hydrophobic kink region of HA_2 (Bentz, 2000a). Analysis by Chanturiya, *et al.* (1999) using model membranes, suggested that the rate-limiting step in membrane hemifusion corresponded to the formation of two adjacent semistalks rather than their merger into a fusion stalk. Therefore, reversible membrane interactions of the N-terminal myristate moiety of p15 alone may be sufficient to initiate the process of hemifusion.

Ectodomain flexibility

Repeated 'flipping' of the N-terminus to create the hydrophobic defect may be facilitated by an intrinsic flexibility of the p15 ectodomain. The major structural feature of the ectodomain, the polyproline helix, is expected to be inherently flexible (chapter 5). According to Guermeur's hierarchial neural network algorithm (Combet *et al.*, 2000), much of the remaining p15 ectodomain is predicted to adopt either random coil or extended strand conformation and, as such, may be conformationally plastic. If the p15 ectodomain is relatively disordered, as has been demonstrated by NMR for a p14 synthetic ectodomain peptide, then little energy would be required to alter the structure of the ectodomain if any such rearrangements are involved in the fusion mechanism. Although the p15 ectodomain lacks a fusion peptide motif, the relative intolerance of this domain to mutation (chapter 6) indicates that the externalized portion of p15 nonetheless plays a critical, as yet undefined, role in the promotion of cell-cell fusion.

TM domain, CRAC and flanking polybasic cluster

The predicted cholesterol-binding motif immediately downstream of the TM anchor (chapter 6) may interact with cholesterol, potentially within membrane microdomains whose lipid composition may be fusion-promoting and/or where the local

concentration of p15 is relatively high. The TM domain GxxxG-like motif (chapter 6) might promote TM helix-helix interactions that serve to oligomerize p15. Furthermore, both the size and shape of the p15 TM anchor is predicted to introduce curvature energy into the donor membrane that may influence the level of p15 self-assembly (perhaps promoting clustering at the fusion site) and/or the formation of high-energy lipid intermediates during fusion (chapter 6).

The adjacent polybasic cluster is presumed to interact strongly with anionic phospholipids (e.g. phosphatidylserine) on the cytosolic face of the bilayer, given the apparent resistance of this region to proteolytic attack in the presence of membranes (chapter 4). The polybasic domain may discourage lipids from the *trans* monolayer from entering a hydrophobic defect introduced into the *cis* monolayer, thereby indirectly promoting the entry of lipids from the apposed membrane to repair the defect and accomplish hemifusion. The polybasic domain may also function at a later stage in the fusion reaction. Perhaps through condensation of anionic phospholipid headgroups in the *trans* leaflet of the donor bilayer, the polybasic cluster may promote the adoption of inverted lipid phases, thereby facilitating the formation and growth of fusion pores. This is the first model to propose a direct role for a polybasic domain in a membrane fusion mechanism.

Non-spanning bilayer insertions

The moderately hydrophobic H2 domain of p15 does not span the bilayer (chapter 4), but is predicted to partition into the membrane, potentially regulated by the proposed domain motion of HL and/or the self-association of H2 (chapter 6). Self-assembly of H2 to form an oligomeric β-sheet structure would not only reduce the energy requirement for

membrane insertion but would also align three glycines along one face of the H2 element that may function analogous to the glycine ridge of other fusion peptides, such as that of HA_2 (chapter 6). If the membrane insertion of H2 occurred once the hemifusion diaphragm was established, it may serve to break that diaphragm, thereby opening a fusion pore, especially if H2 (in β-sheet conformation) interacts with the TM anchor via the predicted glycine face. Late-stage interaction between H2 and the TM anchor could weaken TM helix-helix interactions leading to the loosening of the predicted TM anchor-ring (discussed further in section 7.2.3) and dissociation of the p15 cluster that would be required for expansion of the fusion pore to achieve full cell-cell fusion.

Interestingly, the H2/HL sequence of p15 exhibits similarity to the fusion peptides of several retroviruses (simian Mason-Pfizer virus, squirrel monkey retrovirus, simian retrovirus SRV-1, avian reticuloendotheliosis virus) and HBV, with respect to the presence of an internal PLLV-like motif and surrounding pattern of alternating small (G, A, S) and large, aliphatic (V, L, I) residues (Del Angel *et al.*, 2002; Rodriguez-Crespo *et al.*, 1996). In addition, the p15 H2/HL sequence shows 70% similarity (25% identity) to the fusion peptide of another retrovirus, equine infectious anemia virus (NCBI Accession #P22427; gp45, aa 445-473). The fusogenic form of the retrovirus and HBV fusion peptides is likely an extended β-sheet conformation (Rodriguez-Crespo *et al.*, 1996; Sackett and Shai, 2003), as predicted for the p15 H2 region. These similarities support the prediction that the p15 H2/HL domain may exhibit a fusion-promoting character.

Flanking H2 is the semi-conserved FAST protein FLX sequence. The FLX motif can be functionally exchanged among the various FAST proteins and, thus, is proposed to represent mechanistically equivalent segments within the different FAST proteins

(chapter 6). This finding is significant given the location of the p10 and p14 FLX motifs within externalized putative fusion peptides. The FLX motif was found to exhibit partial similarity to sequences flanking the fusion peptides of SFV and rotavirus (chapter 6). The putative fusion-promoting activity of FLX may be tied to its proximity to the fusion peptide. Perhaps the FLX sequence promotes conformational flexibility within the fusion peptide itself that is necessary during membrane fusion. Although the relationship of the cytoplasmically-localized p15 FLX region with membranes is not known, it should be kept in mind that several membrane-active motifs of enveloped virus fusion proteins have recently been identified which were not originally predicted to bind membranes (Peisajovich and Shai, 2003). Until the FLX region has been thoroughly investigated, a direct role for this motif in p15-induced membrane fusion should not be ruled out.

C-terminal tail

Since much of the endodomain can be deleted while retaining a minimal level of p15-induced syncytium formation, it is concluded that the essential domains for initiation of the fusion process lie upstream of the dispensable 'tail' (residues 98-140). The C-terminal tail may contribute to the stability or folding of the protein, indirectly increasing the efficiency of p15-mediated membrane fusion.

7.2.3. Clustering of p15 at the nucleation site

Extrapolating from the hydrophobic defect model of Bentz (2000a), it is predicted that tight clustering of p15 molecules at the fusion site, possibly in a ring-like configuration, is essential to translate the p15-induced perturbations of the donor membrane into a nucleation point for bilayer merger. Although p15 possesses many possible means of inducing stress into the donor bilayer (in the form of localized

curvature strain and hydrophobic defects; discussed above and diagrammed in Fig. 7.1.), without clustering of p15 molecules to restrict lipid flow, the induced stress would rapidly dissipate and not be communicated to the apposed target bilayer. The most likely domains contributing to p15 self-assembly are the TM anchor and H2. Either domain may promote p15 oligomerization and/or clustering. As discussed above, a conformational change that brings these two domains together may break the p15 cluster as a necessary final step in the fusion process. Assuming the need to accumulate a critical number of p15 molecules at the fusion site, the suboptimal p15 translation initiation sequence (chapter 3) and rapid degradation profile of (presumably nascent) p15 (J. Corcoran, unpublished results) might contribute to the prevention of premature p15 fusogenic (or membrane-destabilizing) activity during transport, analogous to what has been proposed for the p10 FAST protein (Shmulevitz *et al.*, 2004a).

7.2.4. Balance between fusion-promoting motifs and energy barriers

A key theme emerging from ongoing studies of membrane fusion mechanisms is the requirement for the concerted action of multiple fusion-promoting motifs in order to overcome the energy barriers to membrane merger (reviewed by Peisajovich and Shai, 2003). The working model of p15-induced membrane cell-cell fusion described above incorporates this supposition. The relative contribution of various p15 fusion-promoting motifs may differ depending on the condition of the donor and/or target membranes. The overall kinetics of p15-induced syncytium formation are enhanced in Vero cells compared to QM5, which is the opposite of what is observed for the p10 and p14 FAST proteins expressed from the same vector. It would appear that the BRV p15 protein is potentially better suited to merging membranes originating from a monkey cell line,

while the ARV and RRV FAST proteins are better suited at fusing membranes originating from avian cells. Several p15 mutants display significant variance in relative fusogenicity when expressed in the two cell types. The A12C, pro3, P81A, and 97* constructs, in particular, induced syncytium formation in Vero cells, but failed (or nearly failed) to do so in QM5 cells. Also, the dominant-negative effect of those nonfusogenic mutants screened in Vero (G2A and the polyproline mutants) was complete, while it remained partial in QM5 cells (chapter 6). As fusion proteins operate on lipid assemblies, it is certain that the composition of the membranes to be fused influences the fusion reaction. For example, raft-associated lipids (cholesterol and spingolipids) reportedly influence the fusogenic activity of several enveloped virus fusion proteins (reviewed by Rawat *et al.*, 2003). Also, the externalization of phosphatidylserine (a negatively charged phospholipid normally localized to the cytosolic face of the lipid bilayer) at cell-cell contact sites has been implicated in supporting cell-cell fusion during fertilization, myotube development, and the formation of the syncytial trophoblast (Potgens *et al.*, 2002; van den Eijnde *et al.*, 2001), as well as rhabdovirus-mediated membrane fusion (Carneiro *et al.*, 2002).

The impact of membrane structure on the requirement for certain fusion-promoting motifs of p15 may have been serendipitously observed. While BFA treatment early in infection or transfection eliminated p15-induced syncytium formation (presumably due to the inhibition of intracellular transport pathways), late BFA treatment of transfected cells (after p15 has reached the cell surface) facilitated extensive cell-cell fusion mediated by normally nonfusogenic proline mutants, as well as the nonmyristylated, nonfusogenic G2A mutant (data not shown). BFA blocks membrane

traffic between the *cis*- and *trans*-Golgi compartments, leading to the disruption of the trans-Golgi apparatus (reviewed by Pelham, 1991). Golgi disassembly would affect not only the intracellular transport of proteins, but the trafficking of lipids as well. Thus, acquisition of fusogenic potential by certain cell surface-expressed p15 mutants may reflect a BFA-sensitive structural change in the plasma membrane that reduces the necessity of membrane-active motifs in the p15 ectodomain (N-terminal myristate or flexible PPII helix).

7.2.5. Predicted lack of metastability of p15

That fusogenic proteins are primed for fusion and maintained in a metastable fusion-inhibited state until the appropriate trigger induces a fusion-active conformational change, is the paradigm in virus-induced fusion (Stiasny *et al.*, 2001; Weissenhorn *et al.*, 1999). The priming of most viral fusion proteins is controlled by proteolytic cleavage (of either the fusion protein itself, or an associated protein). No such processing is evident in the case of p15. With other viral fusion proteins, the fusion-active conformation is achieved as a consequence of dramatic refolding of the large ectodomains induced by receptor-binding and/or the acid pH of the endosome. The activity of p15 does not require acidic pH and there is no evidence as of yet for the existence of a p15 receptor. Furthermore, with just 20 residues to manipulate, p15 apparently lacks the capability to undergo dramatic ectodomain conformational rearrangements. Thus, it can be perplexing to envision how the extremely minimal p15 ectodomain might participate in the lipid interactions between two apposed bilayers during membrane fusion. It is unlikely that p15 uses energy released upon the conversion from a kinetically-trapped, metastable intermediate to a stable form in order to drive the fusion process. Analogous to the

paradigm of enzyme catalysis, p15 likely accomplishes membrane fusion without inputting energy into the reaction itself, but rather by lowering the energy barrier to the spontaneous rate of reaction. Perturbations introduced into the donor bilayer by p15 would promote the formation of high-energy (i.e. unfavourable) lipidic intermediates in the fusion pathway. To complete the fusion reaction, p15 would also need to stabilize such intermediates (analogous to enzyme transition-state stabilization).

Although the field has converged on the metastability paradigm for membrane fusion-inducing proteins, Epand and Epand (2002, 2003) argue that HA, the prototypical fusion protein, is not held in a metastable state and, although conformational changes are essential for HA-mediated fusion, there is no detectable energy released upon conversion from the neutral- to the low pH-form. Nonetheless, it is still widely believed that significant energy contributions from the reorganization of large protein ectodomains is the essential requirement to overcome the local steric, electrostatic, and hydration-repulsion forces that impede spontaneous membrane merger. Thus, the minimal ectodomains of the highly-fusogenic FAST proteins appeared to be a paradox. However, from an alternate viewpoint, the small p15 ectodomain can be deemed advantageous to the fusion process. The thermodynamic barriers to membrane fusion are minimized at local point-like contact sites between bilayers (Chernomordik and Kozlov, 2003). Thus, if p15 initiates fusion from these sites, the energy requirement is minimized. The large glycoproteins that mediate enveloped virus fusion events themselves contribute to the steric repulsion between bilayers. Even in the 'compact' low energy form, class I fusion protein complexes would project approximately 10-15 nm out from the membrane in which they are anchored if they did not tilt parallel to the bilayer surface during refolding.

Mutations in the hinge regions that allow for this tilting eliminate fusion, even though the coiled-coil rearrangements proceed normally and result in the formation of a stable six-helix bundle (Tamm, 2003). Some of the energy released upon structural rearrangement that is considered to be applied to membrane destabilization may, in fact, be expended on moving these bulky six-helix bundles out of the way in order to allow fusion to proceed – in effect, much of the energy may go towards overcoming the energy barrier such a large protein introduces into the system.

The activity of the enveloped virus fusion proteins is closely tied to the process of receptor-binding. The energy believed to be released by the refolding of these fusion proteins may be necessary solely to bring the viral and target membranes into juxtaposition. The metastability of these fusion proteins likely reflects the need to tie the process of membrane-apposition and subsequent fusion to the appropriate receptor-binding signal. If the need for receptor binding is ignored, the portion of a typical enveloped virus fusion protein that does the bulk of the work promoting fusion (i.e. the ectodomain minus receptor-binding subunit) is of a comparable size to the entire p15 protein. If p15 motifs localized to both sides of the donor membrane function to promote fusion, compared to the 'working' part of other fusion machines, this small protein does not appear so drastically 'minimalistic' after-all. Unlike enveloped virus fusion proteins, p15 is not involved in virus entry and may not require a protein receptor to initiate cell-cell fusion. Thus, p15 requires neither to be held in a metastable state nor the release of a large amount of energy to drag two membranes together, so long as this protein functions from sites of pre-existing close cell-cell contact.

Support for this proposal comes from analysis of the influenza FHA_2 construct, representing the N-terminal 127 residues of HA_2 (Leikina *et al.*, 2001). FHA_2 extends from the HA fusion peptide through the coiled coil and kink region, including part of the downstream antiparallel C-terminal helices, but lacking the TM domain. The structure of trimeric FHA_2 resembles that of the lowest energy form of HA_2 and is thus not associated with a 'spring-loaded' conformational change (Leikina *et al.*, 2001, and references therein). Nonetheless, aided by aggregation via the hydrophobic kink region, FHA_2 mediates hemifusion between bound cells in a low pH-dependent manner (Leikina *et al.*, 2001). Therefore, in the absence of the steric repulsion introduced by the HA_1 subunit, and given pre-existing cell-cell contact, a 127-residue peptide of the HA_2 ectodomain requires neither metastability, nor a large release of energy to initiate bilayer mixing.

Certainly, from liposome-based assays have emerged numerous examples of short stretches of polypeptide (from a variety of fusion proteins) that are membrane-active in isolation (i.e. without the need for extensive, global conformational changes in the native protein). Analysis of the reoviral FAST proteins suggests that a collection of such motifs arranged within a minimal protein structure, acting synergistically from either side of a membrane, is sufficient to accomplish membrane fusion. If so, the small p15 ectodomain would not be a handicap but rather an advantage that minimizes steric repulsion between apposed membranes. The small size of the FAST proteins may be a streamlined adaptation to facilitate membrane fusion efficiently, with little to no structural reorganization in the intermembrane space. Rather than regulation through proteolytic processing and protein-protein interactions controlling triggered conformational changes, regulation of p15 activity may instead primarily rely on environmental control. The

requirement for pre-existing close cell-cell contact, the need to accumulate a critical number of FAST protein molecules at the initiation site, and the dependence on a specific membrane composition at the initiation site, together may be sufficient to keep p15 fusion-incompetent during protein transport, thereby preventing intracellular p15 from inducing massive destabilization of internal membranes prior to its expression at the cell surface.

7.3. Application of the p15 model to other FAST proteins

The working model of p15-induced membrane fusion describes the initiation of the fusion process, at sites of close cell-cell contact, through perturbations of primarily the donor bilayer accomplished by multiple p15 polypeptides clustered at the nucleation point and aided by a fusion-competent lipid platform. The p15 protein does not appear to require proteolytic processing for fusogenic activity, and does not appear to be held in a metastable conformation through protein-protein interactions. These general themes are certainly applicable to the entire FAST protein family, and perhaps to other examples of biological membrane merger as well. Although the ectodomains of p10 and p14 contain HP motifs capable of inducing lipid mixing, at approximately 40-residues each, the ectodomains of both these proteins are likely too small to initiate membrane fusion by contacting and destabilizing a target bilayer positioned more than a few nm away. As with other protein-mediated fusion events, it can be assumed that only motifs externalized within the FAST protein ectodomains are available to mediate contact with the *cis* bilayers of apposed membranes. Thus, it is the ectodomain motifs that likely accomplish hemifusion. These same motifs may influence further steps in the fusion

process, but it seems likely that the formation and growth of fusion pores within the hemifusion diaphragm will rely on the activity of motifs within the TM and endodomains. Although the FAST proteins share certain putative fusion-promoting motifs, the placement of these motifs on either side of the membrane has implications for what stage in the fusion process these domains might function in their respective proteins. For example, the externalized HPs of p10 and p14 (which include the FLX region) potentially induce lipid rearrangements within the *cis* monolayers so as to reverse the leaflet curvature (from positive to negative) in order to form the fusion stalk and accomplish hemifusion. However, the cytosolically-localized H2 domain of p15 (and flanking FLX region) are more likely to interact with the *trans* monolayers, and perhaps reverse the leaflet curvature (from negative to positive) in order to promote fusion pore formation. How these similar motifs might have opposite effects on lipid curvature, depending on their location to either the ecto- or endodomain, is not known. The lipid composition at the site of fusion initiation may promote the necessary curvature intermediates, simply requiring p15 to introduce minor destabilization. The regions of the different FAST proteins that are presumably available to the disparate steps in the fusion process are summarized in Table 7.1.

Table 7.1. **FAST protein motifs available to mediate either early (hemifusion) or late (fusion pore) steps in the fusion process.** Ectodomain motifs are the only ones presumably capable of interacting with the *cis* monolayers to induce hemifusion; endodomain motifs presumable influence the formation and growth of fusion pores.

Protein	Hemifusion	Fusion pore
ARV p10	HP/FLX	TM palmitate polybasic
RRV p14	myristate HP (HL + FLX)	TM polybasic
BRV p15	myristate PP(II) helix	TM polybasic H2/HL FLX

7.4. Future directions

The analysis presented in this thesis has culminated in the proposal of a novel model for how the p15 protein of BRV accomplishes syncytium formation. This working model of p15-mediated cell-cell fusion offers a number of hypotheses that need to be directly tested. Future mutagenesis and functional investigations should target the various motifs that have been identified by analysis of the p15 sequence and are proposed to play a role in the p15 mechanism of fusion: (1) the GxxxG-like motif within the TM anchor; (2) the membrane-proximal CRAC sequence; (3) the membrane-proximal tryptophan residue; (4) the tandem dileucine motifs in the C- terminal tail; and (5) the residues predicted to form the glycine face of H2 in β-sheet conformation. Although it is clear that p15 is the only viral protein required to drive membrane fusion, the implication that p15 activity does not involve a cellular partner should be examined using a cell-free fusion assay. Difficulties encountered when purifying and reconstituting baculovirus-expressed p15 into liposomes has delayed the development of a liposome fusion assay for p15 (D. Top, personal communication). Perhaps p15-based peptides will be more amenable to *in vitro* studies than the full-length p15 protein has been to date.

7.4.1. Employment of a lipid-mixing assay

The model proposed for p15 function predicts that the p15 ectodomain, although lacking a hydrophobic fusion peptide, is capable of accomplishing hemifusion, given close membrane apposition. The activity of the p15 ectodomain, if it is functional when dissociated from the endodomain, likely requires a membrane anchor to enable the energetic 'flipping' (and not just reversible dissociation) of the myristylated N-terminus. Hemifusion induced by the GPI-linked p15 ectodomain expressed on a donor population

of liposomes could be measured by the dequenching (release of self-quenching) of a fluorescent lipid probe (e.g. octadecylrhodamine) loaded in the target liposome population. It is likely that liposome aggregation in this experiment would need to be promoted, perhaps through the use of polyethylene glycol.

Regions within the p15 endodomain, including and proximal to the hydrophobic patch, are proposed to play an important role in completing the p15-mediated fusion reaction (Table 7.1). The role of this region of p15 is proposed to be analogous to the hydrophobic patch areas of the ectodomains of other FAST proteins that are known to induce lipid mixing and, thus, are presumed to promote hemifusion in the process of syncytium formation. Given the ability of the cytosolically-localized p15 FLX sequence to functionally substitute for its ectodomain counterparts in the other FAST proteins (chapter 6), it would be of interest to determine whether a peptide corresponding to a portion of the p15 endodomain could also function in a lipid-mixing assay. If so, the results would support a 'membrane-active' role for the p15 endodomain during fusion.

7.4.2. Testing membrane binding and insertion

Various p15 domains are proposed to interact with lipids during the fusion reaction. The membrane-binding activity of the p15 H2, H2/HL and H2/HL/FLX domains could be tested using peptides corresponding to these regions that are modified with the fluorescent probe 7-nitrobenz-2-oxa-1,3-diazole-4-yl (NBD). The fluorescence emission of the NBD moiety is sensitive to the hydrophobicity of its environment, and will exhibit a blue shift concomitant with an increase in its fluorescence intensity upon peptide binding to phospholipid membranes. The NBD probe will not reveal whether peptides are bound at the surface of the membrane or slightly buried within it. Therefore,

the accessibility of membrane-bound peptides could be examined further by their sensitivity to proteinase K digestion. The membrane-perturbing activity of various p15 domains, including the TM anchor, could be tested by measuring their ability to induce leakage of small unilamellar vesicles preloaded with a fluorescent dye. The model of p15-mediated membrane fusion predicts that several domains (e.g. TM anchor, H2) would induce lipid tilting upon their insertion into the membrane. The effect of these domains on the acyl-chain order within a lipid membrane can be estimated using polarized ATR-FTIR spectroscopy. However, this method will not be able to estimate the orientation of H2 if this region inserts as a β-sheet structure.

7.4.3. Analysis of p15 flexibility

The model presented in Figure 7.1 suggests that the flexibility of several p15 regions is a key feature contributing to the fusogenic potential of the protein. The conformational plasticity of the p15 ectodomain, TM anchor, and FLX region could be tested using CD spectroscopy to measure their relative secondary structure content in aqueous buffer versus a membrane-mimicking environment. Similarly, the proposed rotational motion of the putative HL domain could be measured using NMR. Now that the solution structure of the p14 ectodomain has been determined (Corcoran *et al.*, 2004), it would be of benefit to determine the NMR structure of the p15 ectodomain (and endodomain) under similar conditions in order to allow comparison of these two distinct FAST proteins.

7.4.4. Investigation of p15 self-association

A key aspect to the proposed mechanism of p15 function, not diagrammed in Figure 7.1, is the ability of p15 to assemble in close association at the site of fusion

initiation. The multimeric status of p15 needs to be addressed, perhaps through cross-linking, co-immune precipitation, and/or gel filtration assays. The ability of p15 monomers or multimeric complexes to self-associate could be measured by fluorescence energy transfer experiments employing rhodamine-labeled peptides. Rhodamine fluorescence is quenched when several molecules are in close proximity. Thus, a decrease in rhodamine fluorescence intensity upon mixture of an unlabeled p15 population with a labeled population might indicate co-assembly of p15.

7.4.5. Use of a quantitative fusion assay

A limitation of the mutagenic analysis presented throughout this thesis is the use of the syncytial index assay to monitor relative changes in the fusogenic potential of various constructs. Counting syncytial nuclei is time-consuming, subject to the interpretation (and error) of the investigator, and is a relatively insensitive assay that obscures subtle variation in the activity of different constructs. It would be of value to continue the functional analysis of p15 mutants employing a reporter gene assay to quantify the extent of cell-cell fusion. In such an assay the expression of p15 in a donor cell population would be linked with the expression of a transcriptional activator that would induce the expression of a reporter construct (e.g. luciferase or β-galactosidase; the activity of which could be measured) within the target cell population. Many of the p15 mutants described in this thesis as nonfusogenic, may support initial steps in the fusion process not detected by a syncytial assay. Therefore, it would also be beneficial to develop liposome- or cell-based assays for the quantitation of hemifusion and small pore formation in order to begin to dissect the regions of p15 that contribute to different steps in the overall process of membrane merger.

Continued analysis of BRV p15 should illuminate the details of how this unique FAST protein accomplishes membrane merger. These studies should expand the current understanding of how the union of lipid bilayers proceeds, and may potentially define a novel mechanism of protein-mediated membrane fusion.

REFERENCES

Abe, E., H. Mocharla, T. Yamate, Y. Taguchi, and S. C. Manolagas. 1999. Meltrin-alpha, a fusion protein involved in multinucleated giant cell and osteoclast formation. *Calcif. Tissue Int.* 64:508-15.

Adzhubei, A. A., and M. J. E. Sternberg. 1993. Left-handed polyproline II helices commonly occur in globular proteins. *J. Mol. Biol.* 229:472-93.

Ahmadian, G., J. S. Randhawa, and A. J. Easton. 2000. Expression of the ORF-2 protein of the human respiratory syncytial virus M2 gene is initiated by a ribosomal termination-dependent reinitiation mechanism. *EMBO J.* 19:2681-9.

Allison, S. L., J. Schalich, K. Stiasny, C. W. Mandl, and F. X. Heinz. 2001. Mutational evidence for an internal fusion peptide in flavivirus envelope protein E. *J. Virol.* 75:4268-75.

Allison, S. L., K. Stiasny, K. Stadler, C. W. Mandl, and F. X. Heinz. 1999. Mapping of functional elements in the stem-anchor region of tick-borne encephalitis virus envelope protein E. *J. Virol.* 79:5605-12.

Ames, J. B., R. Ishima, T. Tanaka, J. I. Gordon, L. Stryer, and M. Ikura. 1997. Molecular mechanics of calcium-myristoyl switches. *Nature* 389:198-202.

Andersson, A. M., L. Melin, A. Bean, and R. F. Pettersson. 1997. A retention signal necessary and sufficient for Golgi localization maps to the cytoplasmic tail of a Bunyaviridae (Uukuniemi virus) membrane glycoprotein. *J. Virol.* 71:4717-27.

Antin, P. B., and C. P. Ordahl. 1991. Isolation and characterization of an avian myogenic cell line. *Dev. Biol.* 143:111-21.

Armstrong, R. T., A. S. Kushnir, and J. M. White. 2000. The transmembrane domain of influenza hemagglutinin exhibits a stringent length requirement to support the hemifusion to fusion transition. *J. Cell Biol.* 151:425-37.

Arold, S., P. Franken, M. P. Strub, F. Hoh, S. Benichou, R. Benarous, and C. Dumas. 1997. The crystal structure of HIV-1 Nef protein bound to the Fyn kinase SH3 domain suggests a role for this complex in altered T cell receptor signaling. *Structure* 5:1361-72.

Avitabile, E., G. Lombardi, and G. Campadelli-Fiume. 2003. Herpes simplex virus glycoprotein K, but not its syncytial allele, inhibits cell-cell fusion mediated by the four fusogenic glycoproteins, gD, gB, gH, and gL. *J. Virol.* 77:6836-44.

Bagai, S., and R. A. Lamb. 1996. Truncation of the COOH-terminal region of the paramyxovirus SV5 fusion protein leads to hemifusion but not complete fusion. *J. Cell Biol.* 135:73-84.

Ball, L. J., T. Jarchau, H. Oschkinat, and U. Walter. 2002. EVHI domains: structure, function and interactions. *FEBS Lett.* 513:45-52.

Barre, P., O. Zschornig, K. Arnold, and D. Huster. 2003. Structural and dynamical changes of the bindin B18 peptide upon binding to lipid membranes. A solid-state NMR study. *Biochemistry* 42:8377-86.

Beaton, A. R., J. Rodrigues, Y. K. Reddy, and P. Roy. 2002. The membrane trafficking protein calpactin forms a complex with bluetongue virus protein NS3 and mediates virus release. *Proc. Natl. Acad. Sci. USA* 99:13154-9.

Beltzer, J. P., K. Fieder, C. Fuhrer, I. Geffen, C. Handschin, H. P. Wessels, and M. Spiess. 1991. Charged residues are major determinants of the transmembrane orientation of a signal-anchor sequence. *J. Biol. Chem.* 266:973-8.

Bentz, J. 2000a. Membrane fusion mediated by coiled coils: a hypothesis. *Biophys. J.* 78:886-900.

Bentz, J. 2000b. Minimal aggregate size and minimal fusion unit for the first fusion pore of influenza hemagglutinin-mediated membrane fusion. *Biophys. J.* 78:227-45.

Bentz, J., and A. Mittal. 2003. Architecture of the influenza hemagglutinin membrane fusion site. *Biochim. Biophys. Acta.* 1614:24-35.

Bentz, J., and A. Mittal. 2000. Deployment of membrane fusion protein domains during fusion. *Cell Biol. Int.* 24:819-38.

Bergmann, C. C., D. Maass, M. S. Poruchynsky, P. H. Atkinson, and A. R. Bellamy. 1989. Topology of the non-structural rotavirus receptor glycoprotein NS28 in the rough endoplasmic reticulum. *EMBO J.* 8:1695-703.

Berting, A., C. Fischer, S. Schaefer, W. Garten, H. D. Klenk, and W. H. Gerlich. 2000. Hemifusion activity of a chimeric influenza virus hemagglutinin with a putative fusion peptide from hepatitis B virus. *Virus Res.* 68:35-49.

Binder, H., K. Arnold, A. S. Ulrich, and O. Zschornig. 2000. The effect of Zn(2+) on the secondary structure of a histidine-rich fusogenic peptide and its interaction with lipid membranes. *Biochim Biophys Acta.* 1468:345-58.

Blahak, S., I. Ott, and E. Vieler. 1995. Comparison of 6 different reoviruses of various reptiles. *Vet. Res.* 26:470-6.

Blumenthal, R., M. J. Clague, S. R. Durell, and R. M. Epand. 2003. Membrane fusion. *Chem. Rev.* 103:53-69.

Bochicchio, B., and A. M. Tamburro. 2002. Polyproline II structure in proteins: identification by chiroptical spectroscopies, stability and functions. *Chirality* 14:782-92.

Bodelon, G., L. Labrada, J. Martinez-Costas, and J. Benavente. 2001. The avian reovirus genome segment S1 is a functionally tricistronic gene that expresses one structural and two nonstructural proteins in infected cells. *Virology* 290:181-91.

Boesze-Battaglia, K., F. P. Stefano, M. Fenner, and A. A. J. Napoli. 2000. A peptide analogue to a fusion domain within photoreceptor peripherin/rds promotes membrane adhesion and depolarization. *Biochim. Biophys. Acta.* 1462:343-54.

Bonner, W. M. 1984. Fluorography for the detection of radioactivity in gels. *Methods Enzymol.* 104:460-5.

Bork, P., and M. Sudol. 1994. The WW domain: A signalling site in dystrophin? *Trends Biochem. Sci.* 19:531-3.

Bosch, B. J., R. van der Zee, C. A. de Haan, and P. J. Rottier. 2003. The coronavirus spike protein is a class I virus fusion protein: structural and functional characterization of the fusion core complex. *J. Virol.* 77:8801-11.

Browne, E. P., A. R. Bellamy, and J. A. Taylor. 2000. Membrane-destabilizing activity of rotavirus NSP4 is mediated by a membrane-proximal amphipathic domain. *J. Gen. Virol.* 81:1955-9.

Brunger, A. T. 2000. Structural insights into molecular mechanism of Ca^{2+}-dependent exocytosis. *Curr. Opin. Neurobiol.* 10:293-302.

Bruss, V. 1997. A short linear sequence in the preS domain of the large hepatitis B virus envelope protein required for virion formation. *J. Virol.* 71:4350-7.

Burgoyne, R. D. and M. J. Clague. 2003. Calcium and calmodulin in membrane fusion. *Biochim. Biophys. Acta.* 1614:137-43.

Caballero, M., J. Carabana, J. Ortego, R. Fernandez-Munoz, and M. L. Celma. 1998. Measles virus fusion protein is palmitoylated on transmembrane-intracytoplasmic cysteine residues which participate in cell fusion. *J. Virol.* 72:8198-204.

Carlsson, L., L. E. Nystrom, I. Sundkvist, F. Markey, and U. Lindberg. 1977. Actin polymerizability is influenced by profilin, a low molecular weight protein in non-muscle cells. *J. Mol. Biol.* 115:465-83.

Carr, C. M., C. Chaudhry, and P. S. Kim. 1997. Influenza hemagglutinin is spring-loaded by a metastable native conformation. *Proc. Natl. Acad. Sci. U.S.A.* 94:14306-13.

Carrasco, L. 1995. Modification of membrane permeability by animal viruses. *Adv. Virus Res.* 45:61-111.

Carneiro, F. A., M. L. Bianconi, G. Weissmuller, F. Stauffer, and A. T. Da Poian. 2002. Membrane recognition by vesicular stomatitis virus involves enthalpy-driven protein-lipid interactions. *J. Virol.* 76:3756-64.

Chanturiya, A., E. Leikina, J. Zimmerberg, and L. V. Chernomordik. 1999. Short-chain alcohols promote an early stage of membrane hemifusion. *Biophys. J.* 77:2035-45.

Chasey, D., R. J. Higgins, M. Jeffrey, and J. Banks. 1989. Atypical rotavirus and villous epithelial cell syncytia in piglets. *J Comp Pathol.* 100:217-22.

Chelli, R., F. L. Gervasio, P. Procacci, and V. Schettino. 2002. Stacking and T-shape competition in aromatic-aromatic amino acid interactions. *J. Am. Chem. Soc.* 124:6133-43.

Chen, S. 1991. Myristylation of the envelope glycoprotein of vesicular stomatitis virus. *Intervirology* 32:193-7.

Chen, J. K., J. J. Skehel, and D. C. Wiley. 1999. N- and C-terminal residues combine in the fusion-pH influenza hemagglutinin HA(2) subunit to form an N cap that terminates the triple-stranded coiled coil. *Proc. Nat. Acad. Sci. USA* 96:8967-72.

Chen, Y. A., and R. H. Scheller. 2001. SNARE-mediated membrane fusion. *Nat. Rev. Mol. Cell Biol.* 2:98-106.

Chernomordik, L., M. Kozlov, and J. Zimmerberg. 1995. Lipids in biological membrane fusion. *J. Membr. Biol.* 146:1-14.

Chernomordik, L. V., V. A. Frolov, E. Leikina, P. Bronk, and J. Zimmerberg. 1998. The pathway of membrane fusion catalyzed by influenza hemagglutinin: restriction of lipids, hemifusion, and lipidic fusion pore formation. *J. Cell Biol.* 140:1369-82.

Chernomordik, L. V., and M. M. Kozlov. 2003. Protein-lipid interplay in fusion and fission of biological membranes. *Annu. Rev. Biochem.* 72:175-207.

Chizmadzhev, Y. A., D. A. Kumenko, P. I. Kuzmin, L. V. Chernomordik, J. Zimmerberg, and F. S. Cohen. 1999. Lipid flow through fusion pores connecting membranes of different tensions. *Biophys. J.* 76:2951-65.

Cho, S. J., M. Kelly, K. T. Rognlien, J. A. Cho, J. K. Horber, and B. P. Jena. 2002. SNAREs in opposing bilayers interact in a circular array to form conducting pores. *Biophys. J.* 83:2522-7.

Cleverley, D. Z., and J. Lenard. 1998. The transmembrane domain in viral fusion: essential role for a conserved glycine residue in vesicular stomatitis virus G protein. *Proc. Natl. Acad. Sci. USA* 95:3425-30.

Cole, N. L., and C. Grose. 2003. Membrane fusion mediated by herpesvirus glycoproteins: the paradigm of varicella-zoster virus. *Rev. Med. Virol.* 13:207-22.

Colman, P. M., and M. C. Lawrence. 2003. The structural biology of type I viral membrane fusion. *Nat. Rev. Mol. Cell. Biol.* 4:309-19.

Combet, C., C. Blanchet, C. Geourjon, and G. Deleage. 2000. NPS@: network protein sequence analysis. *TIBS* 25:147-50.

Cooper, A., N. Paran, and Y. Shaul. 2003. The earliest steps in hepatitis B virus infection. *Biochim. Biophys. Acta.* 1614:89-96.

Corcoran, J. 2003. Protein-mediated fusion: new insights from the reptilian reovirus p14 fusion protein. Ph.D. thesis. Dalhousie University, Halifax.

Corcoran, J., and R. Duncan. 2004. Reptilian reovirus utilizes a small type III protein with an external myristylated amino terminus to mediate cell-cell fusion. *J. Virol.* (submitted).

Corcoran, J., R. Syvitski, D. Top, D. Jakeman, and R. Duncan. 2004. An atypical fusion protein from a non-enveloped virus contains a looped internal fusion peptide within its essential 40-residue N-terminal ectodomain (in preparation).

Cordes, F. S., J. N. Bright, and M. S. Sansom. 2002. Proline-induced distortions of transmembrane helices. *J. Mol. Biol.* 323:951-60.

Cuasnicu, P. S., D. A. Ellerman, D. J. Cohen, D. Busso, M. M. Morgenfeld, and V. G. Da Ros. 2001. Molecular mechanisms involved in mammalian gamete fusion. *Arch. Med. Res.* 32:614-8.

Dawe, S., J. Boutilier, and R. Duncan. 2002. Identification and characterization of a baboon reovirus-specific nonstructural protein encoded by the bicistronic S4 genome segment. *Virology* 304:44-52.

Dawe, S., and R. Duncan. 2002. The S4 genome segment of baboon reovirus is bicistronic and encodes a novel fusion-associated small transmembrane protein. *J. Virol.* 76:2131-40.

De Falco, S., M. Ruvo, A. Verdoliva, A. Scarallo, D. Raimondo, A. Raucci, and G. Fassina. 2001. N-terminal myristylation of HBV preS1 domain enhances receptor recognition. *J. Pept. Res.* 57:390-400.

Del Angel, V. D., F. Dupuis, J. P. Mornon, and I. Callebaut. 2002. Viral fusion peptides and identification of membrane-interacting segments. *Biochem. Biophys. Res. Commun.* 293:1153-60.

Dennison, S. M., N. Greenfield, J. Lenard, and B. R. Lentz. 2002. VSV transmembrane domain (TMD) peptide promotes PEG-mediated fusion of liposomes in a conformationally sensitive fashion. *Biochemistry* 41:14925-34.

Denzer, A. J., C. E. Nabholz, and M. Spiess. 1995. Transmembrane orientation of signal-anchor proteins is affected by the folding state but not the size of the N-terminal domain. *EMBO J.* 14:6311-7.

Ding, L., A. Derdowski, J. J. Wang, and P. Spearman. 2003. Independent segregation of human immunodeficiency virus type 1 Gag protein complexes and lipid rafts. *J. Virol.* 77:1916-26.

Dubin, G., and H. Jiang. 1995. Expression of herpes simplex virus type 1 glycoprotein L (gL) in transfected mammalian cells: evidence that gL is not independently anchored to cell membranes. *J. Virol.* 69:4564-8.

Dubovski, P. V., H. Li, S. Takahashi, A. S. Arseniev, and K. Akasaka. 2000. Structure of an analog of fusion peptide from hemagglutinin. *Protein Sci.* 9:786-98.

Duncan, R. 1999. Extensive sequence divergence and phylogenetic relationships between the fusogenic and nonfusogenic orthoreoviruses: a species proposal. *Virology* 260:316-28.

Duncan, R., Z. Chen, S. Walsh, and S. Wu. 1996. Avian reovirus-induced syncytium-formation is independent of infectious progeny virus production and enhances the rate, but is not essential, for virus-induced cytopathology and virus egress. *Virology* 224:453-64.

Duncan, R., J. Corcoran, J. Shou, and D. Stoltz. 2004. Reptilian reovirus: a new fusogenic orthoreovirus species. *J. Virol.* (in press)

Duncan, R., F. A. Murphy, and R. R. Mirkovic. 1995. Characterization of a novel syncytium-inducing baboon reovirus. *Virology* 212:752-6.

Duncan, R., and K. Sullivan. 1998. Characterization of two avian reoviruses that exhibit strain-specific quantitative differences in their syncytium-inducing and pathogenic capabilities. *Virology* 250:263-72.

Durrer, P., Y. Gaudin, R. W. Ruigrok, R. Graf, and J. Brunner. 1995. Photolabeling identifies a putative fusion domain in the envelope glycoprotein of rabies and vesicular stomatitis viruses. *J. Biol. Chem.* 270:17575-81.

Dworak, H. A., and H. Sink. 2002. Myoblast fusion in Drosophila. *Bioessays* 24:591-601.

Eisenberg, D. 1984. Three-dimensional structure of membrane and surface proteins. *Annu. Rev. Biochem.* 53:595-623.

Ender, F., K. Godl, S. Wenzl, and M. Sumper. 2002. Evidence for autocatalytic cross-linking of hydroxyproline-rich glycoproteins during extracellular matrix assembly in Volvox. *Plant Cell* 14:1147-60.

Epand, R. F., and R. M. Epand. 2003. Irreversible unfolding of the neutral pH form of influenza hemagglutinin demonstrates that it is not in a metastable state. *Biochemistry* 42:5052-7.

Epand, R. F., J. C. Macosko, C. J. Russel, Y. K. Shin, and R. M. Epand. 1999. The ectodomain of HA2 of influenza virus promotes rapid pH dependent membrane fusion. *Mol. Biol. Cell* 286:489-503.

Epand, R. M. 1998. Lipid polymorphism and protein-lipid interactions. *Biochim. Biophys. Acta.* 1376:353-68.

Epand, R. M. 2003. Fusion peptides and the mechanism of viral fusion. *Biochim. Biophys. Acta.* 1614:116-21.

Epand, R. M., and R. F. Epand. 2001. Factors contributing to the fusogenic potency of foamy virus. *Biochem. Biophys. Res. Commun.* 284:870-4.

Epand, R. M., and R. F. Epand. 2002. Thermal denaturation of influenza virus and its relationship to membrane fusion. *Biochem. J.* 365:841-8.

Epand, R. M., Y. Shai, J. P. Segrest, and G. M. Anantharamaiah. 1995. Mechanisms for the modulation of membrane bilayer properties by amphipathic helical peptides. *Biopolymers* 37:319-38.

Ernst, H., and A. J. Shatkin. 1985. Reovirus hemagglutinin mRNA codes for two polypeptides in overlapping reading frames. *Proc. Natl. Acad. Sci. USA* 82:48-52.

Feng, S., J. K. Chen, H. Yo, J. A. Simon, and S. L. Schreiber. 1994. Two binding orientations for peptides to the Src SH3 domain: development of a general model for SH3-ligand interactions. *Science* 266:1241-7.

Feng, Y., G. Melacini, J. P. Taulane, and M. Goodman. 1996. Acetyl-terminated and template-assembled collagen-based polypeptides composed of Gly-Pro-Hyp sequences. 2. Synthesis and conformational analysis by circular dichroism, ultraviolet absorbance and optical rotation. *J. Am. Chem. Soc.* 118:10351-8.

Ferlenghi, I., M. Clarke, T. Ruttan, S. L. Allison, J. Schalich, F. X. Heinz, S. C. Harrison, F. A. Rey, and S. D. Fuller. 2001. Molecular organization of a recombinant subviral particle from tick-borne encephalitis virus. *Mol. Cell* 7:593-602.

Ferlenghi, I., B. Gowen, F. de Haas, E. J. Mancini, H. Garoff, M. Sjoberg, and S. D. Fuller. 1998. The first step: activation of the Semliki Forest virus spike protein precursor causes a localized conformational change in the trimeric spike. *J. Mol. Biol.* 283:71-81.

Ferris, P. J., J. P. Woessner, S. Waffenschmidt, S. Kilz, J. Drees, and U. W. Goodenough. 2001. Glycosylated polyproline II rods with kinks as a structural motif in plant hydroxyproline-rich glycoproteins. *Biochemistry* 40:2978-87.

Ferro-Novick, S., and R. Jahn. 1994. Vesicle fusion from yeast to man. *Nature* 370:191-3.

Foster, T. P., J. M. Melancon, and K. G. Kousoulas. 2001. An alpha-helical domain within the carboxyl terminus of herpes simplex virus type 1 (HSV-1) glycoprotein B (gB) is associated with cell fusion and resistance to heparin inhibition of cell fusion. *Virology* 287:18-29.

Fouillot, N., S. Tlouzeau, J. M. Rossignol, and O. Jean-Jean. 1993. Translation of the hepatitis B virus P gene by ribosomal scanning as an alternative to internal initiation. *J. Virol.* 67:4886-95.

Fournier, J. B. 1999. Microscopic membrane elasticity and interactions among membrane inclusions: interplay between the shape, dilation, tilt and tilt-difference modes. *Eur. Phys. J. B.* 11:261-72.

Fra, A. M., Fagioli, C., Finazzi, D., Sitia, R., Alberini, C.M. 1993. Quality control of ER synthesized proteins: an exposed thiol group as a three-way switch mediating assembly, retention and degradation. *EMBO J.* 12:4755-61.

Fredericksen, B. L., and M. A. Whitt. 1995. Vesicular stomatitis virus glycoprotein mutations that affect membrane fusion activity and abolish virus infectivity. *J. Virol.* 69:1435-43.

Frendo, J. L., D. Olivier, V. Cheynet, J. L. Blond, O. Bouton, M. Vidaud, M. Rabreau, D. Evain-Brion, and F. Mallet. 2003. Direct involvement of HERV-W Env glycoprotein in human trophoblast cell fusion and differentiation. *Mol. Cell. Biol.* 23:3566-74.

Freund, C., V. Dotsch, K. Nishizawa, E. L. Reinherz, and G. Wagner. 1999. The GYF domain is a novel structural fold that is involved in lymphoid signaling through proline-rich sequences. *Nat. Struct. Biol.* 6:656-60.

Freund, C., R. Kuhne, S. H. Park, K. Thiemke, E. L. Reinherz, and G. Wagner. 2003. Structural investigation of a GYF domain covalently inked to a proline-rich peptide. *J. Biol. NMR* 27:143-9.

Fritza, S., D. Rapaportb, E. Klannera, W. Neuperta, and B. Westermanna. 2001. Connection of the mitochondrial outer and inner membranes by Fzo1 is critical for organellar fusion. *J. Cell Biol.* 152:683-92.

Fujiki, Y., A. L. Hubbard, S. Fowler, and P. B. Lazarow. 1982. Isolation of intracellular membranes by means of sodium carbonate treatment: application to endoplasmic reticulum. *J. Cell. Biol.* 93:97-108.

Gallaher, W. R., C. DiSimone, and M. J. Buchmeier. 2001. The viral transmembrane superfamily: possible divergence of Arenavirus and Filovirus glycoproteins from a common RNA virus ancestor. *BMC Microbiol.* 1:1.

Gallina, A., and G. Milanesi. 1993. Trans-membrane translocation of a myristylated protein amino terminus. *Biochem. Biophys. Res. Commun.* 195:637-42.

Gallo, S. A., C. M. Finnegan, M. Viard, Y. Raviv, A. Dimitrov, S. S. Rawat, A. Puri, S. Durell, and R. Blumenthal. 2003. The HIV Env-mediated fusion reaction. *Biochim. Biophys. Acta.* 1614:36-50.

Gard, G., and R. W. Compans. 1970. Structure and cytopathic effects of Nelson Bay virus. *J. Virol.* 6:100-6.

Garry, R. F., and S. Dash. 2003. Proteomics computational analyses suggest that hepatitis C virus E1 and pestivirus E2 envelope glycoproteins are truncated class II fusion proteins. *Virology* 307:255-65.

Gaudin, Y. 2000a. Rabies virus-induced membrane fusion pathway. *J. Cell Biol.* 150:601-12.

Gaudin, Y. 2000b. Reversibility in fusion protein conformational changes: the intriguing case of rhabdovirus-induced membrane fusion. *Subcell. Biochem.* 34:379-408.

Gaudin, Y., R. W. Ruigrok, and J. Brunner. 1995. Low-pH induced conformational changes in viral fusion proteins: implications for the fusion mechanism. *J. Gen. Virol.* 76:1541-56.

Gelberg, H. B., W. F. Hall, G. N. Woode, E. J. Basgall, and G. Scherba. 1990. Multinucleate enterocytes associated with experimental group A porcine rotavirus infection. *Vet. Pathol.* 27:453-4.

Gerst, J. E. 2003. SNARE regulators: matchmakers and matchbreakers. *Biochim. Biophys. Acta.* 1614:99-110.

Ghosh, J. K., and Y. Shai. 1999. Direct evidence that the N-terminal heptad repeat of Sendai virus fusion protein participates in membrane fusion. *J. Mol. Biol.* 292:531-546.

Gibbons, D. L., I. Erk, B. Reilly, J. Navaza, M. Kielian, F. A. Rey, J. Lepault. 2003. Visualization of the target-membrane-inserted fusion protein of Semliki Forest virus by combined electron microscopy and crystallography. *Cell* 114:573-83.

Glaser, R. W., M. Grune, C. Wandelt, and A. S. Ulrich. 1999. Structure analysis of a fusogenic peptide sequence from the sea urchin fertilization protein bindin. *Biochemistry* 38:2560-9.

Goff, A., L. S. Ehrlich, S. N. Cohen, and C. A. Carter. 2003. Tsg101 control of human immunodeficiency virus type I Gag trafficking and release. *J. Virol.* 77:9173-82.

Goldberg, J. 1998. Structural basis for activation of ARF GTPase: mechanisms of guanine nucleotide exchange and GTP-myristoyl switching. *Cell* 95:237-48.

Gong, S. C., C. Lai, and M. Esteban. 1990. Vaccinia virus induces cell fusion at acid pH and this activity is mediated by the N-terminus of the 14-kDa virus envelope protein. *Virology* 178:81-91.

Grgacic, E. V. L., and H. Schaller. 2000. A metastable form of the large envelope protein of duck hepatitis B virus: low-pH release results in a transition to a hydrophobic, potentially fusogenic conformation. *J. Virol.* 74:5116-22.

Gruenke, J. A., R. T. Armstrong, W. W. Newcomb, J. C. Brown, and J. M. White. 2002. New insights into the spring-loaded conformational change of influenza virus hemagglutinin. *J. Virol.* 76:4456-66.

Haag, L., H. garoff, L. Xing, L. Hammar, S.-T. Kan, and R. H. Cheng. 2002. Acid-induced movements in the glycoprotein shell of an alphavirus turn the spikes into membrane fusion mode. *EMBO J.* 21:4402-10.

Haan, K. M., S. K. Lee, and R. Longnecker. 2001. Different functional domains in the cytoplasmic tail of glycoprotein B are involved in Epstein-Barr virus-induced membrane fusion. *Virology* 290:106-14.

Hammar, L., S. Markarian, L. Haag, H. Lankinen, A. Salmi, and R. Cheng. 2003. Prefusion rearrangements resulting in fusion peptide exposure in Semliki Forest virus. *J. Biol Chem.* 278:7189-98.

Harty, R. N., M. E. Brown, G. Wang, J. Huibregtse, and F. P. Hayes. 2000. A PPxY motif within the VP40 protein of Ebola virus interacts physically and functionally with a ubiquitin ligase: implications for filovirus budding. *Proc. Natl. Acad. Sci. USA* 97:13871-6.

Hayward, S. 1999. Structural principles governing domain motions in proteins. *Proteins* 36:425-35.

Hemler, M. E. 2003. Tetraspanin proteins mediate cellular penetration, invasion, and fusion events and define a novel type of membrane microdomain. *Annu. Rev. Cell. Dev. Biol.* 19:397-422.

High, S., N. Flint, and B. Dobberstein. 1991. Requirements for the membrane insertion of signal-anchor type proteins. *J Cell Biol.* 113:25-34.

Hirokawa, T., S. Boon-Cheng, and S. Mitaku. 1998. SOSUI: classification and secondary structure prediction system for membrane proteins. *Bioinformatics* 14:378-9.

Hofmann, K., and W. Stoffel. 1993. A database of membrnae spanning protein segments. *Biol. Chem.* 374:166-172.

Holt, M. R., and A. Koffer. 2001. Cell motility: proline-rich proteins promote protrusions. *Trends Cell Biol.* 11:38-46.

Hsiao, J.-C., C.-S. Chung, and W. Chang. 1998. Cell surface proteoglycans are necessary for A27L protein-mediated cell fusion: identification of the N-terminal region of A27L protein as the glycosaminoglycan-binding protein. *J. Virol.* 72:8374-9.

Huang, X., and W. Miller. 1991. A time-ecient, linear space local similarity algorithm. *Adv. Appl. Math* 12:337-357.

Huang, Q., R. P. Sivaramakrishna, K. Ludwig, T. Korte, C. Bottcher, and A. Hermann. 2003. Early steps of the conformational change of influenza virus hemagglutinin to a fusion active state: stability and energetics of the hemagglutinin. *Biochim. Biophys. Acta.* 1614:3-13.

Hughson, F. M. 1997. Enveloped viruses: a common mode of membrane fusion? *Curr. Biol.* 7:R565-9.

Hutchinson, L., H. Browne, V. Wargent, N. Davis-Poynter, S. Primorac, K. Goldsmith, A. C. Minson, and D. C. Johnson. 1992. A novel herpes simplex virus glycoprotein, gL, forms a complex with glycoprotein H (gH) and affects normal folding and surface expression of gH. *J. Virol.* 66:2240-50.

Hwang, W. L., and T. S. Su. 1998. Translational regulation of hepatitis B virus polymerase gene by termination-reinitiation of an upstream minicistron in a length-dependent manner. *J. Gen. Virol.* 79:2181-9.

Ikeda, M., A. Ikeda, L. C. Longan, and R. Longnecker. 2000. The Epstein-Barr virus latent membrane protein 2A PY motif recruits WW domain-containing ubiquitin-protein ligases. *Virology* 268:178-91.

Ilsey, J. L., M. Sudol, and S. J. Winder. 2002. The WW domain: Linking cell signalling to the membrane cytoskeleton. *Cell Signal* 14:183-9.

Jacobs, B. L., and C. E. Samuel. 1985. The reovirus S1 mRNA encodes two primary translation products. *Virology* 143:63-74.

Jahn, R., T. Lang, and T. C. Sudhof. 2003. Membrane fusion. *Cell* 112:519-33.

Jaysinghe, S., K. Hristova, and S. H. White. 2000. http://blanco.biomol.uci.edu/mpex.

Jeetendra, E., C. S. Robinson, L. M. Albritton, and M. A. Whitt. 2002. The membrane-proximal domain of vesicular stomatitis virus G protein functions as a membrane fusion potentiator and can induce hemifusion. *J. Virol.* 76:12300-11.

Jensen, M. J., I. W. Cheney, L. H. Thompson, J. D. Mecham, W. C. Wilson, M. Yamakawa, P. Roy, and B. M. Gorman. 1994. The smallest gene of the orbivirus, epizootic hemorrhagic disease, is expressed in virus-infected cells as two proteins and the expression differs from that of the cognate gene of bluetongue virus. *Virus Res.* 32:353-64.

Jin, H., K. Subbarao, S. Bagai, G. P. Leser, B. R. Murphy, and R. A. Lamb. 1996. Palmitylation of the influenza virus hemagglutinin (H3) is not essential for virus assembly or infectivity. *J. Virol.* 70:1406-14.

Kay, B. K., M. P. Williamson, and M. Sudol. 2000. The importance of being proline: the interaction of proline-rich motifs in signaling proteins with their cognate domains. *FASEB J.* 14:231-41.

Kemble, G. W., T. Danieli, and J. M. White. 1994. Lipid-anchored influenza hemagglutinin promotes hemifusion, not complete fusion. *Cell* 76:383-91.

Kennedy, M. T., H. Brockman, and F. Rusnak. 1996. Contributions of myristoylation to calcineurin structure/function. *J. Biol. Chem.* 271:26517-21.

Kibenge, F. S. B., G. E. Gwaze, R. C. Jones, A. F. Chapman, and C. E. Savage. 1985. Experimental reovirus infection in chickens: observations on early viraemia and virus distribution in bone marrow, liver and enteric tissues. *Avian Pathol.* 14:87-98.

Kielian, M. 2002. Structural surprises from the flaviviruses and alphaviruses. *Mol. Cell* 9:454-6.

Kieliszewski, M. J., and D. T. Lamport. 1994. Extensin: repetitive motifs, functional sites, post-translational codes, and phylogeny. *Plant J.* 5:157-72.

Kim, M., B. W. Chellgren, A. L. Rucker, J. M. Troutman, M. G. Fried, A.-F. Miller, and T. P. Creamer. 2001. Host-guest study of left-handed polyproline II helix formation. *Biochemistry* 40:14376-83.

Kliger, Y., S. G. Peisajovich, R. Blumenthal, and Y. Shai. 2000. Membrane-induced conformational change during the activation of HIV-1 gp41. *J. Mol. Biol.* 301:905-14.

Kogan, M. J., I. Dalcol, P. Gorostiza, C. Lopez-Iglesias, M. Pons, F. Sanz, D. Ludevid, and E. Giralt. 2001. Self-assembly of the amphipathic helix (VHLPPP)8. A mechanism for zein protein body formation. *J. Mol. Biol.* 312:907-13.

Kozak, M. 1991. An analysis of vertebrate mRNA sequences: intimations on translational control. *J. Cell. Biol.* 115:887-903.

Kozak, M. 1987. Effects of intercistronic length on the efficiency of reinitiation by eucaryotic ribosomes. *Mol Cell Biol.* 7:3438-45.

Kozak, M. 1989. The scanning model for translation: an update. *J. Cell. Biol.* 108:229-41.

Kozlov, M. M., and L. V. Chernomordik. 1998. A mechanism of protein-mediated membrane fusion: coupling between refolding of the influenza hemagglutinin and lipid rearrangements. *Biophys. J.* 75:1384-96.

Kozlovsky, Y., L. V. Chernomordik, and M. M. Kozlov. 2002. Lipid intermediates in membrane fusion: formation, structure and decay of hemifusion diaphragm. *Biophys. J.* 83:2634-51.

Kozlovsky, Y., and M. Kozlov. 2002. Stalk model of membrnae fusion: solution of energy crisis. *Biophys. J.* 88:882-95.

Krishtalik, L. I., and W. A. Cramer. 1995. On the physical basis for the cis-positive rule describing protein orientation in biological membranes. *FEBS Lett.* 369:140-3.

Kuhn, R. J., W. Zhang, M. G. Rossman, S. V. Pletnev, J. Corver, E. Lenches, C. T. Jones, S. Mukhopadhyay, P. R. Chipman, E. G. Strauss, T. S. Baker, and J. H. Strauss. 2002. Structure of dengue virus: implications for flavivirus organization, maturation, and fusion. *Cell* 108:717-25.

Kuntz-Simon, G., G. Le Gall-Recule, C. de Boisseson, and V. Jestin. 2002. Muscovy duck reovirus sigma-C protein is atypically encoded by the smallest genome segment. *J. Gen. Virol.* 83:1189-200.

Kweon, D. H., C. S. Kim, and Y. K. Shin. 2003. Insertion of the membrane-proximal region of the neuronal SNARE coiled coil into the membrane. *J. Biol. Chem.* 278:12367-73.

Lambert, C., and R. Prange. 2001. Dual topology of the hepatitis B virus large envelope protein: determinants influencing post-translational pre-S translocation. *J. Biol. Chem.* 276:22265-72.

Lamirande, E. W., D. K. Nichols, J. W. Owens, J. M. Gaskin, and E. R. Jacobson. 1999. Isolation and experimental transmission of a reovirus pathogenic in ratsnake (*Elaphe* species). *Virus Res.* 63:135-41.

Lang, T., D. Bruns, D. Wenzel, D. Riedel, P. Holroyd, C. Thiele, and R. Jahn. 2001. SNAREs are concentrated in cholesterol-dependent clusters that define docking and fusion sites for exocytosis. *EMBO J.* 20:2202-13.

Langosch, D., J. M. Crane, B. Brosig, A. Hellwig, L. K. Tamm, and J. Reed. 2001. Peptide mimics of SNARE transmembrane segments drive membrane fusion depending on their conformational plasticity. *J. Mol. Biol.* 311:709-721.

Leikina, E., D. L. LeDuc, J. C. Macosko, R. Epand, R. Epand, Y.-K. Shin, and L. V. Chernomordik. 2001. The 1-127 HA2 construct of influenza virus hemagglutinin induces cell-cell hemifusion. *Biochemistry* 40:8378-86.

Leland, M. M., G. R. Hubbard, H. T. Sentmore III, K. F. Soike, and J. K. Hilliard. 2000. Outbreak of Orthoreovirus-induced meningoencephalomyelitis in baboons. *Comp. Med.* 50:199-205.

Lescar, J., A. Roussel, M. W. Wien, J. Navaza, S. D. Fuller, G. Wengler, and F. A. Rey. 2001. The fusion glycoprotein shell of Semliki Forest virus: an icosahedral assembly primed for fusogenic activation at endosomal pH. *Cell* 105:137-148.

Li, H., and V. Papadopoulos. 1998. Peripheral-type benzodiazepine receptor function in cholesterol transport. Identification of a putative cholesterol recognition/interaction amino acid sequence and consensus pattern. *Endocrinology* 139:4991-7.

Lin, X., C. A. Derdeyn, R. Blumenthal, J. West, and E. Hunter. 2003. Progressive truncations C terminal to the membrane-spanning domain of simian immunodeficiency virus Env reduce fusogenicity and increase concentration dependence of Env for fusion. *J. Virol.* 77:7067-77.

Liu, Q., and G. Hobom. 2000. Evidence for translation of VP3 of avian polyomavirus BFDV by leaky ribosomal scanning. *Arch. Virol.* 145:407-16.

Loewen, C. J., O. L. Moritz, B. M. Tam, D. S. Papermaster, and R. S. Molday. 2003. The role of subunit assembly in peripherin-2 targeting to rod photoreceptor disk membranes and retinitis pigmentosa. *Mol. Cell. Biol.* 14:3400-13.

Loffler-Mary, H., M. Werr, and R. Prange. 1997. Sequence-specific repression of cotranslational translocation of the hepatitis B virus envelope proteins coincides with the binding of heat shock protein Hsc70. *Virology* 18:144-52.

Lower, R., J. Lower, and R. Kurth. 1996. The viruses in all of us: characteristics and biological significance of human endogenous retrovirus sequences. *Proc. Nat. Acad. Sci. USA* 93:5177-84.

Madhusoodanan, M., and T. Lazaridis. 2003. Investigation of pathways for the low-pH conformational transition in influenza hemagglutinin. *Biophys. J.* 84:1926-39.

Mandl, C. W., F. Guirakhoo, H. Holzmann, F. X. Heinz, and C. Kunz. 1989. Antigenic structure of the flavivirus envelope protein E at the molecular level, using tick-borne encephalitis virus as a model. *J. Virol.* 63:564-71.

Mangasarian, M., V. Piguet, J.-K. Wang, Y.-L. Chen, and D. Trono. 1999. Nef-induced CD4 and major histocompatibility complex class I (MHC-I) down-regulation are governed by distinct determinants: N-terminal alpha helix and proline repeat of Nef selectively regulate MHC-I trafficking. *J. Virol.* 73:1964-73.

Markosyan, R. M., F. S. Cohen, and G. B. Melikyan. 2000. The lipid-anchored ectodomain of influenza virus hemagglutinin (GPI-HA) is capable of inducing nonenlarging fusion pores. *Mol. Biol. Cell* 11:1143-52.

Martin-Belmonte, F., J. A. Lopez-Guerrero, L. Carrasco, and M. A. Alonso. 2000. The amino-terminal nine amino acid sequence of poliovirus capsid VP4 protein is

sufficient to confer N-myristoylation and targeting to detergent-insoluble membranes. *Biochemistry* 39:1083-90.

Martin, L. A., A. J. Meyer, R. S. O'Hara, H. Fu, P. S. Mellor, N. J. Knowles, and P. P. Mertens. 1998. Phylogenetic analysis of African horse sickness virus segment 10: sequence variation, virulence characteristics and cell exit. *Arch. Virol. Suppl.* 14:281-93.

Matlack, K. E. S., W. Mothes, and T. A. Rapoport. 1998. Protein translocation: tunnel vision. *Cell* 92:381-90.

Mayer, B. J. 2001. SH3 domains: complexity in moderation. *J. Cell Sci.* 114:1253-63.

Mayer, B. J., M. Hamaguchi, and H. Harafusa. 1988. A novel viral oncogene with structural similarity to phospholipase C. *Nature* 332:272-5.

McCabe, J. B., and L. G. Berthiaume. 1999. Functional roles for fatty acylated amino-terminal domains in subcellular localization. *Mol. Biol. Cell* 10:3771-86.

McLaughlin, S., and A. Aderem. 1995. The myristoyl-electrostatic switch: a modulator of reversible protein-membrane interactions. *Trends Biochem. Sci.* 20:272-6.

Melikyan, G. B., R. M. Markosyan, H. Hemmati, M. K. Delmedico, D. M. Lambert, and F. S. Cohen. 2000a. Evidence that the transition of HIV-1 gp41 into a six-helix bundle, not the bundle configuration, induces membrane fusion. *J. Cell Biol.* 151:413-23.

Melikyan, G. B., R. M. Markosyan, M. G. Roth, and F. S. Cohen. 2000b. A point mutation in the transmembrane domain of the hemagglutinin of influenza virus stabilizes a hemifusion intermediate that can transit to fusion. *Mol. Biol. Cell.* 11:3765-75.

Melikyan, G. B., J. M. White, and F. S. Cohen. 1995. GPI-anchored influenza hemagglutinin induces hemifusion to both red blood cell and planar bilayer membranes. *J. Cell Biol.* 131:679-91.

Mertens, P. P. C., M. Arella, H. Attoui, S. Belloncik, M. Bergoin, G. Boccardo, T. F. Booth, W. Chiu, J. M. Diprose, R. Duncan, *et al.* 2000. *Reoviridae. In* M. H. V. Van Regenmortel, C. M. Fauquet, D. H. L. Bishop, *et al.* (eds.) Virus Taxonomy: Seventh Report of the International Committee on Taxonomy of Viruses. Academic Press, New York.

Mi, S., X. Lee, X. Li, G. M. Veldman, H. Finnerty, L. Racie, E. LaVallie, X. Y. Tang, P. Edouard, S. Howes, J. C. J. Keith, and J. M. McCoy. 2000. Syncytin is a captive retroviral envelope protein involved in human placental morphogenesis. *Nature* 403:785-9.

Milne, R. S., S. L. Hanna, A. H. Rux, S. H. Willis, G. H. Cohen, and R. J. Eisenberg. 2003. Function of herpes simplex virus type 1 gD mutants with different receptor-binding affinities in virus entry and fusion. *J. Virol.* 77:8962-72.

Monsma, S. A., and G. W. Blissard. 1995. Identification of a membrane fusion domain and an oligomerization domain in the baculovirus GP64 envelope fusion protein. *J. Virol.* 69:2583-95.

Morrison, T. G. 2003. Structure and function of a paramyxovirus fusion protein. *Biochim. Biophys. Acta.* 1614:73-84.

Muga, A., W. Neugebauer, T. Hirama, and W. K. Surewicz. 1994. Membrane interaction and conformational properties of the putative fusion peptide of PH-30, a protein active in sperm-egg fusion. *Biochemistry* 33:4444-8.

Murphy, F. A., C. M. Fauquet, D. H. L. Bishop, S. A. Ghabrial, A. W. Jarvis, G. P. Martelli, M. A. Mayo, and M. D. Summers (eds.). 1995. Virus Taxonomy: Sixth Report of the International Committee on Taxonomy of Viruses. *Arch. Virol.* (suppl.) 10. Springer-Verlag, New York.

Naim, H. Y., B. Amarneh, N. T. Ktistakis, and M. G. Roth. 1992. Effects of altering palmitylation sites on biosynthesis and function of the influenza virus hemagglutinin. *J. Virol.* 66:7585-8.

Namba, K., M. Nishio, K. Mori, N. Miyamoto, M. Tsurudome, M. Ito, M. Kawano, A. Uchida, and Y. Ito. 2001. Involvement of ADAM9 in multinucleated giant cell formation of blood monocytes. *Cell. Immunol.* 213:104-13.

Ni, Y., and R. F. Ramig. 1993. Characterization of avian reovirus-induced cell fusion: the role of viral structural proteins. *Virology* 194:705-14.

Nibert, M. L., L. A. Schiff, and B. N. Fields. 1991. Mammalian reoviruses contain a myristylated structural protein. *J. Virol.* 65:1960-7.

Nibert, M. L., L. A. Schiff, and B. N. Fields. 1996. Reoviruses and their replication, p. 691-730. *In* B. N. Fields, D. M. Knipe, P. M. Howley, *et al.* (eds.), Fundamental Virology, 3rd ed. Lippincott-Raven, Philadelphia.

Niebuhr, K., F. Ebel, R. Frank, M. Reinhard, E. Domann, U. D. Carl, U. Walter, F. B. Gertler, J. Wehland, and T. Chakraborty. 1997. A novel proline-rich motif present in ActA of Listeria monocytogenes and cytoskeletal proteins is the ligand for the EVH1 domain, a protein module present in the Ena/VASP family. *EMBO J.* 16:5433-44.

Nieva, J. L., and A. Agirre. 2003. Are fusion peptides a good model to study viral cell fusion? *Biochim. Biophys. Acta.* 1614:104-15.

Nieva, J. L., and T. Suarez. 2000. Hydrophobic-at-interface regions in viral fusion protein ectodomains. *Biosci Rep.* 20:519-33.

Nilsson, I., S. Witt, H. Kiefer, I. Mingarro, G. von Heijne. 2000. Distant downstream sequence determinants can control N-tail translocation during protein insertion into the endoplasmic reticulum membrane. *J. Biol. Chem.* 275:6207-13.

Nixdorf, R., B. G. Klupp, A. Karger, and T. C. Mettenleiter. 2000. Effects of truncation of the carboxy terminus of pseudorabies virus glycoprotein B on infectivity. *J. Virol.* 74:7137-45.

Olsen, H. B., and N. C. Kaarsholm. 2000. Structural effects of protein lipidation as revealed by LysB29-myristoyl, des(B30) insulin. *Biochemistry* 39:11893-900.

Olsen, K. E. P., and K. B. Andersen. 1999. Palmitoylation of the intracytoplasmic R peptide of the transmembrane envelope protein in Moloney murine leukemia virus. *J. Virol.* 73:8975-91.

Otte, L., U. Wiedemann, B. Schlegel, P. J. R., M. Beyermann, P. Schmieder, G. Krause, R. Volkmer-Engert, J. Schreider-Mergener, and H. Oschkinat. 2003. WW domain sequence activity relationships identified using ligand recognition propensities of 42 WW domains. *Protein Sci.* 12:491-500.

Ozols, J., S. A. Carr, and P. Strittmatter. 1984. Identification of the NH2-terminal blocking group of NADH-cytochrome b5 reductase as myristic acid and the complete amino acid sequence of the membrane-binding domain. *J. Biol. Chem.* 259:13349-54.

Pak, C. C., A. Puri, and R. Blumenthal. 1997. Conformational changes and fusion activity of vesicular stomatitis virus glycoprotein: [^{125}I] iodonaphthylazide photolabeling studies in biological membranes. *Biochemistry* 36:8890-6.

Park, S.-H., W. Shalongo, and E. Stellwagen. 1997. The role of PPII conformations in the calculation of peptide fractional helix content. *Protein Sci.* 6:1694-1700.

Peabody, D. S., and P. Berg. 1986. Termination-reinitiation occurs in the translation of mammalian cell mRNAs. *Mol. Cell. Biol.* 6:2695-703.

Pécheur, E. I., J. Sainte-Marie, A. Bienvene, and D. Hoekstra. 1999. Peptides and membrane fusion: towards an understanding of the molecular mechanism of protein-induced fusion. *J. Membr. Biol.* 167:1-17.

Peisajovich, S. G., O. Samuel, and Y. Shai. 2000. Paramyxovirus F1 protein has two fusion peptides: implications for the mechanism of membrane fusion. *J. Mol. Biol.* 296:1353-65.

Peisajovich, S. G., and Y. Shai. 2001. SIV gp41 binds to membranes both in the monomeric and trimeric states: consequences for the neuropathology and inhibition of HIV infection. *J. Mol. Biol.* 311:249-54.

Peisajovich, S. G., and Y. Shai. 2003. Viral fusion proteins: multiple regions contribute to membrane fusion. *Biochim. Biophys. Acta.* 1614:122-9.

Peitzsch, R. M., and S. McLaughlin. 1993. Binding of acylated peptides and fatty acids to phospholipid vesicles: pertinence to myristoylated proteins. *Biochemistry* 32:10436-43.

Pereira, H. G. 1991. Double-stranded RNA viruses. *Semin. Virol.* 2:39-53.

Persing, D. H., H. E. Varmus, and D. Ganem. 1987. The preS1 protein of hepatitis B virus is acylated at its amino terminus with myristic acid. *J. Virol.* 61:1672-7.

Persson, B., and P. Argos. 1994. Prediction of transmembrane segments in proteins utilising multiple sequence alignments. *J. Mol. Biol.* 237:182-92.

Persson, B., and P. Argos. 1997. Prediction of membrane protein topology utilizing multiple sequence alignments. *J. Protein Chem.* 16:453-7.

Petek, M., B. Felluga, G. Borghi, and A. Baroni. 1967. The Crawley agent: an avian reovirus. *Arch. Gesamte Virusforsch* 21:413-24.

Poggioli, G. J., C. Keefer, J. L. Connolly, T. S. Dermody, and K. L. Tyler. 2000. Reovirus-induced G2/M cell cycle arrest requires s1s and occurs in the absence of apoptosis. *J. Virol.* 74:9562-70.

Poppers, J., M. Mulvey, D. Khoo, and I. Mohr. 2000. Inhibition of PKR activation by the proline-rich RNA binding domain of the herpes simplex virus type 1 Us11 protein. *J. Virol.* 74:11215-21.

Potgens, A. J. G., U. Schmitz, P. Bose, A. Versmold, P. Kaufmann, and H.-G. Frank. 2002. Mechanisms of syncytial fusion: a review. *Placenta* 23:S107-13.

Prange, R., and R. E. Streeck. 1995. Novel transmembrane topology of the hepatitis B virus envelope proteins. *EMBO J.* 14:247-56.

Randazzo, P. A., T. Terui, S. Sturch, H. M. Fales, A. G. Ferrige, and R. A. Kahn. 1995. The myristoylated amino terminus of ADP-ribosylation factor 1 is a phospholipid- and GTP-sensitive switch. *J. Biol. Chem.* 270:14809-15.

Rawat, S. S., M. Viard, S. A. Gallo, A. Rein, R. Blumenthal, and A. Puri. 2003. Modulation of entry of enveloped viruses by cholesterol and spingolipids (review). *Mol. Membr. Biol.* 20:243-54.

Razinkov, V. I., and F. S. Cohen. 2000. Sterols and sphingolipids strongly affect the growth of fusion pores induced by the hemagglutinin of influenza virus. *Biochemistry* 39:13462-8.

Resh, M. D. 1999. Fatty acylation of proteins: new insights into membrane targeting of myristoylated and palmitoylated proteins. *Biochim. Biophys. Acta.* 1451:1-16.

Rey, F. A., F. X. Heinz, C. W. Mandl, C. Kunz, and S. C. Harrison. 1995. The envelope glycoprotein from tick-borne encephalitis virus at 2 Å resolution. *Nature* 375:291-8.

Rodgers, S. E., J. L. Connolly, J. D. Chappell, and T. S. Dermody. 1998. Reovirus growth in cell culture does not require the full complement of viral proteins: identification of a σ1s-null mutant. *J. Virol.* 72:8597-604.

Rodriguez-Crespo, I., J. Gomez-Gutierrez, J. A. Encinar, J. M. Gonzalez-Ros, J. P. Albar, D. L. Peterson, and F. Gavilanes. 1996. Structural properties of the putative fusion peptide of hepatitis B virus upon interaction with phospholipids. Circular dichroism and Fourier-transform infrared spectroscopy studies. *Eur. J. Biochem.* 242:243-8.

Rodriguez-Crespo, I., E. Nuñez, B. Yélamos, J. Gómez-Gutiérrez, J. P. Albar, D. l. Peterson, and F. Gavianes. 1999. Fusogenic activity of hepadnavirus peptides corresponding to sequences downstream of the putative cleavage site. *Virology* 261:133-42.

Rodriguez-Crespo, I., B. Yelamos, J. P. Albar, D. L. Peterson, and F. Gavilanes. 2000. Selective destabilization of acidic phospholipid bilayers performed by the hepatitis B virus fusion peptide. *Biochim. Biophys. Acta.* 1463:419-28.

Ronish, E. W., and S. Krimm. 1974. The calculated circular dichroism of polyproline II in the polarizability approximation. *Biopolymers* 13:1635-51.

Rotzchke, O., and K. Falk. 1994. Origin, structure and motifs of naturally processed MHC class II ligands. *Curr. Opin. Immunol.* 6:45-51.

Ruiz-Gomez, M., N. Coutts, A. Price, M. V. Taylor, and M. Bate. 2000. *Drosophila* dumbfounded: a myoblast attractant essential for fusion. *Cell* 102:189-98.

Sackett, K., and Y. Shai. 2002. The HIV-1 gp41 N-terminal heptad repeat plays an essential role in membrane fusion. *Biochemistry* 41:4678-85.

Sackett, K., and Y. Shai. 2003. How structure correlates to function for membrane associated HIV-1 gp41 constructs corresponding to the N-terminal half of the ectodomain. *J. Mol. Biol.* 333:47-58.

Sakai, T., R. Ohuchi, and M. Ohuchi. 2002. Fatty acids on the A/USSR/77 influenza virus hemagglutinin facilitate the transition from hemifusion to fusion pore formation. *J. Virol.* 76:4603-11.

Salzwedel, K., J. T. West, and E. Hunter. 1999. A conserved tryptophan-rich motif in the membrane-proximal region of the human immunodeficiency virus type 1 gp41 ectodomain is important for Env-mediated fusion and virus infectivity. *J. Virol.* 73:2469-80.

Samuel, C. E. 1989. Polycistronic animal virus mRNAs. *Prog. Nucleic Acid Res. Mol. Biol.* 37:127-53.

Santos, N. C., M. Prieto, and M. A. Castanho. 1998. Interaction of the major epitope region of HIV protein gp41 with membrane model systems. A fluorescence spectroscopy study. *Biochemistry* 37:8674-82.

Sarimento, M., and P. G. Spear. 1979. Membrane proteins specified by herpes simplex virus. IV. Conformation of the virion glycoprotein designated VP7 (B2). *J. Virol.* 29:1159-67.

Sato, M., R. Hresko, and M. Mueckler. 1998. Testing the charge difference hypothesis for the assembly of a eucaryotic multispanning membrane protein. *J. Biol. Chem.* 273:25203-8.

Schagger, H., and G. von Jagow. 1987. Tricine-sodium dodecyl sulfate-polyacrylamide gel electrophoresis for the separation of proteins in the range from 1 to 100 kDa. *Anal. Biochem.* 166:368-79.

Schneider, P. A., M. Schwemmle, and W. I. Lipkin. 1997. Implication of a cis-acting element in the cytoplasmic accumulation of unspliced Borna disease virus RNAs. *J. Virol.* 71:8940-5.

Schoch, C., R. Blumenthal, and M. J. Clague. 1991. A long-lived state for influenza virus-erythrocyte complexes committed to fusion at neutral pH. *FEBS Lett.* 311:221-5.

Schmidt, M., M. F. G. Schmidt, and R. Rott. 1988. Chemical identification of cysteine as palmitoylation site in a transmembrane protein (Semliki Forest virus E1). *J. Biol. Chem.* 263.

Schmidt, M. F. G. 1982. Acylation of viral spike glycoproteins: A feature of enveloped RNA viruses. *Virology* 116:327-38.

Schmidt, M. F. G., M. Bracha, and M. J. Schlesiger. 1979. Evidence for covalent attachment of fatty acids to Sindbis virus glycoproteins. *Proc. Nat. Acad. Sci. USA* 76:1687-91.

Schmidt, M. F. G., and M. J. Schlesinger. 1979. Fatty acid binding to vesicular stomatitis virus glycoprotein: A new type of post-translational modification of the viral glycoprotein. *Cell* 17:813-9.

Schroth, B., H. C. Philipp, M. Veit, M. F. Schmidt, and A. Herrmann. 1996. Deacylation of influenza virus hemagglutinin does not affect the kinetics of low pH induced membrane fusion. *Pflugers Arch.* 431:R257-8.

Schweimer, K., S. Hoffmann, F. Bauer, U. Friedrich, C. Kardinal, S. M. Feller, B. Biesinger, and H. Sticht. 2002. Structural investigation of the binding of a herpesviral protein to the SH3 domain of tyrosine kinase Lck. *Biochemistry* 41:5120-30.

Senes, A., M. Gerstein, and D. M. Engelman. 2000. Statistical analysis of amino acid patterns in transmembrane helices: the GxxxG motif occurs frequently and in association with beta-branched residues at neighboring positions. *J. Mol. Biol.* 296:921-36.

Seth, S., A. Vincent, and R. W. Compans. 2003. Mutations in the cytoplasmic domain of a paramyxovirus fusion glycoprotein rescue syncytium formation and eliminate the hemagglutinin-neuraminidase protein requirement for membrane fusion. *J. Virol.* 77:167-78.

Seykora, J. T., M. M. Myat, L. A. Allen, J. V. Ravetch, and A. Aderem. 1996. Molecular determinants of the myristoyl-electrostatic switch of MARCKS. *J. Biol. Chem.* 271:18797-802.

Shackleton, S., I. Hamer, M. Foti, N. Zumwald, C. Maeder, and J. L. Carpentier. 2002. Role of two dileucine-like motifs in insulin receptor anchoring to microvilli. *J. Biol. Chem.* 277:43631-7.

Shmulevitz, M. 2001. Understanding the mechanism of protein-mediated fusion through structure/function analysis of a nonenveloped virus-encoded 'minimalistic' fusion protein. Ph.D. thesis. Dalhousie University, Halifax.

Shmulevitz, M., and R. Duncan. 2000. A new class of fusion-associated small transmembrane (FAST) proteins encoded by the non-enveloped fusogenic reoviruses. *EMBO J.* 19:902-12.

Shmulevitz, M., J. Corcoran, J. Salsman, and R. Duncan. 2004a. The ER-associated degradation pathway restricts the kinetics of cell-cell fusion induced by a nonenveloped virus membrane fusion protein. *J. Virol.* (submitted).

Shmulevitz, M., R. F. Epand, R. M. Epand, and R. Duncan. 2004b. Structural and functional properties of an unusual internal fusion peptide in a nonenveloped virus membrane fusion protein. *J. Virol.* (in press).

Shmulevitz, M., J. Salsman, and R. Duncan. 2003. Palmitoylation, membrane-proximal basic residues, and transmembrane glycine residues in the reovirus p10 protein are essential for syncytium formation. *J. Virol.* 77:9769-79.

Shmulevitz, M., Z. Yameen, S. J. Dawe, J. Shou, D. O'Hara, I. Holmes, and D. R. 2002. Sequential partially overlapping gene arrangement in the tricistronic S1 genome segments of avian reovirus and Nelson Bay reovirus: implications for translation initiation. *J. Virol.* 76:609-18.

Siligardi, G., and A. F. Drake. 1995. The importance of extended conformations and, in particular, the PII conformation for the molecular recognition of peptides. *Biopolymers* 37:281-92.

Skehel, J. J., and D. C. Wiley. 1998. Coiled coils in both intracellular vesicle and viral membrane fusion. *Cell* 95:871-4.

Skehel, J. J., and D. C. Wiley. 2000. Receptor binding and membrane fusion in virus entry: the influenza hemagglutinin. *Annu. Rev. Biochem.* 69:531-69.

Skehel, J. J., K. Cross, D. Steinhauer, and D. C. Wiley. 2001. Influenza fusion peptides. *Biochem. Soc. Trans.* 29:623-6.

Smit, J. M., R. Bittman, and J. Wilschut. 2001. Deacylation of the transmembrane domains of Sindbis virus envelope glycoproteins E1 and E2 does not affect low-pH-induced viral membrane fusion activity. *FEBS Lett.* 498:57-61.

Sowadski, J. M., C. A. Ellis, and Madhusudan. 1996. Detergent binding to unmyristylated protein kinase A - structural implications for the role of myristate. *J. Bioenerg. Biomembr.* 28:7-12.

Spear, P. G., and R. Longnecker. 2003. Herpesvirus entry: an update. *J. Virol.* 77:10179-85.

Stahl, M. L., C. R. Ferenz, K. L. Kelleher, and R. W. Kriz. 1988. Sequence similarity of phospholipase C with the non-catalytic region of src. *Nature* 332:269-72.

Stapley, B. J., and T. P. Creamer. 1999. A survey of left-handed polyproline II helices. *Protein Sci.* 8:587-95.

Steel, G. J., J. Brownsword, and C. J. Stirling. 2002. Tail-anchored protein insertion into yeast ER requires a novel posttranslational mechanism which is independent of the SEC machinery. *Biochemistry* 41:11914-20.

Stegmann, T., R. W. Doms, and A. Helenius. 1989. Protein-mediated membrane fusion. *Annu. Rev. Biophys. Chem.* 18:187-211.

Steinhauer, D. A., S. A. Wharton, D. C. Wiley, and J. J. Skehel. 1991. Deacylation of the hemagglutinin of influenza A/Aichi/2/68 has no effect on membrane fusion properties. *Virology* 184:445-8.

Stiasny, K., S. L. Allison, C. W. Mandl, and F. X. Heinz. 2001. Role of metastability and acidic pH in membrane fusion by tick-borne encephalitis virus. *J. Virol.* 75:7392-8.

Stiasny, K., S. L. Allison, A. Marchler-Bauer, C. Kunz, and F. X. Heinz. 1996. Structural requirements for low-pH-induced rearrangements in the envelope glycoprotein of tick-borne encephalitis virus. *J. Virol.* 70:8142-7.

Stiasny, K., C. Koessl, and F. X. Heinz. 2003. Involvement of lipids in different steps of the flavivirus fusion mechanism. *J. Virol.* 77:7856-62.

Suarez, T., W. R. Gallaher, A. Agirre, F. M. Goni, and J. L. Nieva. 2000. Membrane interface-interacting sequences within the ectodomain of the human immunodeficiency virus type 1 envelope glycoprotein: putative role during viral fusion. *J. Virol.* 74:8038-47.

Sutton, R. B., J. A. Ernst, and A. T. Brunger. 1999. Crystal structure of the cytosolic C2A-C2B domains of synaptotagmin III: Implications for Ca^{2+}-independent SNARE complex interaction. *J. Cell Biol.* 147:589-98.

Sutton, R. B., D. Fasshauer, R. Jahn, and A. T. Brunger. 1998. Crystal structure of a SNARE complex involved in synaptic exocytosis at 2.4 Å resolution. *Nature* 395:347-53.

Swameye, I., and H. Schaller. 1997. Dual topology of the large envelope protein of duck hepatitis B virus: determinants preventing pre-S translocation and glycosylation. *J. Virol.* 71:9434-41.

Takeda, M., G. P. Leser, C. J. Russell, and R. A. Lamb. 2003. Influenza virus hemagglutinin concentrates in lipid raft microdomains for efficient viral fusion. *Proc. Natl. Acad. Sci. USA* 100:14610-7.

Takeda, Y., I. Tachibana, K. Miyado, M. Kobayashi, T. Miyazaki, T. Funakoshi, H. Kimura, H. Yamane, Y. Saito, H. Goto, T. Yoneda, M. Yoshida, T. Kumagai, T. Osaki, S. Hayashi, I. Kawase, and E. Mekada. 2003. Tetraspanins CD9 and CD81 function to prevent the fusion of mononuclear phagocytes. *J. Cell Biol.* 161:945-56.

Tamm, L. K. 2003. Hypothesis: spring-loaded boomerang mechanism of influenza hemagglutinin-mediated membrane fusion. *Biochim. Biophys. Acta.* 1614:14-23.

Tamm, L. K., X. Han, Y. Li, and A. L. Lai. 2002. Structure and function of membrane fusion peptides. *Biopolymers* 66:249-60.

Taylor, G. M., and D. A. Sanders. 1999. The role of the membrane-spanning domain sequence in glycoprotein-mediated membrane fusion. *Mol. Biol. Cell* 10:2803-15.

Theil, K. W., and C. M. McCloskey. 1991. Rabbit syncytium virus is a Kemorovo serogroup orbivirus. *J. Clin. Microbiol.* 29:2059-62.

Theil, K. W., and L. J. Saif. 1985. *In vitro* detection of porcine rotavirus-like virus (group B rotavirus) and its antibody. *J. Clin. Micro.* 1:844-6.

Tholey, A., R. Pipkorn, D. Bossemeyer, V. Kinzel, and J. Reed. 2001. Influence of myristoylation, phosphorylation, and deamidation on the structural behavior of

the N-terminus of the catalytic subunit of cAMP-dependent protein kinase. *Biochemistry* 40:225-31.

Tieleman, D. P., and J. Bentz. 2002. Molecular dynamics simulation of the evolution of hydrophobic defects in one monolayer of a phosphatidylcholine bilayer: relevance for membrane fusion mechanisms. *Biophys. J.* 83:1501-10.

Tong, S., F. Yi, A. Martin, Q. Yao, M. Li, and R. W. Compans. 2001. Three membrane-proximal amino acids in the human parainfluenza type 2 (HPIV 2) F protein are critical for fusogenic activity. *Virology* 280:52-61.

Tong, S., M. Li, A. Vincent, R. W. Compans, E. Fritsch, R. Beier, C. Klenk, M. Ohuchi, and H. D. Klenk. 2002. Regulation of fusion activity by the cytoplasmic domain of a paramyxovirus F protein. *Virology* 301:322-33.

Tusnády, G. E., and I. Simon. 1998. Principles governing amino acid composition of integral membrane proteins: applications to topological prediction. *J. Mol. Biol.* 283:489-506.

Ulrich, A. S., M. Otter, C. G. Glabe, and D. Hoekstra. 1998. Membrane fusion is induced by a distinct peptide sequence of the sea urchin fertilization protein bindin. *J. Biol. Chem.* 273:16748-55.

Vanderplasschen, A., M. Hollinshead, and G. I. Smith. 1998. Intracellular and extracellular vaccinia virions enter cells by different mechanisms. *J. Gen. Virol.* 79:877-87.

van den Eijnde, S. M., M. J. B. van den Hoff, C. P. M. Reutelingsperger, W. L. van Heerde, M. E. R. Henfling, C. Vermeij-Keers, B. Schutte, M. Borgers, and F. C. S. Ramaekers. 2001. Transient expression of phosphatidylserine at cell-cell contact areas is required for myotube formation. *J. Cell Science* 114:3631-42.

van Niekerk, M., M. Freeman, J. T. Paweska, P. G. Howell, A. J. Guthrie, A. C. Potgieter, V. van Staden, and H. Huismans. 2003. Variation in the NS3 gene and protein in South African isolates of bluetongue and equine encephalosis viruses. *J. Gen. Virol.* 84:581-90.

van Staden, V., and H. Huismans. 1991. A comparison of the genes which encode non-structural protein NS3 of different orbiviruses. *J. Gen. Virol.* 72:1073-9.

Varela, R., J. Martinez-Costas, M. Mallo, and J. Benavente. 1996. Intracellular posttranslational modifications of S1133 avian reovirus proteins. *J. Virol.* 73:9098-109.

Vazquez, M.-I., and M. Esteban. 1999. Identification of functional domains in the 14-kilodalton envelope protein (A27L) of vaccinia virus. *J. Virol.* 73:9098-109.

Vazquez, M.-I., G. Rivas, D. Cregut, L. Serrano, and M. Esteban. 1998. The vaccinia virus 14-kilodalton (A27L) fusion protein forms a triple coiled-coil structure and interacts with the 21-kilodalton (A17L) virus membrane protein through a C-terminal alpha-helix. *J. Virol.* 72:10126--37.

Veit, M., E. Kretzschmar, K. Kuroda, W. Garten, M. F. Schmidt, H. D. Klenk, and R. Rott. 1991. Site-specific mutagenesis identifies three cysteine residues in the cytoplasmic tail as acylation sites of influenza virus hemagglutinin. *J. Virol.* 65:2491-500.

Vincent, N., C. Genin, and E. Malvoisin. 2002. Identification of a conserved domain of the HIV-1 transmembrane protein gp41 which interacts with cholesteryl groups. *Biochim. Biophys. Acta.* 1567:157-64.

von Heijne, G., and Y. Gavel. 1988. Topogenic signals in integral membrane proteins. *Eur. J. Biochem.* 174:671-8.

Waarts, B. L., R. Bittman, and J. Wilschut. 2002. Sphingolipid and cholesterol dependence of alphavirus membrane fusion. Lack of correlation with lipid raft formation in target liposomes. *J. Biol. Chem.* 277:38141-7.

Wahlberg, J. M., and M. Spiess. 1997. Multiple determinants direct the orientation of signal-anchor proeins: the topogenic role of the hydrophobic signal domain. *J. Cell Biol.* 137:555-62.

Weber, T., B. V. Zemelman, J. A. McNew, B. Westermann, M. Gmachl, F. Parlati, T. H. Sollner, and J. E. Rothman. 1998. SNAREpins: minimal machinery for membrane fusion. *Cell* 92:759-772.

Weimin Wu, B., P. M. Cannon, E. M. Gordon, F. L. Hall, and W. French Anderson. 1998. Characterization of the proline-rich region of murine leukemia virus envelope protein. *J. Virol.* 72:5383-91.

Weissenhorn, W., A. Dessen, L. J. Calder, S. C. Harrison, J. J. Skehel, and D. C. Wiley. 1999. Structural basis for membrane fusion by enveloped viruses. *Mol. Membr. Biol.* 16:3-9.

Westermann, B. 2003. Merging mitochondria matters: cellular role and molecular machinery of mitochondrial fusion. *EMBO Rep.* 3:527-31.

Westermann, B. 2003. Mitochondrial membrane fusion. *Biochim. Biophys. Acta.* 1641:195-202.

White, J. M. 1990. Viral and cellular membrane fusion proteins. *Annu. Rev. Physiol.* 52:675-9.

White, J. M. 1992. Membrane fusion. *Science* 258:917-24.

White, S. H., and W. C. Wimley. 1999. Membrane protein folding and stability: physical principles. *Annu. Rev. Biophys. Biomol. Struct.* 28:319-65.

Whitt, M. A., and J. K. Rose. 1991. Fatty acid acylation is not required for membrane fusion activity or glycoprotein assembly into VSV virions. *Virology* 185:875-8.

Wiley, D. C., and J. J. Skehel. 1987. The structure and function of the hemagglutinin membrane glycoprotein of influenza virus. *Annu. Rev. Biochem.* 56:365-94.

Wilcox, G. E., and R. E. Compans. 1982. Cell fusion induced by Nelson Bay virus. *Virology* 123:312-22.

Williamson, M. P. 1994. The structure and function of proline-rich regions in proteins. *Biochem. J.* 297:249-60.

Wilson, N. F., and W. J. Snell. 1998. Microvilli and cell-cell fusion during fertiization. *Trends Cell. Biol.* 8:93-6.

Winton, J. R., C. N. Lannan, J. L. Fryer, R. P. Hedrick, T. R. Meyers, J. A. Plumb, and T. J. Yanamoto. 1987. Morphological and biochemical properties of four members of a novel group of reoviruses isolated from aquatic animals. *J. Gen. Virol.* 68:353-64.

Wolfe, C. A., J. Cladera, S. Ladha, S. Senior, R. Jones, and P. O'Shea. 1999. Membrane interactions of the putative fusion peptide (MF alpha P) from fertilin-alpha, the mouse sperm protein complex involved in fertilization. *Mol. Membr. Biol.* 16:257-63.

Wolffe, E. J., S. Vijaya, and B. Moss. 1995. A myristylated membrane protein encoded by the vaccinia virus L1R open reading frame is the target of potent neutralizing monoclonal antibodies. *Virology* 211:53-63.

Wolfsberg, T. G., and J. M. White. 1996. ADAMs in fertilization and development. *Dev. Biol.* 180:389-401.

Woody, R. W. 1992. Circular dichroism and conformation of unordered polypeptides. *Adv. Biophys. Chem.* 2:37-79.

Xiang, Q., C. Rasmussen, N. L. Glass. 2002. The ham-2 locus, encoding a putative transmembrane protein, is required for hyphal fusion in Neurospora crassa. *Genetics* 160:169-80.

Yang, C., and R. W. Compans. 1996. Palmitoylation of the murine leukemia virus envelope glycoprotein transmembrane subunits. *Virology* 221:87-97.

Yang, L., T. A. Harroun, T. M. Weiss, L. Ding, and H. W. Huang. 2001. Barrel-stave model or torroidal model? A case study on melittin pores. *Biophys. J.* 81:1475-85.

Yang, C., C. P. Spies, and R. W. Compans. 1995. The human and simian immunodeficiency virus envelope glycoprotein transmembrane subunits are palmitoylated. *Proc. Natl. Acad. Sci. USA* 92:9871-5.

Yang, R., J. Yang, and D. P. Weliky. 2003. Synthesis, enhanced fusogenicity, and solid state NMR measurements of cross-linked HIV-1 fusion peptides. *Biochemistry* 42:3527-35.

Yao, Y., K. Ghosh, R. F. Epand, R. M. Epand, and H. P. Ghosh. 2003. Membrane fusion activity of vesicular stomatitis virus glycoprotein G is induced by low pH but not by heat or denaturant. *Virology* 310:319-32.

Yasunda, J., M. Nakao, Y. Kawaoka, and H. Shida. 2003. Nedd4 regulates egress of ebola virus-like particles from host cells. *J. Virol.* 77:9987-92.

Yonemoto, W., M. L. McGlone, and S. S. Taylor. 1993. N-myristylation of the catalytic subunit of cAMP-dependent protein kinase conveys structural stability. *J. Biol. Chem.* 268.

Yu, H., J. K. Chen, S. Feng, D. C. Dalgarno, A. W. Brauer, and S. L. Schreiber. 1994. Structural basis for the binding of proline-rich peptides to SH3 domains. *Cell* 76:933-45.

Yuksel, K. U., A. Q. Sun, R. W. Gracy, and K. D. Schnackerz. 1994. The hinged lid of yeast triose-phosphate isomerase. Determination of the energy barrier between the two conformations. *J. Biol. Chem.* 269:5005-8.

Zarripar, A., R. P. Bhattacharyya, and W. A. Lim. 2003. The structure and function of proline recognition domains. *Sci. STKE* 179:RE8.

Zhang, S. X., Y. Han, and G. W. Blissard. 2003. Palmitoylation of the Autographa californica multicapsid nucleopolyhedrovirus envelope glycoprotein GP64: mapping, functional studies, and lipid rafts. *J. Virol.* 77:6265-73.